

Gravitational Lensing by Dark Matter Caustics

Vakif K. Onemli ¹

Department of Physics, University of Florida, Gainesville, FL 32611 USA

Abstract

There are compelling reasons to believe that the dark matter of the universe is constituted, in large part, by non-baryonic collisionless particles with very small primordial velocity dispersion. Such particles are called cold dark matter (CDM). The leading candidates are axions and weakly interacting massive particles (WIMPs). The word “collisionless” indicates that the particles are so weakly interacting that they move purely under the influence of gravity. Galaxies are surrounded by CDM and hence, because of gravity, CDM keeps falling onto galaxies from all directions. CDM infall produces a discrete number of flows and caustics in the halos of galaxies. There are two types of caustics in the halos of galaxies: inner and outer. An outer caustic is a simple fold (A_2) catastrophe located on a topological sphere enveloping the galaxy. An inner caustic is a closed tube whose cross-section is an elliptic umbilic (D_{-4}) catastrophe, with three cusps.

In space, caustics are the boundaries that separate regions with differing numbers of flows. One side of a caustic surface has two more flows than the other. The density of CDM particles becomes very large as one approaches the caustic from the side with the extra flows. Dark matter caustics have specific density profiles and therefore precisely calculable gravitational lensing properties. This dissertation presents a formalism that simplifies the relevant calculations, and apply it to four specific cases. In the first three cases, the line of sight is tangent to a smooth caustic surface. The curvature of the surface at the tangent point is positive, negative, or zero. In the fourth case, the line of sight passes near a cusp. For each case we derive the map between the image and source planes. In some cases, a point source has multiple images and experiences infinite magnification when the images merge. A

¹e-mail: onemli@zephyr.th.u-psud.fr

promising approach to reveal the locations of caustics is to observe the distortions in the images of extended sources (such as radio jets) passing by the caustics.

Acknowledgments

This dissertation is based on a research paper on gravitational lensing by dark matter caustics. Caustic rings of dark matter were discovered by Dr. Pierre Sikivie who graciously allowed me to draw extensively on his work as he served as my guide during the course of the research that yielded this dissertation. I am deeply indebted to him for accepting me as one of his students. It has been a great privilege to work under his supervision in this new area of research in particle astrophysics. This attempt to widen the range of the discussion and to make the material more pedagogical would not have been possible without his help and encouragement. I would like to thank him also for his patience and his willingness to share both his thoughts and his time generously.

It is a pleasure to express my thanks to the other members of my supervisory committee: Dr. James Fry, Dr. David Grossier, Dr. Zongan Qiu, Dr. Pierre Ramond, Dr. Richard P. Woodard, and Dr. John Yelton. I have been honored by their presence on my committee; and benefitted from their contributions as teachers, collaborators, and coordinators throughout the years of my stay at the Physics Department.

I would like to thank Dr. Richard P. Woodard for his unfailing interest, encouragement and support. He was always available to assist me with every kind of problem I had, from physics to personal ones. His enthusiasm and dedication influenced me deeply. I was very fortunate that I had the chance to attend his lectures and collaborate with him. For the “cydonies,” I am forever grateful. Dear Richard, thank you for caring about my career. You will be missed. As in the good old days “all the brothers were valiant.”

My thanks also go to the other members of the Department of Physics of the University of Florida for making my studies enjoyable as well as educational. I would also like to thank my friends, whose support I have relied on; and my collaborators: Dr. Christos Charmousis, Dr. Zongan Qiu, Dr. Pierre Sikivie, Dr. Bayram Tekin, Dr. Murat Tas, and Dr. Richard Woodard, for the insights they shared with me. I thank Carol Lauriault for

carefully editing the manuscript. I am particularly grateful to my grandmother, my parents and my brother for their love and support. Finally, the Gibson Dissertation Fellowship I received is most gratefully acknowledged.

1 Introduction

A large amount of astronomical evidence indicates the existence in the universe of more gravitationally interacting matter than luminous matter. Most of the matter in the universe is dark. The stuff that is responsible for holding galaxies (and clusters of galaxies) together is a peculiar kind of matter that we neither see nor detect by any means. This cosmic mystery began puzzling astronomers in the 1930s and the case still remains open. For a review of the sources and distributions of dark matter, see Sikivie [1] and the references therein.

In 1932, Oort [2] studied the motions of galactic disk stars in the direction perpendicular to the disk. He applied the virial theorem to the distribution of vertical star velocities, and estimated the density of the galactic disk as $\rho_{\text{disk}} \simeq 1.2 \cdot 10^{-23} \frac{\text{gr}}{\text{cm}^3}$. When the density due to the matter seen in stars, interstellar gas, and stellar remnants like white dwarfs is calculated, however, one finds an estimate considerably less than the above value. This implies the existence of dark matter in the disk. Because this dark matter is in the disk rather than the halo, it is expected to be dissipative, hence baryonic in nature.

In 1933, Zwicky [3] used measurements of the line of sight velocities of galaxies in the Coma cluster to estimate the total mass of the cluster using the virial theorem:

$$\langle T \rangle = -\frac{1}{2} \langle U \rangle, \quad (1)$$

where T and U are the kinetic and potential energy of the system respectively. Bracket $\langle \rangle$ denotes time average. In these estimates, however, it is important to remember that the virial theorem is valid for a closed system in mechanical equilibrium and that it applies to the time average of the system. Whether the observed clusters satisfy these requirements is questionable. Nevertheless, assuming the applicability of the theorem, and using for the kinetic energy of N galaxies in the cluster:

$$\langle T \rangle = \frac{1}{2} N \langle mv^2 \rangle, \quad (2)$$

the potential energy of the $\frac{1}{2}N(N-1)$ independent galaxy pairs:

$$\langle U \rangle = -\frac{1}{2}GN(N-1)\frac{\langle m^2 \rangle}{\langle r \rangle}, \quad (3)$$

and taking $N \simeq N-1$, one can estimate the total mass:

$$M = N\langle m \rangle \simeq \frac{2r\langle v^2 \rangle}{G}. \quad (4)$$

By measuring the quantities r and v , it is possible to estimate M . The result obtained was about 400 times the mass in the luminous parts of the cluster galaxies.

During the seventies, the rotation curves (velocity as a function of radial distance from the center) of spiral galaxies began to be measured over much larger distances than before. Spiral galaxies are large scale structures containing billions of stars, arranged in the form of a rotating disk with a central bulge. Assuming that the stars have a circular orbit around the galactic center, the rotation velocity of a star can be calculated by balancing the centrifugal and the gravitational forces:

$$\frac{GM(r)m}{r^2} = \frac{v_{\text{rot}}^2 m}{r}, \quad (5)$$

where $M(r)$ is the mass interior to the orbit radius r , m is the mass of the star and $v_{\text{rot}}(r)$ is the rotation velocity at r . Here, we used the fact that for cylindrically or spherically symmetric distributions, the forces due to the mass lying outside the orbit compensate exactly. We have, therefore

$$v_{\text{rot}}(r) = \sqrt{\frac{GM(r)}{r}}. \quad (6)$$

If we assume that the bulge is spherically symmetric with a constant density of ρ , then $M(r) = \frac{4}{3}\pi r^3 \rho$. Hence, for the innermost part of a galaxy, a rotation curve where $v_{\text{rot}} \sim r$ is expected. For the outside of the galaxy, where $r >$ disc-radius, $M(r)$ is equal to the total mass of the galaxy $M(r) = M_{\text{galaxy}}$, which is a constant. In this case

$$v_{\text{rot}}(r) = \sqrt{\frac{GM_{\text{galaxy}}}{r}} \sim \frac{1}{\sqrt{r}}. \quad (7)$$

The data show, however, that $v_{\text{rot}} \sim \text{constant}$ for large r . This means that $M(r) \sim r$, which implies the existence of a huge unseen mass extending far beyond the visible region. The distribution of globular star clusters suggests a spherical distribution. Theoretical model calculations show that pure disk galaxies have a tendency to become bars (i.e., within the central nucleus, a bar-like structure forms) [4]. Barred galaxies do exist, but they are relatively rare. A spherical halo of dark matter increases the stability of the pure disk structure, producing a ratio of barred spirals consistent with observations [5]. Considerations of the stellar dynamics in elliptical galaxies also imply that they contain a significant fraction of dark matter[6].

These observations lead to the hypothesis of a halo of dark matter whose density is $d_{\text{dm}}(r) \sim \frac{1}{r^2}$ at large r . The halo distribution is usually modelled by the function

$$\rho_{\text{dm}}(r) = \frac{\rho_{\text{dm}}(0)}{1 + \left(\frac{r}{r_0}\right)^2}, \quad (8)$$

where r_0 is called the core radius. For our own galaxy, $v_{\text{rot}} \simeq 220 \frac{\text{km}}{\text{s}}$, r_0 is a few kpc, and $\rho_{\text{dm}}(0) \sim 10^{-23} \frac{\text{gr}}{\text{cm}^3}$.

According to Wilkinson Microwave Anisotropy Probe (WMAP) results [7, 8, 9], the density parameter

$$\Omega = \frac{\rho}{\rho_c} = \frac{8\pi G\rho}{3H_0^2} \quad (9)$$

of the universe has the numerical value $\Omega_{\text{univ}} = 1.02 \pm 0.02$. In Eq. 9 ρ_c is the critical density for closing the universe and H_0 is the present Hubble expansion rate. Most of the energy density of the universe is in the form of vacuum energy $\Omega_\Lambda = 0.73 \pm 0.04$. The density due to matter is $\Omega_m = 0.27 \pm 0.04$ and 0.17 \pm 0.01 of Ω_m is baryonic: $\Omega_b = 0.044 \pm 0.004$. Since the density of luminous matter is $\Omega_{\text{lum.}} < 0.006$, we conclude that some baryons are dark. Recall that there is dark matter associated with the disk of a galaxy. Because it is in the disk rather than in a halo, this dark matter must be dissipative which presumably

means that it is baryonic (disk dark matter must have sufficiently strong interactions to be concentrated in a disk by dissipating its energy while conserving its angular momentum). Likely hiding places for these dark baryons may be black holes, cold white dwarfs, and brown dwarfs (i.e., stars too low in mass to burn by nuclear fusion). Objects of this kind, generically called MACHOs (for massive compact halo objects), have been searched for by looking for the gravitational lensing of background stars by MACHOs that happen to pass close to the line of sight. Many of them have been discovered [10, 11, 12, 13]. We still do not know what makes up most of the missing mass in the universe.

The success of nucleosynthesis in producing the primordial abundances of light elements [14], also requires that $0.011 \leq \Omega_b \leq 0.12$. Studies of large scale structure formation support the view that most of the dark matter consists of non-baryonic, collisionless but gravitationally interacting particles such as axions and/or Weakly Interacting Massive Particles (WIMPs) (like neutralinos, photinos, higgsinos, etc.) [14]. The particles must have small primordial velocity dispersion; for this reason, they also are called “Cold Dark Matter (CDM)” candidates. We discuss these CDM candidates in the next section. Here, and throughout the dissertation, we assume that they exist; and study interesting consequences of their motion in the potential well of a galactic halo. We see that these candidates produce surfaces (which we call caustics) in physical space where the dark matter density is large, because folds exist at the corresponding locations of the sheet on which the particles lie in phase space. The CDM caustics may move about, but they are stable. They also have specific density profiles, and hence precisely calculable gravitational lensing properties. We present a formalism that simplifies the relevant calculations; and apply it to different cases to obtain their lensing signatures [15].

Let us start with a discussion of the phase space (velocity-position space) structure of CDM halos. Since the particles are in three-dimensional (3D) space, the phase space is six-dimensional. The primordial velocity dispersion of the cold dark matter candidates is

of a very small order [16]

$$\delta v_a(t) \sim 1.5 \cdot 10^{-17} \left(\frac{10^{-5} \text{eV}}{m_a} \right)^{4.7/5.7} \left(\frac{t_0}{t} \right)^{2/3}, \quad (10)$$

for axions and

$$\delta v_\chi(t) \sim 10^{-11} \left(\frac{\text{GeV}}{m_\chi} \right)^{1/2} \left(\frac{t_0}{t} \right)^{2/3}, \quad (11)$$

for WIMPs, where t_0 is the present age of the universe, and m_a and m_χ are respectively the masses of the axion and the WIMP. Calculations for $\delta v_a(t)$ and $\delta v_\chi(t)$ are given in Sections 2.2 and 2.1, respectively. These estimates of primordial velocity dispersions are approximate, but in the context of this dissertation and of galaxy formation in general, δv_a and δv_χ are entirely negligible. Therefore, CDM particles lie on a very thin 3D sheet in 6D phase space. The thickness of the sheet is the primordial velocity dispersion δv of the particles. Moreover, the present average number density n of the particles can be expressed in terms of their energy density in units of the critical density. For axions

$$n_a(t_0) = \frac{1.5 \cdot 10^{64}}{\text{pc}^3} \Omega_a \left(\frac{h}{0.7} \right)^2 \left(\frac{10^{-5} \text{eV}}{m_a} \right), \quad (12)$$

see Section 2.2. Likewise, for WIMPs

$$n_\chi(t_0) = \frac{1.5 \cdot 10^{50}}{\text{pc}^3} \Omega_\chi \left(\frac{h}{0.7} \right)^2 \left(\frac{\text{GeV}}{m_\chi} \right), \quad (13)$$

see Section 2.1. The large exponents indicate that the density of cold dark matter particles is enormous in terms of astronomical length scales. Since they are effectively collisionless, the particles experience only gravitational forces. These are universal and vary only on huge distances compared to the interparticle distance. Hence the sheet on which the particles lie in phase space is continuous. It cannot break and its evolution is constrained by topology. If each of the aforementioned CDM candidates is present, the phase space sheet has a layer for each species, with a thickness proportional to the corresponding velocity dispersion.

The phase space sheet is located on the 3D hypersurface of points (\vec{r}, \vec{v}) : $\vec{v} = H(t)\vec{r} + \Delta\vec{v}(\vec{r}, t)$, where $H(t) = \frac{\dot{a}}{a}$ is the Hubble expansion rate and $\Delta\vec{v}(\vec{r}, t)$ is the peculiar

velocity field. Figure 1 shows a 2D section of phase space along the (z, \dot{z}) plane. The wiggly line is the intersection of the 3D sheet on which the particles lie in phase space with the plane of the figure. The thickness of the line is the velocity dispersion δv , whereas the amplitude of the wiggles in the line is the peculiar velocity Δv . If there were no peculiar velocities, the line would be straight, since in that case $\dot{z} = H(t)z$. The peculiar

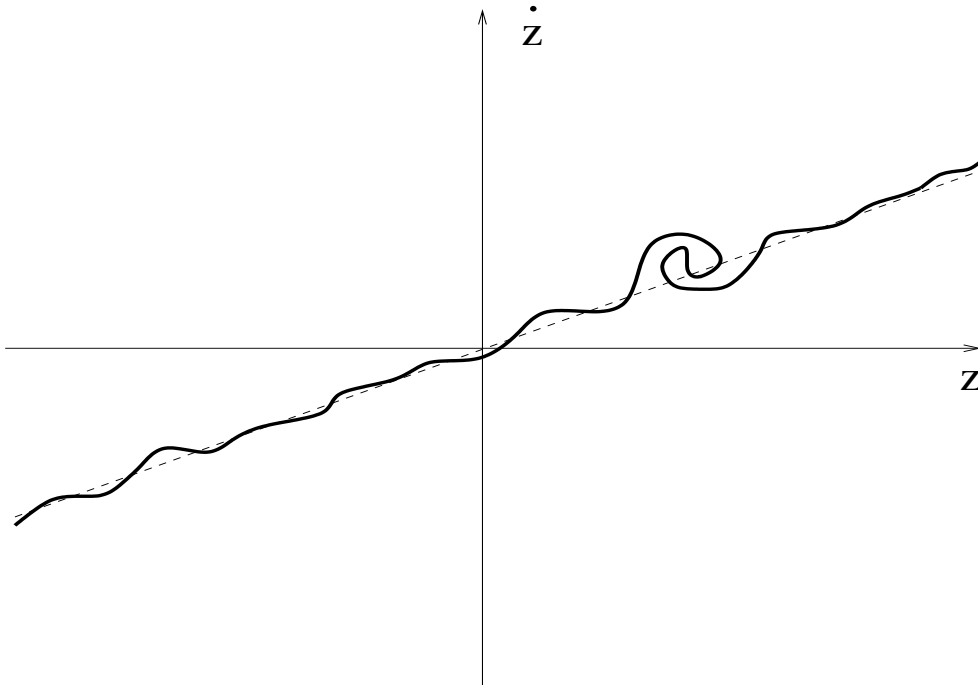


Figure 1: The wiggly line is the intersection of the (z, \dot{z}) plane with the 3D sheet on which the collisionless dark matter particles lie in phase space. The thickness of the line is the primordial velocity dispersion. The amplitude of the wiggles in the \dot{z} direction is the velocity dispersion associated with density perturbations. Where an overdensity grows in the nonlinear regime, the line winds up in clockwise fashion. One such overdensity is shown.

velocities are associated with density perturbations and grow by gravitational instability as $\Delta v \sim t^{2/3}$. On the other hand the primordial velocity dispersion decreases on average as $\delta v \sim t^{-2/3}$, consistent with Liouville’s theorem. When a large overdensity enters the nonlinear regime, the particles in the vicinity of the overdensity fall back onto it. This implies that the phase space sheet “winds up” in clockwise fashion wherever an overdensity

grows in the nonlinear regime. One such overdensity is shown in Fig. 1. Before density perturbations enter the nonlinear regime, there is only one value of velocity (i.e., a single flow) at a typical location in physical space, because the phase space sheet covers physical space only once. On the other hand, inside an overdensity in the nonlinear regime, the sheet wraps up in phase space, turning clockwise in any two dimensional cut (z, \dot{z}) of that space. The physical space coordinate axis z is in an arbitrary direction, and \dot{z} is its associated velocity. The outcome of this process in a galactic halo is an odd number of flows at any physical point in the halo [17]. One flow is associated with particles falling through the galaxy for the first time ($n = 1$); another is associated with particles falling through the galaxy for the second time ($n = 2$), and so on (Fig. 2).

At the boundary between two regions, one of which has n flows and the other $n + 2$ flows, the physical space density is very large because the phase space sheet has a fold there. At the fold, the phase space sheet is tangent to velocity space and hence, in the limit of zero velocity dispersion ($\delta v = 0$), the physical space density diverges, since it is the integral of the phase space density over velocity space. The structure associated with such a phase space fold is called a “caustic” [18, 16, 19]. Generically, caustics are surfaces in physical space, since they separate regions with differing number of flows. One side of a caustic surface has two more flows than the other. Because caustic surfaces occur wherever the number of flows changes, they are topologically stable, in direct analogy with domain walls. It is easy to show (Section 3.2) that, in the limit of zero velocity dispersion, the density diverges as $d \sim \frac{1}{\sqrt{\sigma}}$ when the caustic is approached from the side with $n + 2$ flows, where σ is the distance to the caustic. If the velocity dispersion is small, but nonzero, the divergence is cut off so that the density at the caustic is no longer infinite, but merely very large.

Zel’dovich [20] emphasized the importance of caustics in large scale structure formation, and suggested using the name “pancakes” for them. The reason galaxies tend to lie

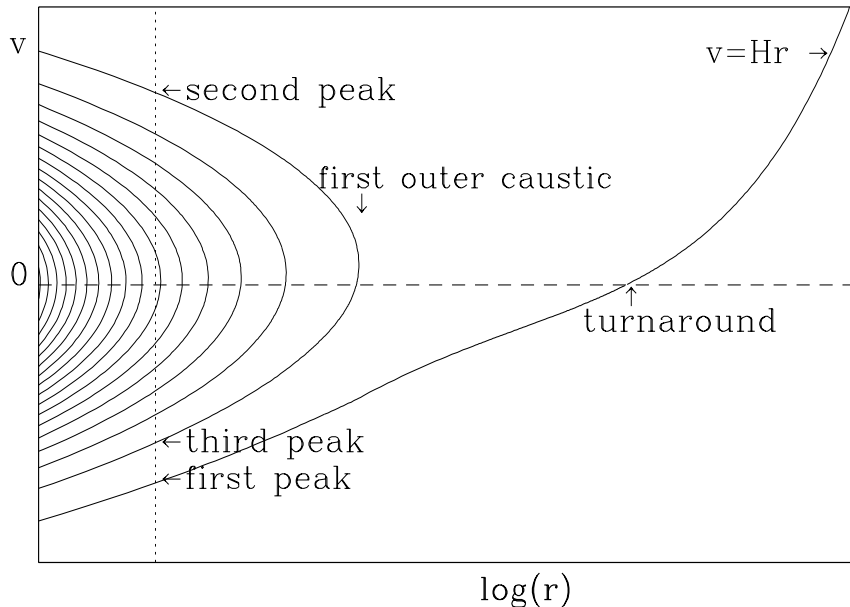


Figure 2: Snapshot of the phase space distribution of CDM particles in a galactic halo. For simplicity, spherical symmetry is assumed: r is galactocentric distance and v is radial velocity. The solid line indicates the location of the particles. The dotted line corresponds to observer position. Each intersection of the solid and dotted lines corresponds to a CDM flow at the observer’s location. “Turnaround” refers to the moments in a particle’s history when it has zero radial velocity with respect to the galactic center. A “caustic” appears wherever the phase space line folds back. Particles pile up and hence the density diverges there.

on surfaces [21] such as “the Great Wall” is undoubtedly that the 3D sheet on which the dark matter particles and baryons lie in phase space acquires folds on very large scales, producing caustics appropriately called Zel’dovich pancakes. Sikivie [16] derived the minimal CDM caustic structure that must occur in galactic halos [16]. There are two types of caustics in the halos of galaxies: inner and outer. The outer caustics are simple fold (A_2) catastrophes located on topological spheres surrounding the galaxy.

We saw above that where a localized overdensity is growing in the nonlinear regime, the line at the intersection of the phase space sheet with the (z, \dot{z}) plane winds up in a clockwise fashion. The onset of this process is shown in Fig. 1. Of course, the picture is

qualitatively the same in the (x, \dot{x}) and (y, \dot{y}) planes. In this view, the process of galactic halo formation is the winding up of the phase space sheet of collisionless dark matter particles. When the galactic center is approached from any direction, the local number of flows increases. First, there is one flow, then three flows, then five, seven. . . . The boundary between the region with one (three, five, . . .) and the region with three (five, seven, . . .) flows is the location of a caustic, which is topologically a sphere surrounding the galaxy (Fig. 2). When these caustic spheres are approached from the inside, the density diverges as $d \sim \frac{1}{\sqrt{\sigma}}$ in the zero velocity dispersion limit. Outer caustics occur where a given outflow reaches its furthest distance from the galactic center before falling back in.

The inner caustics are rings [18]. They are located near where the particles with the most angular momentum in a given inflow reach their distance of closest approach to the galactic center before going back out. In the absence of angular momentum, the caustic rings collapse to a caustic point at the center whereas the outer caustics are unaffected. A caustic ring is more precisely a closed tube with a special structure. Its transverse cross-section is a closed line with three cusps, one of which points away from the galactic center (Fig. 3). In the language of Catastrophe Theory, such a singularity is called a D_{-4} (or *elliptic umbilic*) catastrophe [16]. We call it a “tricuspl.” The existence of these caustics and their topological properties are independent of any assumptions of symmetry. Their derivations are discussed in Section 3.

Dark matter caustics have very well-defined density profiles, and hence calculable gravitational lensing signatures [22]. In this dissertation we derive these signatures in a number of specific cases. In the limit of zero velocity dispersion ($\delta v = 0$), the density diverges when one approaches a caustic surface on the side that has two extra flows, as the inverse square root of the distance to the surface. This divergence is cut off if there is velocity dispersion, because the location of the caustic surface gets smeared over some distance δx . For the dark matter caustics in galactic halos, δx and δv are related [18] by

$$\delta x \sim \frac{R \delta v}{v}, \quad (14)$$

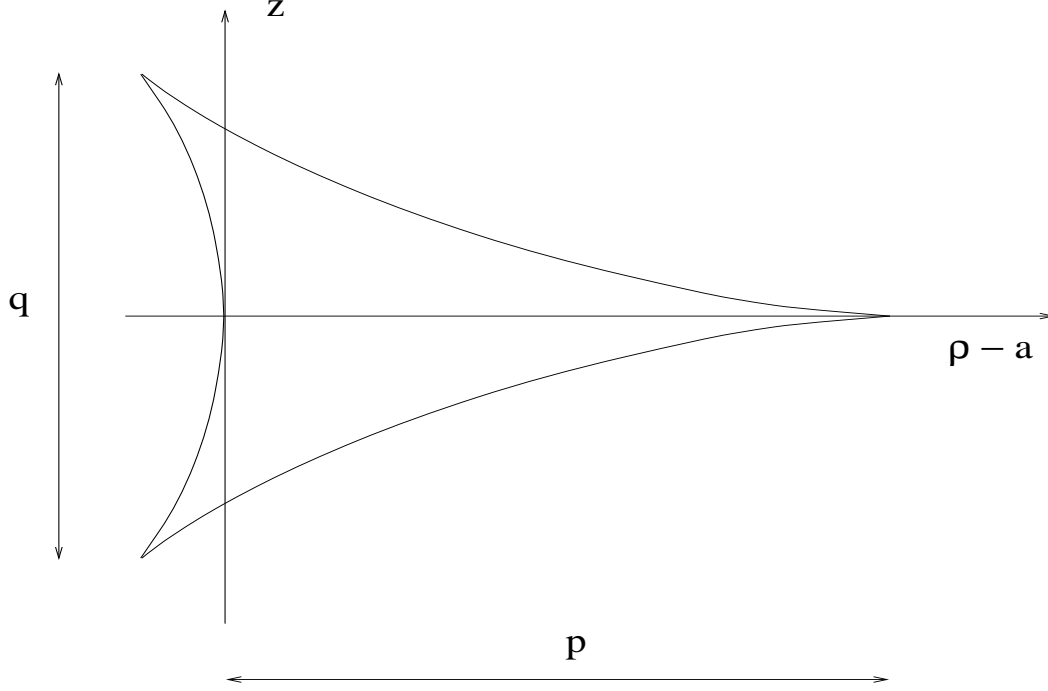


Figure 3: Cross-section of a caustic ring in the case of axial and reflection symmetry, and $p, q \ll a$.

where v is the order of magnitude of the velocity of the particles in the flow and R is the distance scale over which that flow turns around (i.e., changes its direction). For a galaxy like our own, $v = 500$ km/s and $R = 200$ kpc are typical orders of magnitude.

As mentioned earlier, the primordial velocity dispersion of the leading cold dark matter candidates is very small. Using the estimates of δv given above, one finds that axion caustics in galactic halos are typically smeared over

$$\delta x_a \sim 5 \cdot 10^9 \text{ cm} \left(\frac{10^{-5} \text{ eV}}{m_a} \right)^{4.7/5.7} \quad (15)$$

as a result of their primordial velocity dispersion; whereas WIMP caustics are smeared over

$$\delta x_\chi \sim 3 \cdot 10^{15} \text{ cm} \left(\frac{\text{GeV}}{m_\chi} \right)^{1/2} . \quad (16)$$

It should be kept in mind, however, that a cold dark matter flow may have an effective velocity dispersion that is larger than its primordial velocity dispersion. Effective velocity

dispersion occurs when the sheet on which the dark matter particles lie in phase space is wrapped up on scales that are small compared to the galaxy as a whole. It is associated with the clumpiness of the dark matter falling onto the galaxy. The effective velocity dispersion of a flow may vary from point to point, taking larger values where more small scale structure has formed; and taking the minimum primordial value where no small scale structure has formed. For a coarse-grained observer, the dark matter caustic is smeared over δx given by Eq. 14 where δv is the effective velocity dispersion of the flow.

Little is known about the size of the effective velocity dispersion of dark matter flows in galactic halos. Sikivie [23], however, interpreted a triangular feature in the IRAS map of the Milky Way as the imprint on baryonic matter of the caustic ring of dark matter nearest to us. The sharpness of the feature’s edges implies an upper limit of 20 pc on the distance δx over which that caustic is smeared; and hence an upper limit of order 50 m/s on the effective velocity dispersion of the corresponding flow.

The gravitational lensing effects of a caustic surface are largest when the line of sight is near tangent to the surface, because the contrast in column density is largest there. The effects depend on the curvature of the caustic surface at the tangent point in the direction of the line of sight: the smaller the curvature, the larger the effects. A caustic is an oriented surface because one side has two more flows than the other. We considered three cases of gravitational lensing by a smooth caustic surface. In the first case, the line of sight is near tangent to a caustic surface that curves toward the side with two extra flows. We call such a surface “concave.” In the second case, the surface is “convex,” (i.e., it curves away from the side with two extra flows). In the third case, the caustic surface has zero curvature at the tangent point (the radius of curvature is infinite), but the tangent line is entirely outside the side with two extra flows. Caustic surfaces may have cusps. The outer dark matter caustics of galactic halos are smooth topological spheres, which have no singularities, but the inner caustics of galactic halos are closed tubes whose cross-section

has three cusps. Therefore, the fourth case we consider has a line of sight near a cusp, and parallel to the plane of the cusp.

Gravitational lensing produces a map of an object surface onto an image surface. The magnification is the inverse of the Jacobian of this map. Because dark matter caustics have well-defined density profiles, it is a neat mathematical exercise to calculate their gravitational lensing characteristics. The images of extended sources may show distortions that can be unambiguously attributed to lensing by dark matter caustics in the limit of perfect observations. We see that in three of the cases considered, a point source can have multiple images. In those cases when two images merge, the Jacobian of the map vanishes and the magnification diverges. So, at least in theory, it seems that gravitational lensing is a very attractive tool for investigating dark matter caustics. Observation of the calculated lensing signatures would give direct evidence for caustics and CDM.

We have been particularly motivated by the possibility [22] that the observer might be able to distinguish between axions and WIMPs by determining the distance over which the caustics are smeared. The nearby caustic, whose position is revealed [23] by a triangular feature in the IRAS map of the Milky Way plane, is only 1 kpc away from us in the direction of observation. By observing the gravitational lensing due to that caustic, one may be able to measure δx as small as 10^{13} cm, assuming an angular resolution of $3 \cdot 10^{-9}$ radians. If δx turned out to be that small, the WIMP dark matter hypothesis would be severely challenged (Eq. 16).

Unfortunately, as shown below, the gravitational lensing due to a caustic only a kpc away from us is too weak to be observed with current instruments. It is well known that gravitational lensing effects are proportional to $\frac{D_L D_{LS}}{D_S}$ where D_S, D_L and D_{LS} are respectively the distances from the observer to the source, from the observer to the lens, and from the lens to the source. We see below that, for the gravitational lensing effects of dark matter caustics to be observable using the current technology, the lenses and sources

must be as far away as possible (at the cosmological distances of order Gpc). Even then, the observation of such effects will be difficult. Unfortunately, at Gpc distances it is not possible to measure δx as small as Eqs. 15 and 16 with foreseeable technology. So, it seems unlikely that one will be able to distinguish between dark matter candidates on the basis of the gravitational lensing characteristics of the caustics they form. Henceforth, unless otherwise stated, the velocity dispersion is set equal to zero.

The outline of this dissertation is as follows. Section 2 is devoted to the review of the main CDM candidates. In Sections 2.1 and 2.2 we study the WIMPs and axions, respectively. Each candidate's status in particle physics and production mechanism in the early universe are discussed. Calculations show that their velocity dispersions are negligible. In Section 3, we study the caustics associated with the infall of collisionless dark matter particles onto a galaxy. In Section 3.1 a general discussion of caustics is given. Caustic surfaces are introduced in Section 3.2. We prove the existence of CDM caustics and classify them as *outer* and *inner*. We show that the outer caustics are topological spheres and the inner caustics are rings with three cusps. We find $n + 2$ flows (where n is always odd) inside an outer caustic; and n -flows outside. Estimates of the radii and fold coefficients of the outer caustics (based on the self similar infall model) are given in Section 3.4.2. We find $n + 4$ flows inside the caustic rings; and $n + 2$ outside. In Section 3.5.2, we give a detailed analysis of the caustic rings under the additional assumptions that the flow is axially and reflection symmetric; and that the transverse dimensions of the ring, p and q , are small compared to the ring radius a . In Section 3.5.3, we show that under these assumptions, the flow near the ring is described in terms of five parameters: a , b , τ_0 , u and s . We study the differential geometry of the ring surfaces produced by this flow in Section 3.5.4. We conclude the section by estimating the density profiles of the caustic rings, using the self-similar infall model.

In Section 4.1, the general formalism of gravitational lensing is reviewed. We show how the calculations can be streamlined for the case of gravitational lensing by dark matter

caustics. In Section 4.2, we calculate the gravitational lensing properties of dark matter caustics in the four cases mentioned above. In Section 5, we summarize our conclusions.

2 Cold Dark Matter Candidates

2.1 Weakly Interacting Massive Particles (WIMPs)

WIMPs is an acronym for weakly interacting massive particles. In this section we derive some properties of WIMPs, in particular their velocity dispersion, $\delta_\chi \equiv \sqrt{\langle v_\chi^2 \rangle}$, where $\langle \rangle$ indicates averaging, and χ denotes a WIMP. First, we briefly introduce some relevant concepts and calculational tools[14, 24, 25, 26].

The key to understanding thermodynamics in an expanding universe is the comparison of the particle interaction rates and the expansion rate of the universe [14]. The interaction rate per particle of a species is defined as

$$\Gamma_{\text{int}}(t) \equiv n \langle \sigma_{\text{int}} |\vec{v}| \rangle(t) \quad (17)$$

where $n(t)$ is the number density of target particles, \vec{v} is the relative velocity, and σ_{int} is the interaction cross-section. Since σ_{int} is a function of energy and interacting particles have random thermal velocities, averaging of the combination $\sigma_{\text{int}} |\vec{v}|$ is necessary. The expansion rate of the universe is given by $H(t) \equiv \dot{R}(t)/R(t)$, where $R(t)$ is the scale factor of the comoving coordinates. Since in the relativistic regime, $n(t)$ scales as $R^{-3}(t)$, and $\langle \sigma_{\text{int}} \vec{v} \rangle$ is typically a declining function of energy, $\Gamma_{\text{int}}(t)$ decreases at least as fast as $R^{-3} \sim t^{-3/2}$. In the non-relativistic regime, $n(t)$ and hence $\Gamma_{\text{int}}(t)$ decreases exponentially. The $H(t)$, on the other hand, changes in time as t^{-1} in both regimes. Thus, $\Gamma_{\text{int}}(t)/H(t) \rightarrow \infty$, as $t \rightarrow 0$. In time, crossover between $\Gamma_{\text{int}}(t)$ and $H(t)$ is unavoidable. This means that there is a certain time t_D , called decoupling time, such that $\Gamma_{\text{int}}(t_D) \simeq H(t_D)$. After t_D , a particle species effectively stops interacting with the rest of the matter; and its distribution evolves independently.

Next let us consider WIMPs in particular. We assume that they carry a quantum number, like R parity in the case of the lightest supersymmetric partner (LSP), that keeps

them stable. Thus, the number of WIMPs per comoving volume can only change via annihilation processes mediated by Z^0 , such as the two-body final state annihilations:

$$\chi\bar{\chi} \leftrightarrow X\bar{X} \quad (18)$$

where X denotes particle species (like ν , e^- , μ^- , π^- , u , d , s , etc.). A bar indicates the anti-particle. We represent the average annihilation cross-section summed over all annihilation channels (not only the two-body final state annihilations) by $\langle\sigma_{\text{ann}}|\vec{v}|\rangle$. Let us also assume that there is no particle number asymmetry between χ 's and $\bar{\chi}$'s, or that it is negligible. When T drops below m_χ , the χ particles become nonrelativistic and their energy density $\rho_\chi \simeq m_\chi n_\chi$ is Boltzmann suppressed as long as it is in thermal equilibrium. Their number density is given by

$$n_\chi \simeq g_\chi \left(\frac{m_\chi T}{2\pi}\right)^{3/2} \exp(-m_\chi/T) \quad (19)$$

where $T(t)$ is the temperature and g_χ is the number of internal degrees of freedom of the χ 's (such as spin, color, etc.). The number of internal degrees of freedom g_i of a species, in general, is an important quantity in the calculations (because each adds independently to the number and energy densities, pressure, etc.). For example, photons have two polarization states, hence $g_\gamma = 2$; neutrinos have only one polarization state, therefore $g_\nu = 1$; and electrons and muons have $g_{e^-, \mu} = 2$, since they have two spin states. Internal degrees of freedom of the antiparticles are counted independently; and their number is the same as for the particles. It is clear from Eq. 19 that if a massive species remained in thermal equilibrium until the present, its abundance would be negligible. On the other hand, if the annihilations of the species stop at a temperature $T_F = T(t_F)$, called the freeze-out temperature, n_χ would decrease only as R^{-3} after t_F , exceeding its equilibrium value. Such particles could have a significant relic abundance even today.

Using Eqs. 17 and 19, the annihilation rate of χ can be written as

$$\Gamma_{\text{ann}} \simeq g_\chi \left(\frac{m_\chi T}{2\pi}\right)^{3/2} \exp(-m_\chi/T) \langle\sigma_{\text{ann}}|\vec{v}|\rangle. \quad (20)$$

The average of $\sigma_{\text{ann}}|\vec{v}|$ for the annihilation reactions is given [14] as

$$\langle\sigma_{\text{ann}}|\vec{v}|\rangle \equiv \sigma_0 \left(\frac{T}{m_\chi}\right)^n, \quad (21)$$

(where $n = 0$ for s-wave annihilation, $n = 1$ for p-wave annihilation, etc.). The σ_0 for a WIMP with mass in the range $T \leq m_\chi \leq m_{Z^0}$ is

$$\sigma_0 \simeq \frac{c}{2\pi} G_F^2 m_\chi^2, \quad (22)$$

where G_F is the Fermi constant. The value c depends on the number of annihilation channels and whether $\bar{\chi}$ is distinct from χ (Dirac-type) or not (Majorana-type). Eqs. 20-22 yield

$$\Gamma_{\text{ann}}(T) \simeq \frac{c G_F}{(2\pi)^{5/2}} g_\chi \left(\frac{m_\chi}{T}\right)^{1/2-n} T^2 m_\chi^3 \exp(-m_\chi/T). \quad (23)$$

The Hubble parameter $H(T)$ can be determined from the Friedmann equation for the early universe:

$$H^2(t) = \frac{8\pi G}{3} \rho(t), \quad (24)$$

where G is the Newton's constant and $\rho(t)$ is the total energy density. Since the energy density of a nonrelativistic species in thermal equilibrium is exponentially suppressed compared to that of a relativistic species (assuming for the moment that no other species is out of equilibrium), summing only the energy densities of the relativistic particles in thermal equilibrium at a given temperature is sufficient. Hence, the energy density has the form of the Stefan-Boltzmann law:

$$\rho(T) \simeq \frac{\pi^2}{30} g_{\text{eff}}(T) T^4. \quad (25)$$

Here we introduce the effective degeneracy factor $g_{\text{eff}}(T)$, which counts the total number of internal degrees of freedom of the particles that are relativistic and in thermal equilibrium at temperature T (particle species whose mass $m_i \ll T$). The expression for $g_{\text{eff}}(T)$ also contains the factor $7/8$ for fermions relative to bosons. It is useful to calculate $g_{\text{eff}}(T)$ for a temperature (say, 1 TeV) at which all the particles of the Standard Model were

relativistic and in thermal equilibrium. The total number of internal degrees of freedom of the gauge and Higgs bosons is 28 (the Higgs boson is spinless, hence it has just one spin state. The W^\pm and Z^0 bosons are massive spin $s = 1$ particles, hence each have $2s + 1 = 3$ spin states. The photon and each of the eight gluons are massless spin 1 particles, therefore each has 2 helicity states: $+1$ and -1 . If we add them up, the total number of bosonic degrees of freedom is $9 \cdot 2 + 3 \cdot 3 + 1 = 28$) and for fermions it is 90. (Each of the six quarks comes in 3 colors and 2 spins. Each of the three charged leptons has two spin states. Each of the three neutrinos has one helicity state. Therefore, the total fermionic particle degeneracy is $6 \cdot 6 + 3 \cdot 2 + 3 \cdot 1 = 45$. Because of the anti-particles, the total fermionic degeneracy doubles, hence $2 \cdot 45 = 90$). Thus,

$$g_{\text{eff}}(T = 1\text{TeV}) = 28 + \frac{7}{8} \cdot 90 = 106.75 \quad . \quad (26)$$

For some species of particles, as happens for neutrinos, the interaction rate becomes smaller than the expansion rate. Those particles will have lower equilibrium temperatures than the photons (see below), but will still remain relativistic. To allow this possibility, we introduce a specific temperature T_i for each kind of relativistic particle and define the total number of effective degrees of freedom as

$$g_{\text{eff}}(T) \equiv \sum_{i=\text{boson}} g_i \left(\frac{T_i}{T} \right)^4 + \frac{7}{8} \sum_{j=\text{fermion}} g_j \left(\frac{T_j}{T} \right)^4 \quad . \quad (27)$$

A useful formula can immediately be obtained by inserting Eq. 25 into the Friedmann equation (Eq. 24)

$$H^2 = \frac{8\pi G}{3} \frac{\pi^2}{30} g_{\text{eff}} T^4 = 2.76 \frac{g_{\text{eff}} T^4}{m_{\text{Pl}}^2} \quad (28)$$

where G is given as the inverse square of the Planck mass $\equiv m_{\text{Pl}}$, or

$$H = \frac{1.66}{m_{\text{Pl}}} \sqrt{g_{\text{eff}}} T^2 \quad . \quad (29)$$

Since the scale factor $R(t) \sim \sqrt{t}$ in the era of radiation domination, $H(t) = \dot{R}/R = 1/(2t)$. Thus, we find the time-temperature relation in the radiation domination:

$$t = 0.3 \frac{m_{\text{Pl}}}{\sqrt{g_{\text{eff}}} T^2}. \quad (30)$$

This formula is valid at temperatures around 1 MeV, where most of nucleosynthesis and neutrino decoupling occurred.

Annihilations effectively stop at temperature $T_F = T(t_F)$ when the ratio of the rates $\Gamma(T_F)/H(T_F) \sim 1$. Then, Eqs. 23-25 yield

$$\frac{\Gamma(T_F)}{H(T_F)} \simeq \frac{c\sqrt{90}}{(2\pi)^4} \frac{G_F^2}{\sqrt{G}} \frac{g_\chi}{\sqrt{g_{\text{eff}}}} \left(\frac{m_\chi T}{2\pi}\right)^{1/2-n} m_\chi^3 \exp(-m_\chi/T) \sim 1. \quad (31)$$

If the χ 's are Dirac-type particles, $c \simeq 5$ and $n = 0$. Taking $g_\chi = 2$ and $g_{\text{eff}} \simeq 60$, the logarithm of Eq. 31 yields

$$\frac{m_\chi}{T_F} \simeq 16.4 + \frac{1}{2} \ln\left(\frac{m_\chi}{T_F}\right) + 3 \ln\left(\frac{m_\chi}{\text{GeV}}\right). \quad (32)$$

In this equation, to leading order, $m_\chi/T_F \sim 16.4$. Iterating in this order, the logarithmic term corrects the result as

$$\frac{m_\chi}{T_F} \simeq 17.8 + 3 \ln\left(\frac{m_\chi}{\text{GeV}}\right). \quad (33)$$

Although $n_\chi R^3$ freezes out at $T_F \sim m_\chi/20$, the energy distribution of the WIMPs is kept thermalized by collisions with ν, e , etc. (e.g. , $\nu + \chi \rightarrow \nu + \chi$), down to the decoupling temperature $T_D \sim \text{MeV}$ where all the WIMP interactions effectively stop and WIMPs stream freely. Neutrino decoupling takes place also at this temperature. To see that the decoupling temperature of neutrinos is indeed around an MeV, consider, for example, the interactions between relativistic charged leptons and neutrinos. A typical process maintaining thermal equilibrium, such as $\nu_e^- + e^+ \rightarrow \nu_\mu + \mu^+$ mediated by W^+ , has a weak interaction cross-section:

$$\sigma_{\text{weak}} \sim \frac{\alpha^2 s}{(s - m_W^2)^2} \sim \frac{\alpha^2 s}{m_W^4}, \quad (34)$$

where s is the square of the total four momenta of the incoming or outgoing particles (which is also equal to the square of the total energy in the center of momentum frame), m_W is the mass of the W^+ boson and $\alpha = 1/137$. Since s is of order the energy squared of the reacting particles, and average energy is proportional to T , the cross-section can be expressed as

$$\sigma_{\text{weak}} \sim \frac{\alpha^2 T^2}{m_W^4}. \quad (35)$$

The interaction rate $\Gamma_{\text{weak}} = n \langle \sigma_{\text{weak}} |\vec{v}| \rangle$ is thus

$$\Gamma_{\text{weak}} \sim \frac{\alpha^2 T^5}{m_W^4}, \quad (36)$$

where we have used $|\vec{v}| = c = 1$ and the number density for a relativistic fermion species $n_i = \frac{3}{4} \left(\frac{\zeta(3)}{\pi^2} g_i T^3 \right) \sim T^3$. Comparing the above rate with the Hubble expansion rate $H \sim T^2/m_{\text{Pl}}$ (using Eq. 29), we have

$$\frac{\Gamma_{\text{weak}}}{H} \sim \frac{\alpha^2 T^3 m_{\text{Pl}}}{m_W^4}. \quad (37)$$

The decoupling occurs when the above ratio drops below unity, implying

$$T_D \sim \left(\frac{m_W^4}{\alpha^2 m_{\text{Pl}}} \right)^{\frac{1}{3}} \sim 4 \text{ MeV}. \quad (38)$$

Turning back to the case of WIMPs, being non-relativistic at t_D , the χ s satisfy

$$\frac{1}{2} m_\chi \langle v_\chi^2 \rangle_{T_D} = \frac{3}{2} T_D. \quad (39)$$

Therefore the velocity dispersion of the WIMPs at t_D is

$$\delta v_\chi(T_D) = \sqrt{\langle v_\chi^2 \rangle_{T_D}} = \sqrt{\frac{3T_D}{m_\chi}}. \quad (40)$$

For any free particle moving in an expanding universe, momentum decreases in inverse proportion to the scale factor: $p(T) = p(T_D) (R(T_D)/R(T))$. The velocity dispersion of the WIMPs as a function of time is therefore

$$\delta v_\chi(t) = \sqrt{\frac{3T_D}{m_\chi}} \frac{R(t_D)}{R(t)}. \quad (41)$$

The ratio $R(t_D)/R(t)$ can be determined using conservation of entropy, which implies $T \sim 1/R$ (see below). For a numerical estimate of the ratio today, depending on the decoupling era of χ s, we can either use the present temperature of the CMBR photons $T_{0\gamma}$ or the temperature of the relic neutrinos $T_{0\nu}$. The latter can be calculated from $T_{0\gamma}$. The difference between $T_{0\gamma}$ and $T_{0\nu}$ is due to the early decoupling of neutrinos and the subsequent annihilation of electron-positron pairs: $e^-e^+ \rightarrow \gamma\gamma$ near $T = 1$ MeV. To understand this so called “reheating” effect of photons, we recall that the expansion of the universe is adiabatic, and hence the entropy of particles in thermal equilibrium $S(T) = R^3(T) (\rho(T) + p(T)) / T$ is conserved. Using the relativistic expressions for the energy density $\rho(T) = \pi^2 g_{\text{eff}}^* T^4 / 30$ and the pressure $p(T) = \rho(T) / 3$, the entropy can be written as $S(T) = 2\pi^2 g_{\text{eff}}^* (R(T)T)^3 / 45$. Here we define

$$g_{\text{eff}}^* \equiv \sum_{i=\text{bos}} g_i \left(\frac{T_i}{T} \right)^3 + \frac{7}{8} \sum_{j=\text{fer}} g_j \left(\frac{T_j}{T} \right)^3 . \quad (42)$$

Thus,

$$g_{\text{eff}}^* (R(T)T)^3 = C \quad (43)$$

is a conserved quantity. After decoupling, neutrinos move freely. They remain in a thermal Fermi-Dirac distribution with a temperature $T_\nu = T_D R(T_D) / R(T) = K R^{-1}(T)$ provided $T_\nu \gg m_\nu$, and their entropy $S_\nu(T)$ is separately conserved. If we consider the rest of the particles in thermal equilibrium, using Eq. 43, we calculate their temperature as $T = (C / g_{\text{eff}}^*)^{1/3} R^{-1}(T)$. Since at the time of decoupling, photons, neutrinos, and the rest of the matter had the same temperature, $(C / g_{\text{eff}}^*(T_D))^{1/3} = K$. Thus, in spite of the decoupling of neutrinos, as long as g_{eff} does not change they all continue to have the same temperature. However g_{eff} changes when the temperature of the universe falls below $T \simeq m_e$. Below this temperature, the mean energy of photons is not sufficient to create e^-e^+ pairs. Hence annihilations $e^-e^+ \rightarrow \gamma\gamma$ exhaust the e^-e^+ pairs. Therefore, for $T_D > T \geq m_e$, photons ($g_\gamma = 2$) are in equilibrium with electrons ($g_{e^-} = 2$) and positrons

($g_{e^+} = 2$) giving $g_{\text{eff}}^* = 2 + (7/8) \cdot 4 = 11/2$. For $T \ll m_e$, however, only photons are relativistic, giving $g_{\text{eff}}^* = 2$. If we apply the conservation of entropy Eq. 43 to the particles which are in equilibrium with radiation before and after e^-e^+ annihilation, we find

$$\frac{(R(T)T_\gamma)_{T \ll m_e}^3}{(R(T)T_\gamma)_{T \geq m_e}^3} = \frac{(g_{\text{eff}}^*)_{T \geq m_e}}{(g_{\text{eff}}^*)_{T \ll m_e}} = \frac{11}{4}. \quad (44)$$

Just before e^-e^+ annihilation, neutrinos (although they were decoupled) had the same temperature as photons:

$$(R(T)T_\nu)_{T \geq m_e} = (R(T)T_\gamma)_{T \geq m_e} = K. \quad (45)$$

Using the above equation in Eq. 44, we obtain

$$\begin{aligned} (R(T)T_\gamma)_{T \ll m_e} &= \left(\frac{11}{4}\right)^{1/3} (R(T)T_\nu)_{T \geq m_e} \\ &= \left(\frac{11}{4}\right)^{1/3} (R(T)T_\nu)_{T \ll m_e}. \end{aligned} \quad (46)$$

In the last equation the constancy of $(R(T)T_\nu)$ is used. After e^-e^+ annihilation, g_{eff}^* does not change any more. Therefore, the relation

$$T_\nu = \left(\frac{4}{11}\right)^{1/3} T_\gamma \quad (47)$$

remains valid even today.

Now, let's turn back to the estimation of the velocity dispersion given in Eq. 41. If χ s decouple before $T \geq m_e$, they are not affected by the reheating. Therefore,

$$\delta v_\chi = \sqrt{\frac{3T_D}{m_\chi}} \frac{T_\nu}{T_D}. \quad (48)$$

Let us estimate the present value of the above δv_χ numerically. We take $T_D \sim 1\text{MeV}$ and $m_\chi \sim 100\text{GeV}$. Since the present value of $T_\gamma = 2.725\text{K} = 2.348 \cdot 10^{-13}\text{GeV}$, using Eq. 47 we find $T_\nu = 1.945\text{K} = 1.676 \cdot 10^{-13}\text{GeV}$. Thus, from Eq. 48, we obtain the present value of the velocity dispersion as

$$\delta v_\chi(t_0) = 9.180 \cdot 10^{-12} \sqrt{\frac{1\text{GeV}}{m_\chi}} \sqrt{\frac{1\text{MeV}}{T_D}}, \quad (49)$$

where t_0 denotes the present age of the universe. To insert the time dependence of δ_χ back, using Eq. 41, we write

$$\delta v_\chi(t) = \sqrt{\frac{3T_D}{m_\chi} \frac{R(t_D)}{R(t)}} = \sqrt{\frac{3T_D}{m_\chi} \frac{R(t_D)}{R(t_0)} \frac{R(t_0)}{R(t)}}. \quad (50)$$

Because $\sqrt{\frac{3T_D}{m_\chi} \frac{R(t_D)}{R(t_0)}}$ is the present value of the velocity dispersion $\delta v_\chi(t_0)$ estimated in Eq. 49 and $R(t) \sim t^{\frac{2}{3}}$ in the era of matter domination, we have

$$\begin{aligned} \delta v_\chi(t) &= \delta v_\chi(t_0) \frac{R(t_0)}{R(t)} = \delta v_\chi(t_0) \left(\frac{t_0}{t}\right)^{\frac{2}{3}} = 9.180 \cdot 10^{-12} \sqrt{\frac{1\text{GeV}}{m_\chi}} \sqrt{\frac{1\text{MeV}}{T_D}} \left(\frac{t_0}{t}\right)^{\frac{2}{3}} \\ &\simeq 10^{-11} \left(\frac{\text{GeV}}{m_\chi}\right)^{\frac{1}{2}} \left(\frac{\text{MeV}}{T_D}\right)^{\frac{1}{2}} \left(\frac{t_0}{t}\right)^{\frac{2}{3}}. \end{aligned} \quad (51)$$

If on the other hand, χ s decouple after $T \simeq m_e$, they benefit from the reheating caused by e^+e^- annihilation, and

$$\delta v_\chi = \sqrt{\frac{3T_D}{m_\chi} \frac{T_\gamma}{T_D}}. \quad (52)$$

Then, in this case,

$$\delta v_\chi(t) = 1.286 \cdot 10^{-11} \sqrt{\frac{1\text{GeV}}{m_\chi}} \sqrt{\frac{1\text{MeV}}{T_D}} \left(\frac{t_0}{t}\right)^{\frac{2}{3}}, \quad (53)$$

which is not very different from the value obtained in Eq. 51.

The present average WIMP number density $n_\chi(t_0)$ can be expressed in terms of $\Omega_\chi \equiv \frac{\rho_\chi(t_0)}{\rho_c(t_0)}$, which is the present WIMP energy density in units of the critical density ρ_c :

$$n_\chi(t_0) = \frac{\rho_\chi(t_0)}{m_\chi} = \frac{\rho_c(t_0)\Omega_\chi}{m_\chi}. \quad (54)$$

Recall that the Friedmann equation for a flat universe is

$$H^2(t_0) = \frac{8\pi G}{3} \rho_c(t_0), \quad (55)$$

where $H(t_0) \equiv \frac{\dot{R}(t_0)}{R(t_0)}$ is the present Hubble expansion rate of the universe. Therefore the present critical density is

$$\rho_c(t_0) = 8.1 \cdot 10^{-11} h^2 (\text{eV})^4 = 4.85 \cdot 10^{82} \frac{h^2}{(\text{pc})^4}, \quad (56)$$

where we used $H(t_0) = h 100 \frac{\text{km}}{\text{s} \cdot \text{Mpc}} = h 3.34 \cdot 10^{-10} \frac{1}{\text{pc}}$. Using Eqs. 54, 56 and the conversion $\text{eV} = 1.564 \cdot 10^{23} \frac{1}{\text{pc}}$ we find

$$n_\chi(t_0) = \frac{1.5 \cdot 10^{50}}{\text{pc}^3} \Omega_\chi \left(\frac{h}{0.7} \right)^2 \left(\frac{\text{GeV}}{m_\chi} \right). \quad (57)$$

We next discuss another leading species of cold dark matter candidates, namely axions.

2.2 Axions

Axions have been postulated to solve the strong CP problem of Quantum Chromodynamics (QCD). QCD is the theory of strong interactions. It is a gauge theory on the gauge group $SU(3)$ of “color.” Its dynamical variables are a color octet of gauge fields A_μ^a , called gluons, and a family of color triplet spinor fields q_f , called quarks. The flavour index f , labels the various triplets. A_μ^a is analogous to the vector potential of electrodynamics. Here, in addition to the spacetime index μ , the gauge field carries the $SU(3)$ group index a . In an analogy with Quantum Electrodynamics (QED), the action for the gauge sector is at first taken to be

$$\mathcal{L}_{\text{gauge}} = -\frac{1}{4} \int d^4x G^{a\mu\nu} G_{\mu\nu}^a \quad (58)$$

where

$$G_{\mu\nu}^a = \partial_\mu A_\nu^a - \partial_\nu A_\mu^a + g f^{abc} A_\mu^b A_\nu^c \quad (59)$$

is the gluon field strength tensor, g is the gauge coupling, and f^{abc} are the structure constants of the $SU(3)$ algebra: $[T^a, T^b] = i f^{abc} T^c$. The analogy between QCD and QED, however, fails where the vacuum structure of the theories is concerned. In both theories, the

vacuum configuration of the theory is characterized by the vanishing of the field strength tensor $F_{\mu\nu}$. In QED, however, all the vector potentials which yield $F_{\mu\nu} = 0$, are related to each other by a gauge transformation. For any vacuum configuration, A_μ can be made to vanish by a gauge transformation; see the Appendix. Thus the QED vacuum is unique. In QCD, on the other hand, not all solutions of $G_{\mu\nu}^a = 0$ are related to each other by a gauge transformation. These physically distinct vacuum states can be classified by the set of integers, n , and hence the most general ground state $|\Theta\rangle$, called Θ -vacuum, can be expressed as a superposition of all the degenerate states $|n\rangle$:

$$|\Theta\rangle = \sum_{n=-\infty}^{\infty} \exp(-in\Theta)|n\rangle, \quad (60)$$

where the extra parameter Θ has period 2π , and needs to be measured; see the Appendix. The effects of the Θ -vacuum can be included in the Lagrangian density of QCD by the addition of a topological term

$$\mathcal{L}_\Theta = -\frac{g^2\Theta}{32\pi^2} G^{a\mu\nu*} G_{\mu\nu}^a = \partial_\mu K_\mu, \quad (61)$$

where (Eq. 480)

$$K_\mu \equiv -\epsilon_{\mu\nu\rho\sigma} \text{Tr}(A_\nu \partial_\rho A_\sigma - i\frac{2g}{3} A_\nu A_\rho A_\sigma). \quad (62)$$

Such a term affects neither the equations of motion nor the perturbative aspects of the theory (Feynman rule for the vertex associated with a four-divergence would necessarily have a multiplicative factor of the sum of the momenta at the vertex which vanishes automatically due to momentum conservation). Therefore, the existence of the Θ -term in a Lagrangian does not necessarily mean that physics depends on it. As remarked in the above, Classical Electrodynamics and perturbative QED are unaffected by the presence of such a term in their Lagrangians. In QED, if there are non-perturbative effects, they are absolutely negligible. This is because, the essential structure of a non-perturbative effect can be represented by $e^{-\frac{1}{\alpha_e}}$, which vanishes as the coupling constant $\alpha_e \rightarrow 0$ (when

the interaction is turned-off) and can not be expanded in a Taylor series in α_e . Since $\alpha_e = 1/137$, the Θ -dependence would be highly suppressed. Non-perturbative effects, however, produce Θ -dependence in QCD. These effects must be present in the theory, otherwise QCD would not produce the phenomenology at low energies.

To illustrate the claim given in Eq. 61, we evaluate the vacuum to vacuum transition amplitude in the $SU(3)$ gauge theory:

$$\langle \Theta' | e^{-iHt} | \Theta \rangle = \sum_{m,s} e^{im\Theta'} e^{is\Theta} \langle m | e^{-iHt} | s \rangle . \quad (63)$$

Recall that the expectation value $\langle m | e^{-iHt} | s \rangle$ can be written as the path integral over all $[A_\mu^a]_{s-m}$ that connects the m th vacuum with the s th vacuum:

$$\langle m | e^{-iHt} | s \rangle = \int [DA_\mu]_{s-m} \exp(-i \int \mathcal{L}_{\text{gauge}} d^4x) . \quad (64)$$

Then Eq. 63 becomes

$$\begin{aligned} \langle \Theta' | e^{-iHt} | \Theta \rangle &= \sum_{s,m} e^{-i(s-m)\Theta} e^{im(\Theta' - \Theta)} \int [DA_\mu]_{s-m} \exp(-i \int \mathcal{L}_{\text{gauge}} d^4x) \\ &= \delta(\Theta - \Theta') \sum_n e^{in\Theta} \int [DA_\mu]_n e^{-i \int d^4x \mathcal{L}_{\text{gauge}}} , \end{aligned} \quad (65)$$

where the delta function is obtained by summing over m , after s was replaced by $n = s - m$. The phase factor $e^{in\Theta}$ can be absorbed into the action using

$$n = \frac{g^2}{32\pi^2} \int d^4x G^{a\mu\nu*} G_{\mu\nu}^a , \quad (66)$$

where g is the strong coupling constant and $*G^{a\mu\nu} = \frac{1}{2}\epsilon^{\mu\nu\lambda\rho} G^{a\lambda\rho}$ is the dual field strength tensor. Therefore, the effective QCD Lagrange density is the sum of

$$\mathcal{L}_\Theta = -n\Theta = -\frac{\Theta g^2}{32\pi^2} \int d^4x G^{a\mu\nu*} G_{\mu\nu}^a , \quad (67)$$

$\mathcal{L}_{\text{gauge}}$ and the Dirac Lagrangian density for the quark fields:

$$\mathcal{L}_{QCD} = \sum_f \left[\bar{q}_f i \not{D} q_f - (m_f q_{Lf}^\dagger q_{Rf} + h.c.) \right] - \frac{1}{4} G^{a\mu\nu} G_{\mu\nu}^a - \frac{\Theta g^2}{32\pi^2} G^{a\mu\nu*} G_{\mu\nu}^a , \quad (68)$$

where we define $\not{D} \equiv \gamma^\mu D_\mu = \gamma^\mu (\partial_\mu - igA_\mu^a T^a)$, $q_{Lf} \equiv (1/2)(1 - \gamma_5)q_f$ and $q_{Rf} \equiv (1/2)(1 + \gamma_5)q_f$. The scale dependence of the strong coupling constant g is given at one loop by

$$\alpha_s(\mu) \equiv \frac{g^2(\mu)}{4\pi} = \frac{2\pi}{(11 - \frac{2}{3}n_f) \ln(\frac{\mu}{\Lambda_f})}, \quad (69)$$

where n_f is the number of quark flavors with mass less μ and Λ_f is the appropriate QCD scale. The m_f denote the quark masses. They originate in the electroweak sector of the Standard Model which must violate CP to explain $K_L \rightarrow 2\pi$. Hence, m_f are complex numbers in general.

In the Standard Model, the Θ term receives a contribution due to electroweak effects involving the m_f . To see the reason, consider the effect in the path integral

$$Z[\eta, \bar{\eta}, j_\mu] = \int [Dq][D\bar{q}][DA] \exp \left(i \int d^4x [\mathcal{L}_{QCD} + \bar{q}\eta + \bar{\eta}q + j_\mu A^\mu] \right), \quad (70)$$

of a redefinition of all the quark fields

$$q_f \rightarrow q'_f = \exp(i\beta_f \gamma_5) q_f, \quad (71)$$

where α_f are a set of real phases. Recall that $\{\gamma_\mu, \gamma_5\} = 0$, $\gamma_5^\dagger = \gamma_5 = \gamma_5^{-1}$ and $\gamma_5 \gamma_\mu = -\gamma_\mu \gamma_5$. Therefore,

$$\begin{aligned} \exp(i\beta_f(x)\gamma_5)\gamma_\mu &= \sum_{n=0}^{\infty} \frac{(i\beta_f(x))^n}{n!} \gamma_5^n \gamma_\mu = \gamma_\mu \sum_{n=0}^{\infty} \frac{(i\beta_f(x))^n}{n!} (-1)^n \gamma_5^n \\ &= \gamma_\mu \exp(-i\beta_f(x)\gamma_5), \end{aligned} \quad (72)$$

hence,

$$\begin{aligned} \bar{q}'_f(x) &= q_f^\dagger(x) \gamma^0 = (e^{i\beta_f(x)\gamma_5} q_f(x))^\dagger \gamma^0 = q_f^\dagger(x) e^{-i\beta_f(x)\gamma_5^\dagger} \gamma^0 \\ &= q_f^\dagger(x) \gamma^0 e^{i\beta_f(x)\gamma_5} = \bar{q}_f(x) e^{i\beta_f(x)\gamma_5}. \end{aligned} \quad (73)$$

The transformations of the terms in the exponent of Eq. 70 can then be calculated easily:

$$\bar{q}'_f i \gamma_\mu \partial^\mu q'_f = \bar{q}_f e^{i\beta_f(x)\gamma_5} i \gamma_\mu \partial^\mu e^{i\beta_f(x)\gamma_5} q_f \quad (74)$$

$$= \bar{q}_f e^{i\beta_f(x)\gamma_5} i\gamma_\mu \left[(i\partial^\mu \beta_f(x)\gamma_5) e^{i\beta_f(x)\gamma_5} q_f + e^{i\beta_f(x)\gamma_5} \partial^\mu q_f \right] \quad (75)$$

$$= -(\partial^\mu \beta_f(x)) \bar{q}_f e^{i\beta_f(x)\gamma_5} \gamma_\mu \gamma_5 e^{i\beta_f(x)\gamma_5} q_f + \bar{q}_f i \not{\partial} q_f = -(\partial^\mu \beta_f(x)) \bar{q}_f \gamma_\mu \gamma_5 q_f + \bar{q}_f i \not{\partial} q_f, \quad (76)$$

and

$$\bar{q}'_f \gamma_\mu A^\mu q'_f = \bar{q}_f \gamma_\mu e^{-i\beta_f(x)\gamma_5} A^\mu e^{i\beta_f(x)\gamma_5} q_f = \bar{q}_f \gamma_\mu A^\mu q_f. \quad (77)$$

The mass term in \mathcal{L}_{QCD} is

$$\mathcal{L}_{\text{mass}} = -\frac{1}{2} \sum_f m_f \bar{q}_f (1 + \gamma_5) q_f - \frac{1}{2} \sum_f m_f^* \bar{q}_f (1 - \gamma_5) q_f. \quad (78)$$

Since the chiral transformation gives

$$m_f \bar{q}'_f q'_f = m_f \bar{q}_f e^{i2\beta_f(x)\gamma_5} q_f = m_f [\cos(2\beta_f) \bar{q}_f q_f + i \sin(2\beta_f) \bar{q}_f \gamma_5 q_f], \quad (79)$$

$$m_f \bar{q}'_f \gamma_5 q'_f = m_f \bar{q}'_f \gamma_5 e^{i2\beta_f(x)\gamma_5} q_f = m_f [\cos(2\beta_f) \bar{q}_f \gamma_5 q_f + i \sin(2\beta_f) \bar{q}_f q_f], \quad (80)$$

the $\mathcal{L}_{\text{mass}}$ transforms to

$$\mathcal{L}'_{\text{mass}} = -\frac{1}{2} \sum_f m'_f \bar{q}_f (1 + \gamma_5) q_f - \frac{1}{2} \sum_f m'^*_f \bar{q}_f (1 - \gamma_5) q_f, \quad (81)$$

where

$$m'_f = m_f e^{i2\beta_f(x)}, \quad (82)$$

$$m'^*_f = m_f^* e^{-i2\beta_f(x)}. \quad (83)$$

Finally, the measure for the path integral over quark fields transforms [27] as

$$[dq][d\bar{q}] \rightarrow \exp\left(\frac{-ig^2}{32\pi^2} \int d^4x G^{a\mu\nu*} G^a_{\mu\nu} \sum_f 2\beta_f\right) [dq][d\bar{q}]. \quad (84)$$

Hence:

$$Z = Z[\eta', \bar{\eta}', j_\mu] = \int [dq][d\bar{q}][DA] \exp\left(i \int d^4x [\mathcal{L}_{\beta(x)} + \bar{q}\eta' + \bar{\eta}'q + j_\mu A^\mu]\right), \quad (85)$$

where, in the source terms, we shifted the chiral transformation from the fields to the sources:

$$\eta'_f(x) \equiv e^{i\beta_f(x)\gamma_5}\eta(x) , \quad (86)$$

$$\bar{\eta}'_f(x) \equiv \bar{\eta}(x)e^{i\beta_f(x)\gamma_5} , \quad (87)$$

and

$$\begin{aligned} \mathcal{L}_{\beta(x)} = \sum_f \left\{ \bar{q}_f i \not{D} q_f - \left(e^{i2\beta_f} m_f q_{L_f}^\dagger q_{R_f} + h.c. \right) - (\partial^\mu \beta_f) \bar{q}_f \gamma_\mu \gamma_5 q_f \right\} \\ - \frac{1}{4} G^{a\mu\nu} G_{\mu\nu}^a - \frac{(\Theta + 2 \sum_f \beta_f) g^2}{32\pi^2} G^{a\mu\nu*} G_{\mu\nu}^a . \end{aligned} \quad (88)$$

Using Noether's theorem, which relates the divergence of the current associated with an infinitesimal continuous transformation on the fields to the change in the Lagrangian density under that transformation, we calculate the current associated with the chiral transformations:

$$q'_f(x) = (1 + i\beta_f(x)\gamma_5)q_f(x) + O(\beta_f^2(x)) , \quad (89)$$

$$\bar{q}'_f(x) = \bar{q}(x)(1 + i\beta_f(x)\gamma_5) + O(\beta_f^2(x)) . \quad (90)$$

The infinitesimal form of Eq. 88 is

$$\mathcal{L}_{\beta(x)} = \mathcal{L}_{QCD} - \sum_f [(\partial^\mu \beta_f) \bar{q}_f \gamma_\mu \gamma_5 q_f + i2\beta_f(m_f q_{L_f}^\dagger q_{R_f} + h.c.) + \frac{\beta_f g^2}{16\pi^2} G^{a\mu\nu*} G_{\mu\nu}^a] . \quad (91)$$

The current associated with the transformation (Eq. 90) is

$$J_\mu^5 = - \sum_f \frac{\partial \mathcal{L}_\beta}{\partial(\partial^\mu \beta_f)} = \sum_f \bar{q}_f \gamma_\mu \gamma_5 q_f . \quad (92)$$

Noether's theorem states

$$\partial^\mu J_\mu^5 = - \sum_f \frac{\partial \mathcal{L}_\beta}{\partial \beta_f} = \sum_f i2(m_f q_{L_f}^\dagger q_{R_f} + h.c.) + \frac{g^2}{16\pi^2} G^{a\mu\nu*} G_{\mu\nu}^a . \quad (93)$$

The explicit dependence of \mathcal{L}_β on $\beta_f(x)$ in Eq. 90 yields the non-conserved axial vector current

$$\partial_\mu J_5^\mu = \partial_\mu \left(\sum_f \bar{q}_f \gamma_\mu \gamma_5 q_f \right) = \sum_f [i2(m_f q_{L_f}^\dagger q_{R_f} + h.c.) + \frac{g^2}{16\pi^2} G^{a\mu\nu*} G_{\mu\nu}^a]. \quad (94)$$

The first term on the right hand side is due to the fermion mass, whereas the second is due to the anomaly which is a quantum mechanical effect (in fact the anomaly term is proportional to $g^2 \hbar$).

Equation 88 implies [28] that the physics of the theory defined by \mathcal{L}_{QCD} is unchanged under the *global* (spacetime independent) transformations:

$$\begin{aligned} q_f &\rightarrow e^{i\beta_f \gamma_5} q_f \\ m_f &\rightarrow e^{-i2\beta_f} m_f \\ m_f^* &\rightarrow e^{i2\beta_f} m_f^* \\ \Theta &\rightarrow \Theta - 2 \sum_f \beta_f. \end{aligned} \quad (95)$$

In general, this set of transformations is not a symmetry of the theory because, when the dynamical variables q_f are transformed, the parameters, m_f and Θ , are needed to be transformed, to leave the Lagrangian invariant. If the physics were Θ independent (transforming Θ would not make any difference), then one would recover the classical result that the theory has an axial $U_A(1)$ symmetry when $m_f = 0$ (m_f transformations would not exist). We know, however, that $U_A(1)$ is explicitly broken because otherwise there would be a fourth pseudo Nambu-Goldstone boson η' , in addition to the three pions, with $m_{\eta'} < \sqrt{3}m_\pi$. This can only be understood if physics is Θ -dependent. In this case, Eq. 95 is not a symmetry even in the massless limit, because the parameter Θ is transformed. Hence, $U_A(1)$ is broken even when the quark masses are zero. (If there is Θ -dependence $\partial_\mu J_5^\mu \neq 0$, due to the $G^{a\mu\nu*} G_{\mu\nu}^a$ -term, even if $m_f = 0$. Hence the anomaly explicitly breaks $U_A(1)$). Therefore, QCD must have Θ -dependence through non-perturbative effects

(as noted earlier, the Θ -term is a four-divergence and hence does not contribute in the perturbative quantum theory). These effects that break $U_A(1)$ are known as QCD instanton effects; see the Appendix. The instanton in QCD describes a classically forbidden, but quantum mechanically allowed vacuum tunneling, in which the charge $Q_f^5 = \int d^3x q_f^\dagger \gamma_5 q_f$ associated with $U_A(1)$ symmetry is not conserved. Therefore, the instantons explicitly violate $U_A(1)$. The probability amplitude of an instanton event (see the Appendix)

$$\mathcal{A} \sim \exp\left(-\frac{2\pi}{\alpha_s(\mu)}\right), \quad (96)$$

where μ is the inverse of the instanton size and α_s is defined in Eq. 69. This amplitude can not be expanded in a Taylor series in α_s . Thus, the instanton is indeed a non-perturbative effect. At a finite T , using Eq. 69, we have

$$\mathcal{A} \sim \exp\left(-\frac{2\pi}{\alpha_s(T)}\right) = \left(\frac{\Lambda_{QCD}}{T}\right)^{11-\frac{2}{3}n_f}. \quad (97)$$

At high temperatures non-perturbative (instanton) effects are suppressed. Around $T \sim \Lambda_{QCD}$, instanton effects fully turn-on and strongly break $U_A(1)$ symmetry of QCD.

The terms $i\bar{q}_f \gamma_5 q_f$ and $G^{a\mu\nu*} G_{\mu\nu}^a$ are P and CP odd. Hence their presence in the theory (in the $\mathcal{L}_{\text{mass}}$ and \mathcal{L}_Θ , respectively) leads in general to P and CP violation. Moreover, the transformations given in Eq. 95 allow us to change the m_f (for each flavor) and Θ . The apparent source of CP violation can be moved among the m_f and Θ , by changing the phases of the quark masses. Since there are six transformations on seven parameters, we can not find a definition of quark fields that sets all the parameters real. We might choose, for example, the Θ as zero, m_u, m_d, \dots, m_b as real and m_t as complex. One combination that can not be removed from the theory is $\Theta - \text{Arg} \prod_f m_f = \Theta - 2 \sum_f \beta_f$. Hence, the Θ dependence of QCD comes only through the combination of parameters

$$\bar{\Theta} \equiv \Theta - \text{Arg} \prod_f m_f = \Theta - 2 \sum_f \beta_f. \quad (98)$$

Let us also note that the transformations given in Eq. 95 leaves the $\bar{\Theta}$ invariant. For example lets transform the up-quark field only, then for the invariance, we have

$$\begin{aligned} q_u &\rightarrow e^{i\beta_u\gamma^5} q_u \\ \text{Arg}(m_u) &\rightarrow \text{Arg}(m_u) - 2\beta_u \\ \Theta &\rightarrow \Theta - 2\beta_u, \end{aligned} \tag{99}$$

and hence

$$\bar{\Theta} \rightarrow \bar{\Theta}. \tag{100}$$

Let us suppose that $\bar{\Theta} \neq 0$. Then, no matter how we shuffle the phases of quark masses, it is impossible to set $\Theta = 0$, and $\text{Arg}(m_f) = 0, \forall f$. Therefore, it is inevitable to have some CP violation, with an upper limit consistent with the experiments.

As we remarked, when $\bar{\Theta} \neq 0$, the $\bar{\Theta}$ term in \mathcal{L}_{QCD} violates the P and T (and hence CP) symmetries. Since

$$P : E_i^a \rightarrow -E_i^a \quad B_i^a \rightarrow B_i^a \tag{101}$$

and

$$T : E_i^a \rightarrow E_i^a \quad B_i^a \rightarrow -B_i^a, \tag{102}$$

$G^{a\mu\nu*}G_{\mu\nu}^a = -4E_i^a B_i^a$ is odd under P and T . Therefore, the $\bar{\Theta}$ -term would induce a CP violating term in the effective π -N coupling and produce an electric dipole moment for the neutron. It is of order [29, 30, 31, 32, 33, 34] $d_n \simeq 5 \cdot 10^{-16} |\bar{\Theta}| e \cdot \text{cm}$. Comparison with the experimental bound $d_n \leq 10^{-25} e \cdot \text{cm}$ constrains [35] $\bar{\Theta} \leq 10^{-10}$. This fine tuning requirement on the parameter $\bar{\Theta}$ is known as “the strong CP problem.” It is puzzling that the two independent contributions in the $\bar{\Theta}$, Θ due to the vacuum structure of QCD, and $2\sum_f \beta_f$ due to the electroweak effects involving quark masses, seem to cancel each other.

The most elegant solution of the strong CP puzzle is to replace the parameter $\bar{\Theta}$ by a dynamical field $\bar{\Theta}(x)$. This is achieved by introducing a Higgs field whose expectation value

v_{PQ} spontaneously breaks a postulated global $U(1)_{PQ}$ Peccei-Quinn (PQ) Symmetry [36, 37]. The axion is the Nambu-Goldstone boson associated with this *spontaneous* symmetry breaking. The defining properties of PQ symmetry are[28]:

- 1) it is an exact global symmetry of the classical theory, before anomalies,
- 2) it is broken spontaneously,
- 3) it is broken explicitly by the QCD instanton effects which make the theory Θ dependent.

To see how the PQ mechanism works, consider the theory defined by

$$\begin{aligned} \mathcal{L}_{QCD+PQ} = & -\frac{1}{4}G_{\mu\nu}^a G^{a\mu\nu} + \frac{1}{2}\partial_\mu\phi^*\partial^\mu\phi - \frac{\Theta}{32\pi^2}G_{\mu\nu}^a \tilde{G}^{a\mu\nu} \\ & + \sum_f \left[\bar{q}_f \not{D} q_f - (K_f q_{L_f}^\dagger q_{R_f} \phi + h.c.) \right] - V(\phi^*\phi) , \end{aligned} \quad (103)$$

where ϕ is a complex scalar field. Under $U(1)_{PQ}$, $\phi \rightarrow e^{i\alpha}\phi$ and $q_f \rightarrow e^{i\alpha\gamma_5/2}q_f$. The potential V is a ‘‘Mexican hat’’ potential; hence, $U(1)_{PQ}$ is spontaneously broken:

$$\langle\phi(x)\rangle = v_{PQ}e^{i\alpha(x)} . \quad (104)$$

The quarks acquire masses: $m_f = K_f v_{PQ} e^{i\alpha(x)}$, and hence

$$\bar{\Theta}(x) = \Theta - \text{Arg}\left(\prod_f m_f\right) = \Theta - \text{Arg}\left(\prod_f K_f\right) - \sum_f \alpha(x) = \Theta - \text{Arg}\left(\prod_f K_f\right) - N\alpha(x) . \quad (105)$$

In this toy model N is the number of quarks. Notice that here $\bar{\Theta}(x)$ is a function of the dynamical field $\alpha(x)$, whereas in Eq. 95 $\bar{\Theta}$ is fixed. One can adopt a convention such that $\Theta - \text{Arg}(\prod_f m_f) = 0$. In Eq. 103 the non-perturbative effects which make the theory $\bar{\Theta}$ -dependent produce an effective potential for $\bar{\Theta}$. The field $\bar{\Theta}$ relaxes to the minimum of that potential. Therefore the axion is not massless but acquires a small mass due to non-perturbative QCD (instanton) effects. The zero temperature mass is given in terms of up and down quark masses m_u and m_d , and the pion mass m_π [38, 39] as

$$m_a = \frac{\sqrt{m_u m_d}}{m_u + m_d} \frac{m_\pi f_\pi}{f_a} , \quad (106)$$

where $f_a = \frac{v_{PQ}}{N}$ and f_π are the axion and pion decay constants, and N is a positive integer that describes the color anomaly of $U_{PQ}(1)$. (Axion models have N degenerate vacua [40]). Numerically,

$$m_a \simeq 6 \cdot \text{eV} \left(\frac{10^6 \text{ GeV}}{f_a} \right) . \quad (107)$$

We now study the cosmological implications of axion models [41, 42, 43]. Let the potential for $\phi(x)$ in Eq. 103 be

$$V(\phi) = \frac{\lambda}{4} (|\phi|^2 - v_{PQ}^2)^2 . \quad (108)$$

At extremely high temperatures $U_{PQ}(1)$ symmetry is restored, $\langle \phi(x) \rangle = 0$. As the universe expands and cools below $T_{PQ} \simeq v_{PQ}$, the potential looks like a ‘‘Mexican hat’’ and is minimized for

$$\phi = v_{PQ} \exp(i\alpha(x)) . \quad (109)$$

Notice that $V(\phi)$ is independent of $\alpha(x)$. This massless degree of freedom is the axion: $a(x) \equiv v_{PQ}\alpha(x)$. The system settles down in one of the continuously degenerate ground states which are all equally likely. At much lower temperatures $T \sim \Lambda_{QCD}$, axions acquire mass. This is because $U(1)_{PQ}$ is *explicitly* broken by non-perturbative QCD (instanton) effects at low temperatures. At high temperatures these effects are suppressed. When T approaches Λ_{QCD} , instanton effects turn on. They produce the effective potential

$$\tilde{V}(\bar{\Theta}) = m_a^2(T) \frac{v_{PQ}^2}{N^2} (1 - \cos(\bar{\Theta})) , \quad (110)$$

where [44]

$$m_a(T) \simeq 0.1 m_a \left(\frac{\Lambda_{QCD}}{T} \right)^{3.7} . \quad (111)$$

The minimum of the total potential is at the CP conserving value $\bar{\Theta}(x) = N\alpha(x) = 0$. The axion develops mass m_a , due to the curvature of the potential at the minimum. The effective Lagrangian density for the axion field is obtained by setting $\alpha(x) = \frac{a(x)}{v_{PQ}}$:

$$\mathcal{L}_{\text{eff}} = \frac{1}{2} \partial_\mu a \partial^\mu a - m_a^2(T) \frac{v_{PQ}^2}{N^2} \left(1 - \cos\left(\frac{Na}{v_{PQ}}\right) \right) , \quad (112)$$

where we implicitly assumed that the signature of the spacetime is $(+ - - -)$. Variation of the action $S = \int d^4x \sqrt{-g} \mathcal{L}_{\text{eff}}$ yields the sine-Gordon equation for $\alpha(x)$:

$$\square \alpha(x) + \frac{1}{N} m_a^2(T) \sin(N\alpha(x)) = 0, \quad (113)$$

where d'Alembertian $\square \equiv (1/\sqrt{-g}) \partial_\mu (\sqrt{-g} g^{\mu\nu} \partial_\nu)$. In a Friedmann universe where

$$ds^2 = dt^2 - R^2(t) d\vec{x} \cdot d\vec{x} \quad (114)$$

Eq. 113 reads

$$\ddot{\alpha} + 3H(t)\dot{\alpha} - \frac{1}{R^2(t)} \nabla^2 \alpha + \frac{1}{N} m_a^2(T(t)) \sin(N\alpha) = 0. \quad (115)$$

Near the minima, the potential (Eq. 110) $\tilde{V}(\alpha) \simeq \frac{1}{2} m_a^2 v_{PQ}^2 \alpha^2$. Hence, $\sin(N\alpha) \simeq N\alpha$ in Eq. 115. In that case, the solution of Eq. 115 is a linear superposition of eigenmodes with definite comoving wave vector \vec{k} :

$$\alpha(\vec{x}, t) = \int d^3k \alpha(\vec{k}, t) e^{i\vec{k} \cdot \vec{x}}, \quad (116)$$

where the $\alpha(\vec{k}, t)$ satisfy

$$\left(\partial_t^2 + 3 \frac{\dot{R}(t)}{R(t)} \partial_t + \frac{k^2}{R^2(t)} + m_a^2(t) \right) \alpha(\vec{k}, t) = 0. \quad (117)$$

We are interested in the $k = 0$ mode of vacuum misalignment contribution. The other contributions (of similar magnitude) are discussed by Chang, Hagmann and Sikivie [45]. Then Eq. 115 becomes

$$\ddot{\alpha} + 3H(t)\dot{\alpha} + m_a^2(t)\alpha = 0. \quad (118)$$

This is the equation of a damped harmonic oscillator with time dependent parameters. Since the axion is massless when $T \simeq T_{PQ}$, no initial value α_1 of α is preferred dynamically. Although $\alpha \simeq 0$ today, there is no reason to expect that was the case initially. Therefore, α_1 is chosen by some stochastic process. For $m_a = 0$ (as is the case for $T \gg \Lambda_{QCD}$), the

solution of Eq. 118 is obtained by inserting the ansatz $\alpha = t^p$ to the differential equation and solving the resulting algebraic equation $p^2 + p/2 = 0$. The most general solution is

$$\alpha = \alpha_1 + \alpha_2 t^{-1/2} . \quad (119)$$

Quickly α approaches α_1 , which is a constant, and starts to oscillate when T approaches the critical temperature T_1 where [14]

$$m_a(T_1(t_1)) \sim 3H(T_1(t_1)) = \frac{3}{2t_1} . \quad (120)$$

To be more specific let's define the critical temperature as

$$m_a(T_1(t_1)) t_1 = \frac{3}{2} . \quad (121)$$

We will see below (Eq. 139) that $\Omega_a \sim 0.4$ when $m_a \sim 6 \cdot 10^{-6} \text{eV}$ (Eq. 107). In that case T_1 is about 1GeV (Eq. 128). The typical wavelength of these modes is of the horizon size back then. The corresponding momenta of the particle excitations at birth are therefore:

$$p_a(t_1) \sim 1/d_H = 1/t_1 = \frac{\sqrt{g_{\text{eff}}}}{0.3} \frac{T_1^2}{m_{\text{Pl}}} \sim 1.6 \cdot 10^{-9} \text{eV} \left(\frac{10^{12} \text{GeV}}{f_a} \right)^{\frac{2}{5.7}} , \quad (122)$$

where we used time-temperature relation Eq. 30. Since their mass at that time $m_a(t_1) \sim 2.4 \cdot 10^{-9} \text{eV} (10^{12} \text{GeV}/f_a)^{\frac{2}{5.7}}$, they were semi-relativistic. Axions, however, gain mass rapidly. As the temperature drops to $T \simeq \Lambda_{QCD} \sim 200 \text{MeV}$, their mass increases by a factor of $230 \cdot (10^{12} \text{GeV}/f_a)^{\frac{3.7}{5.7}}$, and axions suddenly become non-relativistic. Because the axion couplings are small, energy dissipation of the modes is negligible. The coherent oscillations produced by the vacuum misalignment are good dark matter candidates.

The present velocity dispersion of these axions can be calculated using Eq. 122 and the conservation of entropy (Eq. 43):

$$g_{\text{eff}}^*(T_1) T_1^3 R^3(T_1) = g_{\text{eff}}^*(T_{0\gamma}) T_{0\gamma}^3 R^3(T_{0\gamma}) , \quad (123)$$

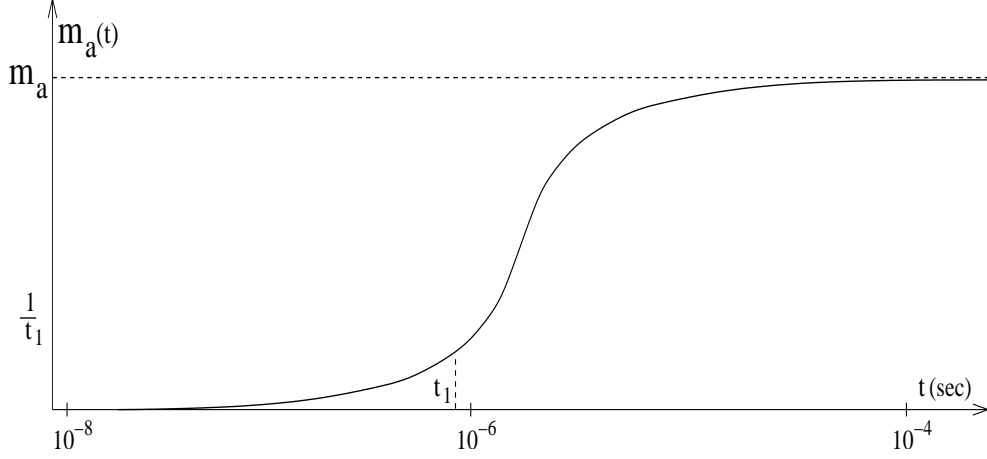


Figure 4: Switch-on of the axion mass in the early universe.

where $g_{\text{eff}}^*(T_1) \sim 60$ and $g_{\text{eff}}^*(T_{0\gamma}) = 2$,

$$\delta v_a(t_0) \equiv v_a(t_0) = \frac{p_a(t_1) R(t_1)}{m_a R(t_0)} \sim \frac{1}{m_a t_1} \frac{R(t_1)}{R(t_0)} = \frac{1}{m_a t_1} \left(\frac{g_{\text{eff}}^*(T_{0\gamma})}{g_{\text{eff}}^*(T_1)} \right)^{\frac{1}{3}} \frac{T_{0\gamma}}{T_1}. \quad (124)$$

To estimate the velocity dispersion we need to calculate t_1 and T_1 . Using Eqs. 107 and 111 we find

$$m_a(T) \sim 1.5 \cdot 10^{-9} \text{eV} \left(\frac{10^{12} \text{GeV}}{f_a} \right) \left(\frac{\text{GeV}}{T} \right)^{3.7}. \quad (125)$$

Taking $g_{\text{eff}} \sim 60$ in the time-temperature relation (Eq. 30), we recast Eq. 125 to read

$$m_a(T) \sim 3.1 \cdot 10^{-51} (\text{GeV})^{\frac{5.7}{2}} \left(\frac{10^{12} \text{GeV}}{f_a} \right) t^{\frac{3.7}{2}}. \quad (126)$$

Then definition 121 yields

$$t_1 \sim 4 \cdot 10^{-7} \text{sec} \left(\frac{f_a}{10^{12} \text{GeV}} \right)^{\frac{2}{5.7}} \sim 6.1 \cdot 10^{17} (\text{GeV})^{-1} \left(\frac{f_a}{10^{12} \text{GeV}} \right)^{\frac{2}{5.7}}. \quad (127)$$

The corresponding temperature is

$$T_1 \sim 0.9 \cdot \text{GeV} \left(\frac{10^{12} \text{GeV}}{f_a} \right)^{\frac{1}{5.7}}. \quad (128)$$

Inserting Eqs. 111, 127 and 128, in Eq. 124 we estimate the present value of the axion velocity dispersion as

$$\delta v_a(t_0) \sim 1.5 \cdot 10^{-17} \left(\frac{10^{-5} \text{eV}}{m_a} \right)^{\frac{4.7}{5.7}}. \quad (129)$$

Since $\delta v_a(t) = \delta v_a(t_0) (R(t_0)/R(t)) = \delta v_a(t_0) (t_0/t)^{\frac{2}{3}}$ we have

$$\delta v_a(t) = 1.5 \cdot 10^{-17} \left(\frac{10^{-5} \text{eV}}{m_a} \right)^{\frac{4.7}{5.7}} \left(\frac{t_0}{t} \right)^{\frac{2}{3}} . \quad (130)$$

Let us now calculate the energy density of the axion field due to vacuum misalignment. The energy density ρ of a homogeneous scalar field around the minimum of its potential is

$$\rho = \frac{v_{PQ}^2}{2} [\dot{\alpha}^2 + m_a^2(t)\alpha^2] . \quad (131)$$

The Virial Theorem implies

$$\langle \dot{\alpha}^2 \rangle = m^2 \langle \alpha^2 \rangle = \frac{\rho}{v_{PQ}^2} . \quad (132)$$

Multiplying Eq. 118 by $\dot{\alpha}$ and using Eqs. 131-132 we obtain

$$\frac{\dot{\rho}}{\rho} = \frac{\dot{m}}{m} - 3 \frac{\dot{R}}{R} , \quad (133)$$

whose solution yields

$$\rho = \text{const.} \frac{m_a(t)}{R^3(t)} . \quad (134)$$

This equation means that as long as the axion mass varies adiabatically, the number of axions per comoving volume is conserved. Because the initial energy in the coherent oscillations is $\rho_1 = v_{PQ}^2 m_a^2(t_1) \alpha_1^2 / 2$, it is easy to estimate the present energy density ρ_0 :

$$\rho_0 = \rho_1 \frac{m_a(t_0)}{m_a(t_1)} \frac{R^3(t_1)}{R^3(t_0)} = \frac{1}{2} v_{PQ}^2 m_a(t_1) m_a \frac{R^3(t_1)}{R^3(t_0)} \alpha_1^2 . \quad (135)$$

Using the conservation of entropy (Eq. 43), we find

$$\rho_0 \sim \frac{1}{60} v_{PQ}^2 m_a(t_1) m_a \frac{T_{0\gamma}^3}{T_1^3} \alpha_1^2 . \quad (136)$$

If the universe never inflated, our presently observable universe should have 10^{30} causally disconnected domains when the α oscillations started. Therefore it is reasonable to assume

that each of the domains had arbitrarily chosen initial amplitudes and take α_1 as the *rms* average of the uniform distribution from $-\pi/N$ to π/N :

$$(\alpha_1)_{rms} = \left[\frac{N}{2\pi} \int_{-\frac{\pi}{N}}^{\frac{\pi}{N}} d\alpha_1 \alpha_1^2 \right]^{1/2} = \frac{\pi}{\sqrt{3}N} . \quad (137)$$

If, on the other hand, the universe inflated after the PQ symmetry breaking, then our observable universe originated from a single domain. Although α_1 had the same value everywhere in our universe, it is arbitrary. Any value is equally likely. To determine Θ_1 in this case, measurement of the axion mass and density are necessary. Assuming $\alpha \sim \frac{\pi}{\sqrt{3}N}$, and using Eqs. 107, 125 and 128 in Eq. 136, we find

$$\rho_0 \sim 3.5 \cdot 10^{-30} \frac{\text{gr}}{\text{cm}^3} \left(\frac{f_a}{10^{12} \text{GeV}} \right)^{\frac{6.7}{5.7}} . \quad (138)$$

Dividing by the critical density $\rho_c = \frac{3H^2}{8\pi G}$, we obtain

$$\Omega_a \sim 0.4 \cdot \left(\frac{f_a}{10^{12} \text{GeV}} \right)^{\frac{6.7}{5.7}} \left(\frac{0.7}{h} \right)^2 , \quad (139)$$

where h is defined as usual by $H_0 = h \text{ 100km/sec} \cdot \text{Mpc}$.

Finally, following the same steps between Eqs. 54 and 57, we express the present axion number density n_a in terms of Ω_a , the present axion energy density in units of the critical density:

$$n_a(t_0) = \frac{1.5 \cdot 10^{64}}{\text{pc}^3} \Omega_a \left(\frac{h}{0.7} \right)^2 \left(\frac{10^{-5} \text{ eV}}{m_a} \right) . \quad (140)$$

As can be seen from the large exponents in Eqs. 57 and 140, WIMPs and axions exist in enormous numbers on astronomical length scales. Moreover, they have negligible velocity dispersion δv_χ and δv_a implied by the exponents in Eqs. 51 and 130. Because of their small velocity dispersions, they are cold dark matter (CDM) particles. CDM particles are so weakly interacting (collisionless) that they have moved purely under the influence of gravity since they decoupled. Galaxies are surrounded by unseen CDM, and hence, because of gravity, CDM particles keep falling in and out of galaxies from all directions.

This continuous flow produces a discrete number of flows anywhere in the halo of a galaxy. This simple observation has rather interesting consequences. Caustics occur where the flow number jumps from n to $n + 2$, with n being an odd number. Generically, caustics are the surfaces in space which separate these regions with differing numbers of flows. The number density of CDM particles becomes very large as one approaches the caustic from the side with the two extra flows. The following section is devoted to the analysis of the CDM caustic surfaces in galactic halos.

3 Cold Dark Matter Caustics

In this section, I make extensive use of the explanations and derivations given in [16]. We have seen in the Introduction that, before the onset of galaxy formation, the collisionless (weakly interacting) CDM particles lie on a time dependent thin 3D sheet in 6D phase space. The thickness of this sheet is the primordial velocity dispersion δv . At the onset of galaxy formation, the particles in a neighborhood of an overdensity fall onto it. As a result, the phase space sheet winds up clockwise wherever galaxies grow (Fig. 1). Outside overdensities, at a location in physical space, there is only one value of velocity (i.e., one single flow, the Hubble flow). There, the phase space sheet covers physical space once. Hence, in Fig. 1, away from the overdensity the plot is one to one. On the other hand, inside an overdensity, the phase space sheet covers physical space multiple times, but always an odd number of times, implying that there are an odd number of flows at such locations in physical space (Figs. 1 and 2). CDM caustics are associated with these flows [16]. We examine them rigorously in the next section.

3.1 Caustics in General

Let us consider a flow of CDM particles with zero (or negligible) velocity dispersion. To study the motion of the particles, we adopt a parametrization of the 3D phase space sheet by labelling each particle with an arbitrary 3-component parameter $\vec{\alpha} = (\alpha_1, \alpha_2, \alpha_3)$. The phase space sheet location at time t is specified by the map $\vec{\alpha} \rightarrow \vec{x}(\vec{\alpha}, t)$ where \vec{x} is the position in physical space of particle $\vec{\alpha}$ at time t . The velocity of particle $\vec{\alpha}$ is $\vec{v} = \frac{\partial \vec{x}}{\partial t}(\vec{\alpha}, t)$. Let $\vec{\alpha}_j(\vec{r}, t)$, with $j = 1 \dots n$, be the solutions of

$$\vec{r} = \vec{x}(\vec{\alpha}, t) . \tag{141}$$

Here n is the number of distinct flows at spatial location \vec{r} and time t . In general, the number of solutions n jumps by 2 on certain surfaces which are the locations of caustics.

The total number of particles is:

$$\begin{aligned}
N &= \int d^3\alpha \frac{d^3N}{d\alpha_1 d\alpha_2 d\alpha_3}(\vec{\alpha}) \\
&= \int d^3r \sum_{j=1}^n \frac{d^3N}{d\alpha_1 d\alpha_2 d\alpha_3}(\vec{\alpha}_j(\vec{r}, t)) \frac{1}{|\det\left(\frac{\partial\vec{x}}{\partial\vec{\alpha}}\right)|_{\vec{\alpha}_j(\vec{r}, t)}}. \tag{142}
\end{aligned}$$

The density of particles in physical space can be extracted from the above equation:

$$d(\vec{r}, t) = \sum_{j=1}^n \frac{d^3N}{d\alpha_1 d\alpha_2 d\alpha_3}(\vec{\alpha}_j(\vec{r}, t)) \frac{1}{|D(\vec{\alpha}, t)|_{\vec{\alpha}_j(\vec{r}, t)}}, \tag{143}$$

where

$$D(\vec{\alpha}, t) \equiv \det\left(\frac{\partial\vec{x}}{\partial\vec{\alpha}}\right) \equiv \det(\mathcal{D}), \tag{144}$$

and \mathcal{D} is the Jacobian. As expected, the density $d(\vec{r}, t)$ is a reparametrization invariant: if we reparametrize the particles $\vec{\alpha} \rightarrow \vec{\beta}$, such that the n distinct flows $\beta_j(\vec{r}, t)$ are the solutions of $\vec{r} = \vec{x}(\vec{\beta}, t)$, then:

$$\begin{aligned}
\frac{d^3N}{d\alpha_1 d\alpha_2 d\alpha_3} &\rightarrow \frac{d^3N}{\left|\det\left(\frac{\partial\vec{\alpha}}{\partial\vec{\beta}}\right)\right| d\beta_1 d\beta_2 d\beta_3}, \\
\det\left(\frac{\partial\vec{x}}{\partial\vec{\alpha}}\right) &\rightarrow \det\left(\frac{\partial\vec{x}}{\partial\vec{\beta}} \frac{\partial\vec{\beta}}{\partial\vec{\alpha}}\right) = \det\left(\frac{\partial\vec{x}}{\partial\vec{\beta}}\right) \det\left(\frac{\partial\vec{\beta}}{\partial\vec{\alpha}}\right), \tag{145}
\end{aligned}$$

and hence, the density retains its form given in Eq. 143 with $\vec{\alpha}$ replaced by $\vec{\beta}$.

Caustics are wherever the density diverges (i.e. wherever $D(\vec{\alpha}, t) = 0$). Thus, the map $\vec{\alpha} \rightarrow \vec{x}$ is singular at the location of the caustics. Generically the zeros of $D(\vec{\alpha}, t)$ are simple (i.e., the matrix $\frac{\partial\vec{x}}{\partial\vec{\alpha}}$ has a single vanishing eigenvalue). The condition that one eigenvalue vanishes imposes one constraint on the three parameters $\vec{\alpha}$. Therefore, the location of a caustic is generically determined by two independent labels, hence it is a 2D surface in physical space.

3.2 Caustic Surfaces

Let's consider a generic caustic surface at a fixed time t . Using the reparametrization invariance $\vec{\alpha} \rightarrow \vec{\beta}(\vec{\alpha}, t)$ of the flow, let's parametrize the particles near the caustic such that the surface is at $\beta_3 = 0$. Also let's choose a Cartesian coordinate system in a neighborhood of point P on the caustic surface such that \hat{z} is the perpendicular direction to the surface, whereas \hat{x} and \hat{y} are the parallel directions. Hence, in this neighborhood $\partial z/\partial\beta_1 = \partial z/\partial\beta_2 = 0$. Thus, we have

$$D = \frac{\partial z}{\partial\beta_3} \det \left(\frac{\partial(x, y)}{\partial(\beta_1, \beta_2)} \right) , \quad (146)$$

around P. The two dimensional matrix $\partial(x, y)/\partial(\beta_1, \beta_2)$ is nonsingular, whereas $\partial z/\partial\beta_3 = 0$ at $\beta_3 = 0$, hence, by construction D vanishes at $\beta_3 = 0$, where the caustic surface is. By Taylor expanding, we have up to the second order in β_3 :

$$z = z_0 + B\beta_3^2 . \quad (147)$$

We may choose the positive z -direction in such a way that $B > 0$. Then, since $\partial z/\partial\beta_3 = 2\sqrt{B(z - z_0)}$, the determinant becomes

$$D = 2\sqrt{B(z - z_0)} \det \left(\frac{\partial(x, y)}{\partial(\beta_1, \beta_2)} \right) \quad \text{for } z > z_0 . \quad (148)$$

Hence, near a caustic surface located at $z = z_0$, the density diverges as $\frac{1}{\sqrt{z - z_0}}$ on the side of the surface where $z > z_0$. Figure 5.A below depicts a 2D cut of phase space in the (z, \dot{z}) plane. The particles lie on the curve which is at the intersection of the phase space sheet with the (z, \dot{z}) plane. The label β_3 gives the position of the particles on this curve. The caustics, which are located at $z = z_1$ and $z = z_2$, extend in the x and y directions. Figure 5.B depicts the density $d(z)$ which diverges as $1/\sqrt{z - z_1}$ for $z \rightarrow z_1$ with $z > z_1$, and as $1/\sqrt{z_2 - z}$ for $z \rightarrow z_2$ with $z < z_2$. There is only one flow for $z < z_1$ and for $z > z_2$, whereas there are three distinct flows in the region $z_1 < z < z_2$. The number of flows changes by

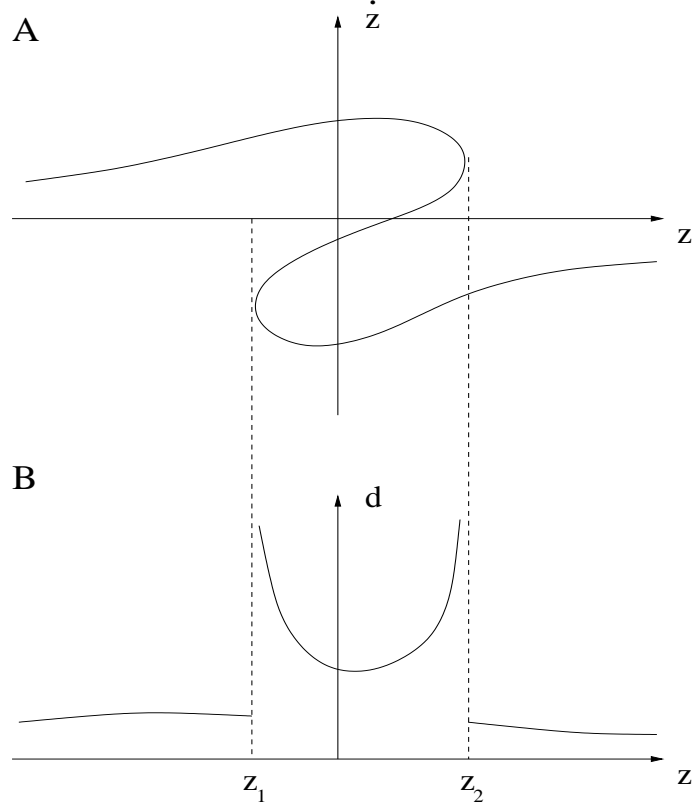


Figure 5: A generic surface caustic. A) In phase space. B) In physical space. The two dimensions (x and y) into which the caustic extends as a surface are not shown. The physical space density d diverges at those locations (z_1 and z_2) where the phase space sheet folds back.

two at the locations of the caustics. The phase space sheet has a fold at $z = z_1$ and $z = z_2$, where $\partial z / \partial \beta_3 = 0$. Hence the velocity space is tangent to the fold. Therefore, in physical space the particles pile up at z_1 and z_2 where the sheet folds back. More rigorously, if we represent the 2D phase space density near a fold in the limit $\delta v \rightarrow 0$ by

$$\frac{d^2 N}{dz d\dot{z}} = N \delta(z - C(\dot{z})^2), \quad (149)$$

where C and N are numbers, then, the density

$$\begin{aligned} d &= \int \frac{d^2 N}{dz d\dot{z}} d\dot{z} = N \int \delta(z - C(\dot{z})^2) d\dot{z} = \int \left\{ \frac{\delta(\dot{z} - \sqrt{\frac{z}{C}})}{|-2C\sqrt{\frac{z}{C}}|} + \frac{\delta(\dot{z} + \sqrt{\frac{z}{C}})}{|2C\sqrt{\frac{z}{C}}|} \right\} d\dot{z}, \\ &= \frac{N}{\sqrt{Cz}} \equiv \frac{A}{\sqrt{z}}, \end{aligned} \quad (150)$$

where A will be called the “fold coefficient.” Notice that d diverges as $z \rightarrow 0$ where the caustic is located.

3.3 CDM Infall in Galactic Halos and Caustics

In this section we will introduce the caustics associated with the infall of CDM particles into the potential well of a galactic halo. The existence and structure of the caustics will be studied in Sections 3.4.1 and 3.5.1 in detail, using the discussion given here. We set the velocity dispersion equal to zero ($\delta v = 0$) in our considerations. A small non-vanishing velocity dispersion would provide a cutoff, such that the density at the caustic would become very large rather than infinite.

We have already seen in the introduction that the process of galaxy formation involves winding up of the phase space sheet of CDM particles which produces a discrete number of flows at a location in space. If the galactic center is approached from an arbitrary direction, the local number of flows increases. First there is one flow, then there are three flows, then five etc. (Fig. 2). The boundary between the region with one (three, five, . . .) and the region with three (five, seven, . . .) flows is the location of a caustic which is topologically a sphere surrounding the galaxy. As will be shown in Section 3.4.2, when these spheres are approached from the side with the two extra flows the density diverges as $\frac{1}{\sqrt{\sigma}}$ where σ is the distance to the surface. We called these spheres “outer caustics.” It is a little more difficult to see the existence of “inner caustics” in addition to the outer caustics; they can not be seen in Fig. 2. Inner caustic rings occur if the CDM particles carry angular momentum with respect to the center. In the limit of zero angular momentum a caustic ring becomes a caustic point at the center, whereas the outer caustics are unaffected.

Let us first discuss the case where the overdensity is spherically symmetric and all the CDM particles have zero angular momentum. Then, the particles move in and out of the galaxy in radial orbits. As a result, the galactic center is a caustic point and the density

associated with each flow diverges as $\frac{1}{r^2}$, where r is the radial coordinate. Caustic point is a degenerate case since we assumed spherical symmetry and radial orbits.

To see the inner caustics, one has to consider the flow of the particles which carry angular momentum with respect to the center. In this case, as will be seen in Section 3.4.1, outer caustics which surround the galaxy also exist.

Let us now consider the case where the collisionless CDM particles move in and out of the galaxy only under the effect of gravity and rotate due to the angular momentum they carry. Figure 6 depicts the successive time frames of a set of CDM particles falling through a galaxy. This sequence is inevitable, for a flow in and out of the potential well of a galactic halo. In Fig. 6.A, the particles are about to fall onto the galaxy for the first time in their history. They make up a closed 2D surface, a topological “sphere,” surrounding the galaxy in 3D physical space. We call this surface the first “turnaround sphere” (in fact, Fig. 6 depicts the intersection of this turnaround sphere with the plane of the figure, as it evolves in time). To be more definite, we assume that the particles carry net angular momentum about the vertical axis in this plane (i.e., the turnaround sphere is spinning about the vertical). The particles near the top (bottom) of the sphere in frame A, carry little angular momentum and end up near the bottom (top) of the sphere in frame F, after falling through the galaxy. The particles near the equator carry the most angular momentum. When the turnaround sphere crosses itself near frame C, they form a ring in the spatial section perpendicular to the plane of the figure. The radius of the ring decreases in time down to some minimum value, reached near frame D, and then increases again during the out flow. Outside this ring, the region inside the sphere which has not turned itself inside out makes a doughnut. When this doughnut is pinched out in spacetime (in frames C and D), as will be shown later in this section, a caustic ring occurs in space. We will designate this ring as the location of the “inner caustic.” The radius of the sphere at the second turnaround in frame F is smaller than the first turnaround radius

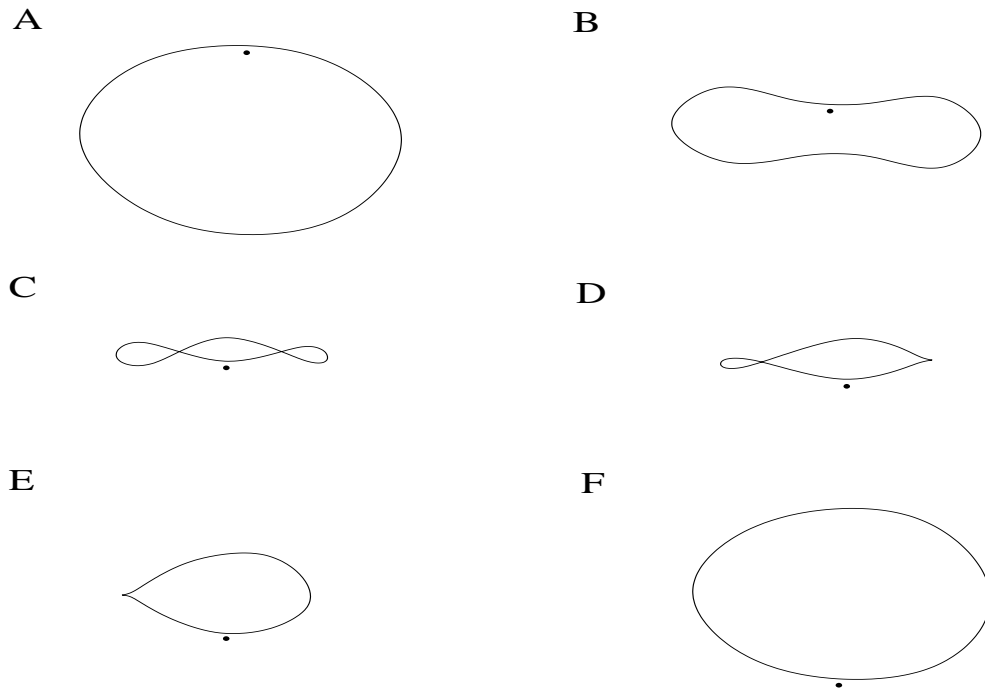


Figure 6: Infall of a turnaround sphere. The closed lines are at the intersections of the sphere with the plane of the figure at six successive times. The sphere has net angular momentum about the vertical axis. It crosses itself between frames B and C. The cusps in frames D and E are at the intersection of a caustic ring with the plane of the figure. The dot, which represents a particle in the flow, is introduced to keep track of the sequences in the flow. The whole infall sphere completes the process of turning inside out just after frame E.

because of the deepening of the potential well of the galaxy due to the infall occurring in the meantime. The second turnaround sphere falls back in, repeating the same sequence of Fig. 6, although it gets fuzzier due to the gravitational scattering of inhomogeneities in the galaxy, and so on. There is another generic surface caustic associated with the m th turnaround, where $m = 2, 3, 4, \dots$. We will call these “outer caustics.” At the location of the outer caustics, the number of flow changes by two (this is also true for the inner caustic rings as well), and particles pile up since the phase space sheet in this location is tangent to velocity space (Fig. 2). There is no change in the number of flow near the first turnaround ($m = 1$), hence there is no caustic associated with it. Outer caustics, in

fact, are located near where the particles of a given outflow reach their maximum radius before falling back in. To illustrate this, let us parametrize the flow at a given time t by $\vec{x}(\alpha, \beta, t_0; t)$, where t_0 is the time the particle was at last turnaround, α and β label the particles on the turnaround sphere at that time. For example, polar and azimuthal angles, which tell us where the particle was on the turnaround sphere, can be used to label the particles. The vector, \vec{x} , is therefore the location of the particle $\vec{\alpha} \equiv (\alpha, \beta, t_0)$ at time t in physical space. Let us define: $\vec{x}_{t_0} \equiv \frac{\partial \vec{x}}{\partial t_0}$, $\vec{x}_\alpha \equiv \frac{\partial \vec{x}}{\partial \alpha}$, $\vec{x}_\beta \equiv \frac{\partial \vec{x}}{\partial \beta}$, and $\dot{\vec{x}} \equiv \frac{\partial \vec{x}}{\partial t}$. Therefore, the determinant $D(t_0, \alpha, \beta; t) = \det \left(\frac{\partial \vec{x}}{\partial \vec{\alpha}} \right)$ can be written as

$$D = \vec{x}_{t_0} \cdot (\vec{x}_\alpha \times \vec{x}_\beta). \quad (151)$$

The remaining discussion will focus on the flow at a fixed time t (we will discuss on the snapshot of the flow at time t). As a result, we do not show the t dependence any further. The existence of outer and inner caustics in the presence of angular momentum will be proven in Sections 3.4.1 and 3.5.1, respectively.

3.4 Outer Caustic Spheres

3.4.1 The Existence of Outer Caustic Spheres

Let us reconsider now the evolution of the spheres in the frames of Fig. 6.A-F and, after frame F. In the beginning, all the later infall spheres, which have greater t_0 , are outside the sphere $\{\vec{x}(\alpha, \beta, t_0) : \forall \alpha, \beta\}$ of frame B, and t_0 increases in the outward direction. Because the particles on the sphere are moving inward (hence $\dot{\vec{x}}(\alpha, \beta, t_0)$ is pointing inward for all (α, β)), the vectors $\{\vec{x}_{t_0}(\alpha, \beta, t_0) : \forall \alpha, \beta\}$ point outward. In frame E the initial infall sphere is just about to complete the process of turning itself inside out. Except for the particle at the cusp, all the particles on the sphere have already started their out flow. After frame E the process is completed. Hence, inside the sphere there are later infall spheres and t_0 increases in the inward direction. Thus, even though the particles on the sphere in frame F flowing outward (hence $\dot{\vec{x}}(\alpha, \beta, t_0)$ is pointing outward for all (α, β)),

the vectors $\{\vec{x}_{t_0}(\alpha, \beta, t_0) : \forall \alpha, \beta\}$ point inward. Note that $\dot{\vec{x}}$ is always in the direction of motion and \vec{x}_{t_0} points opposite to it, since t_0 decreases in the direction of motion (particles in the direction of the motion started to fall earlier, hence they have smaller t_0). After frame F, $\vec{x}_{t_0}(\alpha, \beta, t_0)$ will remain inward until the particle $\vec{x}(\alpha, \beta, t_0)$ reaches the next turnaround where it starts to fall back again. After the turnaround the motion is inward and $\vec{x}_{t_0}(\alpha, \beta, t_0)$ is outward. Therefore, at some point in the evolution $\vec{x}_{t_0}(\alpha, \beta, t_0)$ either vanishes or becomes parallel to the sphere $\{\vec{x}(\alpha, \beta, t_0) : \forall \alpha, \beta\}$. At that point $D = 0$, since $\vec{x}_\alpha \times \vec{x}_\beta$ is perpendicular to the sphere. At a given fixed time the collection of all these points makes up a closed continuous surface (topological sphere) in space. Or, we can go back in time and choose the initial sphere $\{\vec{x}(\alpha', \beta', t_0(\alpha', \beta')) : \forall \alpha', \beta'\}$ such that at the future given fixed time $\{\vec{x}_{t_0}(\alpha', \beta', t_0(\alpha', \beta')) : \forall \alpha', \beta'\}$ is parallel to $\{\vec{x}(\alpha', \beta', t_0(\alpha', \beta')) : \forall \alpha', \beta'\}$, where $D = 0$. Therefore, the initial sphere $\{\vec{x}(\alpha', \beta', t_0(\alpha', \beta')) : \forall \alpha', \beta'\}$ will have simultaneously vanishing D at the given fixed time, making up a caustic which we call an *outer* caustic.

To visualize that we really have a closed continuous caustic surface in the flow of CDM particles in three dimensional space, recall that the particles that fell in can not reach their last turn around radius again. Therefore, at any radial direction \hat{r} from the center of the galactic halo, there are locations where the number of flows jumps from $n + 2$ to n , where n is an odd number. As \vec{r} traces out all the directions in the sky, all these locations make up a closed surface (for a fixed n) due to the continuity of the flow. In phase space, the 3D phase space sheet folds back at the locations where the surfaces are. Hence, at the folds the velocity space is tangent to the phase space sheet and in physical space particles pile up at the locations of the corresponding folds. The number density diverges (in the limit $\delta v = 0$) at the surfaces because it is the integral of the phase space density over velocity space.

3.4.2 Density Profiles of Outer Caustic Spheres

Outer caustics are closed surfaces (topological spheres) near the $(n + 1)$ th turn-around radii with $n = 1, 2, 3, \dots$. Indeed the number of flows changes by two at the turnarounds because of the fall back of the particles. There is no caustic associated with the first turn-around (Fig. 2).

The outer caustics are described by simple “fold” (A_2) catastrophes. Their density profile is

$$d_n(\sigma) = \frac{A_n}{\sqrt{\sigma}} \Theta(\sigma) \quad (152)$$

for small σ , where σ is the distance to the caustic, $\Theta(\sigma)$ is the Heaviside function, and A_n is a constant which we call the “fold coefficient.” We choose $\sigma > 0$ on the side with two extra flows (i.e., towards the galactic center). Therefore, when an outer caustic is approached from the inside, the density diverges as $\sim \frac{1}{\sqrt{\sigma}}$, abruptly falling to zero on the outside. The observation [46] of arc-like shells surrounding giant elliptical galaxies can be interpreted [47] as outer caustics in the distribution of baryonic matter falling onto those galaxies.

To estimate A_n in Eq. 152, consider the time evolution of CDM particles which are falling out of a galactic halo for the n th time and then falling back in. Let R_n be the turn-around radius. We assume that the rotation curve of the galaxy is flat near $r = R_n$ with time-independent rotation velocity v_{rot} . The gravitational potential is then

$$V(r) = v_{\text{rot}}^2 \ln \left(\frac{r}{R_n} \right) \quad . \quad (153)$$

The particles have a trajectory $r(t)$ such that

$$\left| \frac{dr}{dt} \right| = \sqrt{2(E - V(r))} = v_{\text{rot}} \sqrt{2 \ln \left(\frac{R_n}{r} \right)} \quad , \quad (154)$$

where E is the energy per unit mass. Equation 154 neglects the angular momentum of the particles. This is a good approximation at turnaround since the particles are far from their distance of closest approach to the galactic center. Finally, we assume that the flow

is stationary. In that case the number of particles flowing per unit solid angle and per unit time, $\frac{dN}{d\Omega dt}$, is independent of t and r , and the caustic is located exactly at the $(n + 1)$ th turnaround radius R_n .

Let us emphasize that none of the assumptions spherical symmetry, flat rotation curve, time independence of the gravitational potential, radial orbits, and stationarity of the flow affect the existence of the outer caustics or the fact that they have the density profile given by Eq. 152. The assumptions are made only to obtain estimates of the coefficients A_n .

The mass density of particles, $d_n(r)$, follows from the equality: $2\frac{dN}{d\Omega dt}dt = \frac{d_n(r)}{m}r^2dr$, where m is the mass of each particle. The factor of 2 appears because there are two distinct flows, out and in. Using Eq. 154, we obtain the density distribution near the n th outer caustic:

$$d_n(r) = 2\frac{dM}{d\Omega dt}\Big|_n \frac{1}{r^2 v_{\text{rot}} \sqrt{2 \ln\left(\frac{R_n}{r}\right)}} \quad , \quad (155)$$

where $\frac{dM}{d\Omega dt} \equiv m\frac{dN}{d\Omega dt}$. Near the caustic, $\ln\left(\frac{R_n}{r}\right) = \frac{\sigma}{R_n}$ where $\sigma = R_n - r$. Inserting this into Eq. 155 and comparing it with Eq. 152, we find

$$A_n = \frac{\sqrt{2}}{v_{\text{rot}}}\frac{dM}{d\Omega dt}\Big|_n R_n^{-3/2} \quad . \quad (156)$$

Estimates of R_n and $\frac{dM}{d\Omega dt}\Big|_n$ can be extracted from ref. [48, 49] for the case of self-similar infall [50, 51]. The infall is called *self-similar* if it is time-independent after all distances are rescaled by the turn-around radius $R(t)$ at time t and all masses are rescaled by the mass $M(t)$ interior to $R(t)$. In the case of zero angular momentum and spherical symmetry, the infall is self-similar if the initial overdensity profile has the form $\frac{\delta M_i}{M_i} = \left(\frac{M_0}{M_i}\right)^\epsilon$ where M_0 and ϵ are parameters [50]. In CDM theories of large scale structure formation, ϵ is expected to be in the range 0.2 to 0.35 [48, 49]. In that range, the galactic rotation curves predicted by the self-similar infall model are flat [50].

The R_n and $\left.\frac{dM}{d\Omega dt}\right|_n$ do not depend sharply upon ϵ . Our estimates are for $\epsilon = 0.2$ because they can be most readily obtained from ref. [48, 49] in that case. For $\epsilon = 0.2$, the radii of the $(n + 1)$ th turnaround spheres are approximately

$$\{R_n : n = 1, 2, \dots\} \simeq (240, 120, 90, 70, 60, \dots) \text{ kpc} \cdot \left(\frac{v_{\text{rot}}}{220 \text{ km/s}}\right) \left(\frac{0.7}{h}\right) \quad . \quad (157)$$

Moreover, one has

$$\left.\frac{dM}{d\Omega dt}\right|_n \frac{1}{v_{\text{rot}}} = F_n \sqrt{2} \frac{v_{\text{rot}}^2}{4\pi G} \quad , \quad (158)$$

with

$$\{F_n : n = 1, 2, \dots\} \simeq (20, 8, 5, 4, 3, \dots) 10^{-2} \quad . \quad (159)$$

Combining Eqs. 156 - 159, we find

$$\begin{aligned} \{A_n : n = 1, 2, \dots\} \sim (2, 2, 2, 3, 3, \dots) \cdot \frac{10^{-5} \text{ gr}}{\text{cm}^2 \text{ kpc}^{1/2}} \\ \cdot \left(\frac{v_{\text{rot}}}{220 \text{ km/s}}\right)^{1/2} \left(\frac{h}{0.7}\right)^{3/2} \quad . \quad (160) \end{aligned}$$

Generally the outer caustics are “concave” (i.e., they are curved toward the side which has two extra flows). Their radius of curvature is of order R_n . The lensing by concave caustic surfaces is discussed in Section 4.2.2.

Next, we will discuss *inner* caustics which, as we will soon see, have the shape of rings (closed tubes) and are located near where the particles with the most angular momentum in a given inflow reach their distance of closest approach to the galactic center before moving back out of the galaxy.

3.5 Inner Caustic Rings

3.5.1 The Existence of Inner Caustic Rings

During each infall-outfall sequence, the sphere of Fig. 6 turns itself inside out. For example, a particle (represented by a dot throughout the frames of Fig. 6) which is part of the flow

and is just inside the sphere in frame A, appears outside the sphere in frame F. There is, therefore, a ring in space-time of points which are inside the sphere last. The intersection of this space-time ring with the plane of the figure is at two space-time points, one located at the cusp in frame D, the other at the cusp in frame E. Although the cusp in frame D is smoothed out in frame E, and the cusp in frame E does not exist in frame D, since there is a continuous flow of spheres falling in and out that are continuous deformations of one another, the cusp-ring just defined is a persistent feature in space. Here, we should note that it is possible mathematically to turn a sphere inside out by means of continuous deformations which allow the surface to pass through itself without puncturing, ripping, creasing, pinching, or introducing any sharp points in to the intermediate stages. This process is called the “sphere eversion” [52, 53, 54] in topology. In our problem, however, the particles of the sphere are constrained to move purely under the effect of gravity and the angular momentum they carry. When a sphere is pushed bottom up and top down through itself as in Fig. 6.B, a ring shaped fold occurs where the sphere intersects itself as in Fig. 6.C. This ring-fold can not be eliminated without creating a sharp crease (the cusps of Fig. 6.D and Fig. 6.E) in the physical process we are considering. In the mathematical-sphere-eversion process, the ring is pulled down on the sphere becoming smaller and then the ring is squeezed so that its two sides touch and merge.

We, now want to show that the cusp-ring, as defined early in the previous paragraph, is a caustic location (cusps in Fig. 6.D-E are at the intersections of a cusp-ring with the plane of the figure). Consider Fig. 7 that zooms in to the neighborhood of space and time where the infall sphere is completing the process of turning itself inside out. Coordinates x and z are chosen as shown in the figure. The \hat{y} direction is into the plane of the figure and parallel to the ring at point E . We parametrize the flow in a small neighborhood of the ring by $\vec{\alpha} = (\alpha, \beta, t_0)$ such that $\frac{\partial x}{\partial \beta} = \frac{\partial z}{\partial \beta} = 0$. As before, t_0 labels successive infall spheres and may be taken to be the time of their last turnaround. Thus:

$$D = \frac{\partial y}{\partial \beta} \left(\frac{\partial x}{\partial \alpha} \frac{\partial z}{\partial t_0} - \frac{\partial x}{\partial t_0} \frac{\partial z}{\partial \alpha} \right). \quad (161)$$

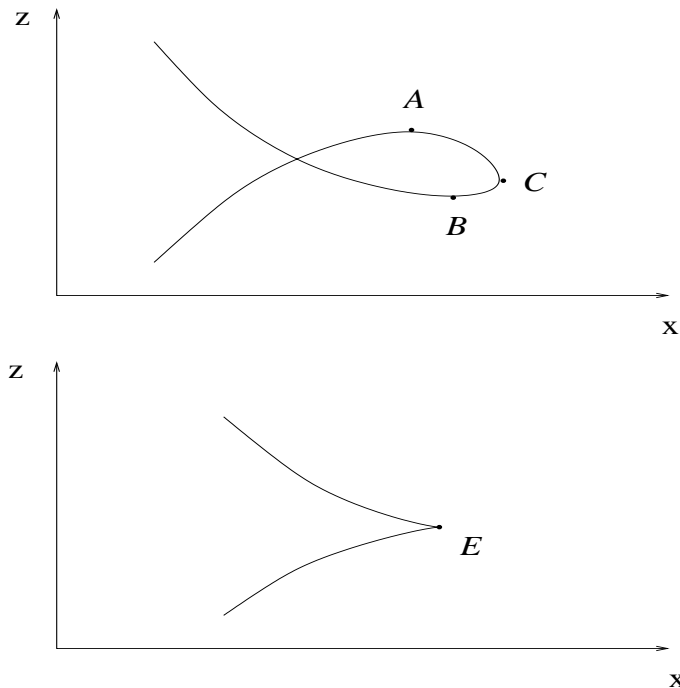


Figure 7: An infall sphere near the location where and when it completes the process of turning itself inside out. The curves are the intersections of the sphere with the plane of the figure at two successive times, corresponding to frames C and D in Fig. 6. Parameter α labels points along the line. $\frac{\partial z}{\partial \alpha} = 0$ at points A and B . $\frac{\partial x}{\partial \alpha} = 0$ at point C . Points A , B and C move to point E , which thus is the location of a caustic since $D = 0$ there.

In the top figure of Fig. 7, the infall sphere is about to reach to the ring. Parameter α labels points (particles) along the curve. At points A and B , $\frac{\partial z}{\partial \alpha} = 0$ because the tangent vectors to the curve at these points are parallel to the \hat{x} -direction. At point C , on the other hand, $\frac{\partial x}{\partial \alpha} = 0$ because the tangent at C is parallel to the \hat{z} -direction. In the bottom figure of Fig. 7, the infall sphere reaches the ring. Points A , B and C of the top figure have moved to point E in the bottom figure. Hence $\frac{\partial z}{\partial \alpha} = \frac{\partial x}{\partial \alpha} = 0$ and, therefore, from Eq. 161, we have $D = 0$ at point E . Thus, E is a caustic location. Since, in general, D only has a simple zero at point E , E is in fact a location of a *surface* caustic. In the discussion that follows, we will show that the complete inner caustic surface is a closed tube and E is a point on this tube.

To see the tube topology, consider Fig. 6.B. The vector $\vec{x}_{t_0} = \frac{\partial \vec{x}}{\partial t_0}$ (not shown explic-

itly) points outward everywhere on the infall sphere since the later (earlier) infall spheres, which have greater (smaller) t_0 , are outside (inside) of this one. In other words, t_0 increases in the outward direction. In Fig. 6.F, however, where the sphere completes the process of turning itself inside out, all the later (earlier) infall spheres are inside (outside) of this one. Therefore, \vec{x}_{t_0} points inside everywhere on this sphere. This implies that during the infall-outfall, \vec{x}_{t_0} either vanishes or becomes parallel to the sphere at some space-time points. $D = 0$ at such points, hence they are the location of caustics. Since D is a continuous function of $\vec{\alpha} = (\alpha, \beta, t_0)$, the caustic must lie on a closed surface (vanishing of D constrains the three parameters leaving only two independent ones, hence we have a surface). Now, if we follow the motion of points which are near the North (South) pole of the sphere in Fig. 6.B and, end up near the South (North) pole in Fig. 6.E, we see that \vec{x}_{t_0} always points up (down). It does not reverse its direction. Hence, \vec{x}_{t_0} does not vanish and is not parallel to the sphere at any time between these two frames for these points. Therefore, within a cylindrical region extending from North to South in the spatial volume under consideration D does not vanish. This implies that inner caustics do not exist in this cylindrical region. On the other hand, for the points near the equator in Fig. 6, \vec{x}_{t_0} points outward during infall and points inward during outfall. For example, at the East (West) pole in Fig. 6, \vec{x}_{t_0} points outward from frame A to the the end of frame D (frame E) and points inward in frames E and F (in frame E). Thus if we track a point near the equator, at some time \vec{x}_{t_0} either vanishes or is parallel to the sphere, hence D vanishes. The points where this happens lie on a closed surface which wraps outside of the previously defined cylinder. Therefore, the surface is a tube located near the equator, where the particles with the most angular momentum are at their distance of closest approach.

According to the Brouwer's Hairy Ball (or Fixed Point) Theorem, an everywhere nonzero tangent vector field on the 2-sphere does not exist. Any continuous tangent vector field on the sphere must have at least one point where the vector is zero. Finding examples

is easy. Since the sphere with one point removed is homeomorphic to the plane, using the fact that a constant (and thus nonzero) vector field on the plane exists, we can obtain a vector field on the once-punctured sphere. Or, consider a line L tangent to the unit sphere S in R^3 at the point N . For every plane P containing L , consider the intersection of P with S . These create a family of circles C on S all separated from each other, except that they all contain the point N . Now define a vector field on S at each point x , using the tangent direction of the unique circle C through x , with a magnitude equal to the distance from the point N . Hence, the zero vector is at N . Another way of stating the theorem is that given a ball with hairs all over it, it is impossible to comb the hairs continuously and have all the hairs lay flat so that they change direction smoothly over the whole surface. At least one hair must be sticking straight up. This implies, as a corollary, that somewhere on the surface of the Earth, at any moment there is at least one point with zero horizontal wind velocity.

Consider now the angular momentum distribution on the turnaround sphere. This is a special continuous two-dimensional vector field on the sphere which has two zeros at the poles where the net angular momentum axis crosses the sphere. When we tracked the particles in the neighborhood of these angular momentum zeros, we found that their \vec{x}_{t_0} does not vanish and is not parallel to the sphere at any time during the infall-outfall process. Therefore the inner caustics appear only in the flow of particles which are some distance away from both zeros. Since that set of particles has the topology of a closed ribbon ($I \times S^1$ where I is a closed interval in R), and the previously defined caustic ring (the set of points E which are in the turnaround sphere last) goes around this closed ribbon once, the inner caustic must be a closed surface with one handle (i.e., a closed tube).

Figure 8 depicts the snapshot of the flow near the caustic. The curves are where the simultaneous (same t) infall spheres corresponding to five different initial times: $t_{01} > t_{02} > \dots > t_{05}$ intersect the plane of the figure near the caustic. The five numbered dots

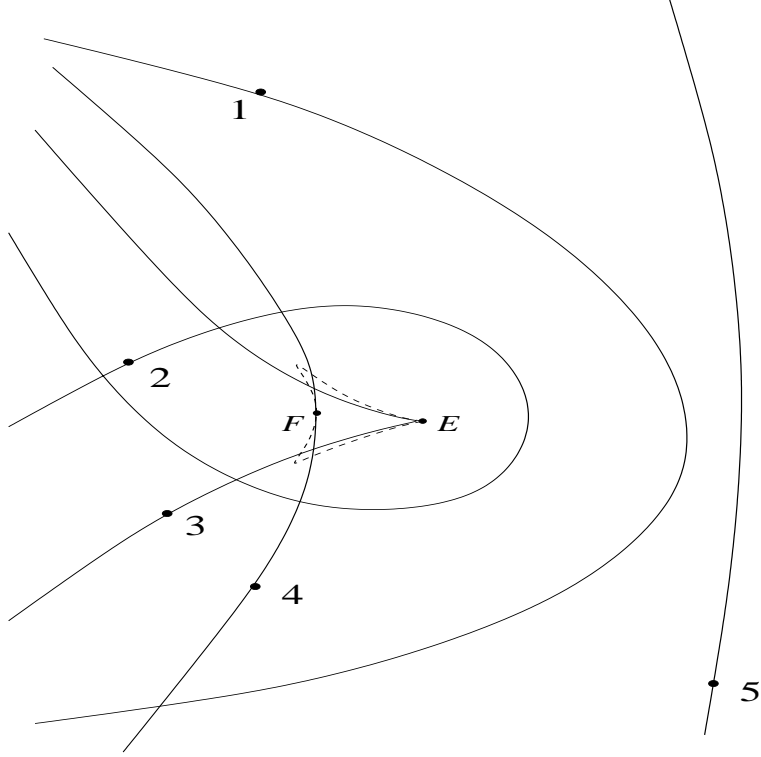


Figure 8: Qualitative description of the flow near a caustic ring. The solid lines are at the intersection of five simultaneous infall spheres corresponding to different initial times $t_{05} < t_{04} < \dots < t_{01}$. The five numbered points are at $\vec{x}(\alpha, t_{0k}), k = 1, \dots, 5$, for some value of α . Points E and F are defined in the text. The closed dashed line is at the intersection of the caustic tube with the plane of the figure. There are four flows inside the dashed line whereas outside there are two. The galactic center is to the left of the figure.

show the positions $\vec{x}(\alpha, t_{0k}), k = 1, \dots, 5$, for a fixed α and five different initial times and following the dots gives one a qualitative picture of the flow in time. The t_{01} sphere is falling in but has not yet crossed itself, as in frame Fig. 6.B. The t_{02} sphere has crossed itself but has not yet completed the process of turning itself inside out, as in frame Fig. 6.C. The t_{03} sphere is just completing the process of turning itself inside out, as in frame Fig. 6.D. The cusp at point E is the location of a caustic for the reason given earlier. Let α_E be the value of α at E and hence, $\vec{x}(\alpha_E, t_{03})$ be the position of E in space. The particles at the cusp are moving to the left. Thus at (α_E, t_{03}) , $\dot{\vec{x}}$ is pointing to the left, whereas \vec{x}_{t_0} is pointing to the right of the t_{03} infall sphere. Although time t increases in the direction

of motion, initial time t_0 decreases (earlier infall spheres are older, hence t increases in the direction of motion, or equivalently they have smaller birthday t_0). Therefore $\frac{\partial}{\partial t_0} \sim -\frac{\partial}{\partial t}$.

For smaller initial times, such as t_{05} , the spheres move to the right; hence $\dot{\vec{x}}$ points to the right of the infall sphere, whereas \vec{x}_{t_0} points to the left. Let t_{04} be the initial time and F be the point where $\vec{x}_{t_0}(\alpha_E, t_0)$ crosses the t_{04} sphere. Then, according to Eq. 151, $D = \vec{x}_{t_0} \cdot (\vec{x}_\alpha \times \vec{x}_\beta)$ vanishes at F because \vec{x}_{t_0} is on the sphere and $(\vec{x}_\alpha \times \vec{x}_\beta)$ is perpendicular to the sphere at F . Thus F is the location of a caustic as well. Now, let us consider any other point which is far from both E and F . At such a point there are two flows because the sphere passes such a point twice, once on the way in and once on the way out. Consider also a point between E and F . At such a point there are four flows because the sphere passes by four times. We can count these flows on Fig. 8 at fixed t as follows: twice for initial time t_0 between t_{02} and t_{03} (down and up flows), once between t_{03} and t_{04} (in flow), and once between t_{04} and t_{05} (outflow). Therefore, there is a finite compact region whose boundary in the plane of Fig. 8 is shown by the dashed lines. Inside the region there are four flows (down, up, in and out), while outside there are two (in the left of the region, down and up; in the right, in and out). The boundary of this region is the location of the tube caustic. If the successive spheres all fall in exactly the same way, the caustic ring is stationary. In general, however, the trajectories of successive spheres change slowly in time t , due to the growth of the halo during the infall and inhomogeneities. As a result the caustic ring moves about.

3.5.2 Axially Symmetric Caustic Ring

In this section we assume that the dark matter flow in and out of the galaxy is axially (rotationally) symmetric about \hat{z} and reflection symmetric under $z \rightarrow -z$. We use the following parametrization of the flow. Let $R(t_0)$ be the turnaround radius in the $z = 0$ plane at time t_0 . Then let $\vec{x}(\theta_0, \varphi_0, t_0; t)$ be the position at time t of the particle that was at the location of polar and azimuthal angles (θ_0, φ_0) on the sphere of radius $R(t_0)$ at

time t_0 . With this choice, we keep the size of the sphere that we use to label the particles comparable to the size of the growing galaxy. The density is given by Eqs. 143 and 144 with $\vec{\alpha} = (\theta_0, \varphi_0, t_0)$. There are n flows outside the closed tube, whereas there are $n + 2$ flows inside, as described in a general fashion in the previous section.

Although the flow is in 3D space, in general, the dimension along the tube is irrelevant as far as the caustic properties are concerned. Particles are actually moving in this direction, however the motion is a simple rotation along the azimuthal direction. To discover the essential properties of the caustic tubes, it is sufficient to consider the cross-section perpendicular to the trivial direction. Thus, the flow is in effect two dimensional, even in the absence of axial symmetry. The essential properties of caustics are invariant under continuous deformations. To proceed further, we will assume axial symmetry of the flow in this section. Therefore, let's throw away the irrelevant φ coordinate and choose $\rho(\alpha, t_0; t)$ and $z(\alpha, t_0; t)$ as the cylindrical coordinates at time t of the ring of particles which start to fall-in with the polar angle $\theta_0 = \frac{\pi}{2} - \alpha$ at initial time t_0 . We then can write the number of particles

$$N = \int \rho d\rho dz 2\pi d(\rho, z, t) = \int d\alpha dt_0 d\phi \frac{d^3 N}{d\alpha dt_0 d\phi}(\alpha, t_0, \phi) = \int d\alpha dt_0 \frac{d^2 N}{d\alpha dt_0}(\alpha, t_0) \quad . \quad (162)$$

In the last equation, changing variables $(\alpha, t_0) \rightarrow (\rho, z)$, we obtain

$$N = \int d\rho dz \sum_{j=1}^{n(\rho, z, t)} \frac{d^2 N}{d\alpha dt_0}(\alpha, t_0) \frac{1}{|D_2(\alpha, t_0)|} \Big|_{(\alpha, t_0) = (\alpha, t_0)_j(\rho, z, t)} \quad , \quad (163)$$

where the determinant of the Jacobian

$$D_2(\alpha, t_0) = \det \left(\frac{\partial(\rho, z)}{\partial(\alpha, t_0)} \right) \quad , \quad (164)$$

and $(\alpha, t_0)_j$, with $j = 1 \dots n$, are the solutions of $\rho = \rho(\alpha, t_0; t)$, $z = z(\alpha, t_0; t)$, and n is a function of ρ , z , and t . Comparing Eqs. 162 and 164, we find

$$d(\rho, z, t) = \frac{1}{2\pi\rho} \sum_{j=1}^{n(\rho, z, t)} \frac{d^2 N}{d\alpha dt_0}(\alpha, t_0) \frac{1}{|D_2(\alpha, t_0)|} \Big|_{(\alpha, t_0) = (\alpha, t_0)_j(\rho, z, t)} \quad . \quad (165)$$

Under a reparametrization of the flow $(\alpha, t_0) \rightarrow [\alpha'(\alpha, t_0), t'_0(\alpha, t_0)]$, the determinant transforms according to

$$D_2(\alpha, t_0) = D'_2(\alpha', t'_0) \det \left(\frac{\partial(\alpha', t'_0)}{\partial(\alpha, t_0)} \right). \quad (166)$$

In particular, for an α -dependent time shift:

$$\alpha' = \alpha, \quad t'_0 = t_0 + \Delta t_0(\alpha), \quad (167)$$

the Jacobian of the transformation $\det \left(\frac{\partial(\alpha', t'_0)}{\partial(\alpha, t_0)} \right) = 1$, and

$$D_2(\alpha, t_0) = D'_2(\alpha', t'_0). \quad (168)$$

Therefore, reparametrizations of type Eq. 167 leaves the determinant D_2 unchanged.

3.5.3 Flow near an Axially Symmetric Caustic Ring

In section 3.3 we qualitatively described the CDM flow near a ring caustic, as summarized in Fig. 8. In this section, we give a quantitative description of ring caustics in the case of axial and reflection symmetry. Reflection symmetry is automatic if the caustic is tight, namely if the transverse dimensions p and q of the caustic are small compared to the tube radius. We will assume that the caustics are tight.

Recall that the flow is reparametrization invariant. In Fig. 8 we describe the flow at given time t . The time of observation is fixed. However, we use initial time t_0 to label the particles. Now, let us introduce a Cartesian coordinate system on Fig. 8 by choosing the point E as the origin, the horizontal axis as the x -axis, and the vertical axis as the z -axis. In the reflection symmetric case, points E and F have $z = 0$. Let us label the particles on the $z = 0$ axis by $(\alpha, \tau = 0)$ and relabel the flow by shifting the initial time t_0 in an α dependent way: $\alpha \rightarrow \alpha, t_0 \rightarrow \tau = t_0 + \Delta t_0(\alpha)$ such that $z(\alpha, \tau = 0) = 0$ for all α . Physically this means that we relabel the particle going through the cusp at E by $(\alpha, \tau) = (0, 0)$ and all the other particles on the negative x -axis ($z = 0$), by $(\alpha, \tau = 0)$. Due to the reflection

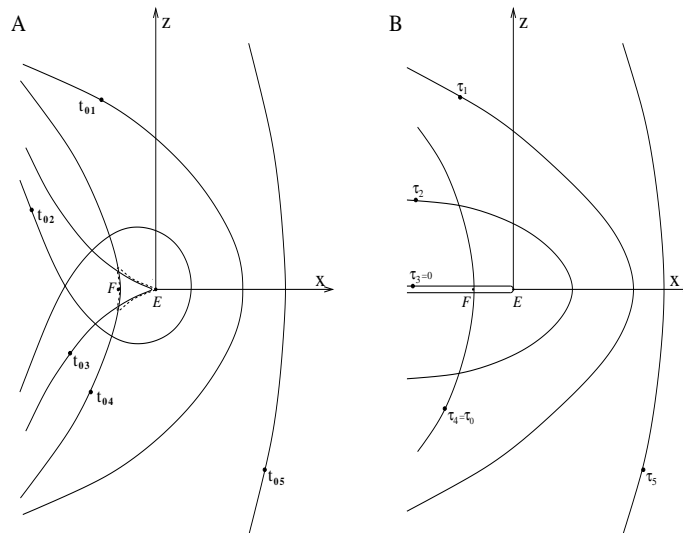


Figure 9: Qualitative descriptions of the reflection symmetric flow near a caustic ring. A) Same as Fig. 8 except that now the flow has reflection symmetry and we introduce a coordinate system whose origin is at the cusp E . $\alpha = 0$ at E . The x -coordinates of the particles labelled by $\pm\alpha$ are the same whereas their z -coordinates have the opposite sign. B) We reparametrize the flow by shifting t_0 in an α dependent way: $t_0 \rightarrow \tau = t_0 + \Delta t_0(\alpha)$ such that $z(\alpha, \tau = 0) = 0$ for all α . We label the particle at the cusp by $(\alpha, \tau) = (0, 0)$ and all the other particles on the negative x -axis by $(\alpha, \tau = 0)$. Due to the reflection symmetry, we have $(z, x) \rightarrow (-z, x)$ under $(\alpha, \tau) \rightarrow (-\alpha, \tau)$. This fixes the labelling for the rest of the particles in the flow.

symmetry, we must have $(z, x) \rightarrow (-z, x)$ under $(\alpha, \tau) \rightarrow (-\alpha, \tau)$. We are interested in the caustics in the flow. The properties of a caustic depend on the flow near the caustic only. It does not matter what happens in the flow away from the caustic. Therefore, we want to expand the flow (x and z) near the caustic in powers of the parameters α and τ keeping terms up to second order only. Let's start with the shell of particles that is going through the cusp. This particular shell is in fact a line segment on the x - z plane where $z = 0$ and $x < 0$. Recall that the parameter τ is chosen as zero for this line. Hence, the parametrization satisfying the above symmetry requirements is

$$z = 0 \quad x = -\frac{1}{2}s \alpha^2, \quad (169)$$

for this line of particles of the flow, where s is an arbitrary constant. Now, let's expand

the flow around the cusp where $\alpha = \tau = 0$ by writing the most general second order polynomials:

$$\begin{aligned} z &= c_1 \alpha + c_2 \tau + c_3 \alpha^2 + c_4 \alpha\tau + c_5 \tau^2 , \\ x &= d_1 \alpha + d_2 \tau + d_3 \alpha^2 + d_4 \alpha\tau + d_5 \tau^2 . \end{aligned} \quad (170)$$

Due to reflection symmetry, z must be odd whereas x must be even under $(\alpha, \tau) \rightarrow (-\alpha, \tau)$. We then have $c_2 = c_3 = c_5 = 0$ in z and $d_1 = d_4 = 0$ in x . Applying the condition that at $\tau = 0$, $z = 0$ and $x = -\frac{1}{2}s\alpha^2$, we identify $c_1 = 0$ and $d_3 = -\frac{1}{2}s$. Renaming the constants as $c_4 \equiv b$, $d_2 \equiv -u\tau_0$, $d_5 \equiv \frac{1}{2}u$ where u and τ_0 are constants, we have

$$z = b\alpha\tau , \quad (171)$$

$$x = \frac{1}{2}u [(\tau - \tau_0)^2 - \tau_0^2] - \frac{1}{2}s\alpha^2 . \quad (172)$$

If we call ρ_0 the ρ -coordinate of point E where $\alpha = \tau = 0$, we have $x = \rho - \rho_0$. Equation 172 can then be written as

$$\rho = a + \frac{1}{2}u(\tau - \tau_0)^2 - \frac{1}{2}s\alpha^2 , \quad (173)$$

where we introduce a new constant

$$a \equiv \rho_0 - \frac{1}{2}u\tau_0^2 \equiv \rho_0 - p , \quad (174)$$

which will turn out to be the inner tube radius (ρ -coordinate of point F where $\alpha = 0$ and $\tau = \tau_0$) and $p = \frac{1}{2}u\tau_0^2$, the longitudinal dimension of the tube. The parameters b , u and s are positive.

The parameter b is positive because the flow is from top to bottom, $\frac{dz}{dt} < 0$, (bottom to top, $\frac{dz}{dt} > 0$) for particles with $\alpha > 0$ ($\alpha < 0$). Remember that particles closer to the $z = 0$ plane reached the turn around sphere earlier; therefore, they have smaller t_0 , and hence smaller τ . Although time t increases in the direction of motion, τ decreases. Hence,

for particles with $\alpha > 0$ ($\alpha < 0$), $\frac{dz}{d\tau} \sim -\frac{dz}{dt} > 0$ ($\frac{dz}{d\tau} \sim -\frac{dz}{dt} < 0$). Since $\frac{dz}{d\tau} = b\alpha$, the constant $b > 0$. Thus, $b\alpha$ is the negative of the velocity in the z direction of the particle coming in at an angle α . For particles with $\alpha = 0$ the velocity in the z direction is zero, because they move in the $z = 0$ plane.

The parameter u is positive because the particles with $\alpha = 0$ are accelerated outward by the angular momentum barrier, hence $\rho = a + \frac{1}{2}u(\tau - \tau_0)^2 \geq a$. Thus, u is the acceleration of the particles away from the distance of closest approach. The parameter s is positive because at $\tau = 0$, the particles with $\alpha \neq 0$ are at $\rho = \rho_0 - \frac{1}{2}s\alpha^2 < \rho_0$. The parameter τ_0 , which is the time it takes a particle to go from the cusp to the radius of closest approach, can either be positive or negative. Since $p = \frac{1}{2}u\tau_0^2 > 0$, $a = \rho_0 - p$ is always smaller than ρ_0 (i.e., point F is always closer to the galactic center than point E , as noted earlier).

The determinant of the Jacobian $D_2(\alpha, \tau) \equiv \det \mathcal{D}(\alpha, \tau)$ where

$$\mathcal{D}(\alpha, \tau) \equiv \begin{pmatrix} \frac{\partial \rho}{\partial \alpha} & \frac{\partial z}{\partial \alpha} \\ \frac{\partial \rho}{\partial \tau} & \frac{\partial z}{\partial \tau} \end{pmatrix} = \begin{pmatrix} -s\alpha & b\tau \\ u(\tau - \tau_0) & b\alpha \end{pmatrix}, \quad (175)$$

is

$$D_2(\alpha, \tau) = -b[u\tau(\tau - \tau_0) + s\alpha^2], \quad (176)$$

and vanishes for

$$\alpha = \pm \sqrt{\frac{u}{s}\tau(\tau_0 - \tau)}, \quad (177)$$

with $0 < \tau < \tau_0$ if $\tau_0 > 0$, and $\tau_0 < \tau < 0$ if $\tau_0 < 0$. Since the CDM density diverges where D_2 vanishes, by substituting Eq. 177 into Eqs. 171 and 173, we find parametric ($\tau =$ parameter) equations describing the cross-section of the caustic surface in the (ρ, z) -plane:

$$\rho = a + \frac{1}{2}u(\tau - \tau_0)(2\tau - \tau_0), \quad (178)$$

$$z = \pm b \sqrt{\frac{u}{s}\tau^3(\tau_0 - \tau)}. \quad (179)$$

Figure 3 shows a plot of the cross-section. Both $\rho(\tau)$ and $z(\tau)$ are extremized for $\tau = \frac{3}{4}\tau_0$, where $\rho = a - \frac{1}{8}p$ and $z = \pm \frac{\sqrt{27}}{8} \frac{b}{\sqrt{us}} p$. At $\tau = 0$, $\rho = a + p$ and $z = 0$. At $\tau = \tau_0$, $\rho = 0$ and $z = 0$. Thus, the dimensions of the cross section in the $\hat{\rho}$ and \hat{z} directions are

$$p = \frac{1}{2}u\tau_0^2 \quad \text{and} \quad q = \frac{\sqrt{27}}{4} \frac{b}{\sqrt{us}} p \quad , \quad (180)$$

respectively. The caustic has three cusps: one at $\tau = 0$ where $(\rho, z) = (a + p, 0)$; and two at $\tau = \frac{3}{4}\tau_0$ where $(\rho, z) = (a - \frac{1}{8}p, \pm \frac{1}{2}q)$.

The three cusps are related by Z_3 transformations. To show this, let us rescale the parameters:

$$T = \frac{\tau}{\tau_0} \quad , \quad A = \sqrt{\frac{s}{u}} \frac{1}{\tau_0} \alpha \quad , \quad (181)$$

and rescale and shift (in the $\hat{\rho}$ direction) the coordinates:

$$Z = \frac{2}{b} \sqrt{\frac{s}{u}} \frac{1}{\tau_0^2} z \quad , \quad X = \frac{2}{u\tau_0^2} (\rho - a) - \frac{1}{4} \quad , \quad (182)$$

Eqs. 171 and 173 then become

$$Z = 2AT \quad , \quad X = (T - 1)^2 - A^2 - \frac{1}{4} \quad . \quad (183)$$

These relations are invariant under the discrete transformation:

$$\begin{aligned} Z' &= -X \sin(-2\pi/3) + Z \cos(-2\pi/3) = -\frac{1}{2}Z + \frac{\sqrt{3}}{2}X \quad , \\ X' &= X \cos(-2\pi/3) + Z \sin(-2\pi/3) = -\frac{\sqrt{3}}{2}Z - \frac{1}{2}X \quad , \\ T' &= -\frac{1}{2}T + \frac{\sqrt{3}}{2}A + \frac{3}{4} \quad , \quad A' = -\frac{\sqrt{3}}{2}T - \frac{1}{2}A + \frac{\sqrt{3}}{4} \quad . \end{aligned} \quad (184)$$

Notice that the cube of this transformation is the identity: $Z''' = Z$, $X''' = X$, $A''' = A$, and $T''' = T$. In the X-Z plane, the transformation is a rotation by 120° . It transforms the three cusps of the caustic into one another. Thus, after the rescaling, the caustic has a Z_3 symmetry. Hereafter, we will call the shape of Fig. 3 “tricuspid.” In the language of

Catastrophe Theory, the tricusp is a D_{-4} catastrophe. The apparent reason for the two cusps which are not on the $\hat{\rho}$ -axis in Fig. 3 is that both

$$\frac{d\rho}{d\tau} = \frac{u}{2}(4\tau - 3\tau_0) , \quad (185)$$

and

$$\frac{dz}{d\tau} = \pm \frac{b}{2} \sqrt{\frac{u}{s} \frac{(3\tau_0 - 4\tau)}{\sqrt{\frac{u}{\tau} - 1}}} , \quad (186)$$

vanish for $\tau = \frac{3}{4}\tau_0$. The simultaneous vanishing of $\frac{d\rho}{d\tau}$ and $\frac{dz}{d\tau}$ is, however, not an accident peculiar to our assumptions of symmetry and/or our limiting the expansion of ρ and z to terms of second order in α and τ . This claim is easy to prove. Notice that the equation for the location of a generic caustic in 2 dimensions:

$$D_2(\alpha, \tau) = \frac{\partial\rho}{\partial\alpha} \frac{\partial z}{\partial\tau} - \frac{\partial\rho}{\partial\tau} \frac{\partial z}{\partial\alpha} = 0 \quad , \quad (187)$$

defines $\alpha(\tau)$ such that $[\rho(\tau) = \rho(\alpha(\tau), \tau), z(\tau) = z(\alpha(\tau), \tau)]$ is a parametric representation of the caustic location. Wherever $\rho(\tau)$ has an extremum, $z(\tau)$ is expected to have an extremum as well, since

$$\frac{d\rho}{d\tau} = \frac{\partial\rho}{\partial\alpha} \frac{d\alpha}{d\tau} + \frac{\partial\rho}{\partial\tau} = 0 , \quad (188)$$

implies

$$\frac{\partial\rho}{\partial\tau} = - \frac{\partial\rho}{\partial\alpha} \frac{d\alpha}{d\tau} . \quad (189)$$

And Eq. (187) yields

$$\frac{\partial\rho}{\partial\alpha} \left[\frac{\partial z}{\partial\tau} + \frac{\partial z}{\partial\alpha} \frac{d\alpha}{d\tau} \right] = 0 , \quad (190)$$

which implies

$$\frac{dz}{d\tau} = \frac{\partial z}{\partial\alpha} \frac{d\alpha}{d\tau} + \frac{\partial z}{\partial\tau} = 0 , \quad (191)$$

if $\frac{\partial\rho}{\partial\alpha}$ and $\frac{d\alpha}{d\tau}$ are finite. In the same way, it can be shown that the vanishing of $\frac{dz}{d\tau}$ implies that $\frac{d\rho}{d\tau} = 0$. The cusp at point E may appear to have a different origin. Its apparent reason is that $z \sim \pm\tau^{\frac{3}{2}}$ near $\tau = 0$ which is at the boundary of the range of τ . This,

however, is an artifact of the parametrization we have used. Indeed, we saw that the three cusps can be transformed to each other due to a Z_3 symmetry, hence the cusp on the $\hat{\rho}$ -axis can be given the same parametrization as the other two. In conclusion, the appearance of three cusps in the cross-section of a ring caustic is neither an accidental consequence of the assumed axial and reflection symmetries nor is it due to the expansion including only second order terms in Eq. 170.

Inside (outside) the tricusp, there are four (two) flows. To count the distinct flows, let us restrict ourselves to the $z = 0$ plane, where either $\alpha = 0$ or $\tau = 0$. If $\alpha = 0$, then $\rho = a + \frac{1}{2}u(\tau - \tau_0)^2 > a$. If $\tau = 0$, then $\rho = a + \frac{1}{2}u\tau_0^2 - \frac{1}{2}s\alpha^2 < \rho_0$. Thus, for $z = 0$ and $\rho > a$, with $\alpha = 0$, there are two flows parametrized by

$$(\alpha, \tau_+) = \left(0, \tau_0 + \sqrt{\frac{2}{u}(\rho - a)} \right), \quad (\alpha, \tau_-) = \left(0, \tau_0 - \sqrt{\frac{2}{u}(\rho - a)} \right). \quad (192)$$

Both of the flows have

$$\frac{\partial z}{\partial t}(\alpha = 0) = -\frac{\partial z}{\partial \tau}(\alpha = 0) = 0, \quad (193)$$

whereas

$$\frac{\partial \rho}{\partial t}(\alpha = 0, \tau_+) = -\frac{\partial \rho}{\partial \tau}(\alpha = 0, \tau_+) = -u(\tau_+ - \tau_0) = -\sqrt{2u(\rho - a)}, \quad (194)$$

$$\frac{\partial \rho}{\partial t}(\alpha = 0, \tau_-) = -\frac{\partial \rho}{\partial \tau}(\alpha = 0, \tau_-) = -u(\tau_- - \tau_0) = +\sqrt{2u(\rho - a)}. \quad (195)$$

Thus, we call the flow (α, τ_+) , for which $\frac{\partial \rho}{\partial t} < 0$, the “in” flow and the flow (α, τ_-) , for which $\frac{\partial \rho}{\partial t} > 0$, the “out” flow. For $z = 0$, ($\alpha \neq 0, \tau = 0$) and hence $\rho = \rho_0 - \frac{1}{2}s\alpha^2 < \rho_0$, there are two other flows parametrized by

$$(\alpha_+, \tau) = \left(\sqrt{\frac{2}{s}(\rho_0 - \rho)}, 0 \right), \quad (\alpha_-, \tau) = \left(-\sqrt{\frac{2}{s}(\rho_0 - \rho)}, 0 \right), \quad (196)$$

for both of which

$$\frac{\partial \rho}{\partial t}(\tau = 0) = -\frac{\partial \rho}{\partial \tau}(\tau = 0) = u\tau_0, \quad (197)$$

whereas

$$\begin{aligned}\frac{\partial z}{\partial t}(\alpha_+, \tau = 0) &= -\frac{\partial z}{\partial \tau}(\alpha_+, \tau = 0) = -b\alpha_+ = -b\sqrt{\frac{2}{s}(\rho_0 - \rho)}, \\ \frac{\partial z}{\partial t}(\alpha_-, \tau = 0) &= -\frac{\partial z}{\partial \tau}(\alpha_-, \tau = 0) = -b\alpha_- = +b\sqrt{\frac{2}{s}(\rho_0 - \rho)}.\end{aligned}\quad (198)$$

Thus, we call the flow $(\alpha_+, \tau = 0)$, for which $\frac{\partial z}{\partial t} < 0$ as the “down” flow and the flow $(\alpha_-, \tau = 0)$, for which $\frac{\partial z}{\partial t} > 0$ as the “up” flow. Therefore, in the $z = 0$ plane, there are four flows (in, out, down and up) for $a < \rho < \rho_0$, whereas there are two flows (down and up) for $\rho < a$, and two flows (in and out) for $\rho > \rho_0$.

Away from the cusps, the caustic is a generic surface caustic, as described in Section 3.2. Thus, if one approaches the boundary of the tricusp from the inside and away from any of the cusps, as will be shown for a sample point below, the density diverges as $d \sim \frac{1}{\sqrt{\sigma}}$ where σ is the distance to the boundary. If the boundary is approached from the outside, away from any of the cusps, then the density remains finite until the boundary is reached. To illustrate this, let us again restrict ourselves to the $z = 0$ plane and calculate D_2 as $\rho - a \rightarrow 0_+$ and $\rho - a \rightarrow 0_-$. In the former case there are four flows (up, down, in and out), while in the latter there are only two (up and down). The caustic is caused by the appearance of the extra in and out flows in the region $\rho > a$. For $z = 0$, and $\rho - a \rightarrow 0_+$, the in and out flows have $(\alpha, \tau) = (0, \tau_0 \pm \sqrt{\frac{2}{u}(\rho - a)})$, respectively. Therefore the determinant (176) is

$$D_2 = \mp b\tau \sqrt{2u(\rho - a)}. \quad (199)$$

Since $\tau \rightarrow \tau_0$ as $\rho - a \rightarrow 0_+$ when $\alpha = 0$, $D_2 \simeq \mp b\tau_0 \sqrt{2u(\rho - a)}$ for the in and out flows, the density associated with these flows diverges as $\frac{1}{\sqrt{\rho - a}}$. The two other flows (down and up) yield finite contributions to the density. At $z = 0$, for the down and up flows $(\alpha_{\pm}, \tau) = (\pm \sqrt{\frac{2}{s}(\rho_0 - \rho)}, 0)$. Hence, the determinant

$$D_2 = -bs\alpha_{\pm}^2 = -2b(\rho_0 - \rho) = -2b(a + p - \rho). \quad (200)$$

Therefore, in the limits $\rho - a \rightarrow 0_+$, ($\rho > a$), and $\rho - a \rightarrow 0_-$, ($\rho < a$), $|D_2| \rightarrow 2bp$ for the down and up flows. The contribution of each flow to the density, in both regions, is $\frac{1}{2bp}$.

Near the cusps, the behavior depends upon the direction of approach. For $z = 0$ and $\rho - \rho_0 \rightarrow 0_-$ (inside the caustic tube), there are four flows: in, out, up and down. For $\rho - \rho_0 \rightarrow 0_+$ (outside the caustic tube), there are two flows: in and out. In the region $\rho < \rho_0$, in addition to the extra down and up flows, which both diverge in the limit $\rho - \rho_0 \rightarrow 0_-$, one of the common flows (out flow if $\tau_0 > 0$, in flow if $\tau_0 < 0$) of the regions also diverges in both limits $\rho - \rho_0 \rightarrow 0_{\pm}$, whereas the other (in flow if $\tau_0 > 0$, out flow if $\tau_0 < 0$) remains finite. Notice that near the cusp (unlike the case $\rho - a < 0$ where both of the down and up flows remain finite as one approaches the caustic from the outside), there is a flow which diverges as one approaches the caustic from the outside of the tube. Hence, the cusps are more divergent than the folds.

Let us first calculate the density due to the down and up flows which exist only in the region $\rho < \rho_0$, for $z = 0$ and $\rho - \rho_0 \rightarrow 0_-$. Recall (Eq. 196) that in the $z = 0$ plane, for the up and down flows, $\tau = 0$ and $\alpha^2 = \frac{2}{s}(\rho - \rho_0)$. Then, $D_2 = -bs\alpha^2 = 2b(\rho_0 - \rho)$, and hence $d \sim \frac{1}{\rho_0 - \rho}$. Let us now calculate the density due to the in and out flows which exist for both $\rho < \rho_0$ and $\rho > \rho_0$. For $\rho - \rho_0 \rightarrow 0_-$, let us write $\rho \equiv \rho_0 - \sigma$ where $\sigma \rightarrow 0_+$. Then, Eq. 192 gives for the in and out flows

$$(\alpha, \tau_{\pm}) = \left(0, \tau_0 \pm \sqrt{\tau_0^2 - \frac{2}{u}\sigma}\right), \quad (201)$$

respectively. Thus, using Eq. 176, we find

$$D_2 = -bu \left[\pm \tau_0 |\tau_0| \sqrt{1 - \frac{\sigma}{p} + \tau_0^2 - \frac{2}{u}\sigma} \right]. \quad (202)$$

If $\tau_0 > 0$ the in flow gives, to first order in σ ,

$$D_2 \simeq -bu \left[2\tau_0^2 - \frac{3}{u}\sigma \right]. \quad (203)$$

As $\sigma \rightarrow 0$, $D_2 \rightarrow -2bu\tau_0^2 = -4bp$. Hence the density of the in flow $d \sim \frac{1}{4bp}$ is finite for $\tau_0 > 0$. The out flow, however, has a divergent density for $\tau_0 > 0$. Since $D_2 \simeq b\sigma = b(\rho_0 - \rho)$, the density is $d \sim \frac{1}{\rho_0 - \rho}$. If $\tau_0 < 0$, the flows are time reversed: the out flow becomes the in flow and vice versa. Indeed, Eq. 202 gives $D_2 \simeq b\sigma$, hence $d \sim \frac{1}{\rho_0 - \rho}$ for the in flow, and $D_2 \simeq -bu[2\tau_0^2 - \frac{3}{u}\sigma]$, which yields $d \sim \frac{1}{4bp}$ for the out flow. For the region $\rho > \rho_0$, in the limit $\rho - \rho_0 \rightarrow 0_+$, $\rho = \rho_0 + \sigma$ where $\sigma \rightarrow 0_+$. Then, for the in and out flows $(\alpha, \tau_{\pm}) = (0, \tau_0 \pm \sqrt{\tau_0^2 + \frac{2}{u}\sigma})$ and $D_2 = -bu[\pm\tau_0|\tau_0|\sqrt{1 + \frac{\sigma}{p}} + \tau_0^2 + \frac{2}{u}\sigma]$. Therefore, the in and out flows have the same density as for the in and out flows where $\rho - \rho_0 \rightarrow 0_-$. If $\tau_0 > 0$, the in flow is finite: $d \sim \frac{1}{4bp}$ and the out flow is divergent: $d \sim \frac{1}{\rho - \rho_0}$. If $\tau_0 < 0$, flows are time reversed, hence the in flow has $d \sim \frac{1}{\rho - \rho_0}$ and the out flow has $d \sim \frac{1}{4bp}$.

Finally, let us calculate the density near the cusp at $\rho = \rho_0$ and as $z \rightarrow 0_{\pm}$. Since $\rho = \rho_0 - u\tau_0\tau + \frac{u}{2}\tau^2 - \frac{s}{2}\alpha^2$, at $\rho = \rho_0$ where $(\tau, \alpha) = (0, 0)$,

$$-u\tau_0\tau + \frac{u}{2}\tau^2 - \frac{s}{2}\alpha^2 = 0. \quad (204)$$

Near the cusp, where $(\rho, z) = (\rho_0, 0_{\pm})$, $(\tau, \alpha) \neq (0, 0)$ and α and τ are independent since the point of interest is not exactly on the caustic surface. The determinant $D_2 = -b[u\tau^2 - u\tau_0\tau + s\alpha^2]$ can be written at $\rho = \rho_0$, using Eq. 204 as

$$D_2 = -bu[2\tau^2 - 3\tau_0\tau]. \quad (205)$$

Since $\frac{z}{\alpha} = b\tau$, D_2 at ρ_0 can also be written as

$$D_2 = -u \left[\frac{2}{b} \frac{z^2}{\alpha^2} - 3\tau_0 \frac{z}{\alpha} \right]. \quad (206)$$

Since near the cusp $\frac{z}{\alpha} = b\tau \rightarrow 0$, $(\frac{z}{\alpha})^2$ can be neglected next to $\frac{z}{\alpha}$ in the above equation. This is equivalent to neglecting the $u\tau^2$ term next to $u\tau$ in Eq. 204. Therefore, from Eq. 204 and Eq. 206 we obtain

$$\alpha^2 \simeq -2\frac{u}{s}\tau_0\tau = -2\frac{u}{bs}\tau_0\frac{z}{\alpha} \Rightarrow \alpha \simeq \left[-2\frac{u}{bs}\tau_0z \right]^{1/3}, \quad (207)$$

and

$$D_2 \simeq 3u\tau_0 \frac{z}{\alpha} = -3 \left[\frac{u^2 b \tau_0^2 s |z|^2}{2} \right]^{1/3}, \quad (208)$$

for *one* of the flows. Hence $d \sim \frac{1}{|z|^{2/3}}$ for this flow. Thus, we find that, the density also diverges in this particular limit near the cusp.

The tube caustic collapses to a line caustic in the limit $\tau_0 \rightarrow 0$ with $\frac{b}{\sqrt{us}}$ fixed. In this limit

$$p = \frac{1}{2}u\tau_0^2 \rightarrow 0, \quad q = \frac{\sqrt{27}}{4} \frac{b}{\sqrt{us}} p \rightarrow 0, \quad (209)$$

$$D_2 \rightarrow -b(u\tau^2 + s\alpha^2), \quad \rho \rightarrow a + \frac{1}{2}(u\tau^2 - s\alpha^2). \quad (210)$$

Therefore, we can rewrite

$$D_2 = -2\sqrt{b^2 [(\rho - a) + s\alpha^2]^2} = -2\sqrt{-b^2 [(\rho - a)^2 + s^2\alpha^4 + s\alpha^2(u\tau^2 - s\alpha^2)]}, \quad (211)$$

where we replaced $\rho - a$ by $\frac{1}{2}(u\tau^2 - s\alpha^2)$ using Eq. 211. Since $z = b\alpha\tau$, we might write

$$D_2 = -2\sqrt{b^2(\rho - a)^2 + usz^2}. \quad (212)$$

Hence the density

$$d(\rho, z) = \frac{1}{2\pi\rho} \frac{d^2N}{d\alpha dt_0} \frac{1}{\sqrt{b^2(\rho - a)^2 + usz^2}}, \quad (213)$$

in the $\tau_0 \rightarrow 0$ limit. When p and q are finite, but much smaller than a , Eq. 213 is approximately valid for $p, q \ll \sigma \ll a$ since the terms of order τ_0 in Eqs. 171, 173 and 176 are negligible in this regime.

3.5.4 Differential Geometry of an Axially Symmetric Caustic Ring

In this section, the differential geometric properties of the axially symmetric caustic ring are studied. At the end, we calculate the principal curvature radii, which are needed for lensing applications, at an arbitrary point on the ring surface. Any surface in R^3 is uniquely determined by certain local invariant quantities called first and second fundamental forms. Following [55], let us derive the fundamental forms for the ring surfaces.

Let $\vec{X} = \vec{X}(\tau, \phi)$ be a coordinate patch on a surface. The differential of the map $\vec{X} = \vec{X}(\tau, \phi)$ at (τ, ϕ) is a one to one linear map

$$d\vec{X} = \vec{X}_\tau d\tau + \vec{X}_\phi d\phi , \quad (214)$$

with $\vec{X}_\tau \equiv \frac{\partial \vec{X}}{\partial \tau}$, $\vec{X}_\phi \equiv \frac{\partial \vec{X}}{\partial \phi}$, of the vectors $(d\tau, d\phi)$, which extend from (τ, ϕ) to $(\tau + d\tau, \phi + d\phi)$ in the $\tau\phi$ -plane, on to the vectors $\vec{X}_\tau d\tau + \vec{X}_\phi d\phi$ parallel to the tangent plane of the surface at $\vec{X}(\tau, \phi)$. Notice that, we are using the symbols $d\tau$ and $d\phi$ both for the differentials of the coordinate functions in the $\tau\phi$ -plane and for the components of a vector in the $\tau\phi$ -plane. In the same way, we denote $\vec{X}_\tau d\tau + \vec{X}_\phi d\phi$ by $d\vec{X}$. Recall that, since

$$\vec{X}(\tau + d\tau, \phi + d\phi) = \vec{X}(\tau, \phi) + d\vec{X} + O(d\tau^2, d\tau d\phi, d\phi^2) , \quad (215)$$

the vector $d\vec{X}$ is a first order approximation to the vector $\vec{X}(\tau + d\tau, \phi + d\phi) - \vec{X}(\tau, \phi)$ from the point $\vec{X}(\tau, \phi)$ on the patch, to the neighboring point $\vec{X}(\tau + d\tau, \phi + d\phi)$. Consider the quantity:

$$\begin{aligned} I \equiv ds^2 &\equiv (\vec{X}_\tau d\tau + \vec{X}_\phi d\phi) \cdot (\vec{X}_\tau d\tau + \vec{X}_\phi d\phi) \\ &= (\vec{X}_\tau \cdot \vec{X}_\tau) d^2\tau + 2(\vec{X}_\tau \cdot \vec{X}_\phi) d\tau d\phi + (\vec{X}_\phi \cdot \vec{X}_\phi) d^2\phi \\ &\equiv \mathbf{E} d^2\tau + 2\mathbf{F} d\tau d\phi + \mathbf{G} d^2\phi . \end{aligned} \quad (216)$$

The function I is called the first fundamental form of $\vec{X} = \vec{X}(\tau, \phi)$. The first fundamental coefficients \mathbf{E} , \mathbf{F} and \mathbf{G} are functions of τ and ϕ . Let us find the first fundamental form (i.e., the metric), on the caustic surface. The three vector

$$\vec{X}(\tau, \phi) = \rho(\tau) \cos(\phi) \hat{x} + \rho(\tau) \sin(\phi) \hat{y} + z(\tau) \hat{z} \quad (217)$$

completely describes the surface. The functions $\rho(\tau)$ and $z(\tau)$ are given in Eq. 179, which we copy here

$$\rho = a + \frac{1}{2}u(\tau - \tau_0)(2\tau - \tau_0) , \quad z = \pm b \sqrt{\frac{u}{s} \tau^3 (\tau_0 - \tau)} . \quad (218)$$

Since

$$\vec{X}_\tau = \rho' \cos(\phi)\hat{x} + \rho' \sin(\phi)\hat{y} + z'\hat{z}, \quad \vec{X}_\phi = -\rho \sin(\phi)\hat{x} + \rho \cos(\phi)\hat{y}, \quad (219)$$

where prime denotes $\frac{\partial}{\partial \tau}$, the first fundamental form coefficients for the caustic ring are

$$\mathbf{E} = \vec{X}_\tau \cdot \vec{X}_\tau = \rho'^2 + z'^2, \quad \mathbf{F} = \vec{X}_\tau \cdot \vec{X}_\phi = 0, \quad \mathbf{G} = \vec{X}_\phi \cdot \vec{X}_\phi = \rho^2. \quad (220)$$

Therefore,

$$ds^2 = (\rho'^2 + z'^2)d\tau^2 + \rho^2 d\phi^2. \quad (221)$$

Using Eq. 179 the explicit metric of the surface is found

$$ds^2 = \frac{1}{4} \left[u(3\tau_0 - 4\tau)^2 \left[u + \frac{b^2\tau}{s(\tau_0 - \tau)} \right] d\tau^2 + [2a + u(\tau_0 - \tau)(\tau_0 - 2\tau)]^2 d\phi^2 \right]. \quad (222)$$

The area \mathcal{A} of the caustic surface can be obtained readily since

$$\mathcal{A} = 2 \int_0^{2\pi} d\phi \int_0^{\tau_0} d\tau \sqrt{\det g} \quad (223)$$

where the determinant of the metric is $\mathbf{EG} - \mathbf{F}^2 > 0$. Because I is positive definite, its coefficients must satisfy $\mathbf{E} > 0$, $\mathbf{G} > 0$, and $\mathbf{EG} - \mathbf{F}^2 > 0$. This can easily be verified. Since \vec{X}_τ and \vec{X}_ϕ are independent, $\vec{X}_\tau \neq 0$, $\vec{X}_\phi \neq 0$, and hence $\mathbf{E} = \vec{X}_\tau \cdot \vec{X}_\tau = |\vec{X}_\tau|^2 > 0$, $\mathbf{G} = \vec{X}_\phi \cdot \vec{X}_\phi = |\vec{X}_\phi|^2 > 0$. The determinant

$$\begin{aligned} \det(g) = \mathbf{EG} - \mathbf{F}^2 &= (\vec{X}_\tau \cdot \vec{X}_\tau)(\vec{X}_\phi \cdot \vec{X}_\phi) - (\vec{X}_\tau \cdot \vec{X}_\phi)(\vec{X}_\tau \cdot \vec{X}_\phi) \\ &= (\vec{X}_\tau \times \vec{X}_\phi) \cdot (\vec{X}_\tau \times \vec{X}_\phi) = |\vec{X}_\tau \times \vec{X}_\phi|^2 > 0. \end{aligned} \quad (224)$$

On the caustic surface we have

$$\det(g) = (\rho'^2 + z'^2)\rho^2 = \frac{u}{16}(3\tau_0 - 4\tau)^2 \left(u + \frac{b^2\tau}{s(\tau_0 - \tau)} \right) [2a + u(\tau_0^2 - 3\tau_0\tau + 2\tau^2)]^2. \quad (225)$$

For simplicity, if we choose $\frac{us}{b^2} = 1$, we find the area as

$$\mathcal{A} = \frac{8\pi}{105} p (35a + 29p). \quad (226)$$

The non-vanishing, independent components of the Riemann and Ricci tensors of the caustic ring surface are

$$R_{\tau\phi\tau\phi} = \frac{\rho z'(\rho'z'' - z'\rho'')}{(\rho'^2 + z'^2)} = -\frac{ub^2 \tau_0(3\tau_0 - 4\tau)(2a + u(\tau_0^2 - 3\tau_0\tau + 2\tau^2))}{8(\tau_0 - \tau)(b^2\tau + us(\tau_0 - \tau))}, \quad (227)$$

$$R_{\tau\tau} = \frac{z'(\rho'z'' - z'\rho'')}{\rho(\rho'^2 + z'^2)} = -\frac{ub^2 \tau_0(3\tau_0 - 4\tau)}{2(\tau_0 - \tau)(b^2\tau + us(\tau_0 - \tau))(2a + u(\tau_0^2 - 3\tau_0\tau + 2\tau^2))}, \quad (228)$$

$$R_{\phi\phi} = \frac{\rho z'(\rho'z'' - z'\rho'')}{(\rho'^2 + z'^2)^2} = -\frac{sb^2 \tau_0(2a + u(\tau_0^2 - 3\tau_0\tau + 2\tau^2))}{2(3\tau_0 - 4\tau)(b^2\tau + us(\tau_0 - \tau))^2}, \quad (229)$$

respectively. Components of the Ricci tensor can also be written as

$$R_{ij} = g_{ij} \frac{z'(\rho'z'' - z'\rho'')}{\rho(\rho'^2 + z'^2)^2}. \quad (230)$$

Therefore, the Ricci scalar is

$$R = 2 \frac{z'(\rho'z'' - z'\rho'')}{\rho(\rho'^2 + z'^2)^2} = \frac{-4sb^2\tau_0}{(3\tau_0 - 4\tau)(b^2\tau + us(\tau_0 - \tau))^2(2a + u(\tau_0^2 - 3\tau_0\tau + 2\tau^2))}. \quad (231)$$

The Gaussian curvature of the surface is calculated as

$$\mathcal{K} = \frac{R_{\tau\phi\tau\phi}}{\det(g)} = \frac{z'(\rho'z'' - z'\rho'')}{\rho(\rho'^2 + z'^2)^2} = \frac{1}{2}R, \quad (232)$$

and will also be obtained as the product of the principal curvatures later in this section.

In order to calculate the principal curvature radii and the Gauss curvature of the surface, we need to calculate the second fundamental form II . To find II , we need the unit normal vector $\hat{N} = \frac{\vec{X}_\tau \times \vec{X}_\phi}{|\vec{X}_\tau \times \vec{X}_\phi|}$, which is a function of τ and ϕ , with differential $d\hat{N} = \hat{N}_\tau d\tau + \hat{N}_\phi d\phi$. Observe that $0 = d(1) = d(\vec{N} \cdot \vec{N}) = 2 d\vec{N} \cdot \vec{N}$. Thus $d\vec{N}$ is parallel to the tangent plane at \vec{X} . The quantity

$$\begin{aligned} II &\equiv -d\vec{X} \cdot d\hat{N} = -(\vec{X}_\tau d\tau + \vec{X}_\phi d\phi) \cdot (\hat{N}_\tau d\tau + \hat{N}_\phi d\phi) \\ &= -\vec{X}_\tau \cdot \hat{N}_\tau d^2\tau - (\vec{X}_\tau \cdot \hat{N}_\phi + \vec{X}_\phi \cdot \hat{N}_\tau) d\tau d\phi - \vec{X}_\phi \cdot \hat{N}_\phi d^2\phi \\ &\equiv \mathbf{L} d^2\tau + 2\mathbf{M} d\tau d\phi + \mathbf{N} d^2\phi, \end{aligned} \quad (233)$$

is called the second fundamental form of $\vec{X} = \vec{X}(\tau, \phi)$. \mathbf{L} , \mathbf{M} and \mathbf{N} are called the second fundamental coefficients, and are continuous functions of τ and ϕ . We can express the second fundamental coefficients in terms of \hat{N} and the second derivatives of \vec{X} , using the fact that \vec{X}_τ and \vec{X}_ϕ are perpendicular to \hat{N} for all (τ, ϕ) :

$$0 = (\vec{X}_\tau \cdot \hat{N})_\tau = \vec{X}_{\tau\tau} \cdot \hat{N} + \vec{X}_\tau \cdot \hat{N}_\tau \Rightarrow \mathbf{L} = -\vec{X}_\tau \cdot \hat{N}_\tau = \vec{X}_{\tau\tau} \cdot \hat{N} \quad (234)$$

$$0 = (\vec{X}_\phi \cdot \hat{N})_\phi = \vec{X}_{\phi\phi} \cdot \hat{N} + \vec{X}_\phi \cdot \hat{N}_\phi \Rightarrow \mathbf{N} = -\vec{X}_\phi \cdot \hat{N}_\phi = \vec{X}_{\phi\phi} \cdot \hat{N} . \quad (235)$$

Using the remaining two identities

$$0 = (\vec{X}_\tau \cdot \hat{N})_\phi = \vec{X}_{\tau\phi} \cdot \hat{N} + \vec{X}_\tau \cdot \hat{N}_\phi \Rightarrow -\vec{X}_\tau \cdot \hat{N}_\phi = \vec{X}_{\tau\phi} \cdot \hat{N} \quad (236)$$

$$0 = (\vec{X}_\phi \cdot \hat{N})_\tau = \vec{X}_{\phi\tau} \cdot \hat{N} + \vec{X}_\phi \cdot \hat{N}_\tau \Rightarrow -\vec{X}_\phi \cdot \hat{N}_\tau = \vec{X}_{\phi\tau} \cdot \hat{N} . \quad (237)$$

we find

$$\mathbf{M} = -\frac{1}{2}(\vec{X}_\tau \cdot \hat{N}_\phi + \vec{X}_\phi \cdot \hat{N}_\tau) = \vec{X}_{\tau\phi} \cdot \hat{N} = \vec{X}_{\phi\tau} \cdot \hat{N} . \quad (238)$$

Therefore, the second fundamental form

$$\begin{aligned} II &= \mathbf{L}d^2\tau + 2\mathbf{M}d\tau d\phi + \mathbf{N}d^2\phi \\ &= \vec{X}_{\tau\tau} \cdot \hat{N}d^2\tau + 2\vec{X}_{\tau\phi} \cdot \hat{N}d\tau d\phi + \vec{X}_{\phi\phi} \cdot \hat{N}d^2\phi = d^2\vec{X} \cdot \hat{N} , \end{aligned} \quad (239)$$

where we define $d^2\vec{X} \equiv \vec{X}_{\tau\tau}d^2\tau + 2\vec{X}_{\tau\phi}d\tau d\phi + \vec{X}_{\phi\phi}d^2\phi$. For the caustic ring, the unit normal

$$\hat{N} = \frac{\vec{X}_\tau \times \vec{X}_\phi}{|\vec{X}_\tau \times \vec{X}_\phi|} = \frac{\rho' \hat{z} - z'(\cos \phi \hat{x} + \sin \phi \hat{y})}{\sqrt{\rho'^2 + z'^2}} , \quad (240)$$

and the second fundamental coefficients are

$$\mathbf{L} = \vec{X}_{\tau\tau} \cdot \hat{N} = \frac{\rho' z'' - z' \rho''}{\sqrt{\rho'^2 + z'^2}} , \quad \mathbf{N} = \vec{X}_{\phi\phi} \cdot \hat{N} = \frac{z' \rho}{\sqrt{\rho'^2 + z'^2}} , \quad (241)$$

$$\mathbf{M} = \vec{X}_{\tau\phi} \cdot \hat{N} = 0 . \quad (242)$$

Now, let P be a point on the surface, $\vec{X} = \vec{X}(\tau, \phi)$ a patch containing P , and $\vec{X} = \vec{X}(\tau(t), \phi(t))$ a curve C through P where t is an arbitrary real parameter in an interval I . For instance,

$$s = s(t) \equiv \int_{t_0}^t \left| \frac{d\vec{X}}{dt} \right| dt, \quad (243)$$

where the constant $t_0 \in I$ and $t_0 < t$, can be used to parametrize the curve. Notice that, $s(t)$ is the length of the arc segment of the curve between $\vec{X}(t_0)$ and $\vec{X}(t)$, hence $X(s)$ is called “a natural representation” of a curve. Note also that, a representation in terms of arc length is not unique, because, it depends on the chosen initial point t_0 (where $s = 0$). The tangent vector $\vec{\mathbf{t}}$ to C at $\vec{X}(s)$ is defined as

$$\vec{\mathbf{t}} = \vec{\mathbf{t}}(s) \equiv \frac{d\vec{X}}{ds}(s), \quad (244)$$

where $\vec{\mathbf{t}}$ is a unit vector since

$$\vec{\mathbf{t}} = \frac{d\vec{X}}{ds} = \frac{d\vec{X}}{dt} \frac{dt}{ds} = \frac{d\vec{X}}{dt} \bigg/ \frac{ds}{dt}. \quad (245)$$

From Eq. 243, however, we obtain

$$\frac{ds}{dt} = \left| \frac{d\vec{X}}{dt} \right|, \quad (246)$$

hence Eq. 245 becomes

$$\vec{\mathbf{t}} = \frac{d\vec{X}}{ds} = \frac{d\vec{X}}{dt} \bigg/ \left| \frac{d\vec{X}}{dt} \right|, \quad (247)$$

and, $|\vec{\mathbf{t}}| = 1$, as claimed. We will define all the geometric quantities along the curve in terms of a natural representation, as in the case of the unit tangent vector $\vec{\mathbf{t}}$, however, all of these quantities can be re-expressed in terms of an arbitrary parameter t , by using the chain rule and Eq. 246.

The first derivative of the tangent vector $\vec{\mathbf{t}}(s)$, denoted by $\vec{\mathbf{k}}(s)$, is called the curvature vector on C at the point $\vec{X}(s)$, hence

$$\vec{\mathbf{k}} = \vec{\mathbf{k}}(s) = \frac{d\vec{\mathbf{t}}}{ds}(s) = \frac{d^2\vec{X}}{ds^2}(s), \quad (248)$$

or, using Eq. 246

$$\vec{\mathbf{k}} = \frac{d\vec{\mathbf{t}}}{ds} = \frac{d\vec{\mathbf{t}}}{dt} \bigg/ \left| \frac{d\vec{X}}{dt} \right|. \quad (249)$$

Since $\vec{\mathbf{t}}$ is a unit vector, $\vec{\mathbf{k}} = \frac{d\vec{\mathbf{t}}}{ds}$ is orthogonal to $\vec{\mathbf{t}}$:

$$0 = d(1) = \frac{d}{ds}(\vec{\mathbf{t}} \cdot \vec{\mathbf{t}}) = 2 \frac{d\vec{\mathbf{t}}}{ds} \cdot \vec{\mathbf{t}}. \quad (250)$$

Therefore $\vec{\mathbf{k}}(s)$ is parallel to the normal plane. The direction of $\vec{\mathbf{k}}$ is the direction in which the curve is turning. The magnitude of the curvature vector $\kappa = |\vec{\mathbf{k}}(s)|$ is called the curvature of C at $\vec{X}(s)$. In fact, geometrically, κ is equal to the rate of change of the direction of the tangent vector with respect to the arc length. To prove the claim let us call the angle between the unit tangent $\vec{\mathbf{t}}(s)$ at $\vec{X}(s)$ and $\vec{\mathbf{t}}(s + \Delta s)$ at a neighboring point $\vec{X}(s + \Delta s)$ as $\Delta\theta$. Since $\vec{\mathbf{t}}$ is a unit vector, $|\vec{\mathbf{t}}(s + \Delta s) - \vec{\mathbf{t}}(s)|$ is the base of an isosceles triangle with sides of unit length. Hence $|\vec{\mathbf{t}}(s + \Delta s) - \vec{\mathbf{t}}(s)| = 2 \sin(\frac{\Delta\theta}{2}) = \Delta\theta + O((\Delta\theta)^2)$.

Then,

$$\kappa = \left| \frac{d\vec{\mathbf{t}}}{ds} \right| = \left| \lim_{\Delta s \rightarrow 0} \frac{\vec{\mathbf{t}}(s + \Delta s) - \vec{\mathbf{t}}(s)}{\Delta s} \right| = \lim_{\Delta s \rightarrow 0} \frac{\Delta\theta + O((\Delta\theta)^2)}{\Delta s}, \quad (251)$$

or, we may write

$$\kappa = \lim_{\Delta s \rightarrow 0} \left[\frac{\Delta\theta}{\Delta s} \left(1 + \frac{O((\Delta\theta)^2)}{\Delta\theta} \right) \right]. \quad (252)$$

Since

$$\lim_{\Delta s \rightarrow 0} \Delta\theta = 0 \Rightarrow \lim_{\Delta s \rightarrow 0} \frac{O((\Delta\theta)^2)}{\Delta\theta} = 0, \quad (253)$$

the curvature

$$\kappa = \lim_{\Delta s \rightarrow 0} \frac{\Delta\theta}{\Delta s} = \frac{d\theta}{ds}. \quad (254)$$

Thus, along a curve that has a rapidly changing tangent direction with respect to arc length, such as a with a small radius, the curvature is large. The reciprocal of the curvature is denoted by

$$R = \frac{1}{\kappa} = \frac{1}{|\vec{\mathbf{k}}(s)|}, \quad (255)$$

and is called the radius of curvature at $\vec{X}(s)$. A point on C where the curvature vector $\vec{\mathbf{k}} = 0$, is called a point of inflection. Thus, at a point of inflection the curvature κ is zero and R is infinite. If κ is identically zero along a curve C , then $\frac{d\vec{\mathbf{t}}}{ds} = 0$, and by integrating we find, $\vec{\mathbf{t}} = \frac{d\vec{X}}{ds} = \vec{a}$, where $\vec{a} = \text{const.} \neq 0$. Thus $\vec{X} = \vec{a}s + \vec{b}$, where $\vec{a} = \text{const.}$ which implies that C is a straight line through \vec{b} , and parallel to \vec{a} . Furthermore, on a surface, we can define a normal curvature vector. The normal curvature vector to C at P , denoted by $\vec{\mathbf{k}}_n$, is the vector projection of the curvature vector $\vec{\mathbf{k}}$ of C at P on to the unit normal vector \hat{N} of the surface at P :

$$\vec{\mathbf{k}}_n = (\vec{\mathbf{k}} \cdot \hat{N})\hat{N}. \quad (256)$$

The component of $\vec{\mathbf{k}}_n$ in the direction of \hat{N} , denoted by $\kappa_n \equiv \vec{\mathbf{k}} \cdot \hat{N}$, is called the normal curvature of C at P . The normal curvature can be re-expressed using Eq. 249

$$\kappa_n = \vec{\mathbf{k}} \cdot \hat{N} = \frac{d\vec{\mathbf{t}}}{dt} \cdot \hat{N} / \left| \frac{d\vec{X}}{dt} \right|. \quad (257)$$

Now, using the fact that $\vec{\mathbf{t}}$ is perpendicular to \hat{N} along C :

$$\frac{d}{dt}(\vec{\mathbf{t}} \cdot \hat{N}) = 0 \Rightarrow \frac{d\vec{\mathbf{t}}}{dt} \cdot \hat{N} = -\vec{\mathbf{t}} \cdot \frac{d\hat{N}}{dt}, \quad (258)$$

we find

$$\kappa_n = -\vec{\mathbf{t}} \cdot \frac{d\hat{N}}{dt} / \left| \frac{d\vec{X}}{dt} \right| = -\frac{d\vec{X}}{dt} \cdot \frac{d\hat{N}}{dt} / \left| \frac{d\vec{X}}{dt} \right|^2, \quad (259)$$

where we replaced $\vec{\mathbf{t}}$ using Eq. 247. The above equation can be written more explicitly as

$$\kappa_n = - \left[\vec{X}_\tau \frac{d\tau}{dt} + \vec{X}_\phi \frac{d\phi}{dt} \right] \cdot \left[\hat{N}_\tau \frac{d\tau}{dt} + \hat{N}_\phi \frac{d\phi}{dt} \right] / \left[\vec{X}_\tau \frac{d\tau}{dt} + \vec{X}_\phi \frac{d\phi}{dt} \right] \cdot \left[\vec{X}_\tau \frac{d\tau}{dt} + \vec{X}_\phi \frac{d\phi}{dt} \right], \quad (260)$$

and hence

$$\kappa_n = \frac{\mathbf{L}(d\tau/dt)^2 + 2\mathbf{M}(d\tau/dt)(d\phi/dt) + \mathbf{N}(d\phi/dt)^2}{\mathbf{E}(d\tau/dt)^2 + 2\mathbf{F}(d\tau/dt)(d\phi/dt) + \mathbf{G}(d\phi/dt)^2}. \quad (261)$$

Observe that κ_n , as a function of $d\tau/dt$ and $d\phi/dt$, depends only upon the ratio $(d\tau/dt)/(d\phi/dt)$, namely the direction of $d\tau/d\phi$, hence

$$\kappa_n = \frac{\mathbf{L}(d\tau)^2 + 2\mathbf{M}(d\tau)(d\phi) + \mathbf{N}(d\phi)^2}{\mathbf{E}(d\tau)^2 + 2\mathbf{F}(d\tau)(d\phi) + \mathbf{G}(d\phi)^2} = \frac{II}{I}, \quad (262)$$

where $(d\tau)^2 + (d\phi)^2 \neq 0$. The two perpendicular directions on the surface, for which the κ_n take maximum and minimum values, are called “the principal directions,” and the corresponding normal curvatures, κ_1 and κ_2 , are called “the principal curvatures.” If κ_n has a maximum or minimum, κ^* , for $(d\tau^*, d\phi^*)$, then

$$\begin{aligned}\frac{\partial \kappa_n}{\partial d\tau} \Big|_{(d\tau^*, d\phi^*)} &= \frac{I II_{d\tau} - II I_{d\tau}}{I^2} \Big|_{(d\tau^*, d\phi^*)} = 0, \\ \frac{\partial \kappa_n}{\partial d\phi} \Big|_{(d\tau^*, d\phi^*)} &= \frac{I II_{d\phi} - II I_{d\phi}}{I^2} \Big|_{(d\tau^*, d\phi^*)} = 0.\end{aligned}\quad (263)$$

Multiplying both equations by I , and using the identity

$$\frac{II}{I} \Big|_{(d\tau^*, d\phi^*)} = \kappa_n \Big|_{(d\tau^*, d\phi^*)} = \kappa^*, \quad (264)$$

we obtain

$$(II_{d\tau} - \kappa^* I_{d\tau}) \Big|_{(d\tau^*, d\phi^*)} = 0, \quad (II_{d\phi} - \kappa^* I_{d\phi}) \Big|_{(d\tau^*, d\phi^*)} = 0. \quad (265)$$

Since $II_{d\tau} = 2(\mathbf{L} d\tau + \mathbf{M} d\phi)$, $I_{d\tau} = 2(\mathbf{E} d\tau + \mathbf{F} d\phi)$, $II_{d\phi} = 2(\mathbf{M} d\tau + \mathbf{N} d\phi)$ and $I_{d\phi} = 2(\mathbf{F} d\tau + \mathbf{G} d\phi)$, Eq. 265 yields

$$\begin{aligned}(\mathbf{L} d\tau^* + \mathbf{M} d\phi^*) - \kappa^*(\mathbf{E} d\tau^* + \mathbf{F} d\phi^*) &= 0, \\ (\mathbf{M} d\tau^* + \mathbf{N} d\phi^*) - \kappa^*(\mathbf{F} d\tau^* + \mathbf{G} d\phi^*) &= 0.\end{aligned}\quad (266)$$

The above is a homogeneous system of equations and will have a nontrivial solution $(d\tau^*, d\phi^*)$ (or nontrivial principal direction $d\tau^*/d\phi^*$) if

$$\det \begin{pmatrix} \mathbf{L} - \kappa^* \mathbf{E} & \mathbf{M} - \kappa^* \mathbf{F} \\ \mathbf{M} - \kappa^* \mathbf{F} & \mathbf{N} - \kappa^* \mathbf{G} \end{pmatrix} = 0. \quad (267)$$

Therefore, by expanding, we find that a number κ is a principal curvature, if it is a solution of the equation

$$(\mathbf{EG} - \mathbf{F}^2)\kappa^2 - (\mathbf{EN} + \mathbf{GL} - 2\mathbf{FM})\kappa + (\mathbf{LN} - \mathbf{M}^2) = 0. \quad (268)$$

The discriminant δ of Eq. 268 is

$$\begin{aligned}\delta &= (\mathbf{EN} + \mathbf{GL} - 2\mathbf{FM})^2 - 4(\mathbf{EG} - \mathbf{F}^2)(\mathbf{LN} - \mathbf{M}^2) , \\ &= (\mathbf{EN} - \mathbf{GL})^2 + 4(\mathbf{EM} - \mathbf{FL})(\mathbf{GM} - \mathbf{FN})\end{aligned}\quad (269)$$

$$= 4 \left(\frac{\mathbf{EG} - \mathbf{F}^2}{\mathbf{E}^2} \right) (\mathbf{EM} - \mathbf{FL})^2 + \left(\mathbf{EN} - \mathbf{GL} - \frac{2\mathbf{F}}{\mathbf{E}}(\mathbf{EM} - \mathbf{FL}) \right)^2 . \quad (270)$$

The discriminant $\delta \geq 0$ since $\mathbf{EG} - \mathbf{F}^2 > 0$ (Eq. 224). We have $\delta = 0$ if and only if $\mathbf{EM} - \mathbf{FL} = 0$ and $\mathbf{EN} - \mathbf{GL} - \frac{2\mathbf{F}}{\mathbf{E}}(\mathbf{EM} - \mathbf{FL}) = 0$, which implies $\mathbf{EM} - \mathbf{FL} = 0$ and $\mathbf{EN} - \mathbf{GL} = 0$, or equivalently, $\frac{\mathbf{E}}{\mathbf{L}} = \frac{\mathbf{F}}{\mathbf{M}} = \frac{\mathbf{G}}{\mathbf{N}} \equiv \lambda$. Thus, Eq. 268 has either a single real root, $\kappa = \frac{1}{\lambda}$, if $\delta = 0$, or two distinct real roots, κ_1 and κ_2 . Dividing Eq. 268 by $\mathbf{EG} - \mathbf{F}^2 > 0$, we obtain

$$\kappa^2 - 2\mathcal{H}\kappa + \mathcal{K} = 0 , \quad (271)$$

where

$$\mathcal{H} \equiv \frac{1}{2}(\kappa_1 + \kappa_2) = \frac{\mathbf{EN} + \mathbf{GL} - 2\mathbf{FM}}{2(\mathbf{EG} - \mathbf{F}^2)} , \quad (272)$$

is the average of the principal curvatures and is called the mean curvature at P , and

$$\mathcal{K} \equiv \kappa_1\kappa_2 = \frac{\mathbf{LN} - \mathbf{M}^2}{\mathbf{EG} - \mathbf{F}^2} , \quad (273)$$

is the product of the principal curvatures and is called the Gaussian curvature at P . Hence the roots of Eq. 271 are

$$\kappa_{1,2} = \mathcal{H} \pm \sqrt{\mathcal{H}^2 - \mathcal{K}} , \quad (274)$$

$$\kappa_{1,2} = \frac{\mathbf{EN} + \mathbf{GL} - 2\mathbf{FM} \pm \sqrt{(\mathbf{GL} - \mathbf{EN})^2 + 4(\mathbf{EM} - \mathbf{FL})(\mathbf{GM} - \mathbf{FN})}}{2(\mathbf{EG} - \mathbf{F}^2)} . \quad (275)$$

For the caustic surface, we have $\mathbf{F} = \mathbf{M} = 0$; therefore

$$\kappa_{1,2} = \frac{1}{2} \left[\frac{\mathbf{L}}{\mathbf{E}} + \frac{\mathbf{N}}{\mathbf{G}} \pm \frac{|\mathbf{GL} - \mathbf{EN}|}{\mathbf{EG}} \right] , \quad (276)$$

and hence, we choose $\kappa_1 = \frac{\mathbf{L}}{\mathbf{E}}$ and $\kappa_2 = \frac{\mathbf{N}}{\mathbf{G}}$. When explicitly calculated in terms of the caustic parameters, they yield

$$\kappa_1 = \frac{\mathbf{L}}{\mathbf{E}} = \frac{\rho' z'' - z' \rho''}{(\rho'^2 + z'^2)^{3/2}} = \mp \frac{1}{2} \frac{b}{\sqrt{usp}} \frac{1}{\sqrt{\tau_0}} \left[3 - 4 \frac{\tau}{\tau_0} \right]^{-1} \left[1 - \left(1 - \frac{b^2}{us} \right) \frac{\tau}{\tau_0} \right]^{-3/2} , \quad (277)$$

$$\kappa_2 = \frac{\mathbf{N}}{\mathbf{G}} = \frac{z'}{\rho\sqrt{\rho'^2 + z'^2}} = \pm \frac{1}{\rho} \left[1 + \frac{us}{b^2} \left(\frac{\tau_0}{\tau} - 1 \right) \right]^{-1/2}, \quad (278)$$

where ρ is given explicitly in terms of the parameters in Eq. 179. Then, we can verify the Gaussian curvature found in Eqs. 232:

$$\mathcal{K} = \kappa_1\kappa_2 = \frac{z'(\rho'z'' - z'\rho'')}{\rho(\rho'^2 + z'^2)^2} = -\frac{b^2 s}{\rho \left(3 - 4\frac{\tau}{\tau_0} \right) (us(\tau_0 - \tau) + b^2\tau)^2}. \quad (279)$$

The principal curvatures, κ_1 and κ_2 , are the inverse of the principal curvature radii R_1 and R_2 . The lensing by a caustic surface depends on the curvature radius R of the surface along the line of sight. Therefore, we will need the curvature radii of the caustic ring surface at an arbitrary point $(\alpha_1(\tau_1), \tau_1)$ on the surface. R is given by the Euler's theorem:

$$\frac{1}{R} = \frac{(\cos \omega)^2}{R_1} + \frac{(\sin \omega)^2}{R_2}, \quad (280)$$

where

$$R_1(\tau_1) = \frac{1}{\kappa_1(\tau_1)} = -2\frac{\sqrt{su}}{b} p \sqrt{\frac{\tau_1}{\tau_0}} |3 - 4\frac{\tau_1}{\tau_0}| \left(1 - \left(1 - \frac{b^2}{su} \right) \frac{\tau_1}{\tau_0} \right)^{\frac{3}{2}} \quad (281)$$

in the direction of the cross-sectional plane of the caustic ring,

$$R_2(\tau_1) = \frac{1}{\kappa_2(\tau_1)} = \pm \frac{\sqrt{su}}{b} \sqrt{\frac{\tau_0}{\tau_1} - 1 + \frac{b^2}{su} \left(a + \frac{u}{2}(\tau_0 - \tau_1)(\tau_0 - 2\tau_1) \right)}, \quad (282)$$

in the direction perpendicular to the cross-sectional plane, and ω is the angle between the line of sight and the direction associated with R_1 . In this dissertation, we adopt the convention that R is positive (negative) if, along the line of sight, the surface curves toward (away from) the side with two extra flows. If R is positive, the surface is called ‘‘concave’’ (Fig. 12). If R is negative, the surface is called ‘‘convex’’ (Fig. 13). In Eq. 282, the + sign pertains if $0 \leq \frac{\tau_1}{\tau_0} \leq \frac{3}{4}$; the - sign pertains if $\frac{3}{4} \leq \frac{\tau_1}{\tau_0} \leq 1$. R_1 is always negative except at the three cusps, where it vanishes. R_2 diverges at the cusp in the $z = 0$ plane.

For $0 \leq \frac{\tau_1}{\tau_0} \leq \frac{3}{4}$, there is a pair of lines of sight for which the curvature vanishes. They are at angles:

$$\omega = \pm \arctan \sqrt{-\frac{R_2}{R_1}} \quad (283)$$

relative to the cross-sectional plane. Gravitational lensing by a fold of zero curvature is discussed in Section 4.2.3.

3.5.5 Density Profiles of Axially Symmetric Caustic Rings

As we have seen the inner caustics [18] are closed tubes whose cross-section, shown in Fig. 3, is a D_{-4} catastrophe [16]. They are located near where the particles with the most angular momentum in a given inflow are at their distance of closest approach to the galactic center. For simplicity, we study caustic rings which are axially symmetric about the z -direction as well as reflection symmetric with respect to the $z = 0$ plane. In galactocentric cylindrical coordinates, the flow at such a caustic ring is described by Eqs. 171 and 173.

Recall that the physical space density is given by Eq. 165:

$$d(\rho, z) = \frac{1}{\rho} \sum_{j=1}^n \frac{dM}{d\Omega d\tau}(\alpha, \tau) \frac{\cos(\alpha)}{|D_2(\alpha, \tau)|} \Big|_{(\alpha_j(\rho, z), \tau_j(\rho, z))}, \quad (284)$$

where we define $\frac{dM}{d\Omega d\tau} = \frac{dM}{2\pi \cos(\alpha) d\alpha d\tau}$ as the mass falling in per unit time and unit solid angle. The parameters $\alpha_j(\rho, z)$ and $\tau_j(\rho, z)$, with $j = 1, \dots, n$, are the solutions of $\rho(\alpha, \tau) = \rho$ and $z(\alpha, \tau) = z$, where $n(\rho, z)$ is the number of flows at (ρ, z) . Outside the caustic tube $n = 2$, whereas inside $n = 4$. The determinant $D_2(\alpha, \tau)$ is defined in Eq. 175. In the limit of zero velocity dispersion, the density of dark matter particles is infinite at the location of caustic surfaces. Thus, the location of the caustic ring surface is obtained by demanding that $D_2(\alpha, \tau) = 0$ in Eq. 176, which implied $\alpha(\tau) = \pm \sqrt{\frac{u}{s}\tau(\tau_0 - \tau)}$ with $0 \leq \frac{\tau}{\tau_0} \leq 1$ (Eq. 177). Hence, we obtained $\rho(\tau) = a + \frac{u}{2}(\tau - \tau_0)(2\tau - \tau_0)$ and $z(\tau) = \pm b\sqrt{\frac{u}{s}\tau^3(\tau_0 - \tau)}$ in Eqs. 179, for the location of the tricusp outline.

Near the surface of a caustic ring, but away from the cusps, the density profile is that of a simple fold: $d(\sigma) = \frac{A}{\sqrt{\sigma}}\Theta(\sigma)$, with $\sigma > 0$ inside the tricusp. Next, we calculate the fold coefficient A at arbitrary points other than the cusps, on the surface of a caustic ring. As a warm-up, we start with a special point, marked by a star in Fig. 10. We then obtain the density profile near the cusps.

A sample point

As an example, we determine the fold coefficient A at $(\rho, z) = (a, 0)$ (Fig. 10).

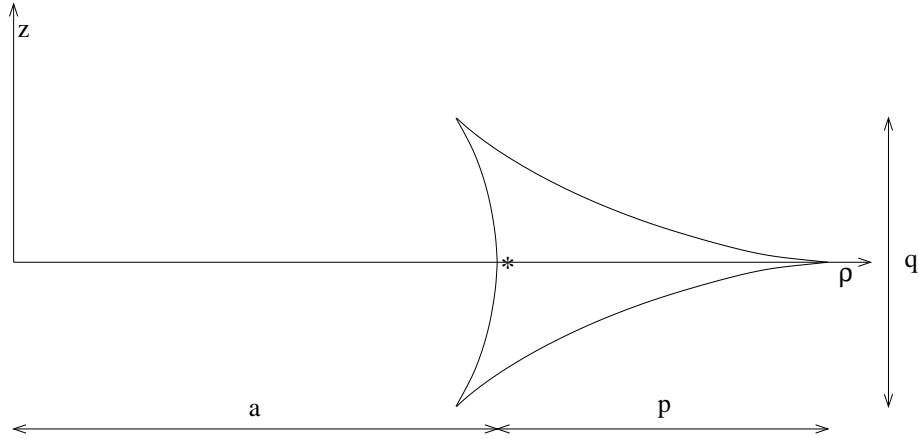


Figure 10: Cross-section of a caustic ring in the case of axial and reflection symmetry. The transverse dimensions in the $\hat{\rho}$ and \hat{z} directions are p and q , respectively. The ring radius is a . The star indicates the sample location $(\rho \simeq a, z = 0)$. For clarity, we took $p, q \sim a$. For actual caustic rings, $p, q \ll a$.

Setting $\alpha = z = 0$, $\sigma = \rho - a = \frac{1}{2}u(\tau - \tau_0)^2$ and $\tau \simeq \tau_0$, we have

$$|D_2(\tau)| \simeq 2b\sqrt{p\sigma} \quad . \quad (285)$$

Including the factor 2 for in and out flows, Eq. 284 yields

$$d(\sigma) = \frac{dM}{d\Omega dt} \frac{1}{ab} \frac{1}{\sqrt{p\sigma}} \quad . \quad (286)$$

Therefore,

$$A_0 = \frac{d^2 M}{d\Omega dt} \frac{1}{ab} \frac{1}{\sqrt{p}} \quad , \quad (287)$$

where the subscript 0 is used to indicate that A is being evaluated at the sample point.

To obtain a numerical estimate for A_0 , we again use the self-similar infall model [50, 51, 48, 49] with $\epsilon = 0.2$. For the n th ring, we have [18],

$$\{a_n : n = 1, 2, \dots\} \simeq (39, 19.5, 13, 10, 8, \dots) \text{kpc} \cdot \left(\frac{j_{\max}}{0.27}\right) \left(\frac{0.7}{h}\right) \left(\frac{v_{\text{rot}}}{220 \text{ km/s}}\right) \quad , \quad (288)$$

where j_{\max} is a parameter, with a specific value for each halo, which is proportional to the amount of angular momentum that the dark matter particles have [48, 49]. Also,

$$\left. \frac{d^2 M}{d\Omega dt} \right|_n = f_n v_n \frac{v_{\text{rot}}^2}{4\pi G} \quad , \quad (289)$$

where v_n is the velocity of the particles in the n th caustic ring, and the dimensionless coefficients f_n characterize the density of the n th in and out flow. In the self-similar model [18],

$$\{f_n : n = 1, 2, \dots\} \simeq (13, 5.5, 3.5, 2.5, 2, \dots) \cdot 10^{-2} \quad (290)$$

for $\epsilon = 0.2$. The f_n are like the F_n in Eq. 158, but they describe the n th in and out flow near the caustic ring, whereas the F_n describe that flow near turnaround.

Combining Eqs. 287 and 289, we have

$$A_{0,n} = \frac{v_{\text{rot}}^2}{4\pi G} \frac{f_n}{a_n} \frac{v_n}{b_n} \frac{1}{\sqrt{p_n}} \quad . \quad (291)$$

It was shown in reference [16] that b_n and v_n are of the same order of magnitude. Moreover, Sikivie [23] interpreted the ten rises in the rotation curve of the Milky Way as the effect of caustic rings. In that case, the widths p_n of caustic rings are determined from the observed widths of the rises. Typically one finds $p_n \sim 0.1 a_n$. Using this and $v_n \sim b_n$, Eq. 291 yields the estimates

$$\begin{aligned} \{A_{0,n} : n = 1, 2, \dots\} &\sim (3, 4, 4, 5, 5, \dots) \cdot \frac{10^{-4} \text{ gr}}{\text{cm}^2 \text{ kpc}^{1/2}} \\ &\cdot \left(\frac{0.27}{j_{\max}}\right)^{3/2} \left(\frac{h}{0.7}\right)^{3/2} \left(\frac{v_{\text{rot}}}{220 \text{ km/s}}\right)^{1/2} \quad . \end{aligned} \quad (292)$$

At the point under consideration, $(\rho, z) = (a, 0)$, the surface of the caustic ring is convex for all lines of sight (i.e., all tangents at that point are on the side with two extra flows). If the line of sight is in the $z = 0$ plane, the curvature radius is a . If the line of sight is perpendicular to the $z = 0$ plane, the curvature radius is $2\frac{b^2}{su}p$. Lensing by a convex caustic surface is discussed in Section 4.2.2.

To obtain the lensing properties of the caustic ring surface at an arbitrary point, we need the curvature radii R given in Eq. 280 and the coefficient A at all locations. We derive A everywhere on the surface in the next two sections.

The fold coefficient everywhere

We choose an arbitrary point on the tricusp (i.e., on the surface of the caustic ring). Its parameters are (α_1, τ_1) with α_1 given in terms of τ_1 by Eq. 177. The physical coordinates (ρ_1, z_1) are given in terms of τ_1 by Eqs. 179. We assume that the point is not at one of the three cusps. The latter are located at $\tau_1 = 0$, at $\tau_1 = \frac{3}{4}\tau_0$ with $\alpha_1 > 0$, and at $\tau_1 = \frac{3}{4}\tau_0$ with $\alpha_1 < 0$.

The vanishing of $D_2(\tau_1) = \det \mathcal{D}(\tau_1)$ implies the existence of a zero eigenvector of the matrix

$$\mathcal{D}(\tau_1) = \begin{pmatrix} -s\alpha_1 & b\tau_1 \\ u(\tau_1 - \tau_0) & b\alpha_1 \end{pmatrix} . \quad (293)$$

Let us define $\theta_1(\tau_1)$ such that

$$\mathcal{D}(\tau_1) \begin{pmatrix} \sin(\theta_1) \\ \cos(\theta_1) \end{pmatrix} = 0 . \quad (294)$$

We have

$$\sin(\theta_1) = \frac{b\tau_1}{\sqrt{(b\tau_1)^2 + (s\alpha_1)^2}} \quad \text{and} \quad \cos(\theta_1) = \frac{s\alpha_1}{\sqrt{(b\tau_1)^2 + (s\alpha_1)^2}} . \quad (295)$$

We define new Cartesian coordinates (σ, η) related to $(\rho - \rho_1, z - z_1)$ by a rotation of angle $\theta_1 + \frac{\pi}{2}$:

$$\begin{pmatrix} \sigma \\ \eta \end{pmatrix} = \begin{pmatrix} -\sin(\theta_1) & -\cos(\theta_1) \\ \cos(\theta_1) & -\sin(\theta_1) \end{pmatrix} \begin{pmatrix} \rho - \rho_1 \\ z - z_1 \end{pmatrix} . \quad (296)$$

We now show that σ is the coordinate in the direction orthogonal to the caustic surface at (ρ_1, z_1) .

Consider small deviations about (α_1, τ_1) in parameter space: $(\alpha, \tau) = (\alpha_1 + \Delta\alpha, \tau_1 + \Delta\tau)$. Equation 175 implies

$$\begin{pmatrix} \Delta\rho \\ \Delta z \end{pmatrix} = \mathcal{D}^T(\tau_1) \begin{pmatrix} \Delta\alpha \\ \Delta\tau \end{pmatrix} + O(\Delta\alpha^2, \Delta\tau^2, \Delta\alpha\Delta\tau) \quad , \quad (297)$$

where T indicates transposition. The expansion of σ in powers of $\Delta\alpha$ and $\Delta\tau$ yields

$$\sigma = O(\Delta\alpha^2, \Delta\tau^2, \Delta\alpha\Delta\tau) \quad , \quad (298)$$

because the first order terms vanish:

$$\left. \frac{\partial\sigma}{\partial\alpha} \right|_{(\alpha_1, \tau_1)} \Delta\alpha + \left. \frac{\partial\sigma}{\partial\tau} \right|_{(\alpha_1, \tau_1)} \Delta\tau = -(\Delta\alpha \quad \Delta\tau) \mathcal{D}(\tau_1) \begin{pmatrix} \sin(\theta_1) \\ \cos(\theta_1) \end{pmatrix} = 0 \quad . \quad (299)$$

The fact that σ is second order in $\Delta\alpha$ and $\Delta\tau$ shows that σ is the coordinate in the direction perpendicular to the caustic surface, and

$$\hat{\sigma} = -\sin(\theta_1)\hat{\rho} - \cos(\theta_1)\hat{z} \quad (300)$$

is the unit normal to the surface, pointing inward. $\theta(\tau_1)$ is the angle between the ρ axis and the tangent line at (ρ_1, z_1) (Fig. 11). To obtain the density profile of the caustic near the point under consideration, we need $D_2(\eta, \sigma)$ to order $\sqrt{\sigma}$. So we calculate σ to second order in powers of $\Delta\alpha$ and $\Delta\tau$, and D_2 and η to first order. We find

$$\sigma = \frac{1}{2}(\Delta\alpha \quad \Delta\tau) \begin{pmatrix} s \sin(\theta_1) & -b \cos(\theta_1) \\ -b \cos(\theta_1) & -u \sin(\theta_1) \end{pmatrix} \begin{pmatrix} \Delta\alpha \\ \Delta\tau \end{pmatrix} \quad , \quad (301)$$

and

$$\begin{aligned} D_2 &= -b[2s\alpha_1\Delta\alpha + u(2\tau_1 - \tau_0)\Delta\tau] \\ \eta &= [u(\tau_1 - \tau_0)\cos\theta_1 - b\alpha_1\sin\theta_1]\Delta\tau - [s\alpha_1\cos\theta_1 + b\tau_1\sin\theta_1]\Delta\alpha \quad . \end{aligned} \quad (302)$$

Eqs. 302 can be inverted to obtain $\Delta\alpha$ and $\Delta\tau$ as functions of D_2 and η . When the result is inserted into Eq. 301, we obtain

$$\sigma(D_2, \eta) = \frac{b}{2\sqrt{(b\tau_1)^2 + (s\alpha_1)^2}} \frac{1}{u\tau_1|3\tau_0 - 4\tau_1|} \left(\tau_1 \left(\frac{D_2}{b} \right)^2 - \frac{us\tau_0\tau_1^2\eta^2}{(b\tau_1)^2 + (s\alpha_1)^2} \right) \quad . \quad (303)$$

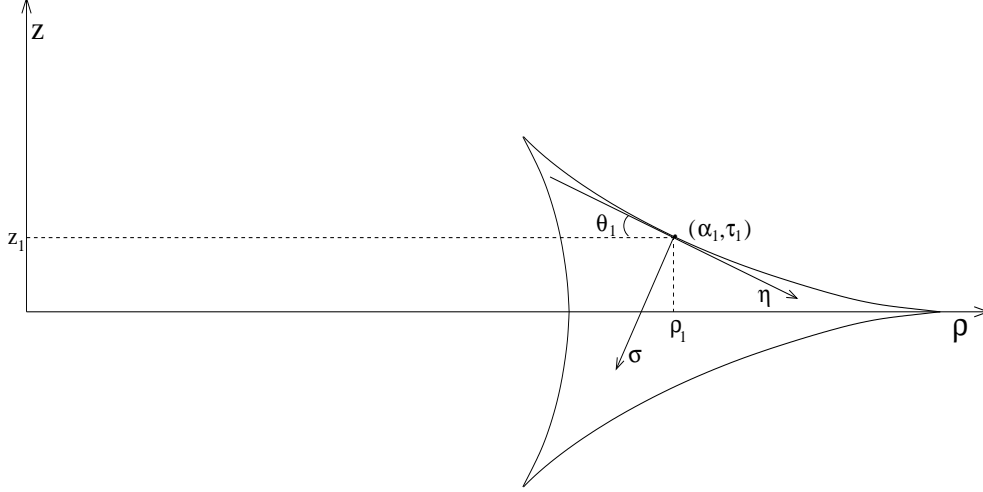


Figure 11: An arbitrary point on the tricuspid is labeled by τ_1 with $\alpha_1 = \alpha_1(\tau_1)$. Its physical coordinates are (ρ_1, z_1) . A new Cartesian coordinate system (σ, η) is defined there such that $\hat{\sigma}$ is perpendicular to the caustic surface. It is rotated relative to the (ρ, z) coordinates by an angle $\theta(\tau_1) + \frac{\pi}{2}$.

This implies

$$D_2(\eta, \sigma) = \sqrt{\frac{b^2}{1 + (\frac{b^2}{us} - 1)\frac{\tau_1}{\tau_0}}\eta^2 + 2b^2u|3\tau_0 - 4\tau_1|\sqrt{\frac{us}{b^2}(\tau_0 - \tau_1)\tau_1 + \tau_1^2}}\sigma. \quad (304)$$

Along the $\hat{\sigma}$ direction ($\eta = 0$), we have

$$D_2(\sigma) = 2C(\tau_1)b\sqrt{\sigma p}, \quad (305)$$

with

$$C(\tau_1) = \sqrt{|3 - 4\frac{\tau_1}{\tau_0}|\sqrt{\frac{us}{b^2}(1 - \frac{\tau_1}{\tau_0})\frac{\tau_1}{\tau_0} + (\frac{\tau_1}{\tau_0})^2}}. \quad (306)$$

Combining Eqs. 284 and 305, and minding the factor of two because two flows contribute, we have

$$d(\tau_1, \sigma) = \frac{A(\tau_1)}{\sqrt{\sigma}}\Theta(\sigma) \quad (307)$$

with

$$A(\tau_1) = \frac{d^2M}{d\Omega dt} \frac{1}{bC(\tau_1)\sqrt{p}} \frac{\cos(\alpha_1)}{\rho(\tau_1)}. \quad (308)$$

In terms of $A_{0,n} = A_n(\tau_1 = \tau_0)$, for which estimates are provided in Eq. 292, we have

$$A_n(\tau_1) = A_{0,n} \frac{a_n}{\rho_n(\tau_1)} \frac{\cos \alpha_1(\tau_1)}{C_n(\tau_1)} . \quad (309)$$

Note that $A(\tau_1)$ diverges at each of the three cusps because C vanishes there. The caustic ring parameters (a, τ, b, u, s) are related to the velocity distribution of the flow at last turnaround [16].

Density near a cusp

In this section, we derive the dark matter density profile near a cusp. For the sake of convenience, we choose the cusp in the $z = 0$ plane at $\rho = a + p \equiv \rho_0$, where $\alpha = \tau = 0$. Very close to the cusp, we may neglect the term of order τ^2 in Eq. 173. Hence,

$$z = b \alpha \tau , \quad \rho = \rho_0 - u \tau_0 \tau - \frac{s}{2} \alpha^2 . \quad (310)$$

The term of order α^2 cannot be neglected. We define new dimensionless quantities [16]:

$$A \equiv \frac{\alpha}{\tau_0} \sqrt{\frac{s}{u}} , \quad T \equiv \frac{\tau}{\tau_0} , \quad X \equiv \frac{\rho - \rho_0}{p} , \quad Z \equiv \frac{z \sqrt{\zeta}}{p} , \quad (311)$$

where $\zeta = \frac{su}{b^2}$. In terms of these, Eq. 310 becomes

$$Z = 2AT , \quad (312)$$

$$X = -2T - A^2 . \quad (313)$$

The determinant of the Jacobian in Eq. 176 becomes

$$D_2(A, T) = 2bp (T - A^2) . \quad (314)$$

Substitution of Eq. 312 into Eq. 313 yields the third order polynomial equation:

$$A^3 + XA + Z = 0 . \quad (315)$$

The discriminant is:

$$\delta = \left(\frac{Z}{2}\right)^2 + \left(\frac{X}{3}\right)^3 . \quad (316)$$

If $\delta > 0$, the cubic equation has one real root, and two complex roots which are complex conjugates of each other. If $\delta < 0$, all the roots are real and unequal. For $\delta = 0$, all the roots are real and at least two are equal. The number of real roots is the number of flows at a given location. The tricusp has two flows outside and four inside. In the neighborhood of a cusp, however, one of the flows of the tricusp is nonsingular and does not participate in the cusp caustic. To include the root corresponding to the nonsingular flow near $(z, \rho) = (0, \rho_0)$, one must keep the term of order τ^2 in Eq. 310.

The equation for the caustic surface in physical space is $\delta = 0$. Indeed, Eq. 314 implies that at the caustic $T = A^2$. Therefore, $Z = 2T^{3/2}$ and $X = -3T$. A straightforward calculation shows that

$$\delta = \frac{D_2}{54bp}(A^4 + 7A^2T - 8T^2). \quad (317)$$

Thus $D_2 = 0$ implies $\delta = 0$, however, the converse is not true: $\delta = 0$ does not imply $D_2 = 0$ because not all flows at the location of the caustic surface are singular.

Eq. 284 for the density becomes

$$d = \frac{1}{2\rho_0bp} \frac{d^2M}{d\Omega dt} \sum_{j=1}^n \frac{1}{|T - A^2|_j}, \quad (318)$$

where the sum is over the flows (i.e., the real roots of the cubic polynomial Eq. 315). If $\delta > 0$, the one real root is

$$A = \left(-\frac{Z}{2} + \sqrt{\delta}\right)^{1/3} + \left(-\frac{Z}{2} - \sqrt{\delta}\right)^{1/3}. \quad (319)$$

This describes the one flow outside the cusp. Using Eqs. 313 and 319 in Eq. 318, we obtain

$$d = \frac{1}{\rho_0bp} \frac{d^2M}{d\Omega dt} \frac{1}{|X - 3\left(-\frac{Z}{2} + \sqrt{\delta}\right)^{2/3} - 3\left(\frac{Z}{2} + \sqrt{\delta}\right)^{2/3}|}. \quad (320)$$

Just above or below the cusp, where $X = 0$ and $|Z| \ll 1$, we have

$$d = \frac{1}{3bp\rho_0} \frac{d^2M}{d\Omega dt} \frac{1}{|Z|^{2/3}}. \quad (321)$$

On the other hand, if we approach the cusp in the plane of the ring from the outside, where $Z = 0$ and $0 < X \ll 1$, we find

$$d = \frac{1}{b \rho_0} \frac{d^2 M}{d\Omega dt} \frac{1}{(\rho - \rho_0)} \quad . \quad (322)$$

Next, we calculate the density inside the cusp, where $\delta < 0$. The three real roots of the polynomial Eq. 315 are

$$A_1 = 2\sqrt{\frac{-X}{3}} \cos \theta \quad (323)$$

$$A_2 = 2\sqrt{\frac{-X}{3}} \cos \left(\theta + \frac{2\pi}{3} \right) \quad (324)$$

$$A_3 = 2\sqrt{\frac{-X}{3}} \cos \left(\theta + \frac{4\pi}{3} \right), \quad (325)$$

where $\cos 3\theta \equiv -\frac{Z}{2} \left(-\frac{3}{X}\right)^{3/2}$ and $0 \leq \theta \leq \frac{\pi}{3}$. Inserting them into Eq. 318 and using Eq. 313, we obtain

$$d = \frac{1}{b p \rho_0} \frac{d^2 M}{d\Omega dt} \left(\frac{1}{-X} \right) \left(\frac{1}{4 \cos^2(\theta) - 1} + \frac{1}{4 \cos^2(\theta + \frac{2\pi}{3}) - 1} + \frac{1}{1 - 4 \cos^2(\theta + \frac{4\pi}{3})} \right) \quad , \quad (326)$$

where each term in the parentheses corresponds to one of the three flows. Adding the individual flow densities yields

$$d = \frac{2}{b p \rho_0} \frac{d^2 M}{d\Omega dt} \frac{1}{|X|} \frac{1}{(\sqrt{3} - \tan \theta) \sin 2\theta} \quad . \quad (327)$$

If we approach the cusp in the galactic plane from the inside, where $Z = 0$ and $0 < -X \ll 1$, we have

$$d = \frac{2}{b \rho_0} \frac{d^2 M}{d\Omega dt} \frac{1}{(\rho_0 - \rho)} \quad , \quad (328)$$

which is twice the result in Eq. 322. The gravitational lensing properties of a cusp are derived, for a special line of sight, in Section 4.2.4.

4 Gravitational Lensing by Dark Matter Caustics

Gravitational lensing techniques have proven useful in studying the distribution of dark matter in the universe. They have been used to reveal the existence of massive compact halo objects (MACHOs) in galaxies [10, 11, 12, 13], and to constrain the mass distribution in galaxy clusters [56, 57, 58]. In this section, we calculate the gravitational lensing properties [15] of dark matter caustics [18, 16, 19]. Gravitational lensing by dark matter caustics has been discussed by Hogan [22]. We confirm Hogan’s results for the case he considered, called the “concave fold” in our nomenclature. We study additional cases and introduce a formalism to facilitate the calculations.

The gravitational lensing effects of a caustic surface are largest when the line of sight is near tangent to the surface because the contrast in column density is largest there. The effects depend on the curvature of the caustic surface at the tangent point in the direction of the line of sight: the smaller the curvature, the larger the effects. A caustic is an oriented surface because one side has two more flows than the other. We will consider three cases of gravitational lensing by a smooth caustic surface. In the first case, the line of sight is near tangent to a caustic surface which curves toward the side with two extra flows, as in Fig. 12. We call such a surface “concave.” In the second case, the surface is “convex”

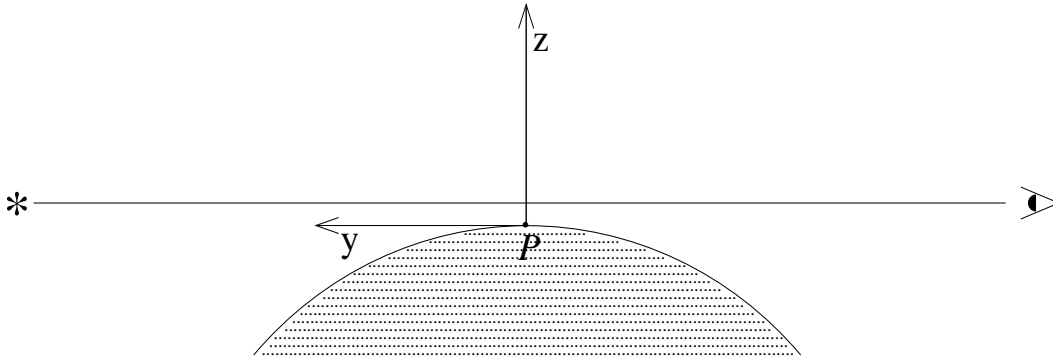


Figure 12: Lensing by a concave fold. The arc is the intersection of the caustic surface with the plane containing the normal (\hat{z}) to the surface and the line of sight (\hat{y}). The shaded area indicates the side with the two extra flows.

(i.e., it curves away from the side with two extra flows as in Fig. 13). In the third case, the

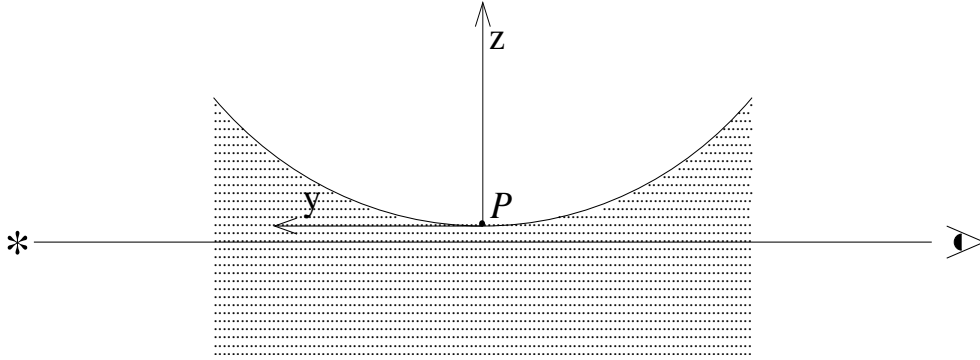


Figure 13: Lensing by a convex fold. Same as Fig. 12 except that now the caustic surface curves away from the side with two extra flows.

caustic surface has zero curvature at the tangent point (the radius of curvature is infinite), but the tangent line is entirely outside the side with two extra flows. Caustic surfaces may have cusps. The outer dark matter caustics of galactic halos are topological spheres which have no cusps, but the inner dark matter caustics of galactic halos are closed tubes whose cross-section is a D_{-4} catastrophe (tricuspid; Fig. 10). The fourth case of gravitational lensing which we consider has a line of sight near a cusp, and parallel to the plane of the cusp (Fig. 14).

Gravitational lensing produces a map of an object surface onto an image surface. The magnification is the inverse of the Jacobian of this map. Because dark matter caustics have well defined density profiles, it is a neat mathematical exercise to calculate their gravitational lensing characteristics. The images of extended sources may show distortions that can be unambiguously attributed to lensing by dark matter caustics in the limit of perfect observations. We see that in three of the cases considered, a point source can have multiple images. In those cases, when two images merge, the Jacobian of the map vanishes and the magnification diverges. So, at least in theory, it seems that gravitational lensing is a very attractive tool for investigating dark matter caustics. Observation of the calculated lensing signatures would give direct evidence for caustics and CDM.

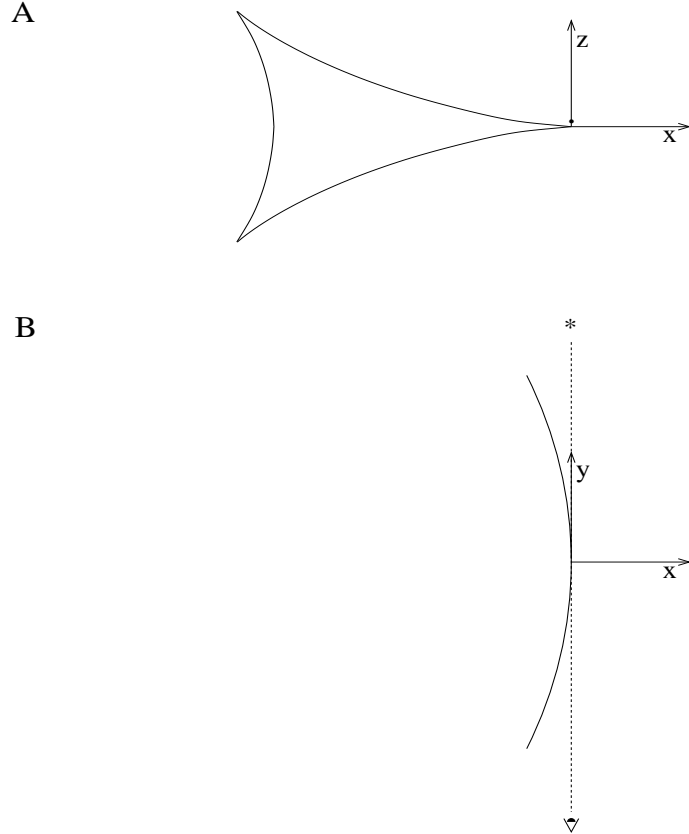


Figure 14: Lensing by the caustic ring cusp at $(z, \rho) = (0, \rho_0)$, with line of sight parallel to the $z = 0$ plane. We define $x \equiv \rho - \rho_0$. A) Side view in the direction of the line of sight. The latter is represented by the dot near $x = z = 0$. B) Top view. The curve is the location of the cusp in the $z = 0$ plane.

We have been particularly motivated by the possibility [22] that the observer might be able to distinguish between axions and WIMPs by determining the distance over which the caustics are smeared. The nearby caustic, whose position is revealed according to ref. [23] by a triangular feature in the IRAS map of the Milky Way plane, is only 1 kpc away from us in the direction of observation. By observing the gravitational lensing due to that caustic, one may be able to measure δx as small as 10^{13} cm, assuming an angular resolution of $3 \cdot 10^{-9}$ radians. If δx turned out to be that small, the WIMP dark matter hypothesis would be severely challenged (Eq. 16). Unfortunately, as will be shown below, the gravitational lensing due to a caustic only a kpc away from us is too weak to be observed

with present instruments. It is well known that gravitational lensing effects are proportional to $\frac{D_L D_{LS}}{D_S}$ where D_S, D_L and D_{LS} are respectively the distances from the observer to the source, from the observer to the lens, and from the lens to the source. We see below that, for the gravitational lensing effects of dark matter caustics to be observable with present technology, the lenses and sources must be as far as possible, at the cosmological distances of order Gpc. Even then, the observation of such effects will be difficult. Unfortunately, at Gpc distances it is not possible to measure δx as small as Eqs. 15 and 16 with foreseeable technology. So it seems unlikely that one will be able to distinguish between dark matter candidates on the basis of the gravitational lensing characteristics of the caustics they form. Henceforth, unless otherwise stated, the velocity dispersion is set equal to zero.

4.1 General Formalism

The first part of this section gives a brief account of the gravitational lensing formalism [59]. In the second part we show how this formalism can be streamlined in the special case of lensing by dark matter caustics.

In linear approximation, the deflection angle $\vec{\theta}$ of a light ray due to a gravitational field is given by

$$\vec{\theta} = \vec{\nabla} \frac{2}{c^2} \int \Phi \, dy, \quad (329)$$

where Φ is the Newtonian potential. We choose the y -axis in the direction of propagation of light. The deflection angle $\vec{\theta}$ is related to the angular shift $\vec{\xi}_I - \vec{\xi}_S$ on the sky of the apparent direction of a source:

$$\vec{\theta}(\vec{\xi}_I) = \frac{D_S}{D_{LS}} (\vec{\xi}_I - \vec{\xi}_S) \quad (330)$$

where D_S and D_{LS} are the distances of the source to the observer and to the lens respectively. $\vec{\xi}_S$ is the angular position of the source in the absence of the lens while $\vec{\xi}_I$ is the angular position of the image with the lens present. The angles carry components in the

x and z -directions: $\vec{\theta} = (\theta_x, \theta_z)$, $\vec{\xi} = (\xi_x, \xi_z)$, etc. Unless otherwise stated, we mean by a vector a quantity with components in the x - and z -directions. We have $\vec{x} = (x, z) = D_L \vec{\xi}_I$.

It is convenient to introduce a 2D potential

$$\psi(\vec{\xi}_I) = \frac{2D_{LS}}{c^2 D_L D_S} \int dy \Phi \quad , \quad (331)$$

so that

$$\vec{\theta} = \frac{D_S}{D_{LS}} \vec{\nabla}_{\xi_I} \psi(\vec{\xi}_I) \quad , \quad (332)$$

where $\vec{\nabla}_{\xi_I} = D_L \vec{\nabla}$, and D_L is the distance of the observer to the lens. Then, Eq. 330 becomes

$$\vec{\xi}_I = \vec{\xi}_S + \vec{\nabla}_{\xi_I} \psi(\vec{\xi}_I) \quad . \quad (333)$$

It gives the map $\vec{\xi}_S(\vec{\xi}_I)$ from the image plane to the source plane. The inverse map may be one to one, or one to many. In the latter case, there are multiple images and infinite magnification when a pair of images merge.

Our problem is to find the image map of a point source when the matter distribution is given. The 2D gravitational potential ψ obeys the Poisson equation:

$$\nabla_{\xi_I}^2 \psi = \frac{8\pi G D_L D_{LS}}{c^2 D_S} \Sigma = 2 \frac{\Sigma}{\Sigma_c} \quad , \quad (334)$$

where $\Sigma(\xi_{Ix}, \xi_{Iz})$ is the column density (i.e., the integral of the volume density along the line of sight):

$$\Sigma(\vec{\xi}_I) = \int dy d(D_L \xi_{Ix}, y, D_L \xi_{Iz}) \quad , \quad (335)$$

and Σ_c is the critical surface density

$$\Sigma_c = \frac{c^2 D_S}{4\pi G D_L D_{LS}} = 0.347 \text{ g/cm}^2 \left(\frac{D_S}{D_L D_{LS}} \text{ Gpc} \right) . \quad (336)$$

A uniform sheet of density Σ_c focuses radiation from the source to the observer.

Equation 334 is solved by

$$\psi(\vec{\xi}_I) = \frac{1}{\pi \Sigma_c} \int d^2 \xi'_I \Sigma(\vec{\xi}'_I) \ln |\vec{\xi}_I - \vec{\xi}'_I| \quad , \quad (337)$$

and hence,

$$\Delta\vec{\xi} \equiv \vec{\xi}_I - \vec{\xi}_S = \vec{\nabla}_{\xi_I} \psi(\vec{\xi}_I) = \frac{1}{\pi \Sigma_c} \int d^2 \xi'_I \Sigma(\vec{\xi}'_I) \frac{\vec{\xi}_I - \vec{\xi}'_I}{(\vec{\xi}_I - \vec{\xi}'_I)^2} . \quad (338)$$

The image structure, distortion, and magnification are given by the Jacobian matrix of the map $\vec{\xi}_S(\vec{\xi}_I)$ from image to source:

$$K_{ij} \equiv \frac{\partial \xi_{Si}}{\partial \xi_{Ij}} = \delta_{ij} - \psi_{ij} , \quad (339)$$

where $\psi_{ij} \equiv \frac{\partial^2 \psi}{\partial \xi_{Ii} \partial \xi_{Ij}}$. Because gravitational lensing does not change surface brightness, the magnification \mathcal{M} is the ratio of image area to source area. Therefore,

$$\mathcal{M} = \frac{1}{|\det(K_{ij})|} . \quad (340)$$

To first order, for $\psi_{ij} \ll 1$,

$$\mathcal{M} = 1 + \nabla_{\xi_I}^2 \psi = 1 + 2 \frac{\Sigma}{\Sigma_c} . \quad (341)$$

To obtain the largest lensing effects, we wish to minimize Σ_c , given in Eq. 336. For fixed D_S , the minimum occurs when the lens is situated half-way between the source and the observer. Also, D_S should be as large as possible. For our estimates, we will assume that the source is at cosmological distances (e.g., $2D_L = 2D_{LS} = D_S = 1\text{Gpc}$, in which case $\Sigma_c = 1.39 \text{ g/cm}^2$).

For a general mass distribution, the gravitational lensing effects are obtained by first calculating the column density, Eq. 335, and then the image shift, Eq. 338. This procedure can be simplified when the lens is a dark matter caustic. We are interested in lines of sight which are tangent to a caustic surface, because the column density Σ has the highest contrast there. We assume that, in the neighborhood of the tangent point, the flow is independent of y except for a shift $\vec{x}(y)$ of the caustic surface with y . The density can then be written as

$$d(x, y, z) = d(x - x(y), z - z(y)) , \quad (342)$$

where $d(x, z)$ is the density of the 2D flow in the plane orthogonal to the line of sight. The flow in the y -direction is irrelevant because lensing depends only on the column density Σ .

In the limit of zero velocity dispersion, a 2D flow is specified by giving the spatial coordinates $\vec{x}(\alpha, \beta, t)$ of the particle labeled (α, β) at time t , for all (α, β, t) . The labels α and β are chosen arbitrarily. At a given time t , $\vec{x}(\alpha, \beta, t) = \vec{x}$ has a discrete number of solutions $(\alpha, \beta)_j(\vec{x}, t)$ labeled by $j = 1, \dots, n(\vec{x}, t)$, where n is the number of distinct flows at (\vec{x}, t) . Here, t is the time at which the light ray passes by the caustic. Henceforth we will not show the time dependence explicitly. The particle density in physical space is

$$d(x, z) = \sum_{j=1}^{n(\vec{x})} \frac{d^2\Lambda}{d\alpha d\beta} \frac{1}{\left| \frac{\partial(x, z)}{\partial(\alpha, \beta)} \right|} \Big|_{(\alpha, \beta) = (\alpha, \beta)_j(\vec{x})}, \quad (343)$$

where Λ is the mass per unit length in the direction of the line of sight and $\frac{d^2\Lambda}{d\alpha d\beta}$ is the Λ density in parameter space. Inserting Eqs. 335 and 342 into Eq. 338 we obtain

$$\vec{\nabla}_{\xi_I} \psi(\vec{\xi}_I = \vec{x}/D_L) = \frac{1}{\pi \Sigma_c} \int dy \int d^2 \xi'_I \frac{\vec{\xi}_I - \vec{\xi}'_I}{|\vec{\xi}_I - \vec{\xi}'_I|^2} d(D_L \xi'_{Ix} - x(y), D_L \xi'_{Iz} - z(y)). \quad (344)$$

When d is replaced by the caustic density Eq. 343, Eq.344 becomes

$$\vec{\nabla}_{\xi_I} \psi(\vec{\xi}_I = \vec{x}/D_L) = \frac{1}{\pi \Sigma_c D_L} \int dy \int dx' dz' \frac{\vec{x} - \vec{x}'}{(\vec{x} - \vec{x}')^2} \sum_{j=1}^n \frac{1}{\left| \frac{\partial(x', z')}{\partial(\alpha, \beta)} \right|} \frac{d^2\Lambda}{d\alpha d\beta} \Big|_{(\alpha, \beta) = (\alpha, \beta)_j(\vec{x}' - \vec{x}(y))}. \quad (345)$$

Changing variables from (x', z') to (α, β) and assuming that the density in parameter space varies only slowly over the region of integration, we rewrite Eq. 345 as

$$\vec{\nabla}_{\xi_I} \psi(\vec{\xi}_I = \vec{x}/D_L) = \frac{1}{\pi \Sigma_c D_L} \frac{d^2\Lambda}{d\alpha d\beta} \int dy \int d\alpha d\beta \frac{\vec{x} - \vec{x}(\alpha, \beta) - \vec{x}(y)}{|\vec{x} - \vec{x}(\alpha, \beta) - \vec{x}(y)|^2}. \quad (346)$$

Further simplification is achieved by defining the complex integral:

$$I(x, z) \equiv \int d\alpha d\beta \frac{1}{x - x(\alpha, \beta) + i(z - z(\alpha, \beta))}, \quad (347)$$

in terms of which the shifts are given by

$$\Delta\xi_x = \frac{\partial\psi}{\partial\xi_{Ix}} = \frac{1}{\pi\Sigma_c D_L} \frac{d^2\Lambda}{d\alpha d\beta} \operatorname{Re} \int dy I(\vec{x} - \vec{x}(y)) \quad , \quad (348)$$

$$\Delta\xi_z = \frac{\partial\psi}{\partial\xi_{Iz}} = -\frac{1}{\pi\Sigma_c D_L} \frac{d^2\Lambda}{d\alpha d\beta} \operatorname{Im} \int dy I(\vec{x} - \vec{x}(y)) \quad . \quad (349)$$

Eqs. 347 and 349 are useful when the caustic has contrast in the two dimensions transverse to the line of sight (e.g., near a cusp).

In many applications, however, the caustic has contrast in only one of the dimensions transverse to the line of sight. Choosing \hat{x} to be the trivial direction, Eq. 334 is reduced to

$$\frac{d^2\psi}{d\xi_I^2}(\xi_I) = \frac{2}{\Sigma_c} \Sigma(z = D_L \xi_I) \quad , \quad (350)$$

and the column density is given by

$$\Sigma(\xi_I) = \int dy d(z - z(y)) \quad . \quad (351)$$

The flow is now effectively one dimensional. Its physical space density is given by

$$d(z) = \sum_{j=1}^{n(z)} \frac{d\Lambda}{d\alpha} \frac{1}{\left| \frac{dz}{d\alpha} \right|} \Big|_{\alpha=\alpha_j(z)} \quad , \quad (352)$$

where Λ is the mass surface density in the two trivial directions (x and y) and $\frac{d\Lambda}{d\alpha}$ is the Λ density in parameter space. The 1D Green's function is $G = \frac{1}{2}(|\xi| + a\xi) + b$, where a and b are arbitrary constants. The shift is

$$\frac{d\psi}{d\xi_I}(\xi_I) = \frac{1}{\Sigma_c} \int d\xi'_I \Sigma(\xi'_I) (\operatorname{Sign}(\xi_I - \xi'_I) + a) \quad . \quad (353)$$

The constant a causes an overall shift of the image, which does not concern us. We choose $a = -1$. Repeating the steps done earlier for the 2D case, Eq. 353 is re-expressed as

$$\Delta\xi = -\frac{2}{\Sigma_c D_L} \frac{d\Lambda}{d\alpha} \int dy \int d\alpha \Theta(-z + z(\alpha) + z(y)) \quad . \quad (354)$$

In the next section Eq. 354 is used to calculate the shifts due to simple folds of dark matter flows, and Eq. 349 is used to calculate the shifts due to a cusp.

4.2 Applications

4.2.1 Lensing by a Concave Fold

We consider a simple fold caustic which has a curvature radius R along the line of sight. We assume that the surface is concave (i.e., it is curved in the direction of the two extra flows; Fig. 12). The outer caustics of dark matter halos are examples of concave caustic surfaces. The convex case is discussed in the next subsection.

In the neighborhood of the point P of closest approach of the line of sight with the caustic surface, we choose coordinates such that \hat{z} is perpendicular to the surface while \hat{x} and the direction \hat{y} of the line of sight are parallel. P has coordinates $x = y = z = 0$. In the $y = 0$ plane, the flow is given by $z(\alpha) = -\frac{1}{2}h\alpha^2$, where h is a positive constant. Using Eq. 352 we find the density in the $y = 0$ plane:

$$d(\sigma) = A \frac{\Theta(\sigma)}{\sqrt{\sigma}} \quad , \quad (355)$$

where $\sigma = -z$, and

$$A = \sqrt{\frac{2}{h}} \frac{d\Lambda}{d\alpha} \quad . \quad (356)$$

For $y \neq 0$, the density is still given by Eq. 355, but with $\sigma = z(y) - z$ and $z(y) = -\frac{y^2}{2R}$.

We calculate the shift using Eq. 354:

$$\begin{aligned} \Delta\xi &= -\frac{2}{\Sigma_c D_L} \frac{d\Lambda}{d\alpha} \int_{-\sqrt{-2Rz}}^{\sqrt{-2Rz}} dy \int d\alpha \Theta\left(-z - \frac{h}{2}\alpha^2 - \frac{y^2}{2R}\right) \\ &= \frac{4\pi}{\Sigma_c} \frac{d\Lambda}{d\alpha} \sqrt{\frac{R}{h}} \Theta(-\xi_I) \xi_I \quad . \end{aligned} \quad (357)$$

Hence

$$\Delta\xi = \xi_I - \xi_S = \eta \xi_I \Theta(-\xi_I) \quad , \quad (358)$$

with

$$\eta = \frac{2\pi A \sqrt{2R}}{\Sigma_c} \quad . \quad (359)$$

One can also obtain this result by calculating the column density:

$$\Sigma(\xi_I) = \int dy d(y, z = \xi_I) = \int dy \frac{A \Theta(-\xi_I D_L - \frac{y^2}{2R})}{\sqrt{-\xi_I D_L - \frac{y^2}{2R}}} = \pi A \sqrt{2R} \Theta(-\xi_I) \quad , \quad (360)$$

and solving Eq. 334:

$$\xi_I - \xi_S = \frac{d\psi}{d\xi_I} = \frac{2}{\Sigma_c} \int d\xi_I \Sigma(\xi_I) = \eta \xi_I \Theta(-\xi_I) \quad . \quad (361)$$

Eqs. 360-361 were first obtained by Hogan [22]. The agreement with Eq. 358 validates the formalism derived in Section 4.1. Figure 15 plots the source position ξ_S versus the image position ξ_I .

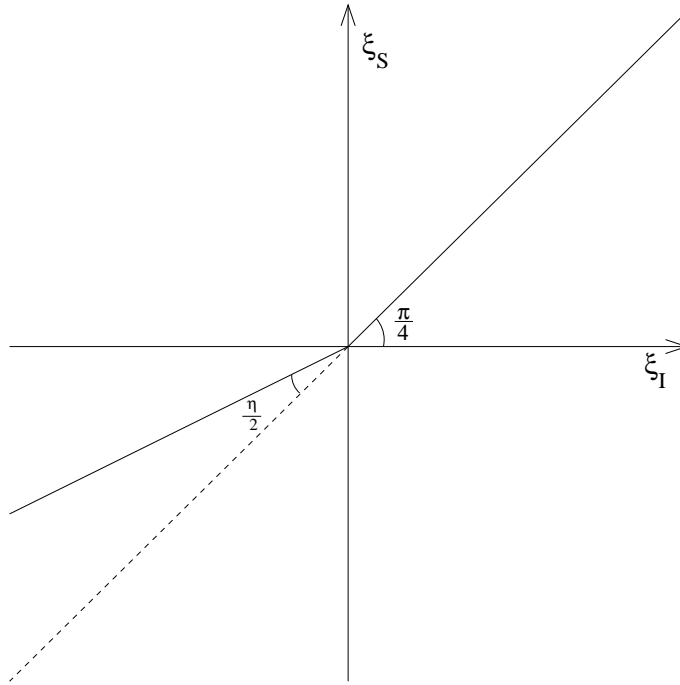


Figure 15: Source position ξ_S as a function of image position ξ_I for lensing by a concave fold. η is given by Eq. 359 in terms of the fold coefficient and the curvature radius of the caustic surface. Estimates of η for the outer caustics of galactic halos are given in Eq. 363.

The magnification is:

$$\mathcal{M} = \frac{d\xi_I}{d\xi_S} = 1 + \eta \Theta(-\xi_I) + 0(\eta^2) \quad . \quad (362)$$

When the line of sight of a moving source crosses the surface of a simple concave fold, the component of its apparent velocity perpendicular to the fold changes abruptly. Also, a discontinuity occurs in the magnification of the image. Both effects are of order η .

We estimate η for the outer caustics of galactic halos using Eqs. 156-159:

$$\{\eta_n = \frac{\sqrt{2} v_{\text{rot}}^2}{G \Sigma_c} \frac{F_n}{R_n} : n = 1, 2, \dots\} \sim (7, 6, 6, 6, 6, \dots) \cdot 10^{-3} \cdot \left(\frac{D_L D_{LS}}{D_S \text{ Gpc}} \right) \left(\frac{v_{\text{rot}}}{220 \text{ km/s}} \right) \left(\frac{h}{0.7} \right) . \quad (363)$$

A magnification of order 10^{-2} seems hard to observe, however, the images of extended sources may be modified in recognizable ways. In particular, straight jets would be seen with an abrupt bend where their line of sight crosses a fold. Indeed, the image is stretched by the factor $1 + \eta$ in the direction perpendicular to the caustic, on the side with the two extra flows. If the jet makes angle α with the normal, it appears bent by an angle $\delta \equiv \frac{1}{2}\eta \sin(2\alpha)$. Searching the sky for bends in extended sources may be a realistic approach to detecting caustic structure in galactic halos [22].

4.2.2 Lensing by a Convex Fold

By definition, a convex fold is curved in the direction opposite to the side with two extra flows (Fig. 13). Using the conventions of the previous subsection, we write the equation for the displacement of the surface along the line of sight as $z(y) = \frac{y^2}{2R}$, and that for the flow as $z(\alpha) = -\frac{1}{2}h\alpha^2$, for small z , with $R, h > 0$. Eqs. 355 and 356 still apply, with $\sigma = y^2/2R - z$. Eq. 354 yields the shift:

$$\Delta\xi = -\frac{8}{\Sigma_c D_L} \frac{d\Lambda}{d\alpha} \left\{ \Theta(-\xi_I) \int_0^\infty dy + \Theta(\xi_I) \int_{\sqrt{2RD_L\xi_I}}^\infty dy \right\} \sqrt{\frac{2}{h} \left(\frac{y^2}{2R} - D_L\xi_I \right)} . \quad (364)$$

We introduce a cut-off L for the integral over large y . L can be thought of as the length scale beyond which our description of the flow is invalid. The above equation becomes

$$\Delta\xi = -\frac{4}{\Sigma_c D_L} \frac{d\Lambda}{d\alpha} \frac{1}{\sqrt{hR}} \left\{ L\sqrt{L^2 - 2RD_L\xi_I} - 2RD_L\xi_I \ln \left(\frac{L + \sqrt{L^2 - 2RD_L\xi_I}}{\sqrt{2RD_L|\xi_I|}} \right) \right\} . \quad (365)$$

By expanding Eq. 365 in powers of $\frac{1}{L}$, and using Eq. 356, we obtain the ξ_I -dependent shift:

$$\Delta\xi = \xi_I - \xi_S = -\frac{\eta'}{\pi} \left[\ln \left(\frac{RD_L |\xi_I|}{2L^2} \right) - 1 \right] \xi_I \quad , \quad (366)$$

where η' (like η in Eq. 359) is given by

$$\eta' = \frac{2\pi A \sqrt{2R}}{\Sigma_c} \quad . \quad (367)$$

The magnification is

$$\mathcal{M} = \frac{d\xi_I}{d\xi_S} = \left| 1 + \frac{\eta'}{\pi} \ln \left(\frac{RD_L |\xi_I|}{2L^2} \right) \right|^{-1} \quad . \quad (368)$$

The cut-off L has an effect on both the magnification and the elongation of the image in the direction normal to the caustic surface, but that effect is ξ_I independent. L has a global effect on the image, as opposed to an effect localized near $\xi_I = 0$. Figure 16 plots ξ_S versus ξ_I . It shows that a convex fold can cause a triple image of a point source. In particular, when the source is exactly behind the caustic ($\xi_S = 0$), the images are at $\xi_I = -\xi_c$, 0, and $+\xi_c$, with

$$\xi_c = \frac{2L^2}{RD_L} \exp \left(-\frac{\pi}{\eta'} + 1 \right) \quad . \quad (369)$$

A point source has a single image sufficiently far from the caustic, say at $\xi_{I1} > 0$. When the line of sight approaches the caustic surface tangent point, two new images appear on top of each other at $\xi_{I2} = \xi_{I3} = -\xi_c/e$. At that moment, the magnification at ξ_{I2} is infinite, and $\xi_S = \eta' \xi_c / e\pi$. As the source crosses the caustic, ξ_{I2} moves toward ξ_{I1} and finally merges with it. When $\xi_{I1} = \xi_{I2} = +\xi_c/e$, the magnification diverges again. After that, only the image at ξ_{I3} remains.

Let us apply the above results to the line of sight in the plane of a caustic ring at the sample point, ($z = 0, \rho = a$), discussed in Section 3.5.5. Setting $R = a_n$ and using Eq. 291 we obtain for the n th ring

$$\eta'_n = \frac{2\pi A_{0,n} \sqrt{2a_n}}{\Sigma_c} = \frac{v_{\text{rot}}^2}{\sqrt{2G\Sigma_c}} \frac{f_n}{\sqrt{a_n p_n}} \frac{v_n}{b_n} \quad . \quad (370)$$

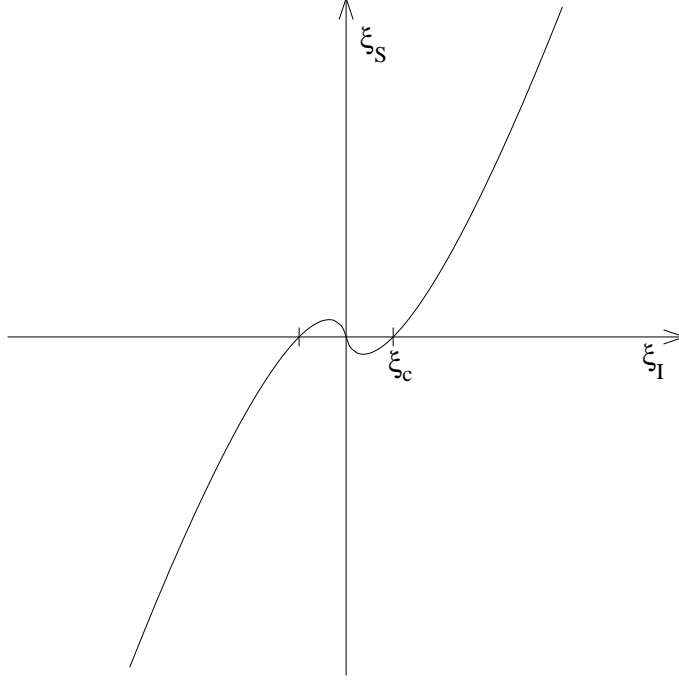


Figure 16: Source position ξ_S as a function of image position ξ_I for lensing by a convex fold. ξ_c is given in Eq. 369.

Using Eq. 292 to estimate $A_{0,n}$, we find

$$\{\eta'_n : n = 1, 2, \dots\} \sim (5, 4, 4, 4, 4, \dots) \cdot 10^{-2} \frac{D_L D_{LS}}{D_S \text{ Gpc}} \cdot \left(\frac{0.27}{j_{\max}}\right) \left(\frac{h}{0.7}\right) \left(\frac{v_{\text{rot}}}{220 \text{ km/s}}\right) . \quad (371)$$

For such small values of η' the angular distance between the triple images is exponentially small and unresolvable with present and foreseeable instruments.

The image of an extended object is stretched in the direction perpendicular to the caustic by the relative amount

$$\mathcal{M} - 1 = -\frac{\eta'}{\pi} \ln \left(\frac{RD_L |\xi_I|}{2L^2} \right) . \quad (372)$$

The image is stretched for $\xi_I < \xi_d$, and compressed for $\xi_I > \xi_d$, where

$$\xi_d = \frac{2L^2}{RD_L} . \quad (373)$$

In the case of the sample point ($z = 0, \rho = a$) with line of sight in the $z = 0$ plane, the cut-off length L (i.e., the distance in the y -direction over which our description of the flow is valid), is of order $\sqrt{2ap}$. In that case $\xi_d \sim 4p/D_L$. Since p/D_L is the transverse angular size of the caustic ring, our description certainly fails for $\xi_I > p/D_L$. So, over the region where our calculation is valid, the image is magnified. The effects are generically of order one percent, increasing to several percent when $\xi_I \sim 10^{-3}\xi_d$, for caustic rings at cosmological distances.

4.2.3 Lensing by a Fold with Zero Curvature

We saw in Section 3.5.4 that the surface of a caustic ring has tangent lines along which the curvature vanishes. One may speculate that the lensing effects of a caustic surface are strongest when the line of sight is tangent to the surface in a direction of zero curvature, because the line of sight stays close to the caustic over greater depths in that case. If the line of sight of an observer looking at the outside profile of a caustic ring is at some point on the profile in a direction of zero curvature, then the equation for the intersection of the caustic surface with the plane containing the outward normal to the surface (\hat{z}) and the line of sight (\hat{y}) is $z(y) = -\frac{y^4}{4U}$ where U is positive and has dimensions of (length)³. In such a case, the cubic term in the Taylor expansion of $z(y)$ is absent because the line of sight remains everywhere outside the caustic ring tube. We did not calculate U for caustic rings, but expect $U \sim (\text{kpc})^3$ in order of magnitude. The flow is given by $z(\alpha) = -\frac{1}{2}h\alpha^2$ with $h > 0$, as before, and Eq. 356 holds.

Using the above expressions for $z(y)$ and $z(\alpha)$ in Eq. 354, we find the shift

$$\begin{aligned}
\Delta\xi &= -\frac{2}{\Sigma_c D_L} \frac{d\Lambda}{d\alpha} \int dy \int d\alpha \Theta\left(-z - \frac{1}{2}h\alpha^2 - \frac{y^4}{4U}\right) \\
&= -\frac{8}{\Sigma_c D_L} \frac{d\Lambda}{d\alpha} \frac{(-4Uz)^{3/4}}{\sqrt{2hU}} \Theta(-\xi_I) \int_0^1 dt \sqrt{1-t^4} \\
&= -\Theta(-\xi_I) (-\xi_0 \xi_I^3)^{1/4} \quad , \tag{374}
\end{aligned}$$

where

$$\xi_0 = (9.89 \frac{A}{\Sigma_c})^4 \frac{U}{D_L} \quad . \quad (375)$$

The magnification is:

$$\mathcal{M} = \left| 1 - \frac{3}{4} \Theta(-\xi_I) \left(-\frac{\xi_0}{\xi_I} \right)^{1/4} \right|^{-1} \quad . \quad (376)$$

Figure 17 shows ξ_S versus ξ_I .

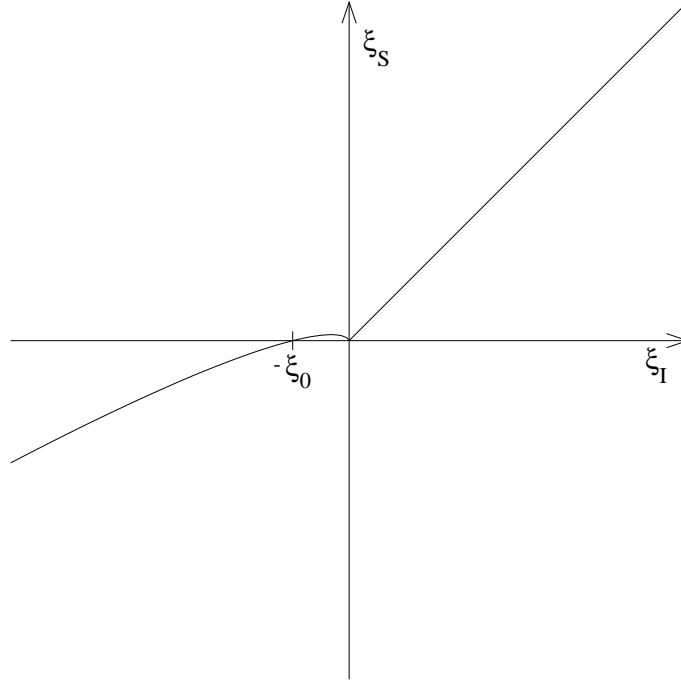


Figure 17: Source position ξ_S as a function of image position ξ_I for lensing by a fold with zero curvature. ξ_0 is given in Eq. 375.

Triple images occur when $|\xi_I| \leq \xi_0$. Unfortunately, for the zero curvature tangents of caustic rings envisaged above, ξ_0 is very small. For $2D_L = 2D_{LS} = D_S = \text{Gpc}$, $A = 3 \cdot 10^{-4} \frac{\text{gr}}{\text{cm}^2 \text{kpc}^2}$, and $U = (\text{kpc})^3$, one finds $\xi_0 = 4 \cdot 10^{-17}$. Hence the triple images cannot be resolved. Also, even at angular distances as small as $\xi_I \sim 10^{-9}$, the magnification and image distortion is only of order 1%.

4.2.4 Lensing by a Cusp

In this section, we investigate a line of sight parallel to the plane ($z = 0$) of a caustic ring, and passing near the cusp at $\rho = \rho_0$ (Fig. 14). We use the 2D lensing equations derived in Section 4.1. The shifts are given by Eq. 349 in terms of the complex integral I of Eq. 347. Using Eq. 310, we have

$$I = \int d\alpha \int d\tau \frac{1}{\rho - a - \frac{1}{2}u\tau_0^2 + u\tau_0\tau + \frac{1}{2}s\alpha^2 + i(z - b\alpha\tau)} \quad . \quad (377)$$

Because we are close to the cusp, the term of order τ^2 is neglected in the denominator of the integrand. In terms of the parameters defined in Eqs. 311,

$$I = \frac{2}{b\sqrt{\zeta}} \int dT \int_{-\infty}^{\infty} \frac{dA}{A^2 - 2i\frac{AT}{\sqrt{\zeta}} + 2T + X + i\frac{Z}{\sqrt{\zeta}}} \quad . \quad (378)$$

The integration over A yields

$$I = \frac{2\pi}{b\sqrt{\zeta}} \int_{\frac{|T|}{\sqrt{\zeta}} < C} \frac{dT}{\sqrt{\frac{T^2}{\zeta} + 2T + X + i\frac{Z}{\sqrt{\zeta}}}} \quad , \quad (379)$$

where $C \equiv \text{Re} \sqrt{\frac{T^2}{\zeta} + 2T + X + i\frac{Z}{\sqrt{\zeta}}} > 0$. Near the cusp ($X, Z \ll 1$) the terms of order T^2 can be neglected since they are unimportant in the denominator of Eq. 378. Equation 379 becomes then

$$I(X, Z) = \frac{2\pi}{b\sqrt{\zeta}} \int \frac{dT}{\sqrt{2T + X + i\frac{Z}{\sqrt{\zeta}}}} \quad , \quad (380)$$

where the integration domain is defined by the inequality:

$$T^4 - \zeta(2T^3 + XT^2) - \frac{\zeta Z^2}{4} < 0 \quad . \quad (381)$$

Let us call T_i ($i = 1, \dots, 4$) the roots of the polynomial on the left hand side of Eq. 381. Near the cusp, three of the roots T_i are near zero and one of the roots is close to 2ζ . Let us call the latter T_4 . In order to find the roots near $T = 0$ we neglect the quartic term and solve the cubic equation:

$$T^3 + \frac{X}{2}T^2 + \frac{Z^2}{8} = 0 \quad . \quad (382)$$

This equation is also obtained by eliminating A from Eqs. 312 and 313. Hence the solutions of Eq. 382 are the values of T for the flows near the cusp. As was discussed in Section 3.5.5, the number of flows is determined by δ , given in Eq. 316. Outside the cusp, where $\delta > 0$, there is a single root T_1 . Inside the cusp where $\delta < 0$, there are three roots T_1 , T_2 and T_3 . Figure 18 shows the quartic polynomial, Eq. 381, for various values of X and Z , and $\zeta = 1$. For a line of sight just outside the cusp, the quartic polynomial is negative

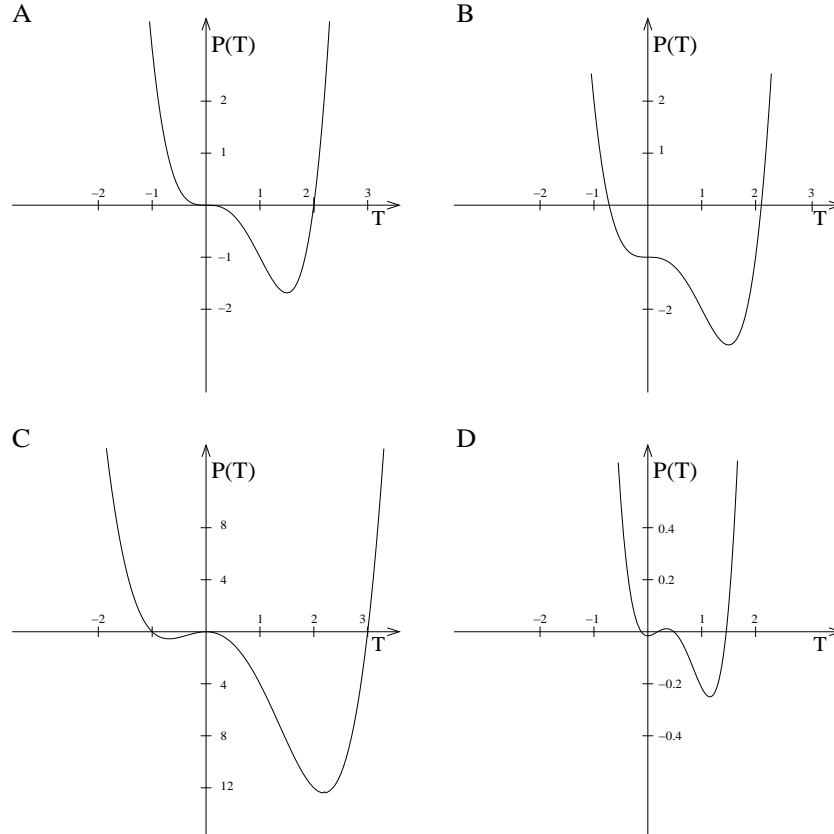


Figure 18: Graphs of the quartic polynomial $P(T) \equiv T^4 - \zeta(2T^3 + XT^2) - \frac{\zeta Z^2}{4}$ for $\zeta = 1$ and $(X, Z) = (0, 0), (0, 2), (1/3, 0)$ and $(-1/3, 0)$; a) through d) respectively.

from T_1 to T_4 with

$$T_1 = -\frac{1}{2} \left(\sqrt{\delta} - \frac{|Z|}{2} \right)^{2/3} - \frac{1}{2} \left(\sqrt{\delta} + \frac{|Z|}{2} \right)^{2/3} - \frac{X}{6} . \quad (383)$$

Eq. 380 becomes in that case:

$$I = \frac{2\pi}{b\sqrt{\zeta}} \left\{ \sqrt{2T_4 + X + i\frac{Z}{\sqrt{\zeta}}} - \sqrt{2T_1 + X + i\frac{Z}{\sqrt{\zeta}}} \right\} . \quad (384)$$

Let us consider the line of sight defined by Fig. 14. Equation 349 gives the shift in the direction perpendicular to the plane of the cusp as

$$\Delta\xi_z = -\frac{1}{\pi\Sigma_c D_L} \frac{d^2\Lambda}{d\alpha d\tau} \operatorname{Im} \int dy I(X - X(y), Z) \quad (385)$$

where $X(y) = -\frac{y^2}{2\rho_0 p}$ is the shift of the cusp as a function of depth. The integral in Eq. 385 with the integrand given by Eqs. 383 and 384 can be done numerically. Here we only give a rough estimate, to determine the order of magnitude and qualitative properties of the lensing effects.

For $X = 0$ and $Z \ll 1$, we have

$$I = \frac{2\pi}{b} \left[2 - \frac{i}{\sqrt{\zeta}} \operatorname{Sign}(Z) |Z|^{1/3} - \frac{1}{2\zeta} |Z|^{2/3} \right] + O(Z) . \quad (386)$$

Because the scaling law $X^3 \sim Z^2$ holds close to the cusp, we expect Eq. 386 to be valid as long as the shift in the x -direction $|\Delta X| \leq |Z|^{2/3}$. Hence Eq. 386 provides a good estimate of $I(X - X(y), Z)$ over a depth $2\Delta y$ with $\Delta y \sim \sqrt{2\rho_0 p} |Z|^{1/3}$. Therefore

$$\Delta\xi_z \sim \frac{2}{\Sigma_c D_L b} \sqrt{\frac{2\rho_0 p}{\zeta}} \frac{d^2\Lambda}{d\alpha d\tau} |Z|^{2/3} \operatorname{Sign}(Z) . \quad (387)$$

Since we are near $\alpha = 0$,

$$\frac{d^2\Lambda}{d\alpha d\tau} = \frac{1}{2\pi\rho_0} \frac{d^2 M}{d\alpha d\tau} = \frac{1}{\rho_0} \frac{d^2 M}{d\Omega dt} . \quad (388)$$

Using this and Eq. 287, we obtain

$$\Delta\xi_z \sim \eta'' |\xi_{Iz}|^{2/3} \operatorname{Sign}(\xi_{Iz}) , \quad (389)$$

where

$$\eta'' \equiv \frac{2\sqrt{2a}}{\zeta^{1/6} \Sigma_c D_L^{2/3}} p^{1/3} A_0 . \quad (390)$$

The contribution to the magnification from distortion in the z -direction is therefore:

$$\mathcal{M}_z \sim \left| 1 - \eta'' \frac{2}{3} |\xi_{Iz}|^{-\frac{1}{3}} \right|^{-1} . \quad (391)$$

Figure 19 plots ξ_{Sz} versus ξ_{Iz} :

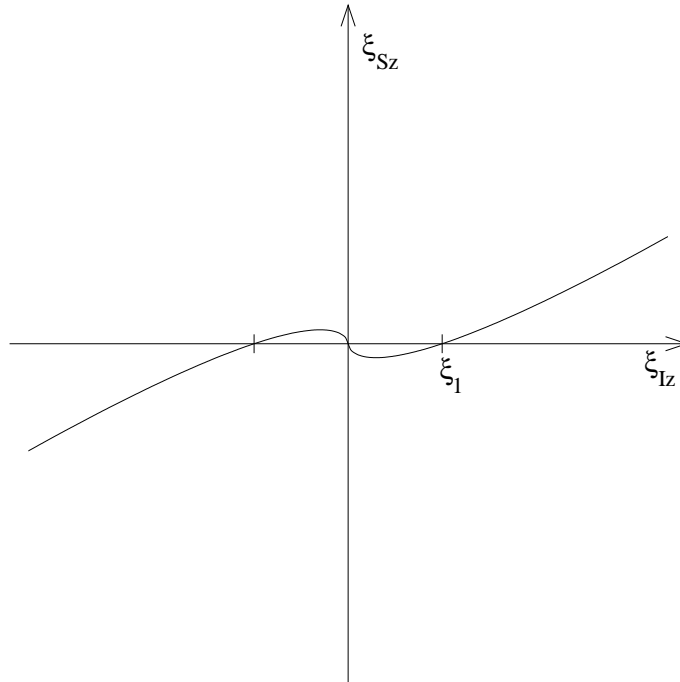


Figure 19: Source position ξ_{Sz} as a function image position ξ_{Iz} for lensing by a cusp along the line of sight described in Fig. 14. $\xi_1 \sim \eta''^3$ where η'' is given by Eq. 390.

For $\xi_{Iz} \leq \xi_1 \sim \eta''^3$, a point source has triple images. For the n th caustic ring, η'' can be estimated using Eqs. 288 and 292, and assuming $p \simeq 0.1a$, $\zeta \sim 1$:

$$\begin{aligned} \{\eta'' : n = 1, 2, \dots\} &\sim (1.5, 1, 0.7, 0.6, 0.5, \dots) \cdot 10^{-4} \frac{D_L^{\frac{2}{3}} D_{LS}}{D_S \text{ Gpc}^{\frac{2}{3}}} \cdot \\ &\cdot \left(\frac{0.27}{j_{\max}} \right)^{\frac{2}{3}} \left(\frac{h}{0.7} \right)^{\frac{2}{3}} \left(\frac{v_{\text{rot}}}{220 \text{ km/s}} \right)^{\frac{4}{3}} . \end{aligned} \quad (392)$$

At cosmological distances, the typical angular separation between the images is of order 10^{-12} . Unfortunately, here again the images are too close to be resolved, however, for an angular distance $\xi_I \sim 10^{-9}$, \mathcal{M}_z is of order 10%, which may be observable. The lensing

properties of a cusp for other lines of sight can be calculated numerically using Eqs. 349 and 377. The latter equation is replaced by Eqs. 384 and 383, and $T_4 = 2\zeta$, if the line of sight is everywhere outside the region with two extra flows.

5 Conclusions

We reviewed the leading cold dark matter (CDM) candidates: axions and weakly interacting massive particles (WIMPs) in Section 2. We discussed each candidate’s status in particle physics and cosmology, its production in the early universe, its energy density and velocity dispersion. We found that the velocity dispersions of the candidates are negligible on astronomical scales; hence, they indeed are “cold.”

In Section 3, we discussed the appearance of caustics in the flow of CDM particles in and out of a galaxy. Caustics are surfaces in space where the density of CDM diverges in the limit of zero velocity dispersion. In this limit the particles lie on a 3D sheet in 6D phase space. The physical space density is the projection of the phase space sheet onto physical space. Caustics occur wherever the phase space sheet folds back in phase space. At the fold the phase space sheet is tangent to velocity space, particles pile up, and hence the number density, which is the integral of the phase space density over velocity space, diverges. Generically caustics are boundary surfaces separating two regions in physical space. One region has n flows and the other has $n + 2$ flows, where n is an odd number. Because the flow of CDM particles is continuous, caustic surfaces are topologically stable. There are two types of CDM caustics in the halos of galaxies: outer and inner. An outer caustic is a simple fold (A_2) catastrophe, located on a topological sphere, surrounding the galaxy. Outer caustics occur where a given outflow reaches its furthest distance from the galactic center before falling back in. We provided estimates of the radii and fold coefficients of the outer caustics, based upon the self similar infall model. An inner caustic is a ring (i.e., a closed circular tube whose cross-section is a D_{-4} catastrophe), with three cusps. Inner caustics are located near where the particles with the most angular momentum in a given inflow reach their closest approach to the galactic center before going back out. Inside the tube there are $n + 4$ flows. Outside the tube there are $n + 2$, where n is again odd. We gave a detailed analysis of caustic rings in the case where the flow of particles is axially and

reflection symmetric and where the transverse dimensions of the ring is tight. In that case, the flow, and hence the caustic, is described by 5 parameters: a , b , s , τ_0 and u . The precise shape of a transverse section of the ring in this limit is shown in Fig. 3. For the inner caustic rings, the curvature radii and fold coefficients depend on the position on the surface of the ring caustic. We derived formulae for these quantities as a function of this position (parametrized by τ_1) and of the five caustic ring parameters (a , b , u , τ_0 , s). A great fraction of the surface of a caustic ring ($0 < |\frac{\tau_1}{\tau_0}| < \frac{3}{4}$) is saddle-shaped and therefore has tangent directions along which the curvature of the surface vanishes. Finally, we derived the mass density profile near a cusp caustic. These quantities were estimated using the self similar infall model.

Gravitational lensing was discussed in Section 4. In general, the shift in image position is the gradient of a potential whose 2D Laplacian is the column density. For an arbitrary mass distribution, the procedure for calculating the shift involves two steps. First the matter density is integrated along the line of sight to obtain the column density. Second, the potential is obtained by convolving the column density with the 2D Green's function. In the case of lensing by dark matter caustics, this procedure can be simplified: the shift is expressed directly as an integral over the parameter space of the dark matter flow forming the caustic. The relevant result is given in Eqs. 347 and 349 if the caustic has contrast in the two dimensions transverse to the line of sight, and in Eq. 354 if the caustic has contrast in only one of the dimensions transverse to the line of sight. We applied our formalism to the gravitational lensing by dark matter caustics in four specific cases. In the first three, the line of sight is tangent to a surface where a simple fold catastrophe is located. The three cases are distinguished by the curvature of the caustic surface at the tangent point in the direction of the line of sight: (1) the surface curves toward the side with two extra flows; (2) the surface curves away from the side with two extra flows; and (3) the surface has zero curvature. In the fourth case (4) studied, the line of sight is at a specific location

close to a cusp catastrophe and parallel to the plane of the cusp. We found that each case has characteristic lensing signatures. In three of the cases (2, 3 and 4) there are multiple images and infinite magnification of point sources when their images merge. In case 1, there are no multiple images. Unfortunately, the effects are small even for dark matter caustic lenses at cosmological distances. The multiple images of a point source cannot be resolved with present instruments. Typical magnifications and image distortions are of order one % to a few %. A promising approach may be to observe the distortions caused by dark matter caustics in the images of extended sources, such as radio jets. This possibility was discussed in case (1).

A Vacua of Non-Abelian Gauge Theory and Instantons

A.1 Description of Non-Abelian Gauge Theory

Let the Lagrangian density be $\mathcal{L}(\Psi(x), \partial_\mu \Psi(x))$, where $\Psi(x)$ denotes an arbitrary field as a function of spacetime coordinate $x^\mu = (x^0, x^1, x^2, x^3)$. We adopt the convention where the spacetime metric tensor has the components $g_{\mu\nu} = \text{diag}(+1, -1, -1, -1)$. Under a local (i.e., x -dependent) gauge transformation

$$\begin{aligned}\Psi(x) &\rightarrow \Psi'(x) = U(x)\Psi(x), \\ \partial_\mu \Psi(x) &\rightarrow (\partial_\mu \Psi(x))' = U(x)\partial_\mu \Psi(x) + (\partial_\mu U(x))\Psi(x),\end{aligned}\tag{393}$$

where $U(x)$ is an element of a Lie Group G . A Lie group is a continuous group generated by the corresponding Lie algebra which is a vector space whose basis consists of N generators $T^a (a = 1, \dots, N)$ that are closed under commutation: $[T^a, T^b] = if^{abc}T^c$. The structure constants f^{abc} are real numbers and they completely define the Lie algebra. We adopt the normalization conditions $\text{Tr}(T^a T^b) = \frac{1}{2}\delta^{ab}$. An element $U(x)$ of G is obtained by exponentiating the algebra:

$$U(x) = e^{-i\omega^a(x)T^a}.\tag{394}$$

Because U is parametrized by $\{\omega^a\}$, the group manifold of G is the space of the possible values of $\{\omega^a\}$. The correspondence between Lie group and Lie algebra is many-to-one. In order to have a one-to-one correspondence between $\{\omega^a\}$ and a group element, the possible values of $\{\omega^a\}$ must be restricted.

Gauge invariance, at the Lagrangian level, means

$$\mathcal{L}(\Psi(x)', (\partial_\mu \Psi(x))') = \mathcal{L}(\Psi(x), \partial_\mu \Psi(x)).\tag{395}$$

This requires invariance under global (i.e., x -independent) transformations. However, since $\partial_\mu U(x) \neq 0$, in Eq. 393, $\partial_\mu \Psi(x)$ does not transform in the same way as $\Psi(x)$. This spoils

the gauge invariance of \mathcal{L} , even if \mathcal{L} is invariant under global transformations. To preserve the invariance we look for a covariant derivative $D_\mu\Psi$ with the transformation property $(D_\mu\Psi(x))' \equiv D'_\mu\Psi'(x) = U(x)(D_\mu\Psi(x))$. Equivalently, since $D'_\mu\Psi'(x) = D'_\mu U(x)\Psi$, we want $D'_\mu U(x)\Psi = U(x)(D_\mu\Psi(x))$ which implies

$$D'_\mu U(x) = U(x)D_\mu, \quad (396)$$

or

$$D'_\mu = U(x)D_\mu U(x)^{-1}. \quad (397)$$

To find D_μ , we introduce a Lie Algebra valued vector field $A_\mu(x) = A_\mu^a(x)T^a$, and try the ansatz

$$D_\mu\Psi(x) = [\partial_\mu - igA_\mu(x)]\Psi(x). \quad (398)$$

If we demand $A_\mu(x)$ to transform as

$$A'_\mu(x) = U(x)A_\mu(x)U^{-1}(x) - \frac{i}{g}(\partial_\mu U(x))U^{-1}(x), \quad (399)$$

the ansatz Eq. 398 gives

$$\begin{aligned} (D_\mu\Psi(x))' &= D'_\mu\Psi'(x) = (\partial_\mu - igA'_\mu(x))U(x)\Psi(x) \\ &= (\partial_\mu U(x))\Psi + U(x)\partial_\mu\Psi(x) \\ &\quad - ig \left[U(x)A_\mu(x)U^{-1}(x) - \frac{i}{g}(\partial_\mu U(x))U^{-1}(x) \right] U(x)\Psi(x), \end{aligned} \quad (400)$$

which yields the required transformation property Eq. 396 for $D_\mu\Psi(x)$:

$$(D_\mu\Psi(x))' = U(x)[\partial_\mu - igA_\mu(x)]\Psi(x) = U(x)D_\mu\Psi(x). \quad (401)$$

Suppose the gauge field is the vacuum configuration; $A_\mu \equiv 0$. If we perform a spacetime dependent gauge transformation Eq. 399, we obtain

$$A_\mu \rightarrow A_\mu(x) = -\frac{i}{g}(\partial_\mu U(x))U^{-1}(x). \quad (402)$$

The form of $A_\mu(x)$ in Eq. 402 is called “pure gauge.”

For an infinitesimal change

$$U_{kl} = \delta_{kl} - iT_{kl}^a \omega^a + O(\omega^2), \quad (403)$$

Eq. 399 becomes

$$T_{kl}^a A_\mu^a = T_{kl}^a A_\mu^a + i\omega^b [T^a, T^b]_{kl} A_\mu^a - \frac{1}{g} T_{kl}^a \partial_\mu \omega^a. \quad (404)$$

Using the commutation relation $[T^a, T^b]_{kl} = if^{abc} T_{kl}^c$, we find

$$\delta A_\mu^a(x) = f^{abc} \omega^b(x) A_\mu^c(x) - \frac{1}{g} \partial_\mu \omega^a(x). \quad (405)$$

To make the gauge fields A_μ^a dynamical variables of the theory we need to add their free Lagrangian density, which should satisfy gauge and Lorentz invariance and should be quadratic in spacetime derivatives of A_μ^a . Thus, we need the generalization of $F_{\mu\nu} F^{\mu\nu}$ of the Abelian case (Maxwell’s theory) where the field strength tensor is $F_{\mu\nu} = \partial_\mu A_\nu - \partial_\nu A_\mu$. We may try to define a field strength tensor of the same form $\partial_\mu A_\nu^a - \partial_\nu A_\mu^a$, however, this transforms in a complicated way under Eq. 405. Recall that $F_{\mu\nu}$ is the curvature (commutator of the covariant derivative) associated with the covariant derivative $D_\mu = \partial_\mu - ieA_\mu$, hence $F_{\mu\nu} = \frac{i}{e} [D_\mu, D_\nu]$, where e is the electric charge. Using this analogy, we find

$$\begin{aligned} [D_\mu, D_\nu] \Psi(x) &= \left\{ \partial_\mu \partial_\nu \Psi(x) - ig \partial_\mu (A_\nu(x) \Psi(x)) - ig A_\mu(x) \partial_\nu \Psi(x) - g^2 A_\mu(x) A_\nu(x) \right\} \\ &\quad - \left\{ \mu \leftrightarrow \nu \right\} = -ig \left\{ \left(\partial_\mu A_\nu(x) - \partial_\nu A_\mu(x) - ig [A_\mu(x), A_\nu(x)] \right) \Psi(x) \right. \\ &\quad \left. - \left(A_\nu(x) \partial_\mu \Psi(x) + A_\mu(x) \partial_\nu \Psi(x) - (\mu \leftrightarrow \nu) \right) \right\} \\ &= -ig \left(\partial_\mu A_\nu(x) - \partial_\nu A_\mu(x) - ig [A_\mu(x), A_\nu(x)] \right) \Psi(x) \\ &\equiv -ig G_{\mu\nu}(x) \Psi(x) = -ig T^a G_{\mu\nu}^a(x) \Psi(x), \end{aligned} \quad (406)$$

where

$$G_{\mu\nu}^a(x) = \partial_\mu A_\nu^a(x) - \partial_\nu A_\mu^a(x) + gf^{abc} A_\mu^b(x) A_\nu^c(x). \quad (407)$$

Let us check that the above form of the field strength tensor transforms in a simple way, determined only by f^{abc} . Because of the transformation property Eq. 397 of the covariant derivative, we have

$$\left([D_\mu, D_\nu]\Psi(x)\right)' = U(\omega(x))\left([D_\mu, D_\nu]\Psi(x)\right). \quad (408)$$

Using Eq. 406 in Eq. 408, we find that $T^a G'_{\mu\nu} U(\omega)\Psi = U(\omega)T^a G_{\mu\nu} \Psi$, or

$$T^a G'_{\mu\nu}(x) = U(\omega(x))\left(T^a G_{\mu\nu}(x)\right)U^{-1}(\omega(x)). \quad (409)$$

Then, the infinitesimal transformation is calculated by inserting Eq. 403 into Eq. 409:

$$\delta G'_{\mu\nu}(x) = f^{abc}\omega^b(x)G_{\mu\nu}^c(x) = i[G_{\mu\nu}(x), \omega(x)], \quad (410)$$

as required.

Up to here, we have been acting the covariant derivative D_μ on fields Ψ which transform as $\delta\Psi_k = -i\omega^a T_{kl}^a \Psi_l$. Now, we want to apply the covariant derivative to Lie Algebra valued objects $V = V^a T^a$. Before proving the form how the covariant derivative acts on the Lie Algebra valued objects, it is useful to introduce a generalized cross product for gauge group vectors $V = V^a T^a$, $W = W^a T^a$ and $X = X^a T^a$, where the dummy index $a = 1, 2, \dots, n$:

$$\vec{V}(x) \equiv (V^1(x), \dots, V^n(x)), \quad \vec{W}(x) \equiv (W^1(x), \dots, W^n(x)), \quad \vec{X}(x) \equiv (X^1(x), \dots, X^n(x)). \quad (411)$$

We define

$$(\vec{V}(x) \times \vec{W}(x))^a \equiv f^{abc}V^b(x)W^c(x), \quad (412)$$

which implies

$$\begin{aligned} (\vec{V}(x) \times \vec{W}(x))^a &= f^{abc}V^b(x)W^c(x) = -i([T^b, T^c])^a V^b(x)W^c(x) \\ &= -i([V(x), W(x)])^a. \end{aligned} \quad (413)$$

Consequently, we can make use of the usual cross product relations like

$$\vec{V} \times \vec{W} = -\vec{W} \times \vec{V}, \quad (414)$$

$$\vec{V} \times (\vec{W} \times \vec{X}) + \vec{W} \times (\vec{X} \times \vec{V}) + \vec{X} \times (\vec{V} \times \vec{W}) = 0, \quad (415)$$

where the later is known as the Jacobi identity. In this new notation Eqs. 405 and 410 can be written, respectively, as

$$\delta \vec{A}_\mu(x) = \vec{\omega}(x) \times \vec{A}_\mu(x) - \frac{1}{g} \partial_\mu \vec{\omega}(x), \quad (416)$$

$$\delta \vec{G}_{\mu\nu}(x) = \vec{\omega}(x) \times \vec{G}_{\mu\nu}(x) \quad (417)$$

Now, we want to show that the covariant derivative of $V = V^a T^a$ must be of the form

$$D_\mu V = \partial_\mu V - ig[A_\mu, V], \quad (418)$$

to have the transformation property $(D_\mu V)' = U(D_\mu V)U^{-1}$. In other words, expressing the covariant derivative as $D_\mu V = T^a (D_\mu V)^a$ and $D_\mu \vec{V} = \{(D_\mu V)^a : a = 1, \dots, n\}$, we will show that

$$D_\mu \vec{V} = \partial_\mu \vec{V} + g \vec{A}_\mu \times \vec{V}, \quad (419)$$

has the required transformation property, in infinitesimal form,

$$\delta(D_\mu \vec{V}) = \vec{\omega} \times (D_\mu \vec{V}) = \vec{\omega} \times (\partial_\mu \vec{V} + g \vec{A}_\mu \times \vec{V}), \quad (420)$$

where

$$\delta \vec{V} = \vec{\omega} \times \vec{V}. \quad (421)$$

In particular, when V is taken as the field strength tensor, we will have $D_\mu G_{\nu\rho} = \partial_\mu G_{\nu\rho} - ig[A_\mu, G_{\nu\rho}]$, where $\delta \vec{G}_{\mu\nu} = \vec{\omega} \times \vec{G}_{\mu\nu}$ as in Eq. 417. Now, to prove the claim Eq. 419 let us calculate the transformation

$$\delta(D_\mu \vec{V}) = \delta(\partial_\mu \vec{V} + g \vec{A}_\mu \times \vec{V}) = \partial_\mu \delta \vec{V} + g \delta \vec{A}_\mu \times \vec{V} + g \vec{A}_\mu \times \delta \vec{V}. \quad (422)$$

Using Eqs. 416 and 421 in Eq. 422 we obtain

$$\begin{aligned}\delta(D_\mu \vec{V}) &= \partial_\mu(\vec{\omega} \times \vec{V}) - (\partial_\mu \vec{\omega}) \times \vec{V} + g(\vec{\omega} \times \vec{A}_\mu) \times \vec{V} + g\vec{A}_\mu \times (\vec{\omega} \times \vec{V}) \\ &= \vec{\omega} \times \partial_\mu \vec{V} + g \left((\vec{\omega} \times \vec{A}_\mu) \times \vec{V} + \vec{A}_\mu \times (\vec{\omega} \times \vec{V}) \right).\end{aligned}\quad (423)$$

Finally, the application of identities 415 in Eq. 423 yield

$$\delta(D_\mu \vec{V}) = \vec{\omega} \times \partial_\mu \vec{V} + g\vec{\omega} \times (\vec{A}_\mu \times \vec{V}) = \vec{\omega} \times (\partial_\mu \vec{V} + g\vec{A}_\mu \times \vec{V}), \quad (424)$$

which is the transformation we wanted in Eq. 420. Thus, we define $D_\mu \equiv \partial_\mu - ig[A_\mu, \]$ or $D_\mu \equiv \partial_\mu + g(\vec{A}_\mu \times \)$. Another relation we want to derive is

$$\begin{aligned}[D_\mu, D_\nu] \vec{V} &= \partial_\mu(\partial_\nu \vec{V} + g\vec{A}_\nu \times \vec{V}) + g\vec{A}_\mu(\partial_\nu \vec{V} + g\vec{A}_\nu \times \vec{V}) - (\mu \leftrightarrow \nu) \\ &= g(\partial_\mu \vec{A}_\nu - \partial_\nu \vec{A}_\mu) \times \vec{V} + g^2(\vec{A}_\mu \times (\vec{A}_\nu \times \vec{V}) - \vec{A}_\nu \times (\vec{A}_\mu \times \vec{V})) \\ &= g(\partial_\mu \vec{A}_\nu - \partial_\nu \vec{A}_\mu + g\vec{A}_\mu \times \vec{A}_\nu) \times \vec{V} \\ &= g \vec{G}_{\mu\nu} \times \vec{V},\end{aligned}\quad (425)$$

where we have used the identities 415. Using result 413 in Eq. 425 we obtain

$$[D_\mu, D_\nu] \vec{V} = -ig[\vec{G}_{\mu\nu}, \vec{V}]. \quad (426)$$

All the pure gauge types of vector potential, defined in 402, are vacuum solutions. This can be shown as follows. For the pure gauge fields

$$\begin{aligned}G_{\mu\nu}(x) &= (\partial_\mu A_\nu(x) - igA_\mu(x)A_\nu(x)) - (\mu \leftrightarrow \nu) = -\frac{i}{g} \left\{ [\partial_\mu (U(x)\partial_\nu U^{-1}(x)) \right. \\ &\quad \left. + U(x) (\partial_\mu U^{-1}(x)) U(x) (\partial_\nu U^{-1}(x))] - [\mu \leftrightarrow \nu] \right\}.\end{aligned}\quad (427)$$

On the other hand, by taking the derivative of the identity $U(x)U^{-1}(x) = I$, we obtain $(\partial_\mu U)U^{-1} + U\partial_\mu U^{-1} = 0$ which gives

$$\partial_\mu U(x) = -U(x) (\partial_\mu U^{-1}(x)) U(x). \quad (428)$$

Replacing $\partial_\nu U(x)$ in Eq. 427 using Eq. 428 one finds

$$G_{\mu\nu}(x) = 0. \quad (429)$$

Recall Eq. 410 that, unlike the Abelian case where $f^{abc} = 0$, $G_{\mu\nu}^a$ transforms nontrivially (under gauge transformation Eq. 399 the field tensor is gauge covariant in the non-Abelian case whereas gauge invariant in the Abelian case). However the trace $\text{Tr}(G_{\mu\nu}G^{\mu\nu}) = \frac{1}{2}G_{\mu\nu}^a G^{a\mu\nu}$ is gauge invariant:

$$\delta[G_{\mu\nu}^a(x)G^{a\mu\nu}(x)] = 2\delta G_{\mu\nu}^a(x)G^{a\mu\nu}(x) = 2f^{abc}\omega^b(x)G_{\mu\nu}^c(x)G^{a\mu\nu}(x) = 0. \quad (430)$$

This is because the indices a and c are antisymmetric in f^{abc} whereas symmetric in $G_{\mu\nu}^c G^{a\mu\nu}$. Therefore,

$$\mathcal{L}_{\text{gauge}} = -\frac{1}{2}\text{Tr}G_{\mu\nu}(x)G^{\mu\nu}(x) = -\frac{1}{4}G_{\mu\nu}^a(x)G^{a\mu\nu}(x), \quad (431)$$

can be used as the kinetic term for the gauge vector field $A_\mu^a(x)$. This is, in fact, the Yang Mills Lagrangian density and in our the discussion we consider only the Yang Mills field theory. The equations of motion are obtained from the condition that the action $S = \int d^4x \mathcal{L}_{\text{gauge}}$ be stationary against arbitrary variations of the gauge fields. Suppressing the explicit spacetime dependence of the fields,

$$\delta S = - \int d^4x \text{Tr}(G_{\mu\nu}\delta G^{\mu\nu}), \quad (432)$$

where $\delta G^{\mu\nu} = (\partial^\mu \delta A^\nu - ig\delta A^\mu A^\nu - igA^\mu \delta A^\nu) - (\mu \leftrightarrow \nu)$. Thus, using $G_{\mu\nu} = -G_{\nu\mu}$, we obtain

$$\delta S = -2 \int d^4x \text{Tr} [G_{\mu\nu}(\partial^\mu \delta A^\nu - ig\delta A^\mu A^\nu - igA^\mu \delta A^\nu)]. \quad (433)$$

Integration of the first term by parts yields

$$\delta S = 2 \int d^4x \text{Tr} [\partial^\mu G_{\mu\nu} + igG_{\mu\nu}(\delta A^\mu A^\nu + A^\mu \delta A^\nu)]. \quad (434)$$

Since $\text{Tr} [G_{\mu\nu} \delta A^\mu A^\nu] = -\text{Tr} [A^\mu G_{\mu\nu} \delta A^\nu]$ we have

$$\delta S = 2 \int dx^4 \text{Tr} [(\partial^\mu G_{\mu\nu} - ig[A^\mu, G_{\mu\nu}]) \delta A^\nu] . \quad (435)$$

Thus the field equations are

$$D^\mu G_{\mu\nu} = \partial^\mu G_{\mu\nu} - ig[A^\mu, G_{\mu\nu}] = 0 , \quad (436)$$

or equivalently,

$$D^\mu G_{\mu\nu}^a = \partial^\mu G_{\mu\nu}^a + gf^{abc} A^{b\mu} G_{\mu\nu}^c = 0 . \quad (437)$$

Using the Jacobi identity,

$$[D_\mu [D_\nu, D_\rho]] + [D_\nu [D_\rho, D_\mu]] + [D_\rho [D_\mu, D_\nu]] = 0 , \quad (438)$$

and Eq. 406, $[D_\mu, D_\nu] = -igG_{\mu\nu}$ we obtain the Bianchi identity:

$$[D_\mu, G_{\nu\rho}] + [D_\nu, G_{\rho\mu}] + [D_\rho, G_{\mu\nu}] = 0 . \quad (439)$$

Let's calculate the above commutators:

$$\begin{aligned} [D_\mu, G_{\nu\rho}] \Psi &= [\partial_\mu - ig[A_\mu, \cdot], G_{\nu\rho}] \Psi = [\partial_\mu, G_{\nu\rho}] \Psi - ig[A_\mu, \cdot, G_{\nu\rho}] \Psi \\ &= \partial_\mu (G_{\nu\rho} \Psi) - G_{\nu\rho} \partial_\mu \Psi - ig([A_\mu G_{\nu\rho} \Psi] - G_{\nu\rho} [A_\mu, \Psi]) \\ &= (\partial_\mu G_{\nu\rho} - ig[A_\mu, G_{\nu\rho}]) \Psi = (D_\mu G_{\nu\rho}) \Psi . \end{aligned} \quad (440)$$

Likewise $[D_\nu, G_{\rho\mu}] = D_\nu G_{\rho\mu}$ and $[D_\rho, G_{\mu\nu}] = D_\rho G_{\mu\nu}$. Hence the Bianchi identity given in Eq. 439 reduces to

$$D_\mu G_{\nu\rho} + D_\nu G_{\rho\mu} + D_\rho G_{\mu\nu} = 0 . \quad (441)$$

By introducing the dual field strength tensor

$${}^* G^{\mu\nu} = \frac{1}{2} \epsilon^{\mu\nu\rho\sigma} G_{\rho\sigma} \quad (442)$$

we can also write the Bianchi identity as

$$D_\mu {}^*G^{\mu\nu} = 0. \quad (443)$$

Here we immediately observe that the (anti)self dual field configurations, where $G_{\mu\nu} = \mp {}^*G_{\mu\nu}$ respectively, automatically satisfy the field equations $D_\mu G^{\mu\nu} = 0$ due to the Bianchi identity. This result is appealing because it is easier to solve the first order self duality equations ${}^*G^{\mu\nu} = G^{\mu\nu}$ rather than second order field equations $D_\mu G^{\mu\nu} = 0$.

The symmetric stress energy tensor is obtained easily by coupling the theory to a background metric $g_{\mu\nu}$:

$$L = -\frac{1}{4}G_{\mu\nu}^a G_{\rho\sigma}^a g^{\mu\rho} g^{\nu\sigma} \sqrt{-g}, \quad (444)$$

and varying the action with respect to $g_{\mu\nu}$:

$$T^{\mu\nu} \equiv -\frac{2}{\sqrt{-g}} \left(\frac{\partial L}{\partial g_{\mu\nu}} - \partial_\rho \frac{\partial L}{\partial g_{\mu\nu,\rho}} + \partial_\rho \partial_\sigma \frac{\partial L}{\partial g_{\mu\nu,\rho\sigma}} \right). \quad (445)$$

Using the identities $\delta g = g g^{\mu\nu} \delta g_{\mu\nu}$ and $\partial g^{\rho\sigma} / \partial g_{\mu\nu} = -(g^{\rho\mu} g^{\nu\sigma} + g^{\rho\nu} g^{\mu\sigma})/2$ we find

$$T^{\mu\nu} = -G^{a\mu\sigma} G^{a\nu}{}_\sigma + \frac{1}{4}g^{\mu\nu} G_{\rho\sigma}^a G^{a\rho\sigma}. \quad (446)$$

We define the electric field $\vec{E} \equiv \vec{E}^a T^a$ and the magnetic field $\vec{B} \equiv \vec{B}^a T^a$, which are elements of the Lie Algebra:

$$\begin{aligned} E^{ai} &= -G^{a0i}, \\ B^{ai} &= -\frac{1}{2}\epsilon^{ijk} G^{ajk} \leftrightarrow G^{aij} = -\epsilon^{ijk} B^{ak}. \end{aligned} \quad (447)$$

In terms of $A^\mu = (A^0, \vec{A})$

$$E^i = \partial^i A^0 - \partial^0 A^i + ig[A^0, A^i], \quad (448)$$

$$B^i = -\epsilon^{ijk}(\partial^j A^k - igA^j A^k). \quad (449)$$

These matrices are not gauge invariant, they transform according to Eq. 410. The equations for non-Abelian electric and magnetic fields can also be written as:

$$\vec{E}^a = -\vec{\nabla} A^{a0} - \frac{\partial \vec{A}^a}{\partial t} + g f^{abc} \vec{A}^b A^{c0}, \quad (450)$$

$$\vec{B}^a = \vec{\nabla} \times \vec{A}^a - \frac{g}{2} f^{abc} \vec{A}^b \times \vec{A}^c. \quad (451)$$

The above equation implies that non-Abelian gauge theories allow magnetic monopoles with magnetic charge density:

$$\rho \equiv \vec{\nabla} \cdot \vec{B}^a = -\frac{g}{2} f^{abc} \vec{\nabla} \cdot (\vec{A}^b \times \vec{A}^c). \quad (452)$$

Total magnetic charge is the surface integral at spatial infinity and there are monopole solutions for which the integral does not vanish.

The components of the dual field tensor 442 are

$$\begin{aligned} *G^{a0i} &= \frac{1}{2} \epsilon^{ijk} G^{ajk} = -B^{ai}, \\ *G^{aij} &= -\epsilon^{ijk} G^{a0k} = \epsilon^{ijk} E^{ak}. \end{aligned} \quad (453)$$

Duality replaces $E^{ai} \rightarrow B^{ai}$ and $B^{ai} \rightarrow -E^{ai}$. The Lagrangian density and energy can be computed in terms of E^{ai} and B^{ai} :

$$\mathcal{L}_{\text{gauge}} = -\frac{1}{4} (-2G^{a0i}G^{a0i} + G^{aij}G^{aij}) = \frac{1}{2} (\vec{E}^a \cdot \vec{E}^a - \vec{B}^a \cdot \vec{B}^a), \quad (454)$$

$$T^{00} = G^{a0i}G^{a0i} - g^{00} \mathcal{L} = \frac{1}{2} (\vec{E}^a \cdot \vec{E}^a + \vec{B}^a \cdot \vec{B}^a) \equiv \mathcal{E}, \quad (455)$$

where \mathcal{E} denotes the energy density. Using Eq. 453 we find

$$*G^{a\mu\nu} G_{\mu\nu}^a = -4\vec{E}^a \cdot \vec{B}^a. \quad (456)$$

The equations of motion 436, in three vector form, reads

$$\vec{\nabla} \times \vec{B}^a = \frac{\partial \vec{E}^a}{\partial t} + g f^{abc} (A_0^b \vec{E}^c + \vec{A}^b \times \vec{B}^c), \quad (457)$$

$$\vec{\nabla} \cdot \vec{E}^a = g f^{abc} \vec{A}^b \cdot \vec{E}^c. \quad (458)$$

They are the generalizations of Maxwell Equations.

A.2 Classical Instanton Solutions of Non-Abelian Gauge Theories

A pure gauge theory can have “static” soliton solutions only in four dimensional Euclidean space [60] (here static means that the solutions are independent of one of the four coordinates). In this section, we will study such a solution, called the instanton, which is characterized by a topological charge and finite action[61, 62, 63, 64, 65]. Instantons are important for the quantum theory, because they describe tunneling between degenerate vacua. Instanton solutions play a crucial role in understanding the quantum theory of gauge theories. We will use most of the results obtained in this section when we discuss the nontrivial vacuum structure of non Abelian gauge theories, later in this Appendix.

We will concentrate on the Euclidean $SU(2)$ gauge theory which is obtained by making the following replacements in the Minkowski space version of the theory:

$$x^0 \rightarrow -ix^4, \quad g_{\mu\nu} = (+, -, -, -) \rightarrow g_{\mu\nu} = (+, +, +, +), \quad (459)$$

where the indices run from 1 to 4 in Euclidean space and $\epsilon^{1234} = 1$ ($\epsilon^{\mu\nu\rho\sigma}$ is a tensor density; it has to be multiplied by the determinant of the transformation when it is transformed. That is why it does not pick up an i under $x^0 \rightarrow -ix^4$). Hence $\partial_0 \rightarrow i\partial_4$, $D_0 \rightarrow iD_4$, and $A_0(x) \rightarrow iA_4(x_E)$. Note that A_0 and ∂_0 are components of vectors hence transform similarly, whereas x^0 is a component of a co-vector and transforms oppositely. Then the fields transform as

$$E_j^M \rightarrow iE_j^E, \quad B_j^M \rightarrow B_j^E. \quad (460)$$

Defining $x^4 \equiv T$ (hence $t = x^0 \rightarrow -ix^4 = -iT$), where T is a real parameter, the transformation of the action is

$$iS_M = i \int d^3x dt \mathcal{L}_M(t, \vec{x}) \rightarrow i \int d^3x (-iT) \mathcal{L}_M(-iT, \vec{x}) = - \int d^4x_E \mathcal{L}_E(x_E) \equiv -S_E, \quad (461)$$

where we define $\mathcal{L}_E(x_E) = -\mathcal{L}_M(-iT, \vec{x})$. Continuation to Euclidean spacetime means that we consider the dynamical evolution of the system in imaginary time. In principle, we

must solve the equations of motion in which the time x^0 is replaced by $-ix^4$. The Lorentz invariance $SO(3,1)$ of the Lagrangian density is replaced by invariance with respect to $SO(4)$ rotations in Euclidean space. The equations of motion determines how the *fields* are to be continued into Euclidean space. For example, for a real scalar field $\phi(x)$, the action in Minkowski spacetime is

$$S_M = \int dt d^3x \left[\frac{1}{2} \left((\partial_0 \phi(x_M))^2 - \nabla^2 \phi(x_M) \right) - U(\phi(x_M)) \right], \quad (462)$$

where U is the potential energy. Let's consider the equations of motion

$$\partial_0^2 \phi(x_M) - \partial_i^2 \phi(x_M) + U'(\phi(x_M)) = 0, \quad (463)$$

where prime denotes the derivative with respect to the field. If we Euclideanize the spacetime so that $\partial_0 \rightarrow i\partial_4$ and $\partial_i \rightarrow \partial_i$, we obtain

$$-\partial_4^2 \phi(x_E) - \partial_i^2 \phi(x_E) + \tilde{U}'(\phi(x_E)) = 0. \quad (464)$$

To have the required $SO(4)$ invariance we must have

$$\phi(x_M) = \phi(x^0 = t, \vec{x}) \rightarrow \phi(x_E) = \phi(x^4 = T, \vec{x}), \quad (465)$$

$$U(\phi(x_M)) \rightarrow \tilde{U}(\phi(x_E)) = -U(\phi(x_E)). \quad (466)$$

Therefore, a real scalar field $\phi(x)$ defined in Minkowski space is replaced by a real scalar field $\phi(x)$ invariant under $SO(4)$ and the potential energy picks up a minus sign. In Euclidean space Eq. 463 is replaced by

$$-\partial_E^2 \phi_E - U'(\phi(x_E)) = 0. \quad (467)$$

The action in Eq. 462 therefore becomes

$$\begin{aligned} S_M &\rightarrow \int (-id^4x) d^3x \left[\frac{1}{2} \left((i\partial_{x^4} \phi(x_E))^2 - \nabla^2 \phi(x_E) \right) + U(\phi(x_E)) \right] \\ &\rightarrow i \int d^4x_E \left[\frac{1}{2} (\partial_E \phi(x_E))^2 - U(\phi(x_E)) \right] = iS_E, \end{aligned} \quad (468)$$

which confirms Eq. 461. The relation between the path integral formulation of the two regimes is therefore

$$\int [dA] e^{iS_M} \rightarrow \int [dA] e^{-S_E} . \quad (469)$$

In the rest of the section, we will drop the index E and adopt the summation convention when the repeated indices are both lower or upper. Using Eqs. 454 and 460 in Eq. 469, we find that the Lagrangian in Euclidean space reads

$$\mathcal{L} = \frac{1}{4} G_{\mu\nu}^a G_{\mu\nu}^a = \frac{1}{2} (E_i^a E_i^a + B_i^a B_i^a) . \quad (470)$$

Non Abelian electric and magnetic fields are assigned to the strength tensor exactly the same way as in Minkowski spacetime: $G_{4i}^a = -E_i^a$, and $G_{ij}^a = -\epsilon_{ijk} B_k^a$. These definitions are consistently yield the above action. The dual field strength tensor $*G_{\mu\nu}^a = \frac{1}{2} \epsilon_{\mu\nu\rho\sigma} G_{\rho\sigma}^a$ has the following components:

$$*G_{4i}^a = B_i^a , \quad *G_{ij}^a = \epsilon_{ijk} E_k^a . \quad (471)$$

Duality replaces $E_i^a \leftrightarrow -B_i^a$, therefore self dual and anti-self dual field configurations satisfy

$$G_{\mu\nu}^a = \pm *G_{\mu\nu}^a \Leftrightarrow E_i^a = \mp B_i^a . \quad (472)$$

Due to the Bianchi identity (Eq. 443), selfdual and anti-selfdual solutions automatically satisfy the equations of motion $D_\mu G_{\mu\nu}^a = 0$. Hence, it is sufficient to find gauge potentials yielding $E_i^a = \mp B_i^a$ to find a solution for the equations of motion.

In Euclidean space the stress energy tensor $T_{\mu\nu} = G_{\mu\sigma}^a G_{\nu\sigma}^a - \frac{1}{4} g_{\mu\nu} G_{\rho\sigma}^a G_{\rho\sigma}^a$ has the following components:

$$\begin{aligned} T_{44} &= \frac{1}{2} (E_i^a E_i^a - B_i^a B_i^a) , \\ T_{ij} &= E_i^a E_j^a - B_i^a B_j^a - \frac{1}{2} \delta_{ij} (E_k^a E_k^a - B_k^a B_k^a) , \\ T_{4i} &= \epsilon_{ijk} E_j^a B_k^a . \end{aligned} \quad (473)$$

All of the above components vanish for the self dual or anti self dual fields (as $E_i^a \rightarrow \mp B_i^a$). Thus, in Euclidean space, the energy momentum tensor for (anti)self dual solutions is identical to zero.

The other $SO(4)$ ($SO(3, 1)$ in Minkowski spacetime) and gauge invariant quantity is given by the pseudoscalar density:

$$\mathcal{T} \equiv \frac{1}{2} \text{Tr} G_{\mu\nu} {}^* G_{\mu\nu} = -E_i^a B_i^a . \quad (474)$$

This term is not considered as a kinetic term because it is a pure divergence, it can be written as

$$\mathcal{T} \equiv \partial_\mu K_\mu \equiv \frac{1}{2g^2} \partial_\mu J_\mu , \quad (475)$$

with

$$K_\mu \equiv \epsilon_{\mu\nu\rho\sigma} \text{Tr} [A_\nu \partial_\rho A_\sigma - i \frac{2g}{3} A_\nu A_\rho A_\sigma] . \quad (476)$$

(Here, let us note that for the group $SU(2)$, one can easily evaluate the traces by introducing Pauli spin matrices $\{\sigma^a; a = 1, 2, 3\}$ as the generators $T^a \equiv \frac{1}{2}\sigma^a$, hence $A_\mu = A_\mu^a \frac{1}{2}\sigma^a$. The identity $\sigma^a \sigma^b = \delta^{ab} + i\epsilon^{abc}\sigma^c$ yields $\text{Tr}(\sigma^a \sigma^b) = 2\delta^{ab}$, $\text{Tr}(\sigma^a \sigma^b \sigma^c) = 2i\epsilon^{abc}$ and one obtains $K_\mu = \frac{1}{2}\epsilon_{\mu\nu\rho\sigma} [A_\nu^a \partial_\rho A_\sigma^a + \frac{g}{3}\epsilon^{abc} A_\nu^a A_\rho^b A_\sigma^c]$.)

Let us prove Eq. 475:

$$\begin{aligned} \mathcal{T} &= \frac{1}{4} \epsilon_{\mu\nu\rho\sigma} \text{Tr} \{ [(\partial_\mu A_\nu - ig A_\mu A_\nu) - (\mu \leftrightarrow \nu)] [(\partial_\rho A_\sigma - ig A_\rho A_\sigma) - (\rho \leftrightarrow \sigma)] \} \\ &= \epsilon_{\mu\nu\rho\sigma} \text{Tr} [(\partial_\mu A_\nu)(\partial_\rho A_\sigma) - ig(\partial_\mu A_\nu)A_\rho A_\sigma - ig A_\mu A_\nu \partial_\rho A_\sigma - g^2 A_\mu A_\nu A_\rho A_\sigma] . \end{aligned}$$

Using the cyclic property of trace, the last term in the above equation can be eliminated.

Renaming $\mu \leftrightarrow \rho$ and $\nu \leftrightarrow \sigma$ in the third term, we obtain

$$\mathcal{T} = \epsilon_{\mu\nu\rho\sigma} \text{Tr} [(\partial_\mu A_\nu)(\partial_\rho A_\sigma) - 2ig(\partial_\mu A_\nu)A_\rho A_\sigma] . \quad (477)$$

It is trivial to show, again using the cyclic property and renaming the necessary indices, that

$$\epsilon_{\mu\nu\rho\sigma} \text{Tr} [(\partial_\mu A_\nu)A_\rho A_\sigma] = \frac{1}{3} \partial_\mu \text{Tr} [A_\nu A_\rho A_\sigma] . \quad (478)$$

Moreover,

$$\epsilon_{\mu\nu\rho\sigma} \text{Tr} [(\partial_\mu A_\nu)(\partial_\rho A_\sigma)] = \epsilon_{\mu\nu\rho\sigma} \partial_\mu \text{Tr} [A_\nu \partial_\rho A_\sigma] , \quad (479)$$

because $\epsilon_{\mu\nu\rho\sigma} \text{Tr} [A_\nu \partial_\mu \partial_\rho A_\sigma] = 0$ due to the symmetry of the partial derivatives and the anti symmetry of the Levi Civita tensor density. Thus we have

$$\mathcal{T} = \partial_\mu \left[\epsilon_{\mu\nu\rho\sigma} \text{Tr} (A_\nu \partial_\rho A_\sigma - i \frac{2g}{3} A_\nu A_\rho A_\sigma) \right] = \partial_\mu K_\mu , \quad (480)$$

as claimed.

Integrating \mathcal{T} over all four space we obtain the topological charge (Pontryagin index) $q[A] \equiv (g^2/8\pi^2) \int d^4x \mathcal{T}$ of the Euclidean field configuration $A^a(x)_\mu$:

$$q[A] = \frac{g^2}{16\pi^2} \int d^4x \text{Tr} G_{\mu\nu} * G_{\mu\nu} = \frac{g^2}{32\pi^2} \int d^4x G_{\mu\nu}^a * G_{\mu\nu}^a , \quad (481)$$

$$= \frac{g^2}{8\pi^2} \oint_{S_\infty^3} d\Sigma_\mu K_\mu + q_{\text{sing}} = \frac{1}{16\pi^2} \oint_{S_\infty^3} d\Sigma_\mu J_\mu + q_{\text{sing}} , \quad (482)$$

where the surface integral is on the boundary of four space, S^3 , with the measure $d\Sigma$, and q_{sing} is included because of the possible solutions that might contribute to the integral independent of their behavior at the boundary (e.g., Dirac-delta like solutions or solutions which yield divergent volume integral Eq. 481 because of their singularities away from the boundary). For nonsingular solutions $q_{\text{sing}} = 0$. Let us note that $q[A]$ is gauge invariant:

$$q' = \frac{g^2}{16\pi^2} \int d^4x \text{Tr} [G_{\mu\nu}^{a'} * G_{\mu\nu}^{a'}] = \frac{g^2}{16\pi^2} \int d^4x \text{Tr} [U G_{\mu\nu}^a U^{-1} U * G_{\mu\nu}^a U^{-1}] = q . \quad (483)$$

The importance of the nonsingular solutions becomes clear in quantization of gauge fields via path integral methods where the integration is over all classical field configurations $A_\mu^a(x)$ in imaginary time that interpolate between the vacua at $x_0 = \pm\infty$. The dominant contributions to this integration comes from the field configurations for which $S^E[A_\mu^a]$ is stationary. Here lies the particular relevance of the (anti)selfdual field configurations which satisfy $G_{\mu\nu}^a = \mp * G_{\mu\nu}^a$. They are solutions of the classical field equations $D_\mu G_{\mu\nu} = 0$ due to the Bianchi identity $D_\mu * G_{\mu\nu} = 0$ which is always satisfied.

Before trying to find solutions of the field equations, let us show that the action for arbitrary Euclidean solutions is bounded below by $|(8\pi^2/g^2)q[A_\mu^a]|$. In Euclidean space we have

$$\text{Tr}[(G_{\mu\nu} \mp *G_{\mu\nu})(G_{\mu\nu} \mp *G_{\mu\nu})] \geq 0, \quad (484)$$

since it is the sum of squares. The above equation implies

$$\text{Tr}[G_{\mu\nu}G_{\mu\nu} + *G_{\mu\nu}*G_{\mu\nu}] \geq \pm 2\text{Tr}[G_{\mu\nu}*G_{\mu\nu}]. \quad (485)$$

In Euclidean space $\epsilon_{\rho\sigma\mu\nu}\epsilon_{\mu\nu\phi\theta} = 2[\delta_{\rho\phi}\delta_{\sigma\theta} - \delta_{\rho\theta}\delta_{\sigma\phi}]$, thus $\text{Tr}[*G_{\mu\nu}*G_{\mu\nu}] = \text{Tr}[G_{\mu\nu}G_{\mu\nu}]$. Then, Eq. 485 gives

$$\text{Tr}[G_{\mu\nu}G_{\mu\nu}] \geq \pm \text{Tr}[G_{\mu\nu}*G_{\mu\nu}]. \quad (486)$$

This means for the action

$$S^E = \frac{1}{2} \int d^4x \text{Tr}[G_{\mu\nu}G_{\mu\nu}] \geq \pm \frac{1}{2} \int d^4x \text{Tr}[G_{\mu\nu}*G_{\mu\nu}]. \quad (487)$$

However, since $\text{Tr}[G_{\mu\nu}G_{\mu\nu}] \geq 0$, the action $S^E \geq 0$. Therefore we obtain the result we want

$$S^E \geq \left| \frac{1}{2} \int d^4x \text{Tr}[G_{\mu\nu}*G_{\mu\nu}] \right| = \frac{8\pi^2}{g^2} |q[A]|. \quad (488)$$

The lower bound is reached (i.e., the equality is satisfied), when $G_{\mu\nu} = \pm *G_{\mu\nu}$. Thus the action has its minimum value $S^E = (8\pi^2/g^2)|q[A]|$ for (anti)self dual solutions. We had already encountered another property of these solutions. They also had zero energy momentum tensor (Eq. 473). We are now ready for the topological interpretation of $q[A]$.

Recalling Eqs. 482 and 485, for nonsingular field configurations, the Euclidean action:

$$S^E = \frac{1}{2} \int d^4x \text{Tr}[G_{\mu\nu}G_{\mu\nu}] \geq \frac{8\pi^2}{g^2} |q[A]| = \frac{1}{2g^2} \oint_{S_\infty^3} d\Sigma_\mu J_\mu. \quad (489)$$

Thus the minimum value of the action depends on the behavior of the gauge fields at infinity. For S^E to be finite, $G_{\mu\nu}$ has to decrease sufficiently fast to zero at Euclidean infinity:

$$\lim_{x^2 \rightarrow \infty} G_{\mu\nu}(x) = 0. \quad (490)$$

Therefore, the potential must go to a pure gauge configuration at infinity:

$$A_\mu \rightarrow -\frac{i}{g}(\partial_\mu U)U^{-1} \quad \text{for } x^2 \rightarrow \infty, \quad (491)$$

which is obtained from $A_\mu = 0$ by a “gauge transformation.” Here the term gauge transformation must be used with precaution. There are so called “large gauge transformations” that yield physically distinct vacua which are gauge inequivalent to the vacuum $A_\mu = 0$. We will discuss this issue, in detail, later in this Appendix. The minimum value of the action is reached by asymptotically pure gauge configurations that yield asymptotically vanishing fields (Eq. 429). The boundary condition Eq. 491 defines a map at infinity. At the infinity of four dimensional Euclidean space E^4 we have boundary S_∞^3 . Equation 491 associates an $SU(2)$ gauge group element $U(x)$ with each point on the boundary 3-sphere S_∞^3 of E^4 . Hence any solution with the behavior of Eq. 491 defines a map:

$$x \rightarrow U(x) : \quad S_\infty^3 \rightarrow SU(2). \quad (492)$$

In fact, since the $SU(2)$ group manifold is topologically the same as S^3 , the solution A_μ with condition Eq. 491 determines a map

$$S_\infty^3 \rightarrow S^3. \quad (493)$$

All maps of the S^3 onto itself are decomposed into homotopy classes by an index $n \in Z$, called winding number. The integer n is simply the number of times S^3 gets covered by the map from S_∞^3 . The trivial vacuum gauge field $A_\mu = 0$ maps all the points of S_∞^3 to a single point of the gauge group space S^3 (which can be identified as the (minus)identity of the group). The trivial map has zero winding number since it does not cover the S^3 .

A.2.1 The Winding Number

Now, we will show that for gauge fields $A_\mu(x)$ with the asymptotic behavior of Eq. 491, the winding number n is given by [61, 62, 63]

$$q[A] = \frac{g^2}{32\pi^2} \int d^4x G_{\mu\nu}^a * G_{\mu\nu}^a = n. \quad (494)$$

Let us start by calculating the current J_μ for a pure gauge $A_\mu = -(i/g)(\partial_\mu U)U^{-1}$:

$$\begin{aligned} J_\mu &= 2g^2 \epsilon_{\mu\nu\rho\sigma} \text{Tr} \left[A_\nu \partial_\rho A_\sigma - i \frac{2g}{3} A_\nu A_\rho A_\sigma \right] \\ &= -2\epsilon_{\mu\nu\rho\sigma} \text{Tr} \left[(\partial_\nu U)U^{-1} \partial_\rho [(\partial_\sigma U)U^{-1}] - \frac{2}{3} (\partial_\nu U)U^{-1} (\partial_\rho U)U^{-1} (\partial_\sigma U)U^{-1} \right]. \end{aligned}$$

Evaluating the term

$$\partial_\rho [(\partial_\sigma U)U^{-1}] = (\partial_\rho \partial_\sigma U)U^{-1} + (\partial_\sigma U) \partial_\rho U^{-1} = (\partial_\rho \partial_\sigma U)U^{-1} - (\partial_\sigma U)U^{-1} (\partial_\rho U)U^{-1}, \quad (495)$$

where we used identity Eq. 428 to write $\partial_\rho U^{-1} = -U^{-1}(\partial_\rho U)U^{-1}$, and inserting back in Eq. 495 we find

$$J_\mu = -2\epsilon_{\mu\nu\rho\sigma} \text{Tr} \left[-(\partial_\nu U)U^{-1} (\partial_\sigma U)U^{-1} (\partial_\rho U)U^{-1} - \frac{2}{3} (\partial_\nu U)U^{-1} (\partial_\rho U)U^{-1} (\partial_\sigma U)U^{-1} \right]. \quad (496)$$

Moreover, if we rename $\sigma \leftrightarrow \rho$ in the first term above and sum up the terms, then

$$J_\mu = -\frac{2}{3} \epsilon_{\mu\nu\rho\sigma} \text{Tr} [(\partial_\nu U)U^{-1} (\partial_\rho U)U^{-1} (\partial_\sigma U)U^{-1}]. \quad (497)$$

Thus, for nonsingular solutions satisfying Eq. 491

$$q[A] = \frac{1}{16\pi^2} \oint_{S_\infty^3} d\Sigma_\mu J_\mu = \frac{-1}{24\pi^2} \oint_{S_\infty^3} d\Sigma_\mu \epsilon_{\mu\nu\rho\sigma} \text{Tr} [(\partial_\nu U)U^{-1} (\partial_\rho U)U^{-1} (\partial_\sigma U)U^{-1}], \quad (498)$$

depends only on the group element $U(x)$. It is interesting that the minimum value of an arbitrary Euclidean action depends only on the properties of $U(x)$ at infinity, and not on the details of the field configurations at finite x . The boundary, S_∞^3 is parametrized by three angles $\psi_1(x)$, $\psi_2(x)$, $\psi_3(x)$, while the group elements U are characterized by three angles $\theta_1(x)$, $\theta_2(x)$, $\theta_3(x)$: $U(x) = U(\theta_a(x))$. Then,

$$\partial_\mu U \equiv \frac{\partial U}{\partial x^\mu} = \frac{\partial \theta_a}{\partial x^\mu} \frac{\partial U}{\partial \theta_a} \equiv (\partial_\mu \theta_a) \partial_a U. \quad (499)$$

Hence,

$$q[A] = \frac{-1}{24\pi^2} \oint_{S_\infty^3} d\Sigma_\mu \epsilon_{\mu\nu\rho\sigma} (\partial_\nu \theta_a) (\partial_\rho \theta_b) (\partial_\sigma \theta_c) \text{Tr} [(\partial_a U)U^{-1} (\partial_b U)U^{-1} (\partial_c U)U^{-1}]. \quad (500)$$

Since $\epsilon_{\mu\nu\rho\sigma}$ is cyclic in $(\nu\rho\sigma)$ and $\text{Tr}[(\partial_a U)U^{-1}(\partial_b U)U^{-1}(\partial_c U)U^{-1}]$ is cyclic in (abc) , we obtain

$$q[A] = \frac{-3!}{24\pi^2} \oint_{S_\infty^3} d\Sigma_\mu \epsilon_{\mu\nu\rho\sigma} (\partial_\nu \theta_1) (\partial_\rho \theta_2) (\partial_\sigma \theta_3) \text{Tr}[(\partial_1 U)U^{-1}(\partial_2 U)U^{-1}(\partial_3 U)U^{-1}] . \quad (501)$$

The measure transform between the coordinate systems as

$$d\theta_1 d\theta_2 d\theta_3 = (\text{Jacobian}) d\psi_1 d\psi_2 d\psi_3 \Rightarrow d\theta_1 d\theta_2 d\theta_3 = d\Sigma_\mu \epsilon_{\mu\nu\rho\sigma} (\partial_\nu \theta_1) (\partial_\rho \theta_2) (\partial_\sigma \theta_3) . \quad (502)$$

Therefore, we can write $q[A]$ in the following form:

$$q[A] = \frac{-1}{4\pi^2} n \oint_{S_{SU(2)}^3} d\theta_1 d\theta_2 d\theta_3 \text{Tr}[(\partial_1 U)U^{-1}(\partial_2 U)U^{-1}(\partial_3 U)U^{-1}] . \quad (503)$$

Now, here the integration is over the group manifold of the gauge group $S_{SU(2)}^3$ instead of the boundary manifold S_∞^3 . The integer $n \in Z$ is there because it denotes how many points of S_∞^3 is mapped to one point of $S_{SU(2)}^3$. Choosing for θ_a , the Euler angles, we can always parametrize an $SU(2)$ group element

$$U(\theta_a) = e^{\frac{i}{2}\theta_1\sigma_3} e^{\frac{i}{2}\theta_2\sigma_2} e^{\frac{i}{2}\theta_3\sigma_3} \Rightarrow U^{-1}(\theta_a) = e^{-\frac{i}{2}\theta_3\sigma_3} e^{-\frac{i}{2}\theta_2\sigma_2} e^{-\frac{i}{2}\theta_1\sigma_3} , \quad (504)$$

where $0 \leq \theta_1 \leq 2\pi$, $0 \leq \theta_2 \leq \pi$, $0 \leq \theta_3 \leq 4\pi$. Then, after trivial cancellations, we find

$$\begin{aligned} \mathcal{U} &\equiv \text{Tr}[(\partial_1 U)U^{-1}(\partial_2 U)U^{-1}(\partial_3 U)U^{-1}] \\ &= -\frac{i}{8} \text{Tr} \left[\sigma_3 e^{\frac{i}{2}\theta_1\sigma_3} \sigma_2 e^{\frac{i}{2}\theta_2\sigma_2} \sigma_3 e^{-\frac{i}{2}\theta_2\sigma_2} e^{-\frac{i}{2}\theta_1\sigma_3} \right] . \end{aligned} \quad (505)$$

In Eq. 505, we can rewrite the term $I \equiv e^{\frac{i}{2}\theta_2\sigma_2} \sigma_3 e^{-\frac{i}{2}\theta_2\sigma_2}$, by power expanding the exponentials, as

$$\begin{aligned} \mathcal{I} &= \sigma_3 + \left(\frac{i}{2}\theta_2\right)[\sigma_2, \sigma_3] + \frac{1}{2!}\left(\frac{i}{2}\theta_2\right)^2 [\sigma_2, [\sigma_2, \sigma_3]] + \frac{1}{3!}\left(\frac{i}{2}\theta_2\right)^3 [\sigma_2, [\sigma_2, [\sigma_2, \sigma_3]]] + \dots \\ &= \sigma^3 \left(1 - \frac{1}{2!}\theta_2^2 + \dots\right) - \sigma_1 \left(\theta_2 - \frac{1}{3!}\theta_2^3 + \dots\right) \\ &= \sigma_3 \cos(\theta_2) - \sigma_1 \sin(\theta_2) . \end{aligned} \quad (506)$$

Then Eq. 505 becomes

$$\begin{aligned}
\mathcal{U} &= -\frac{i}{8} \text{Tr} \left[\sigma_3 e^{\frac{i}{2}\theta_1\sigma_3} \sigma_2 (\sigma_3 \cos(\theta_2) - \sigma_1 \sin(\theta_2)) e^{-\frac{i}{2}\theta_1\sigma_3} \right] \\
&= -\frac{i}{8} \text{Tr} \left[e^{\frac{i}{2}\theta_1\sigma_3} (-i\sigma_1) (\sigma_3 \cos(\theta_2) - \sigma_1 \sin(\theta_2)) e^{-\frac{i}{2}\theta_1\sigma_3} \right] \\
&= -\frac{1}{8} \text{Tr} \left[-i \cos(\theta_2) e^{\frac{i}{2}\theta_1\sigma_3} \sigma_2 e^{-\frac{i}{2}\theta_1\sigma_3} + I \sin(\theta_2) \right] .
\end{aligned}$$

Next, we use the identity

$$e^{\frac{i}{2}\theta_1\sigma_3} \sigma_2 e^{-\frac{i}{2}\theta_1\sigma_3} = \sigma_2 \cos(\theta_1) + \sigma_1 \sin(\theta_1) , \quad (507)$$

which can be verified the same way as in Eq. 506. Thus

$$\begin{aligned}
\mathcal{U} &= -\frac{1}{8} \text{Tr} \left[-i \cos(\theta_2) \cos(\theta_1) \sigma_2 - i \cos(\theta_2) \sin(\theta_1) \sigma_1 + I \sin(\theta_2) \right] \\
&= -\frac{1}{8} \sin(\theta_2) \text{Tr} [I] = -\frac{1}{4} \sin(\theta_2) .
\end{aligned} \quad (508)$$

Finally, we can calculate $q[A]$ using Eqs. 503 and 508:

$$q[A] = -\frac{1}{4\pi^2} n \int_0^{2\pi} d\theta_1 \int_0^{4\pi} d\theta_3 \int_0^\pi d\theta_2 \left(-\frac{1}{4}\right) \sin(\theta_2) = n . \quad (509)$$

Equation 509 can be expressed in Minkowski spacetime. Since $(d^4x)_E = id^4x$; $G_{i4}^a = -iG_{i0}^a$; and $\epsilon^{1230} = -1$ (whereas $\epsilon^{1234} = 1$), we have

$$q_M[A] = \frac{g^2}{32\pi^2} \int d^4x G_{\mu\nu}^a * G_{\mu\nu}^a = -n . \quad (510)$$

The winding number n is a measure of how many times the group manifold $SU(2)$ is covered by the map $U(\theta(x))$, when x spans the whole boundary of the four dimensional Euclidean space, S_∞^3 , once.

We now consider the simplest nontrivial case, $n = 1$, the instanton. Instantons are localized, nonsingular self dual solutions of the classical Euclidean Yang-Mills field equations $D_\mu G_{\mu\nu} = 0$ with one unit of topological charge. They have vanishing Euclidean energy momentum tensor: $T_{\mu\nu} = 0$. In particular the Hamiltonian density $\mathcal{H} = T_{00} = 0$. For instantons the associated action is

$$S^E = \frac{8\pi^2}{g^2} |q[A]| = \frac{8\pi^2}{g^2} . \quad (511)$$

Having defined the instantons, we construct an explicit solution in the next section.

A.2.2 An Explicit Instanton Solution by Construction

We start with making some useful definitions[61, 64]:

$$\sigma_\mu \equiv (\sigma_a, \pm i), \sigma_\mu^\dagger \equiv (\sigma_a, \mp i), \sigma_{\mu\nu} \equiv i(\delta_{\mu\nu} - \sigma_\mu^\dagger \sigma_\nu), {}^* \sigma_{\mu\nu} \equiv \frac{1}{2} \epsilon_{\mu\nu\rho\phi} \sigma_{\rho\phi} = \pm \sigma_{\mu\nu}, \quad (512)$$

where μ and ν runs from one to four, whereas a runs from one to three. Notice that $\sigma_{\mu\nu}$ is self dual if $\sigma_4 = +i$, or anti self dual if $\sigma_4 = -i$. Let's continue with the following ansatz:

$$U \equiv \frac{x_\mu \sigma_\mu^\dagger}{x} = \frac{\vec{x} \cdot \vec{\sigma} \mp i x_4}{\sqrt{\vec{x}^2 + x_4^2}} \Rightarrow U^{-1} = \frac{x_\mu \sigma_\mu}{x} = \frac{\vec{x} \cdot \vec{\sigma} \pm i x_4}{\sqrt{\vec{x}^2 + x_4^2}}, \quad (513)$$

so that

$$A_\mu^{\text{pure}} = -\frac{i}{g} (\partial_\mu U) U^{-1} = \frac{i (x_\mu - \sigma_\mu^\dagger (x_\nu \sigma_\nu))}{g x^2} = \frac{1}{g} \frac{\sigma_{\mu\nu} x_\nu}{x^2}, \quad (514)$$

where we have used the identity $(x_\mu \sigma_\mu)(x_\nu \sigma_\nu^\dagger) = x^2$. For a finite energy solution we need an A_μ which is not a pure gauge over the whole volume. We make the following ansatz for the potential

$$A_\mu = \frac{1}{g} \frac{\sigma_{\mu\nu} x_\nu}{x^2} f(x^2). \quad (515)$$

We require $f(0) = 0$ for regularity at $x = 0$, and $f(\infty) = 1$ for finite energy. To make this a solution, we only need to choose f such that the field strength tensor is self(anti-self) dual: $G_{\mu\nu} = \pm {}^* G_{\mu\nu}$. From Eq. 515 we obtain

$$G_{\mu\nu} = \frac{2}{g} \left\{ \frac{f(1-f)}{x^2} \sigma_{\mu\nu} + \left[f' - \frac{f(1-f)}{x^2} \right] (\sigma_{\mu\rho} x_\rho x_\nu - \sigma_{\nu\rho} x_\rho x_\mu) \right\}, \quad (516)$$

$${}^* G_{\mu\nu} = \frac{2}{g} \left\{ \frac{f(1-f)}{x^2} {}^* \sigma_{\mu\nu} + \left[f' - \frac{f(1-f)}{x^2} \right] \epsilon_{\mu\nu\rho\phi} (\sigma_{\rho\gamma} x_\gamma x_\phi - \sigma_{\phi\gamma} x_\gamma x_\rho) \right\}, \quad (517)$$

where prime denotes derivative with respect to the argument. Thus, $G_{\mu\nu} = \pm {}^* G_{\mu\nu}$, if the second term vanishes

$$f' - \frac{f(1-f)}{x^2} = 0. \quad (518)$$

The general solution satisfying the required boundary conditions is

$$f(x^2) = \frac{c x^2}{c x^2 + \lambda^2}. \quad (519)$$

Note that as $x^2 \rightarrow \infty$, $f(x^2) \rightarrow 1$, hence $A_\mu \rightarrow A_\mu^{\text{pure}}$ as required. The solution with topological charge $q = \mp 1$, has $c = 1$, as we now show. Setting $c = 1$, we find

$$A_\mu = \frac{1}{g} \frac{\sigma_{\mu\nu} x_\nu}{x^2 + \lambda^2}. \quad (520)$$

We can write the vector potential more explicitly:

$$\vec{A} = \frac{1}{g} \frac{(\vec{x} \times \vec{\sigma}) \pm x_4 \vec{\sigma}}{x^2 + \lambda^2} \Rightarrow A_i^a = \frac{2}{g} \frac{(\epsilon_{ija} x_j \pm \delta_{ai} x_4)}{x^2 + \lambda^2}, \quad (521)$$

$$A_4 = \mp \frac{1}{g} \frac{\vec{\sigma} \cdot \vec{x}}{x^2 + \lambda^2} \Rightarrow A_4^a = \mp \frac{2}{g} \frac{x^a}{x^2 + \lambda^2}. \quad (522)$$

The field strength tensor becomes

$$G_{\mu\nu} = \pm {}^* G_{\mu\nu} = \pm \frac{2f(1-f)}{g} \frac{\sigma_{\mu\nu}}{x^2} = \pm \frac{2}{g} \frac{\lambda^2}{(x^2 + \lambda^2)} \sigma_{\mu\nu}, \quad (523)$$

from which we obtain

$$E_i^a = G_{i4}^a = \pm \frac{4}{g} \frac{\lambda^2}{(x^2 + \lambda^2)^2} \delta_i^a. \quad (524)$$

Let us confirm that the topological charge $q[A] = \mp 1$. For self(anti-self) dual fields: $E_i^a = \pm B_i^a$. Then, since $(1/4)G_{\mu\nu}^a {}^* G_{\mu\nu}^a = -E_i^a B_i^a$, we have: $(1/4)G_{\mu\nu}^a {}^* G_{\mu\nu}^a = \mp E_i^a E_i^a$. Hence,

$$q[A] = \frac{g^2}{8\pi^2} \int d^4x \frac{1}{4} G_{\mu\nu}^a {}^* G_{\mu\nu}^a = \mp \frac{6\lambda^4}{\pi^2} \int d^4x \frac{1}{(x^2 + \lambda^2)^4}. \quad (525)$$

In four dimensional Euclidean space $d^4x = d\Omega_3 r^3 dr = \pi^2 r^2 d(r^2)$, thus

$$q[A] = \mp 6\lambda^4 \int_0^\infty \frac{r^2 d(r^2)}{(r^2 + \lambda^2)^4} = \mp 6 \int_0^\infty \frac{z dz}{(1+z)^4} = \mp \left[\frac{1}{3} \frac{1}{(1+z)^3} - \frac{1}{2} \frac{1}{(1+z)^2} \right] \Big|_0^\infty = \mp 1,$$

where we changed the integration variable $r^2 \equiv \lambda^2 z$. Later we will show how instantons are related to tunneling events between physically distinct gauge field vacua. But, before that, we want to study the quantum theory of non Abelian gauge fields in the next section.

A.3 Canonical Formalism and Quantization

Let us turn back and formulate the classical gauge theory using the canonical procedure[61, 66]. The Hamiltonian density and Hamiltonian are obtained using the standard recipe:

$$\mathcal{H} = \Pi_\mu^a \partial_0 A^{a\mu} - \mathcal{L}_{\text{gauge}} , \quad (526)$$

$$H = \int d^3x \mathcal{H} , \quad (527)$$

where Π_μ is the canonical conjugate of the gauge field. From Lagrange density Eq. 454, we find

$$\Pi_0^a(x) = \frac{\partial \mathcal{L}}{\partial(\partial_0 A^{a0})} = 0 , \quad (528)$$

$$\Pi_i^a(x) = \frac{\partial \mathcal{L}}{\partial(\partial_0 A^{ai})} = -G^{a0}{}_i = -E^{ai} . \quad (529)$$

Thus

$$\mathcal{H} = -\vec{E}^a \cdot \frac{\partial \vec{A}^a}{\partial t} - \frac{1}{2}(\vec{E}^a \cdot \vec{E}^a - \vec{B}^a \cdot \vec{B}^a) . \quad (530)$$

Using Eq. 450 we can re-express the first term of Eq. 530

$$\begin{aligned} -\vec{E}^a \cdot \frac{\partial \vec{A}^a}{\partial t} &= \vec{E}^a \cdot (\vec{E}^a + \vec{\nabla} A^{a0} - g f^{abc} \vec{A}^b A^{c0}) \\ &= \vec{E}^a \cdot \vec{E}^a + \vec{\nabla} (A^{a0} \vec{E}^a) - A^{a0} (\vec{\nabla} \cdot \vec{E}^a - g f^{abc} \vec{A}^b \cdot \vec{E}^c) . \end{aligned} \quad (531)$$

Then, Eq. 530 becomes

$$\mathcal{H} = \frac{1}{2}(\vec{E}^a \cdot \vec{E}^a + \vec{B}^a \cdot \vec{B}^a) + \vec{\nabla} (A^{a0} \vec{E}^a) - A^{a0} \vec{D} \cdot \vec{E}^a , \quad (532)$$

where

$$\vec{D} \cdot \vec{E}^a \equiv \vec{\nabla} \cdot \vec{E}^a - g f^{abc} \vec{A}^b \cdot \vec{E}^c . \quad (533)$$

If we try to impose the canonical equal time commutators (Poisson bracket relations in the classical theory), we immediately encounter trouble since $\Pi_0 = 0$ because $\mathcal{L}_{\text{gauge}}$ does not depend on $\partial_0 A^{a0}$. Since A^{a0} is not a dynamical variable, we may eliminate it from

the Hamiltonian by solving for it in terms of the dynamical variables through the classical constraint equation Eq. 458. This constraint equation ($\vec{D} \cdot \vec{E}^a = 0$) is nothing but the variation of the action δS given in Eq. 435 with respect to δA^0 . The component A^{a0} may be expressed in terms of the dynamical variables by inserting \vec{E}^a given in Eq. 450 into the constraint Eq. 458:

$$\nabla^2 A^{a0} - f^{abc} \vec{A}^b \cdot (2\vec{\nabla} A^{c0} + g \frac{\partial \vec{A}^c}{\partial t} + g^2 f^{cpq} A^{p0} \vec{A}^q) + g f^{abc} A^{b0} \vec{\nabla} \cdot \vec{A}^c = 0. \quad (534)$$

The usual procedure however, is to use the gauge invariance and set A^{a0} to zero. In this case Hamiltonian is the energy with density Eq. 455:

$$H = \frac{1}{2} \int d^3x \left((\vec{E}^a)^2 + (\vec{B}^b)^2 \right) = \int d^3x T^{00}. \quad (535)$$

When the canonical commutation relations are imposed

$$\begin{aligned} [A^{ia}(\vec{x}, t), A^{jb}(\vec{x}', t)] &= 0, \\ [E^{ia}(\vec{x}, t), E^{jb}(\vec{x}', t)] &= 0, \\ [E^{ia}(\vec{x}, t), A^{jb}(\vec{x}', t)] &= i\delta^{ij}\delta^{ab}\delta(\vec{x} - \vec{x}'), \end{aligned} \quad (536)$$

Hamilton equations $\frac{\partial \vec{A}^a}{\partial t} = i[H, \vec{A}^a]$ and $\frac{\partial \vec{E}^a}{\partial t} = i[H, \vec{E}^a]$ yield, in the temporal gauge, the definition of the electric field 450 and Ampere's law Eq. 457 (spatial components of Eq. 436) respectively. Let us verify these claims. The Hamilton equation for $\vec{A}^a(x)$ yields

$$\frac{\partial \vec{A}^a}{\partial t}(x) = i[H, \vec{A}^a(x)] = \frac{i}{2} \int d^3y \left\{ [(\vec{E}^b(y))^2, \vec{A}^a(x)] + [(\vec{B}^b(y))^2, \vec{A}^a(x)] \right\}, \quad (537)$$

however, since

$$\begin{aligned} [\vec{B}^b(y), \vec{A}^a(x)] &= [\vec{\nabla}_y \times \vec{A}^b(y) - \frac{g}{2} f^{bcd} \vec{A}^c(y) \times \vec{A}^d(y), \vec{A}^a(x)] = [\vec{\nabla}_y \times \vec{A}^b(y), \vec{A}^a(x)] \\ &= \vec{\nabla}_y \times [\vec{A}^b(y), \vec{A}^a(x)] = 0, \end{aligned} \quad (538)$$

using the distribution law and Eq. 536 we recover the definition of the electric field:

$$\frac{\partial \vec{A}^a}{\partial t}(x) = \frac{i}{2} \int d^3y [(\vec{E}^b(y))^2, \vec{A}^a(x)] = -\vec{E}^a(x). \quad (539)$$

The Hamilton equation for $E^{aj}(x)$ yields

$$\begin{aligned}
\frac{\partial E^{aj}}{\partial t}(x) &= i[H, E^{aj}(x)] = \frac{i}{2} \int d^3y \left[(\vec{B}^b(y))^2, E^{aj}(x) \right] = i \int d^3y B^{bi}(y) [B^{bi}(y), E^{aj}(x)] , \\
&= i \int d^3y B^{bi}(y) \left[\epsilon^{ipq} \partial_{y^p} A^{bq}(y) - \frac{g}{2} f^{bcd} \epsilon^{ipq} A^{cp}(y) A^{dq}(y), E^{aj}(x) \right] , \\
&\equiv \mathcal{I}_a + \mathcal{I}_b ,
\end{aligned} \tag{540}$$

where

$$\begin{aligned}
\mathcal{I}_a &= i \epsilon^{ipq} \int d^3y B^{bi}(y) \partial_{y^p} [A^{bq}(y), E^{aj}(x)] = \epsilon^{ipj} \int d^3y B^{ai}(y) \partial_{y^p} \delta(\vec{x} - \vec{y}) \\
&= \epsilon^{ipj} \int d^3y \left\{ \partial_{y^p} (B^{ai}(y) \delta(\vec{x} - \vec{y})) - (\partial_{y^p} B^{ai}(y)) \delta(\vec{x} - \vec{y}) \right\} \\
&= \epsilon^{ipj} \left\{ \oint_{\infty} d^2\Sigma B^{ai}(x) - \partial_{x^p} B^{ai}(x) \right\} = \epsilon^{jpi} \partial_{x^p} B^{ai}(x) \\
&= \left(\nabla \times \vec{B}^a(x) \right)^j ,
\end{aligned} \tag{541}$$

and

$$\mathcal{I}_b = -\frac{i}{2} g f^{bcd} \epsilon^{ipq} \int d^3y B^{bi}(y) [A^{cp}(y) A^{dq}(y), E^{aj}(x)] \tag{542}$$

$$= -\frac{1}{2} g \left\{ f^{bca} \epsilon^{ipj} B^{bi}(x) A^{cp}(x) + f^{bad} \epsilon^{ijq} B^{bi}(x) A^{dq}(x) \right\} , \tag{543}$$

adding the two terms up we find

$$\mathcal{I}_b = -g f^{abc} \left(\vec{A}^b(x) \times \vec{B}^c(x) \right)^j . \tag{544}$$

Hence

$$\mathcal{I}_a + \mathcal{I}_b = \left(\nabla \times \vec{B}^a(x) - g f^{abc} \vec{A}^b(x) \times \vec{B}^c(x) \right)^j , \tag{545}$$

which implies

$$\frac{\partial \vec{E}^a}{\partial t}(x) = \vec{\nabla} \times \vec{B}^a(x) - g f^{abc} \vec{A}^b \times \vec{B}^c(x) \equiv \vec{D} \times \vec{B}^a . \tag{546}$$

However, the Gauss' law (the time component of Eq. 436), $\vec{D} \cdot \vec{E}^a = 0$, is not found. Note that $\vec{B}^a(x)$, given by Eq. 451, is not a fundamental variable and its definition does not appear in the Hamilton equations either. $\vec{B}^a(x)$ is given by Eq. 451.

In Eq. 399, we have seen that, classically, the theory has a symmetry which leaves the equations of motion invariant. We choose the gauge $A^0(x) = 0$. But this does not completely fix the invariance. The infinitesimal form (Eq. 405) of the residual symmetry transformation is

$$\delta \vec{A}^a(x) = -g^{-1} \vec{D} \omega^a(\vec{x}) \equiv -\frac{1}{g} \vec{\nabla} \omega^a(\vec{x}) + f^{abc} \vec{A}^b(x) \omega^c(\vec{x}). \quad (547)$$

Here, unlike Eq. 405, $\omega(\vec{x})$ is time independent. The time dependent gauge transformations would generate nonzero $A^{a0}(x)$ in view of Eq. 399. Quantum mechanically this residual gauge invariance is expressed through the operator equation[61, 66]:

$$[\vec{D} \cdot \vec{E}^a(x), H] = i \frac{\partial}{\partial t} \vec{D} \cdot \vec{E}^a = i \vec{D} \cdot \dot{\vec{E}}^a = 0. \quad (548)$$

To see that $[\vec{D} \cdot \vec{E}^a(x), H] = 0$, let us first simplify Eq. 548:

$$[\vec{D} \cdot \vec{E}^a(x), H] = i(\partial_i \dot{E}_i^a + g f^{abc} \dot{A}_i^b E_i^c - g f^{abc} A_i^b \dot{E}_i^c). \quad (549)$$

Using $\dot{A}_i^b = -E_i^b$, we obtain

$$[\vec{D} \cdot \vec{E}^a(x), H] = i(\partial_i \dot{E}_i^a - g f^{abc} A_i^b \dot{E}_i^c). \quad (550)$$

On the other hand, from the equations of motion ($D_\nu^{ab} F^{b\nu\mu} = 0$), we have

$$D_i^{ab} F^{bi0} = 0 \quad (551)$$

$$D_0^{ab} F^{b0i} + D_j^{ab} F^{bj i} = -(\partial_0 \delta^{ab} - g f^{abd} A_0^d) E^b + D_j^{ab} F^{bj i} = 0. \quad (552)$$

In the temporal gauge, Eq. 552 becomes

$$\dot{E}_i^a = D_j^{ab} F_{ji}^b. \quad (553)$$

Then the commutator $[\vec{D} \cdot \vec{E}^a(x), H] = i \vec{D} \cdot \dot{\vec{E}}^a$ can be expressed as

$$\begin{aligned} [\vec{D} \cdot \vec{E}^a(x), H] &= i(\delta^{ab} \partial_i \dot{E}_i^b - g f^{abc} A_i^b \dot{E}_i^c) = i D_i^{ab} \dot{E}_i^b = i D_i^{ab} D_j^{bc} F_{ji}^c \\ &= \frac{i}{2} (D_i^{ab} D_j^{bc} - D_j^{ab} D_i^{bc}) F_{ji}^c = \frac{i}{2} [D_i, D_j]^{ac} F_{ji}^c, \end{aligned} \quad (554)$$

where

$$\begin{aligned}
[D_i, D_j]^{ac} &= D_i^{ab} D_j^{bc} - D_j^{ab} D_i^{bc} \\
&= (\delta^{ab} \partial_i - g f^{abe} A_i^e)(\delta^{bc} \partial_j - g f^{bcd} A_j^d) - (\delta^{ab} \partial_j - g f^{abe} A_j^e)(\delta^{bc} \partial_i - g f^{bcd} A_i^d) \\
&= -g f^{acb} (\partial_i A_j^b - \partial_j A_i^b) + g^2 f^{abe} f^{bcd} (A_i^e A_j^d - A_j^e A_i^d) \\
&= -g f^{acb} (\partial_i A_j^b - \partial_j A_i^b) + g^2 (f^{abe} f^{bcd} - f^{abd} f^{bce}) A_i^e A_j^d .
\end{aligned} \tag{555}$$

Using the Jacobi identity, $f^{abe} f^{bcd} - f^{abd} f^{bce} = f^{acb} f^{bde}$, we recast Eq. (555) as

$$\begin{aligned}
[D_i, D_j]^{ac} &= -g f^{acb} (\partial_i A_j^b - \partial_j A_i^b) + g^2 f^{acb} f^{bde} A_i^e A_j^d \\
&= -g f^{acb} (\partial_i A_j^b - \partial_j A_i^b + f^{bpq} A_i^p A_j^q) = -g f^{acb} F_{ij}^b .
\end{aligned} \tag{556}$$

Hence, Eqs. (554) and (556) give

$$[\vec{D} \cdot \vec{E}^a(x), H] = \frac{i}{2} [D_i, D_j]^{ac} F_{ji}^c = -\frac{i}{2} g f^{abc} F_{ij}^b F_{ij}^c = 0 . \tag{557}$$

The commutator vanishes because the indices a and b are antisymmetric in f^{abc} whereas they are symmetric in $F_{ij}^b F_{ij}^c$.

Therefore, an eigenfunction $\Psi[\vec{A}]$ of H can be chosen as a simultaneous eigenfunction of $\vec{D} \cdot \vec{E}^a(x)$. Thus, Gauss' law is imposed on the Hilbert space by choosing the eigenvalue of $\vec{D} \cdot \vec{E}^a(x)$ to be zero

$$\vec{D} \cdot \vec{E}^a(x) \Psi[\vec{A}(x)] = 0 . \tag{558}$$

We are particularly interested in vacuum configurations. Classically the ground state must correspond to time independent minimum energy solution. We have, therefore, $G_{\mu\nu} = 0$. To prove this, consider the action for a time independent solution (i.e., the space integral of the Lagrangian density)[67]:

$$S = S_1 - S_2 = \frac{1}{2} \int d^3x \left(\vec{E}^a \cdot \vec{E}^a - \vec{B}^a \cdot \vec{B}^a \right) . \tag{559}$$

Since the total energy \mathcal{E} is the sum $S_1 + S_2$, its finiteness implies the finiteness of S_1 , S_2 and S . Any solution, if exists, is unstable (not a solution) under the scale transformations:

$$A^{a0}(\vec{x}) \rightarrow \rho\lambda A^{a0}(\lambda\vec{x}) , \quad A^{ai}(\vec{x}) \rightarrow \lambda A^{ai}(\lambda\vec{x}) . \quad (560)$$

Hence

$$\vec{E}^{ai}(\vec{x}) \rightarrow \rho\lambda^2 \vec{E}^{ai}(\vec{y}) , \quad \vec{B}^{ai}(\vec{x}) \rightarrow \lambda^4 \vec{B}^{ai}(\vec{y}) , \quad (561)$$

where $\vec{y} \equiv \lambda\vec{x}$. Therefore,

$$\begin{aligned} S_1 &= (1/2) \int d^3x E^{ai}(\vec{x}) E^{ai}(\vec{x}) \rightarrow S_1 = (1/2) \lambda \rho^2 \int d^3y E^{ai}(\vec{y}) E^{ai}(\vec{y}) , \\ S_2 &= \frac{1}{2} \int d^3x B^{ai}(\vec{x}) B^{ai}(\vec{x}) \rightarrow S_2 = \frac{1}{2} \lambda^4 \int d^3y B^{ai}(\vec{y}) B^{ai}(\vec{y}) , \\ S &= S_1 - S_2 \rightarrow \lambda \rho^2 S_1 - \lambda S_2 , \end{aligned} \quad (562)$$

which should be stationary at $\rho = \lambda = 1$. Thus, the variations of λ and ρ at $\lambda = \rho = 1$ yield $\mathcal{L}_1 - \mathcal{L}_2 = 0$ and $2\mathcal{L}_1 - \mathcal{L}_2 = 0$, respectively. Together they give $\mathcal{L}_1 = \mathcal{L}_2 = 0$, hence $G_{\mu\nu} = 0$ (as expected in the ground state $\vec{E}^a = \vec{B}^a = 0$). This means that (in the temporal gauge) the field $\vec{A}(\vec{x})$ is a pure gauge: $\vec{A}(\vec{x}) = (-i/g)(\nabla U(\vec{x}))U^{-1}(\vec{x})$. Now, to make progress, we make a very important hypothesis regarding gauge transformations. We assume that the allowed gauge transformation matrices $U(\vec{x})$ have the same definite space-time independent limit U_∞ at spatial infinity:

$$\lim_{|\vec{x}| \rightarrow \infty} U(\vec{x}) = U_\infty = \text{const.} \quad (563)$$

Physically, this assumption is necessary at least to have a well defined non-Abelian electric charge. The total electric charge $Q^a \equiv g \int dr f^{abc} \vec{A}^b \cdot \vec{E}^c = \int dr \nabla \cdot \vec{E}^a = \int d\vec{S} \cdot \vec{E}^a$. Under a local gauge transformation charge transforms as

$$Q^a \rightarrow \int d\vec{S} \cdot U^{-1} \vec{E}^a U . \quad (564)$$

If U has a constant limit U_∞ at spatial infinity, Q^a transforms by the global gauge transformation $U_\infty^{-1}Q^aU_\infty$. Otherwise, the transformed charge has no simple relation to the original charge and we must conclude that the non-Abelian electric charge is not well defined. Let us also note that, because of condition that all pure gauge potentials have the same limit at infinity, the possibility of transitions between different the vacuum configurations can not be ruled out by kinetic considerations. Such transitions are only possible if the different vacuum field configurations do not vary at spatial infinity. Otherwise a transition would require an infinite kinetic energy (the integral $\int d^3x(\partial_0 A_i)^2$ would diverge) and an infinite action.

We can regard $U(\vec{x})$ as a continuous mapping of three dimensional space to the gauge group G . Equation 563 identifies spatial infinity as one point. This is equivalent to compactifying the spatial manifold R^3 to S^3 . Thus, we only need to consider the maps of $S^3 \rightarrow G$. A theorem due to Bott [68] states that any continuous mapping of S^3 into a simple Lie group G can be continuously deformed to a mapping into an $SU(2)$ subgroup of G . Therefore, for a gauge theory with simple group structure, it is sufficient to consider $S^3 \rightarrow SU(2)$. The manifold of the $SU(2)$ gauge group is also S^3 . Hence the matrix functions U are mappings of $S^3 \rightarrow S^3$. These can be categorized into homotopy classes labelled by an integer, called the “winding number” (the number of times the spatial S^3 is covered by the group manifold S^3) of the mapping [69]. Class $n = 0$ represents the set of gauge transformations which do not wind the target S^3 at all, and hence are homotopic (continuously deformable) to $U = I$ (the mappings of all points in S^3 to the identity of S^3); transformations of class $n = 1$ are those that wind the target S^3 only once. Remember that the most general element of $SU(2)$ is of the form:

$$U = \exp\left(\pm i\frac{\phi}{2}\hat{x} \cdot \vec{\sigma}\right) = v_0 \pm i\vec{v} \cdot \vec{\sigma} \quad (565)$$

where $\vec{\sigma}$ are the Pauli matrices, $v_0 \equiv \cos(\phi/2)$, $\vec{v} \equiv \hat{x} \sin(\phi/2)$. As ϕ runs from 0 to 2π , map Eq. 565 covers the $SU(2)$ manifold once. Therefore, for the maps of class $n = 1$, replacing

ϕ by a continuous monotonic function $\omega(|\vec{x}|)$ with appropriate boundary conditions, we can write the gauge transformations of the form

$$U_1(x) = \exp(\pm i\vec{\sigma} \cdot \hat{x}\omega(|\vec{x}|)) . \quad (566)$$

To wind S^3 once, as $|\vec{x}|$ runs from 0 to ∞ , $\omega(|\vec{x}|)$ should satisfy

$$\omega(\infty) = \pi, \quad \omega(0) = 0 . \quad (567)$$

As a representative of U_1 , choosing

$$\omega(|\vec{x}|) = \frac{\pi|\vec{x}|}{\sqrt{|\vec{x}|^2 + \lambda^2}} , \quad (568)$$

we have

$$U_1(\vec{x}) = \exp\left(\pm \frac{i\pi\sigma^i x^i}{\sqrt{|\vec{x}|^2 + \lambda^2}}\right) = \cos\left(\frac{\pi|\vec{x}|}{\sqrt{|\vec{x}|^2 + \lambda^2}}\right) \pm i\vec{\sigma} \cdot \hat{x} \sin\left(\frac{\pi|\vec{x}|}{\sqrt{|\vec{x}|^2 + \lambda^2}}\right) , \quad (569)$$

where λ is an arbitrary number. U_1 can also be written, by making the deformation $\sin(\pi|\vec{x}|/\sqrt{|\vec{x}|^2 + \lambda^2}) \rightarrow 2\lambda|\vec{x}|/(|\vec{x}|^2 + \lambda^2)$, as

$$U_1(\vec{x}) = \frac{\lambda^2 - |\vec{x}|^2}{|\vec{x}|^2 + \lambda^2} \pm i2\lambda \frac{\vec{\sigma} \cdot \vec{x}}{|\vec{x}|^2 + \lambda^2} = \sigma^\mu \hat{n}_\mu , \quad (570)$$

where $\sigma^\mu = (I, \mp i\vec{\sigma})$ and the unit vector

$$\hat{n}_\mu = \left(\frac{\lambda^2 - |\vec{x}|^2}{|\vec{x}|^2 + \lambda^2}, -2\lambda \frac{\vec{x}}{|\vec{x}|^2 + \lambda^2} \right) . \quad (571)$$

As \vec{x} ranges over all of 3 dimensional space, n_μ traces out a sphere S^3 in four dimensional spacetime. Thus, indeed, U_1 maps a 3-space onto $S^3 \simeq SU(2)$, covering it once. Equation 563 is satisfied since $U_\infty = -1$. Map Eq. 569 can not be continuously deformed to identity (or to any other $n = 0$ transformations) without violating Eq. 563. Indeed, Eq. 569 only yields a unique limit:

$$U_\infty = \cos(\phi) \pm i\vec{\sigma} \cdot \hat{x} \sin(\phi) , \quad (572)$$

as $|\vec{x}| \rightarrow \infty$ independently of the direction of approach if ϕ is an integer multiple of π . Gauge transformations $U_n(\vec{x})$ of class n , can be taken as $[U_1(\vec{x})]^n$ and A^{ai} is calculated by 402. If $n = 0$, then $U = I$ and we have the trivial vacuum $A^{ai} = 0$. U_1 given in Eq. 570 yields

$$\begin{aligned}\vec{A}(\vec{x}) &= -\frac{i}{g} (\nabla U_1(\vec{x})) U_1^{-1}(\vec{x}) \\ &= \frac{1}{g} \frac{2\lambda}{(|\vec{x}|^2 + \lambda^2)^2} [\mp \vec{\sigma}(|\vec{x}|^2 - \lambda^2) \pm 2\vec{x}(\vec{\sigma} \cdot \vec{x}) + 2\lambda(\vec{x} \times \vec{\sigma})] ,\end{aligned}\quad (573)$$

where we used $U_1^{-1}(\vec{x}) = \frac{\lambda^2 - |\vec{x}|^2}{|\vec{x}|^2 + \lambda^2} \mp i2\lambda \frac{\vec{\sigma} \cdot \vec{x}}{|\vec{x}|^2 + \lambda^2}$ and the identity $\sigma^i(\vec{\sigma} \cdot \vec{x}) = \sigma^i \sigma^j x^j = x^i + i\epsilon^{ijk} x^j \sigma^k$. In the quantum considerations we will show that only $n = 0$ homotopy class leaves the wave function of the system gauge invariant whereas the higher classes change the wave function by a phase. Therefore, homotopically equivalent transformations are also gauge equivalent. U_1 transforms any classical vacuum configuration in class n to one in class $(n+1)$. Hence, any gauge transformation of class $(n+m)$ is a product of a member of class n with a member of class m . The existence of gauge transformations which are not homotopic to the identity is what distinguishes the non-Abelian theory from the Abelian one. In the latter, all gauge transformations fall in the homotopically trivial $n = 0$ class. Thus the vacuum is physically unique in that case.

An analytic expression for the winding number of a gauge transformation $U(x)$ can be given by introducing a second non-conserved topological charge[62]:

$$Q_T(t) = \frac{1}{16\pi^2} \int d^3x J_0(\vec{x}, t) ,\quad (574)$$

where J_μ , defined in Eq. 475, satisfying $\mathcal{T} \equiv (1/2g^2)\partial_\mu J_\mu \equiv (1/4)G_{\mu\nu}^a * G_{\mu\nu}^a$. Recall that first topological charge, defined in Eq. 482, was absolutely gauge invariant winding number $q[A]$ (or the Pontryagin index) of the Euclidean field configuration $A_\mu^a(x)$. The new topological number is related to the issue of how to connect different Minkowski vacua via tunneling events (instantons in Euclidean space). Physically $Q_T[A_\mu^a, t]$ is a number which

characterizes a field configuration $A_\mu(t, \vec{x})$ in three dimensional space at a fixed time t . For an arbitrary field, $Q_T(t)$ is neither an integer nor has topological meaning. But for pure gauges $A_\mu(x) = -\frac{i}{g}(\partial_\mu U(x))U^{-1}(x)$, as shown below, $Q_T(t) \in Z$ gives the homotopy class index (or winding number) of the gauge transformation $U(x)$. Recall Eq. 497 that for a pure gauge

$$J_0 = -\frac{2}{3}\epsilon_{ijk}\text{Tr}[(\partial_i U)U^{-1}(\partial_j U)U^{-1}(\partial_k U)U^{-1}]. \quad (575)$$

Let $x^0 = t$ be fixed and assume that $U(t, \vec{x}) \rightarrow 1$ as $|\vec{x}| \rightarrow \infty$. Using the Euler angles θ^a and going through the same procedure we used for $q[A]$ in section A.2.1, we obtain

$$\begin{aligned} Q_T(t) &= \frac{-1}{12\pi^2} \int d^3x \epsilon_{ijk} (\partial_i \theta_a) (\partial_j \theta_b) (\partial_k \theta_c) \cdot \text{Tr}[(\partial_a U)U^{-1}(\partial_b U)U^{-1}(\partial_c U)U^{-1}] \\ &= \frac{-3!}{12\pi^2} \int d^3x \epsilon_{ijk} (\partial_i \theta_1) (\partial_j \theta_2) (\partial_k \theta_3) \cdot \text{Tr}[(\partial_1 U)U^{-1}(\partial_2 U)U^{-1}(\partial_3 U)U^{-1}] \\ &= \frac{-n}{2\pi^2} \int d\theta_1 d\theta_2 d\theta_3 \left(-\frac{1}{4} \sin(\theta_2)\right) = n. \end{aligned} \quad (576)$$

Note that Q_T can be changed by large gauge transformations whereas q is gauge invariant (Eq. 483). Integrating the four divergence $\partial_\mu J^\mu(x)$ over space and assuming that \vec{J} vanishes faster than $O(1/r^2)$ as $r \rightarrow \infty$ one obtains

$$\partial_0 Q_T(t) = \partial_0 \int d^3x J_0 = \int d^3x \partial_\mu J^\mu. \quad (577)$$

Integrating the above equation over time we find

$$Q_T(\infty) - Q_T(-\infty) = q. \quad (578)$$

The interpretation of this formula is as follows. Euclidean solution $A_\mu(\vec{x}, x_4)$ interpolates between the real time Minkowski potentials $A_\mu(t = \pm\infty, \vec{x})$ in the distant past and future. The imaginary time $x_4 = iT$ is the interpolating parameter. In general, this is not a tunnelling process since $A_\mu(t = -\infty, \vec{x})$ and $A_\mu(t = \infty, \vec{x})$ are not separated by a barrier. However, when the fields $A_\mu(t = \pm\infty, \vec{x})$ are pure gauges (i.e., vacua) so that the $Q_T(t = \pm\infty)$ are their respective homotopy class labels, then the $A_\mu(t = \pm\infty, \vec{x})$ are inequivalent if

$Q_T(t = -\infty) \neq Q_T(t = \infty)$ (i.e., they are separated by a barrier in Minkowski spacetime. Hence, solutions with $q \neq 0$ describe tunneling events between topologically inequivalent vacua and later it will be shown that in Euclidean space the instanton in the $A_4^a = 0$ gauge has exactly this behavior). To see this, observe that the field configuration of pure gauge \vec{A} in Eq. 573 has zero potential energy (the term in the energy functional not containing derivatives of the field A_i with respect to time):

$$\frac{1}{4} \int dx^3 G_{ij}^a G^{aij} = 0, \quad (579)$$

and that there is no zero energy evolution of the system which adiabatically connects configuration Eq. 573, where $Q_T(t = -\infty) = 1$, with the configuration $\vec{A} = 0$, where $Q_T(t = \infty) = 0$. To exemplify why all the paths joining the two field configurations in real time must go over an energy barrier, consider the class of field configurations[63]

$$A_i^{(\gamma)}(\vec{x}) = \gamma A_i^{(1)}(\vec{x}), \quad (580)$$

where $\gamma \in [0, 1]$ is a real time independent parameter and $A_i^{(1)}(\vec{x})$ is the pure gauge classical vacuum in the $n = 1$ class given in Eq. 573. We obtain the pure gauges $A_i = 0$ and $A_i = A_i^1$ for $\gamma = 0$ and $\gamma = 1$, respectively. They both give $G_{ij} = 0$ and hence zero energy for $\gamma = 0, 1$. For $\gamma \in (0, 1)$, however, $A_i^{(\gamma)}(\vec{x})$ is not a pure gauge. Although the electric field G^{0i} still vanishes because $A_0^{(\gamma)} = 0$ and $A_i^{(\gamma)}$ is time independent, the magnetic field $B_i = (1/2)\epsilon_{ijk}G^{jk}$ does not

$$G_{jk} = \gamma(\partial_j A_k^{(1)} - \partial_k A_j^{(1)}) - ig\gamma^2[A_j^{(1)}, A_k^{(1)}] = -ig(\gamma^2 - \gamma)[A_j^{(1)}, A_k^{(1)}] \neq 0, \quad (581)$$

for $\gamma \in (0, 1)$. The energy, $(-1/8) \int d^3x \text{Tr}(G_{ij}G^{ij}) > 0$ for $0 < \gamma < 1$, and proportional to $(g^2/8)(\gamma^2 - \gamma)^2$ (note that $\int d^3x \text{Tr}(G_{ij}G^{ij})$ is finite because $A_i^{(1)}$ falls as $|\vec{x}|^{-2}$ as $|\vec{x}| \rightarrow \infty$ as shown in Eq. 573). As γ varies in the interval $[0, 1]$, in field space $A_i^{(\gamma)}$ plots a path which connects the two classical vacua from $n = 0$ and $n = 1$ sectors. The energy of the configuration can be interpreted as an energy barrier between the two vacua. However, (due

to the nonlinear nature of the Yang-Mills theory) $A_i^{(\gamma)}$ does not solve the field equations, hence the path is classically forbidden; the barrier is impenetrable. In the quantum theory, tunneling will occur across this barrier. A semiclassical description of tunneling can be given by solving the classical equations of motion with imaginary time, thus achieving an evolution which is classically forbidden. The solutions with $q \neq 0$ describe tunnelling between topologically inequivalent vacua. As we will show next, the instanton in the temporal gauge ($A_i^{\text{inst-temp}}, A_4 = 0$), has exactly this behavior. For $x_4 = it \rightarrow -\infty$, $A_i^{\text{inst-temp}} \rightarrow (-i/g)(\partial_i U(\vec{x}))U^{-1}(\vec{x})$, whereas for $x_4 = it \rightarrow \infty$, $A_i^{\text{inst-temp}} \rightarrow 0$. The exact solution of the imaginary time equations of motion interpolates between the $n = 1$ and $n = 0$ vacuum field configuration. Hence the instanton solutions with $q \neq 0$ describe tunnelling between topologically inequivalent vacua. This is another way of saying that we are going under an energy barrier. To be more practical[61], we will now use the explicit instanton solution given in Eq. 522:

$$\vec{A}^{\text{inst}} = \frac{1}{g} \frac{(\vec{x} \times \vec{\sigma}) \pm x_4 \vec{\sigma}}{\vec{x}^2 + x_4^2 + \lambda^2}, \quad A_4^{\text{inst}} = \mp \frac{\vec{\sigma} \cdot \vec{x}}{\vec{x}^2 + x_4^2 + \lambda^2}, \quad (582)$$

and demonstrate the relation between vacuum tunneling and instantons. To bring the instanton field to the temporal gauge we make a gauge transformation

$$A_\mu^{\text{inst}}(x) \rightarrow A_\mu^{\text{inst-temp}}(x) = U(x)A_\mu^{\text{inst}}(x)U^{-1}(x) - \frac{i}{g}(\partial_\mu U(x))U^{-1}(x), \quad (583)$$

such that $A_4^{\text{inst-temp}}(x) = 0$. This yields

$$\partial_4 U(x) = -igU(x)A_4^{\text{inst-temp}} = \pm iU(x) \frac{\vec{\sigma} \cdot \vec{x}}{|\vec{x}|^2 + x_4^2 + \lambda^2}, \quad (584)$$

which can be integrated to give

$$U(\vec{x}, x_4) = \exp \left(\pm i \frac{\vec{\sigma} \cdot \vec{x}}{|\vec{x}|} f(\vec{x}, x_4) \right), \quad (585)$$

with

$$f(\vec{x}, x_4) = \frac{|\vec{x}|}{\sqrt{|\vec{x}|^2 + \lambda^2}} \left[\theta_0 + \arctan \left(\frac{x_4}{\sqrt{|\vec{x}|^2 + \lambda^2}} \right) \right]. \quad (586)$$

By setting the integration constant $\theta_0 = \frac{\pi}{2}$ we find that

$$\lim_{x_4 \rightarrow -\infty} f(\vec{x}, x_4) = 0, \quad (587)$$

$$\lim_{x_4 \rightarrow \infty} f(\vec{x}, x_4) = \omega(|\vec{x}|) = \frac{\pi|\vec{x}|}{\sqrt{|\vec{x}|^2 + \lambda^2}}. \quad (588)$$

Hence

$$\lim_{x_4 \rightarrow -\infty} U(\vec{x}, x_4) = 1, \quad (589)$$

$$\lim_{x_4 \rightarrow \infty} U(\vec{x}, x_4) = U_1(\vec{x}) = \exp\left(\pm i \frac{\pi \vec{\sigma} \cdot \vec{x}}{\sqrt{|\vec{x}|^2 + \lambda^2}}\right), \quad (590)$$

where $U_1(\vec{x})$ is given in Eq. 569. Since $A_4^{\text{inst-temp}} = 0$, the instanton field in the temporal gauge is

$$\vec{A}^{\text{inst-temp}} = \frac{1}{g} U(\vec{x}, x_4) \frac{(\vec{x} \times \vec{\sigma}) \pm x_4 \vec{\sigma}}{\vec{x}^2 + x_4^2 + \lambda^2} U^{-1}(\vec{x}, x_4) - \frac{i}{g} (\nabla U(\vec{x}, x_4)) U^{-1}(\vec{x}, x_4). \quad (591)$$

The first term of the above equation vanishes as $|x_4| \rightarrow \infty$. As $x_4 \rightarrow \mp\infty$, the second term yields the following limits:

$$\lim_{x_4 \rightarrow -\infty} \vec{A}^{\text{inst-temp}} = 0, \quad (592)$$

$$\lim_{x_4 \rightarrow \infty} \vec{A}^{\text{inst-temp}}(\vec{x}) = -\frac{i}{g} (\nabla U_1(\vec{x})) U_1^{-1}(\vec{x}) \quad (593)$$

which is given explicitly in Eq. 573. Thus, the instanton field in the limit $x_4 \rightarrow -\infty$, is the trivial vacuum, whereas in the limit $x_4 \rightarrow \infty$, it has the form of the pure gauge obtained from the large gauge transformations of class $n = 1$. This means that the instanton interpolates, in Euclidean time, between two field configurations differing by a large gauge transformation.

A.4 The Vacuum Angle

Let us now study how quantum theory of the Yang Mills theory responds to gauge transformations[61, 66]. We work in the temporal gauge $A_0^a(x) = 0$. Recall that in this gauge the Hamiltonian is

$$H = \frac{1}{2} \int d^3x (E_i^a(x) E_i^a(x) + B_i^a(x) B_i^a(x)), \quad (594)$$

where $\vec{E}^a(x) = -\partial A_i^a(x)/\partial t$ and $\vec{B}^a(x) = \vec{\nabla} \vec{A}^a(x) - \frac{g}{2} f^{abc} \vec{A}^b \times \vec{A}^c$. The canonical equal time commutators are

$$[A^{ia}(\vec{x}, t), A^{jb}(\vec{x}', t)] = [E^{ia}(\vec{x}, t), E^{jb}(\vec{x}', t)] = 0, \quad (595)$$

$$[E^{ia}(\vec{x}, t), A^{jb}(\vec{x}', t)] = i\delta^{ij}\delta^{ab}\delta(\vec{x} - \vec{x}'). \quad (596)$$

In the functional Schrodinger representation of the quantum theory[70], the operator $A_i^a(\vec{x})$ is diagonal. Let $|a\rangle$ be an eigenstate of $A_i^a(\vec{x})$ with eigenvalue (eigenfunction) $a_i^a(\vec{x})$:

$$A_i^a(\vec{x})|a\rangle = a_i^a(\vec{x})|a\rangle. \quad (597)$$

A_i^a is an operator, a_i is a function. In this representation, a functional differential representation of the conjugate momentum

$$E_i^a(\vec{x}) = i\frac{\delta}{\delta a_i^a(\vec{x})}, \quad (598)$$

is also a differential representation of the above commutators. The state $|\Psi\rangle$ is represented by the wave functional $\Psi[a] = \langle a|\Psi\rangle$. $|\Psi\rangle$ is an eigenstate of the above Hamiltonian, if the wave functional $\Psi[a]$ is a solution of the time independent functional Shrodinger equation:

$$\frac{1}{2} \int d^3x \left(-\frac{\delta}{\delta a_i^a(\vec{x})} \frac{\delta}{\delta a_i^a(\vec{x})} + b_i^a(\vec{x})b_i^a(\vec{x}) \right) \Psi[a] = E_0\Psi[a], \quad (599)$$

where $\vec{b}^a(\vec{x}) = \nabla \times \vec{a}^a(\vec{x}) - \frac{g}{2} f^{abc} \vec{a}^b(\vec{x})\vec{a}^c(\vec{x})$ is the eigenvalue of the diagonal and time independent magnetic field operator. Recall also that in the temporal gauge there is no Hamiltonian equation of motion corresponding to Gauss' law, $\vec{D} \cdot \vec{E}^a = 0$. Therefore, we must add this equation as a constraint on the states, $\vec{D} \cdot \vec{E}^a|\Psi\rangle = 0$. The wave functionals $\Psi[a]$ that satisfy Eq. 599, must also satisfy the functional Gauss' law constraint

$$\vec{D} \cdot \frac{\delta}{\delta \vec{a}(\vec{x})} \Psi[a] = 0. \quad (600)$$

To interpret this constrained let's consider what happens to $\Psi[a]$ under a gauge transformation. When we gauge transform \vec{a}^a , we cause a change in the functional $\Psi[a]$. Any change in the wave functional due to a change in \vec{a}^a is given by

$$\delta\Psi[a] = \int d^3x \frac{\delta\Psi}{\delta a_i^a(\vec{x})} \delta a_i^a(\vec{x}). \quad (601)$$

When the change in $\vec{a}^a(\vec{x})$ is due to a gauge transformation, then (using Eq. 602)

$$\delta a_i^a(\vec{x}) = -\frac{1}{g}(\partial_i \omega^a(\vec{x}) - g f^{abc} \omega^b(\vec{x}) a_i^c(\vec{x})). \quad (602)$$

Therefore, a change in $\Psi[a]$ due to $\delta\vec{a}^a(\vec{x})$ of Eq. 602, is

$$\delta\Psi[\vec{a}] = \frac{i}{g} \left\{ \int d^3x [E_i^a(\vec{x})\Psi[a]] (\partial_i \omega^a(\vec{x}) - g f^{abc} \omega^b(\vec{x}) a_i^c(\vec{x})) \right\}, \quad (603)$$

where we used $\frac{\delta}{\delta a_i^a(\vec{x})} = -iE_i^a(\vec{x})$. Equation 603 can also be written as

$$\delta\Psi[\vec{a}] = \frac{i}{g} \int d^3x \left\{ \partial_i [\omega^a(\vec{x}) E_i^a(\vec{x})] - \omega^a(\vec{x}) \partial_i \vec{E}^a(\vec{x}) - g f^{abc} \omega^b(\vec{x}) a_i^c(\vec{x}) E_i^a(\vec{x}) \right\} \Psi[a], \quad (604)$$

which gives

$$\delta\Psi[\vec{a}] = \frac{i}{g} \left(\int dS \cdot \vec{E}^a(\vec{x}) \omega^a(\vec{x}) - \int dx^3 \omega^a(\vec{x}) (\vec{D} \cdot \vec{E})^a \right) \Psi[\vec{a}]. \quad (605)$$

Notice that the Gauss' law operator $(\vec{D} \cdot \vec{E})^a$ acting on the wave functional $\Psi[a]$ has appeared in Eq. 605. If we assume

$$\lim_{|\vec{x}| \rightarrow \infty} \omega^a(\vec{x}) = 0, \quad (606)$$

the surface term vanishes, and if the wave functional satisfies the Gauss' law constraint, then the right hand side of Eq. 605 vanishes completely, and hence the wave functional is "invariant under a gauge transformation," $\delta\Psi[\vec{a}] = 0$. On the other hand. if we want the wave functional to be gauge invariant, then the functional must satisfy the Gauss' law constraint and the gauge transformation must be of class $n = 0$ which satisfies Eq. 606.

Remember that the transformations which satisfy Eq. 606 are only class $n = 0$ gauge transformations since:

$$\lim_{|\vec{x}| \rightarrow \infty} \omega(\vec{x}) = n\pi. \quad (607)$$

Thus, the Gauss' law constraint implies the physical wave functional to be "class $n = 0$ gauge invariant." Thus, $(\vec{D} \cdot \vec{E})^a$ is the generator of class $n = 0$ gauge transformations under which $\Psi[\vec{a}]$ is invariant. Therefore, we will call the wave functionals obtained by gauge transformations satisfying Eq. 606 "gauge equivalent." Let us also note that, when we say "gauge invariant," we also mean invariant under time independent gauge transformations (i.e., $\omega^a(\vec{x})$ is independent of time. We noted earlier that the temporal gauge condition does not fully fix the gauge. Any transformation that is time independent leaves $A_0^a = 0$). Calling \mathcal{G}_n the unitary operator which implements the gauge transformation in the n th homotopy class (operator representation of $U_n(\vec{x}) = [U_1(\vec{x})]^n$), we have $\mathcal{G}_0 \Psi[\vec{a}] = \Psi[\vec{a}]$. Next we consider the action of \mathcal{G}_1 which takes the n th sector of vacua to the $(n + 1)$ th sector (hence $\mathcal{G}_n \equiv (\mathcal{G}_1)^n$). For this class $\omega \rightarrow \pi$ as $|\vec{x}| \rightarrow \infty$, hence gauge invariance of $\Psi[\vec{a}]$ can not be forced by Gauss' law (Eq. 605). However, since \mathcal{G}_1 commutes with all observables (they are gauge invariant), the only effect it can make on physical states is to change them by a phase:

$$\mathcal{G}_1 \Psi[\vec{a}] = e^{-i\Theta} \Psi[\vec{a}] \quad \text{and hence} \quad \mathcal{G}_n \Psi[\vec{a}] = e^{-in\Theta} \Psi[\vec{a}], \quad (608)$$

where Θ is a free, real parameter. In other words, since under a gauge transformation of class $n \neq 0$, $\Psi[a]$ is not necessarily invariant, but since the Hamiltonian is locally gauge invariant, $[H, (\vec{D} \cdot \vec{E})^a] = 0$, all energy eigenfunctions can be chosen so that they change at most by a constant phase, which is the same for all eigenfunctions: $\Psi[a_n] = \mathcal{G}_n \Psi[a] = e^{-in\Theta} \Psi[a]$, where a_n is the transform of a by a class n gauge transformation $a_n = (U_1)^n a (U_1)^{-n} - \frac{i}{g} (U_1)^n \nabla (U_1)^{-n}$; ($n = 0, \pm 1, \pm 2, \dots$) This is the origin of the famous angle in Yang-Mills theory. We will denote the vacuum state wave functional by $\Psi_\Theta[a]$ and the vacuum state characterized by Θ is called the " Θ -vacuum."

Now, we can ask what the physical vacuum looks like. We have seen that states in different homotopy sectors are not forced to be gauge equivalent by Gauss' law. We have an infinite number of distinct topological vacuum $|n\rangle$ in each sector. Non of these is the true vacuum, since they will tunnel into one another. This is expected since, as we have seen, the Yang-Mills theory has finite action instanton solutions. Therefore, assuming that the tunneling does occur, one can anticipate that the correct vacua will be linear superposition of the topological vacua and are given by $|\Theta\rangle = \sum_{-\infty}^{\infty} e^{-in\Theta}|n\rangle$. In the next paragraph, we make this claim more rigourously, and show that it is plausible.

In Hilbert space, we represent the vacuum associated with the homotopy class index n by the state vector $|n\rangle$, with $\langle n|m\rangle = \delta_{nm}$. The topological charge operator $Q_T = (1/16\pi^2) \int d^3x J_0$ has the property $Q_T|n\rangle = n|n\rangle$. Large gauge transformations change n so that:

$$\mathcal{G}_1|n\rangle = |n+1\rangle, \quad \text{hence} \quad |n\rangle = \mathcal{G}_n|n=0\rangle. \quad (609)$$

Therefore $[Q_T, \mathcal{G}_1] = \mathcal{G}_1$. The state vector $|n\rangle$ is not invariant under \mathcal{G}_n . However, the physical vacuum should be invariant, up to a phase Θ , under gauge transformations (i.e., since $[\mathcal{G}_1, H] = 0$, their eigenstates are common. Then the unitarity of \mathcal{G}_1 implies that the eigenstates $|\Theta\rangle$ of H must satisfy $\mathcal{G}_1|\Theta\rangle = e^{-i\Theta}|\Theta\rangle$). Thus, we superimpose the n -vacua to form the so called Θ vacuum:

$$|\Theta\rangle = \sum_{n=-\infty}^{\infty} e^{in\Theta}|n\rangle. \quad (610)$$

Indeed,

$$\mathcal{G}_1|\Theta\rangle = \sum_{n=-\infty}^{\infty} e^{in\Theta}|n+1\rangle = e^{-i\Theta} \sum_{n=-\infty}^{\infty} e^{i(n+1)\Theta}|n+1\rangle = e^{-i\Theta}|\Theta\rangle, \quad (611)$$

justifying Eq. 608. Different Θ -vacua are orthogonal:

$$\langle\Theta'|\Theta\rangle = \sum_{n,m} e^{i(n\Theta-m\Theta')}\langle m|n\rangle = \sum_n e^{in(\Theta-\Theta')} = 2\pi\delta(\Theta-\Theta') \quad (612)$$

Thus, there exists a continuum of Θ -vacua and each one is a suitable ground state for the physical gauge theory. No gauge invariant operator B ($[B, \mathcal{G}_1] = 0$), can generate transitions between different Θ -vacua[63]:

$$\langle \Theta' | B | \Theta \rangle = \sum_{m,n} e^{in\Theta - im\Theta'} \langle m | B | n \rangle = \sum_{m,n} e^{i(n+p)\Theta - i(m+p)\Theta'} \langle m+p | B | n+p \rangle \quad (613)$$

where p is an arbitrary integer. Bracket $\langle m+p | B | n+p \rangle = \langle m | (\mathcal{G}_1^\dagger)^p B (\mathcal{G}_1)^p | n \rangle = \langle m | B | n \rangle$, since $[B, \mathcal{G}_1] = 0$ and \mathcal{G}_1 is unitary. Therefore, we have

$$\langle \Theta' | B | \Theta \rangle = e^{ip(\Theta - \Theta')} \sum_{m,n} e^{in\Theta - im\Theta'} \langle m | B | n \rangle = e^{ip(\Theta - \Theta')} \langle \Theta' | B | \Theta \rangle, \quad (614)$$

which implies, for all $p \in Z$,

$$(1 - e^{ip(\Theta - \Theta')}) \langle \Theta' | B | \Theta \rangle = 0,$$

or $\langle \Theta' | B | \Theta \rangle = \langle \Theta | B | \Theta \rangle \delta(\Theta - \Theta')$. Hence, each $|\Theta\rangle$ is the vacuum of a separate sector of states.

Here, let us note that we claimed all physical observables commute with the large gauge transformation \mathcal{G}_1 but we consider the wave functions $|n\rangle$ and $|n+1\rangle$ which are related exactly by \mathcal{G}_1 as distinct. Although physics is the same (the observables have the same value) in $|n\rangle$ and in $|n+1\rangle$, as we show below, the existence of distinct vacua changes the Lagrangian density by

$$\mathcal{L}_\Theta = -\frac{g^2}{32\pi^2} \Theta * G^{a\mu\nu} G_{\mu\nu}^a = \frac{g^2}{8\pi^2} \Theta E^{ai} B^{ai}. \quad (615)$$

The new Θ -term, \mathcal{L}_Θ , is a total divergence; it does not effect the equations of motion. However, it changes the quantum theory nonperturbatively in a Θ dependent manner. The relationship between the canonical momentum conjugate to A_i^a and E_i^a (Eq. 529), also changes

$$\Pi_i^a = -E^{ai} - \frac{g^2}{8\pi^2} \Theta B^{ai}. \quad (616)$$

The angle in the Yang Mills theory, therefore, can not be avoided by postulating the (large) gauge invariance of the states. It reappears as an ambiguity in the definition of the Lagrangian, and hence in the canonical variables. Another difference introduced by the Θ -term is the violation of time reversal T and parity P symmetries. Under T , $E_i \rightarrow E_i$, while $B_i \rightarrow -B_i$. Under P , $E_i \rightarrow -E_i$, while $B_i \rightarrow B_i$. Thus, under either T or P , \mathcal{L}_Θ changes sign, while the original Lagrangian density, proportional to $E_i^a E_i^a - B_i^a B_i^a$, is invariant.

To prove the claim Eq. 615, we recall the Feynman-Kac formula which gives the transition amplitude between n -vacua:

$$\lim_{T \rightarrow \infty} \langle m | e^{-TH} | n \rangle = \int [dA]_{n-m} e^{-S_E}, \quad (617)$$

where H is the Hamiltonian of the system and,

$$S_E = \frac{1}{4} \int_{-T/2}^{T/2} d\tau \int d^3x F_{\mu\nu}^a F_{\mu\nu}^a = \frac{1}{2} \int_{-T/2}^{T/2} d\tau \int d^3x (\vec{E}^a \cdot \vec{E}^a + \vec{B}^a \cdot \vec{B}^a) \quad (618)$$

is the Euclidean action between times $-T/2$ and $T/2$. Notice that in Eq. 617 we integrate over Euclidean gauge field configurations which interpolate between the vacua $|n\rangle$ and $|m\rangle$. Thus, the functional integral in Eq. 617 is restricted by the boundary conditions on the winding number $Q_T[A]$:

$$Q_T[A(\vec{x}, \tau = -T/2)] = n \quad \text{and} \quad Q_T[A(\vec{x}, \tau = T/2)] = m, \quad (619)$$

with $q = m - n$. In other words, in Feynman-Kac formula, for $|T| \rightarrow \infty$, we consider configurations which yield finite contributions. Since their Euclidean action is finite, $G_{\mu\nu}$ must vanish at infinity in all Euclidean directions. This means that A_μ is a pure gauge field and yields a mapping from S^3 to the group classified by the winding numbers. Then, we consider the transition amplitude \mathcal{A} between Θ -vacua:

$$\mathcal{A} = \lim_{T \rightarrow \infty} \langle \Theta' | e^{-TH} | \Theta \rangle = \sum_{n,m} e^{i(n\Theta - m\Theta')} \lim_{T \rightarrow \infty} \langle m | e^{-TH} | n \rangle, \quad (620)$$

replacing the summation index m by $p = (m - n)$, we have

$$\mathcal{A} = \sum_{n,p} e^{i(n\Theta - p\Theta' - n\Theta')} \lim_{T \rightarrow \infty} \langle p + n | e^{-TH} | n \rangle . \quad (621)$$

The amplitude $\langle p + n | e^{-TH} | n \rangle = \langle p | e^{-TH} | 0 \rangle$ since $[H, G] = 0$. Therefore,

$$\begin{aligned} \mathcal{A} &= \sum_p \sum_n e^{in(\Theta - \Theta')} e^{-ip\Theta} \lim_{T \rightarrow \infty} \langle p | e^{-TH} | 0 \rangle \\ &= \delta(\Theta - \Theta') \sum_p e^{-ip\Theta} \int [dA]_m e^{-S_E} , \end{aligned} \quad (622)$$

where the δ -function is obtained by summing over n , and Eq. 617 is used. Now we use the formula for topological charge $q = (g^2/32\pi^2) \int d^4x G_{\mu\nu}^a * G_{\mu\nu}^a$, which is an integer, to replace p with q . Hence

$$\begin{aligned} \mathcal{A} &= \delta(\Theta - \Theta') \sum_q \int [dA]_q \exp \left(-S^E - \frac{ig^2}{32\pi^2} \Theta \int d^4x G_{\mu\nu}^a * G_{\mu\nu}^a \right) \\ &= \delta(\Theta - \Theta') \int e^{-S_{\text{eff}}^E} , \end{aligned} \quad (623)$$

where the integration is over all fields, and

$$S_{\text{eff}}^E = \int d^4x_E \mathcal{L}_{\text{eff}}^E = \int d^4x_E \left(\frac{1}{4} G_{\mu\nu}^a G_{\mu\nu}^a + \frac{ig^2}{32\pi^2} \Theta G_{\mu\nu}^a * G_{\mu\nu}^a \right) \quad (624)$$

$$= \int d^4x_E \left(\frac{1}{2} (E_i^a E_i^a + B_i^a B_i^a) + \frac{ig^2}{32\pi^2} \Theta (-4E_i^a B_i^a) \right) . \quad (625)$$

To obtain the action in the Minkowski spacetime, we recall the necessary transformations:

$d^4x_E \rightarrow id^4x_M$, $E_i^E \rightarrow -iE_i^E$. Then, the effective action transforms as

$$\begin{aligned} S_{\text{eff}}^E &\rightarrow \int id^4x \left(\frac{1}{2} (B_i^a B_i^a - E_i^a E_i^a) + \frac{ig^2}{32\pi^2} \Theta (4iE_i^a B_i^a) \right) , \\ &\rightarrow i \int d^4x \left(\frac{1}{4} G_{\mu\nu}^a G^{a\mu\nu} + \frac{g^2}{32\pi^2} \Theta G_{\mu\nu}^a * G^{a\mu\nu} \right) , \end{aligned} \quad (626)$$

where we dropped the index M and used Eqs. 454, 456, and 474. Since $S^E \rightarrow -i \int d^4x_M \mathcal{L}_{\text{eff}}^M$ (Eq. 461), we find the effective action as

$$\mathcal{L}_{\text{eff}}^M = -\frac{1}{4} G_{\mu\nu}^a G^{a\mu\nu} - \frac{g^2}{32\pi^2} \Theta G_{\mu\nu}^a * G^{a\mu\nu} . \quad (627)$$

This proves claim Eq. 615. Since the Θ -angle is an arbitrary real parameter, whose absolute value can only be measured, the Θ -term in Minkowski spacetime can also be chosen with a positive sign.

References

- [1] P. Sikivie. Sources and distributions of dark matter. *Nucl. Phys. Proc. Suppl.*, 43:90, 1995.
- [2] J. Oort. The force exerted by the stellar system in the direction perpendicular to the galactic plane and some related problems. *Bull. Astr. Inst. Netherlands*, 6:249, 1932.
- [3] F. Zwicky. Die Rotverschiebung von extragalaktischen Nebeln. *Helv. Phys. Acta*, 6:110, 1933.
- [4] J. Binney and S. Tremaine. *Galactic Dynamics*. Princeton University Press, Princeton, NJ, 1987.
- [5] J. P. Ostriker and P. J. E. Peebles. A numerical study of the stability of flattened galaxies: or, can cold galaxies survive? *Astrophys. J.*, 186:467, 1973.
- [6] R. P. Saglia, G. Bertin, F. Bertola, J. Danziger, H. Dejonghe, E. M. Sadler, M. Stiavelli, P. T. de Zeeuw, and W. W. Zeilinger. Stellar dynamical evidence for dark halos in elliptical galaxies: the case of NGC 4472, IC 4296, and NGC 7144. *Astrophys. J.*, 403:567, 1993.
- [7] C. L. Bennett, M. Halpern, G. Hinshaw, N. Jarosik, A. Kogut, M. Limon, S. S. Meyer, L. Page, D. N. Spergel, G. S. Tucker, E. Wollack, E. L. Wright, C. Barnes, M. R. Greason, R. S. Hill, E. Komatsu, M. R. Nolta, N. Odegard, H. V. Peiris, L. Verde, and J. L. Weiland. First year Wilkinson Microwave Anisotropy Probe (WMAP) observations: preliminary maps and basic results. *Astrophys. J. Suppl.*, 148:1, 2003.
- [8] D. N. Spergel, L. Verde, H. V. Peiris, E. Komatsu, M. R. Nolta, C. L. Bennett, M. Halpern, G. Hinshaw, N. Jarosik, A. Kogut, M. Limon, S. S. Meyer, L. Page, G. S. Tucker, J. L. Weiland, E. Wollack, and E. L. Wright. First year Wilkinson Microwave

- Anisotropy Probe (WMAP) observations: determination of cosmological parameters. *Astrophys. J. Suppl.*, 148:175, 2003.
- [9] H. V. Peiris, E. Komatsu, L. Verde, D. N. Spergel, C. L. Bennett, M. Halpern, G. Hinshaw, N. Jarosik, A. Kogut, M. Limon, S. S. Meyer, L. Page, G. S. Tucker, , E. Wolack, and E. L. Wright. First year Wilkinson Microwave Anisotropy Probe (WMAP) observations: implications for inflation. *Astrophys. J. Suppl.*, 148:213, 2003.
- [10] B. Paczynski. Gravitational microlensing by the galactic halo. *Astrophys. J.*, 304:1, 1986.
- [11] C. Alcock, C. W. Akerlof, R. A. Allsman, T. S. Axelrod, D. P. Bennett, S. Chan, K. H. Cook, K. C. Freeman, K. Griest, S. L. Marshall, H-S. Park, S. Perlmutter, B. A. Peterson, M. R. Pratt, P. J. Quinn, A. W. Rodgers, C. W. Stubbs, and W. Sutherland. Possible gravitational microlensing of a star in the Large Magellanic Cloud. *Nature*, 365:621, 1993.
- [12] E. Aubourg, P. Bareyre, S. Brehin, M. Gros, M. Lachieze-Rey, B. Laurent, E. Lesquoy, C. Magneville, A. Milsztain, L. Moscoso, F. Queindec, J. Rich, M. Spiro, L. Vigroux, S. Zylberajch, R. Ansari, F. Cavalier, M. Moniez, J. P. Beaulieu, R. Ferlet, P. Grison, A. Vidal-Madjar, J. Guilbert, O. Moreau, F. Tajahmady, E. Maurice, L. Prevot, and C. Gry. Evidence for gravitational microlensing by dark objects in the galactic halo. *Nature*, 365:623, 1993.
- [13] A. Udalski, M. Szymanki, J. Kaluzny, M. Kubiak, W. Krzeminski, M. Mateo, G. W. Preston, and B. Paczynski. The optical gravitational lensing experiment. Discovery of the first candidate microlensing event in the direction of the galactic bulge. *Acta Astron.*, 43:289, 1993.

- [14] E. W. Kolb and M. S. Turner. *The Early Universe*. Addison-Wesley Publishing Company, New York, 1994.
- [15] C. Charmousis, V. Onemli, Z. Qiu, and P. Sikivie. Gravitational lensing by dark matter caustics. *Phys. Rev. D*, 67:103502, 2003.
- [16] P. Sikivie. The caustic ring singularity. *Phys. Rev. D*, 60:063501, 1999.
- [17] P. Sikivie and J. Ipser. Phase space structure of cold dark matter halos. *Phys. Lett. B*, 291:288, 1992.
- [18] P. Sikivie. Caustic rings of dark matter. *Phys. Lett. B*, 432:139, 1998.
- [19] S. Tremaine. The geometry of phase mixing. *MNRAS*, 307:877, 1999.
- [20] Y. B. Zel'dovich. Gravitational instability: an approximate theory for large density perturbations. *Astron. Astrophys.*, 5:84, 1970.
- [21] V. de Lapparent, M. J. Geller, and J. P. Huchra. A slice of the universe. *Ap. J.*, 302:L1, 1986.
- [22] C. Hogan. Gravitational lensing by cold dark matter catastrophes. *Ap. J.*, 527:42, 1999.
- [23] P. Sikivie. Evidence for ring caustics in the Milky Way. *Phys. Lett. B*, 567:1, 2003.
- [24] T. Padmanabhan. *Structure Formation in the Universe*. Cambridge University Press, New York, 1993.
- [25] L. Bergstrom and Ariel Goobar. *Cosmology and Particle Astrophysics*. John Wiley and Sons Ltd., Chichester, UK, 1999.
- [26] B. W. Lee and S. Weinberg. Cosmological lower bound on heavy-neutrino masses. *Phys. Rev. Lett.*, 39:165, 1977.

- [27] K. Fujikawa. Path integral measure for gauge invariant fermion theories. *Phys. Rev. Lett.*, 42:1195, 1979.
- [28] P. Sikivie. Axions in cosmology. *Fundamental Interactions, Cargese, 1981*. Edited by: M. Levy and J. L. Basdevant. Plenum Press, New York, 1982.
- [29] V. Baluni. CP violating effects in QCD. *Phys. Rev. D*, 19:2227, 1979.
- [30] R. J. Crewther, P. D. Di Vecchia, G. Veneziano, and E. Witten. Chiral estimate of the electric dipole moment of the neutron in quantum chromodynamics. *Phys. Lett. B*, 88:123, 1979.
- [31] N. Ramsey. Dipole moments and spin rotations of the neutron. *Phys. Rept.*, 43:409, 1977.
- [32] I. S. Altarev, Yu. V. Borisov, N. V. Borovikova, A. B. Brandin, A. I. Egorov, V. F. Ezhov, S. N. Ivanov, V. M. Lobashev, V. A. Nazarenko, V. L. Ryabov, A. P. Serebrov, and R. R. Taldaev. A new upper limit on the electric dipole moment of the neutron. *Phys. Lett. B*, 102:13, 1981.
- [33] K. F. Smith, N. Crampin, J. M. Pendlebury, D. J. Richardson, D. Shiers, K. Green, A. I. Kilvington, J. Moir, H. B. Prosper, D. Thompson, N. F. Ramsey, B. R. Heckel, S. K. Lamoreaux, P. Ageron, W. Mampe, and A. Steyerl. A search for the electric dipole moment of the neutron. *Phys. Lett. B*, 234:191, 1990.
- [34] I. S. Altarev, Yu. V. Borisov, N. V. Borovikova, S. N. Ivanov, E. A. Kolomensky, M. S. Lasakov, V. M. Lobashev, V. A. Nazarenko, A. N. Pirozhkov, A. P. Serebrov, Yu. V. Sobolev, E. V. Shulgina, and A. I. Egorov. New measurement of the electric dipole moment of the neutron. *Phys. Lett. B*, 276:242, 1992.

- [35] W. B. Dress, P. D. Miller, J. M. Pendlebury, P. Perrin, and N. F. Ramsey. Search for an electric dipole moment of the neutron. *Phys. Rev. D*, 18:9, 1977.
- [36] R. Peccei and H. Quinn. CP conservation in the presence of instantons. *Phys. Rev. Lett.*, 38:1440, 1977.
- [37] R. Peccei and H. Quinn. Constraints imposed by CP conservation in the presence of instantons. *Phys. Rev. D*, 16:1791, 1977.
- [38] S. Weinberg. A new light boson? *Phys. Rev. Lett.*, 40:223, 1978.
- [39] F. Wilczek. Problem of strong P and T invariance in the presence of instantons. *Phys. Rev. Lett.*, 40:279, 1978.
- [40] P. Sikivie. Of axions, domain walls and the early universe. *Phys. Rev. Lett.*, 48:1156, 1982.
- [41] L. Abbott and P. Sikivie. A cosmological bound on the invisible axion. *Phys. Lett. B*, 120:133, 1983.
- [42] J. Preskill, M. Wise, and F. Wilczek. Cosmology of the invisible axion. *Phys. Lett. B*, 120:127, 1983.
- [43] M. Dine and W. Fischler. The not so harmless axion. *Phys. Lett. B*, 120:137, 1983.
- [44] D. Gross, R. Pisarki, and L. Yaffe. QCD and instantons at finite temperature. *Rev. Mod. Phys.*, 53:43, 1981.
- [45] S. Chang, C. Hagmann, and P. Sikivie. Studies of the motion and decay of axion walls bounded by strings. *Phys. Rev. D*, 59:023505, 1998.
- [46] D. F. Malin and D. Carter. Giant shells around normal elliptical galaxies. *Nature*, 285:643, 1980.

- [47] L. Hernquist and P.J. Quinn. Shells and dark matter in elliptical galaxies. *Ap. J.*, 312:1, 1987.
- [48] P. Sikivie, I. Tkachev, and Y. Wang. The velocity peaks in the cold dark matter spectrum on Earth. *Phys. Rev. Lett.*, 75:2911, 1995.
- [49] P. Sikivie, I. Tkachev, and Y. Wang. The secondary infall model of galactic halo formation and the spectrum of cold dark matter particles on earth. *Phys. Rev. D*, 56:1863, 1997.
- [50] J.A. Fillmore and P. Goldreich. Self-similar spherical voids in an expanding universe. *Ap. J.*, 281:1, 1984.
- [51] E. Bertschinger. Self-similar secondary infall and accretion in an Einstein-de Sitter universe. *Ap. J. Suppl.*, 58:39, 1985.
- [52] S. Smale. A classification of immersions of the two-sphere. *Trans. Amer. Math. Soc.*, 90:281, 1959.
- [53] A. Phillips. Turning a sphere inside out. *Sci. Amer.*, 214:112, 1966.
- [54] G. Francis and B. Morin. Arnold Shapiro's eversion of the sphere. *Math. Intelligencer*, 2:200, 1979.
- [55] M. M. Lipschutz. *Theory and Problems of Differential Geometry*. McGraw-Hill, USA, 1969.
- [56] R. Lynds and B. Petrosian. Giant luminous arc in galaxy clusters. *Bull. Am. Astron. Soc.*, 18:1014, 1986.
- [57] G. Soucail, B. Fort, Y. Mellier, and J. P. Picat. A blue ring-like structure in the center of the A370 cluster of galaxies. *Astron. Astrophys. Lett.*, 172:L14, 1987.

- [58] N. Kaiser and G. Squires. Mapping the dark matter with weak gravitational lensing. *Ap. J.*, 404:441, 1993.
- [59] P. Schneider, J. Ehlers, and E.E. Falco. *Gravitational Lenses*. Springer, New York, 1982.
- [60] S. Deser. Absence of static solutions in source free Yang-Mills theory. *Phys. Lett. B*, 64:463, 1976.
- [61] K. Huang. *Quarks Leptons and Gauge Fields*. World Scientific, Singapore, 1992.
- [62] W. Dittrich and M. Reuter. *Selected Topics in Gauge Theories*. Springer Verlag, Berlin, 1986.
- [63] R. Rajaraman. *Solitons and Instantons*. Elsevier, Amsterdam, 1982.
- [64] V. Rubakov. *Classical Theory of Gauge Fields*. Princeton University Press, Princeton, 2002.
- [65] M. Shifman. *Instantons in Gauge Theories*. World Scientific, Singapore, 1994.
- [66] R. Jackiw. Introduction to the Yang-Mills quantum theory. *Rev. Mod. Phys.*, 52:661, 1980.
- [67] C. Itzykson and J. B. Zuber. *Quantum Field Theory*. McGraw-Hill, USA, 1980.
- [68] R. Bott. An application of Morse theory to the topology of Lie groups. *Bull. Soc. Math. France*, 84:251, 1956.
- [69] R. Jackiw and C. Rebbi. Vacuum periodicity in a Yang-Mills quantum theory. *Phys. Rev. Lett.*, 37:172, 1976.
- [70] B. Hatfield. *Quantum Field Theory of Point Particles and Strings*. Addison Wesley, Redwood City, 1989.